CRANFIELD UNIVERSITY

KONSTANTINOS G. KYPRIANIDIS

Multi-disciplinary conceptual design of future jet engine systems

SCHOOL OF ENGINEERING
Department of Power and Propulsion

PhD THESIS
Academic Year 2009-10

Supervisors: Dr. S.O.T. Ogaji and Prof. R. Singh
April 2010

CRANFIELD UNIVERSITY

SCHOOL OF ENGINEERING
Department of Power and Propulsion

PhD THESIS

Academic Year 2009-10

KONSTANTINOS G. KYRPIANIDIS

Multi-disciplinary conceptual design of future jet engine systems

Supervisors: Dr. S.O.T. Ogaji and

Prof. R. Singh

April 2010

This thesis is submitted in partial fulfillment of the requirements for the degree of Doctor of Philosophy

"The bottom line for mathematicians is that the architecture has to be right. In all the mathematics that I did, the essential point was to find the right architecture. It's like building a bridge. Once the main lines of the structure are right, then the details miraculously fit. The problem is the overall design.."

Freeman J. Dyson, *Interview with Donald J. Albers*

Abstract

This thesis describes various aspects of the development of a multi-disciplinary aero engine conceptual design tool, TERA2020 (Techno-economic, Environmental and Risk Assessment for 2020), based on an explicit algorithm that considers: engine performance, engine aerodynamic and mechanical design, aircraft design and performance, emissions prediction and environmental impact, engine and airframe noise, and production, maintenance and direct operating costs.

As part of this research effort, a newly-derived semi-empirical NO_x correlation for modern rich-burn single-annular combustors is proposed. The development of a numerical methods library is also presented, including an improved gradient-based algorithm for solving non-linear equation systems. Common assumptions made in thermo-fluid modelling for gas turbines and their effect on caloric properties are investigated, while the impact of uncertainties on performance calculations and emissions predictions at aircraft system level is assessed. Furthermore, accuracy limitations in assessing novel engine core concepts as imposed by current practice in thermo-fluid modelling are identified.

The TERA2020 tool is used for quantifying the potential benefits from novel technologies for three low pressure spool turbofan architectures. The impact of failing to deliver specific component technologies is quantified, in terms of power plant noise and CO_2 emissions. To address the need for higher engine thermal efficiency, TERA2020 is again utilised; benefits from the potential introduction of heat-exchanged cores in future aero engine designs are explored and a discussion on the main drivers that could support such initiatives is presented. Finally, an intercooled core and conventional core turbofan engine optimisation procedure using TERA2020 is presented. A back-to-back comparison between the two engine configurations is performed and fuel optimal designs for 2020 are proposed.

Whilst the detailed publications and the work carried out by the author, in a collaborative effort with other project partners, is presented in the main body of this thesis, it is important to note that this work is supported by 20 conference and journal papers.

Contribution to knowledge

I. Contribution to the development of a multi-disciplinary aero engine conceptual design tool, within a collaborative environment. The tool is based on an explicit algorithm and is targeted towards identifying an appropriate design space where more complex and time-consuming tools could be utilised. The author's efforts focused on the development of (i) a new engine performance code, (ii) a numerical methods library, (iii) a new emissions prediction and environmental impact code, (iv) and the enhancement of existing codes for engine lifing, direct operating costs and aircraft design and performance.

II. Assessment of future environmentally friendly jet engine systems, using the developed tool, including:

- Assessment of the impact of thermo-fluid modelling uncertainties on performance calculations and emissions predictions at aircraft system level, and identification of accuracy limitations in assessing novel concepts as imposed by current practice in thermo-fluid modelling.
- Quantification of potential benefits from low pressure spool technologies for three turbofan architectures and the impact of failing to deliver specific component technologies, for long and short range applications.
- Quantification of potential benefits from the introduction of heat-exchanged cores in turbofan engines and identification of fuel optimal designs for year 2020 entry into service, for long range applications.

It is likely that detailed studies and such tools exist internally in companies. Nevertheless, it is worth having such a tool and future aero engine assessments available for the broader research community. Whilst the detailed publications and the work carried out by the author, in a collaborative effort with other project partners, is presented in the main body of this thesis, it is important to note that this work is supported by 20 conference and journal papers.

Acknowledgments

The work presented in this thesis has been performed under the project NEWAC (European Commission Contract No. AIP5-CT-2006-030876) and this funding is gratefully acknowledged. In more detail, the work was performed under NEWAC WP1.3, "Techno-Economic and Environmental Risk Analysis", in close collaboration with L. Xu (Chalmers University), A. Alexiou (National Technical University of Athens), and B. Lehmayr (University of Stuttgart). Their contributions in developing the NEWAC TERA2020 framework is acknowledged, and their support in the work presented in this thesis is much appreciated.

I am indebted to Prof. P. Pilidis, Dr. S.O.T. Ogaji and Prof. R. Singh for many reasons; for giving me the opportunity to work at the Department of Power and Propulsion, for their continuous guidance in my research, but above all for encouraging me to be creative. Many thanks go to G. Hargreaves, M. Negus, N. Datt, S. Broe, and L. Pearson for providing solutions to many administrative problems. I would also like to express my most sincere gratitude to Prof. T. Grönstedt, Prof. L. Davidson, M. Vargman, and all my friends and colleagues at Chalmers University for providing a friendly and stimulating working environment, and making my 6-month visit there an unforgettable experience. I am grateful to A.M. Rolt (Rolls-Royce) for providing a valuable insight on conceptual design and intercooled core benefits, as well as for his constructive suggestions on improving TERA2020 and for peer-reviewing the contents of this thesis. Many thanks also go to Prof. A.I. Kalfas for inspiring me to learn more about aero engines, for his encouragement and help in starting this PhD, and for his continuous support in my professional development over the past few years.

I would like to express my appreciation to the reviewers of this work for their constructive suggestions on improving the overall quality and clarity of the thesis and resulting publications. Many thanks go to J.A. Borradaile for the numerous discussions and constructive suggestions which helped put much of his expertise into the TERA2020 tool conceptual design algorithm. Many thanks go to S. Bake (Rolls-Royce Deutschland) for his continuous support on conventional

and lean-burn combustion technology. Discussions with S. Donnerhack (MTU Aero Engines) on intercooled recuperated cores and LPT variable geometry benefits are gratefully acknowledged.

While working for the NEWAC project, I have had the great opportunity of collaborating and exchanging ideas with many people from industry and academia. A. Lundbladh (Volvo Aero), S. Colantuoni (Avio), H. Verdier (Turbomeca), P.C. Madden (Rolls-Royce), J.-M. Rogero (Airbus), M. Andreoletti (Snecma), R. Schaber (MTU Aero Engines), A. Toezser (Arttic), M. Dietz (Arttic), J. Roumeliotis (National Technical University of Athens), S. Bretschneider (University of Stuttgart), O. Arago (University of Stuttgart), D. Au (ISAE/SUPAERO), G. Corchero (Universidad Politechnica de Madrid) have all contributed in different aspects of this work and this is gratefully acknowledged.

I would also like to thank my colleagues at Cranfield University with whom I had the opportunity to work with and exchange ideas: V. Sethi, V. Pachidis, P. Laskaridis, V. Kyritsis, E. Najafi Saatlou, R.S.R. Khan, C. Celis, M. Mohseni, G. Di Lorenzo, D. Fouflias, K. Psarra, J. Janikovic, E. Zanenga, P. Bellocq, F. Colmenares, and D.S. Pascovici.

Many thanks to Mattia, Javi, Ben, Luismi, Guido and Greg for all the great moments with the Sexy Christine's, and for keeping the dream of playing our music all over Europe and America alive. Many thanks to Herc, Vaso, Giorgos, Aspasia, Despoina, Giannhs, Leonidas, Kostas, Konstantinos, Frank, Leo, Nenad, Alekos, Panos, Pavlos, Petros and Ioanna for cherishing me with their friendship. Many thanks to Xiaohui for all the support and encouragement.

This thesis is dedicated to my beloved parents Stella and Giorgos, and sister Athina to whom I am indebted. It is only through their continuous love, support and inspiration that I have managed to come this far.

Konstantinos G. Kyprianidis
April 2010

Contents

List of Figures

List of Tables

Nomenclature

Abbreviations

A/C	Aircraft
ACARE	Advisory Council for Aeronautical Research in Europe
AEO	All Engines Operative
ANOPP	Aircraft Noise Prediction Program
Ar	Argon
ATM	Air Traffic Management
AUTH	Aristotle University of THessaloniki
BP	ByPass
CAEP	Committee on Aviation Environmental Protection
CEA	Chemical Equilibrium with Applications
CEC	Chemical Equilibrium Composition
CFD	Computational Fluid Dynamics
CHALMERS	Chalmers University
CO	Carbon monoxide
CO_2	Carbon dioxide
CRFD	Computational Reactive Fluid Dynamic
CRTF	Counter-Rotating TurboFan
CU	Cranfield University
DAC	Dual-Annular Combustor
DDTF	Direct Drive TurboFan
DOC	Direct Operating Costs
DREAM	valiDation of Radical Engine Architecture systeMs
EDS	Environmental Design Space
EIS	Entry Into Service
$EINO_x$	Nitrogen Oxides Emissions Index

EOR	End Of Runway
ETS	Environmental Tool Suite
EU	European Union
FAA	Federal Aviation Administration
FAR	Federal Aviation Regulations
FLOPS	FLight OPtimization System
FPR	Fan Pressure Ratio
GeSTPAn	General Stationary and Transient Propulsion Analysis
GSP	Gas turbine Simulation Program
GTF	Geared TurboFan
GWP	Global Warming Potential
$H_2O(g)$	Water vapour
HP	High Pressure
HPC	High Pressure Compressor
HPT	High Pressure Turbine
IC	InterCooled aero engine
ICAO	International Civil Aviation Organization
IP	Intermediate Pressure
IPC	Intermediate Pressure Compressor
IPCC	Intergovernmental Panel on Climate Change
IPT	Intermediate Pressure Turbine
IRA	Intercooled Recuperated Aero engine
ISA	International Standard Atmosphere
JAA	Joint Aviation Authorities
LP	Low Pressure
LPT	Low Pressure Turbine
LR	Long Range
LT	Long Term
LTO	Landing and Take-Off
MDO	Multi-Disciplinary Optimisation
Mid-Cr	Mid-Cruise
MMC	Metal Matrix Composite
MOPEDS	MOdular Performance and Engine Design System
MT	Medium Term
MTOW	Maximum Take-Off Weight
N_2	Nitrogen

NASA	National Aeronautics and Space Administration
NCP	National Cycle Program
NEWAC	NEW Aero engine Core concepts
NGV	Nozzle Guide Vanes
NLR	Nationaal Lucht- en Ruimtevaartlaboratorium
NO_x	Nitrogen oxides
NPSS	Numerical Propulsion System Simulation
NTUA	National Technical University of Athens
O_2	Oxygen
OEI	One Engine Inoperative
OEM	Original Equipment Manufacturer
OEW	Operating Empty Weight
OH	Hydroxyl Radical
PARTNER	Partnership for AiR Transportation Noise and Emissions Reduction
PIANO	Project Interactive ANalysis and Optimisation
PROOSIS	PRopulsion Object Oriented SImulation Software
RANS	Reynolds-Averaged NavierStokes equations
RRAP	Rolls-Royce Aerothermal Performance
SAC	Single Annular Combustor
SILENCE(R)	Significantly lower community exposure to aircraft noise
SLS	Sea-Level Static
SoA	State of the Art
SP	Sub-Programme
SPL	Sound Pressure Levels
SR	Short Range
RQL	Rich-burn/Quick-quench/Lean-burn
TBO	Time Between Overhaul
TERA	Techno-economic, Environmental and Risk Assessment
TERA2020	Techno-economic, Environmental and Risk Assessment for 2020
TET	Turbine Entry Temperature
TLC	Through Life Costs
T/O	Take-Off
TOC	Top Of Climb
TOW	Take-Off Weight
TRL	Technology Readiness Level

UHBR	Ultra-High Bypass Ratio
UPM	Universidad Politechnica de Madrid
USTUTT	University of Stuttgart
VGV	Variable Guide Vanes
VITAL	enVIronmenTALly friendly aero engines
VIVACE	Value Improvement through a Virtual Aeronautical Collaborative Enterprise
WATE	Weight Analysis of Turbine Engines
WP	Work-Package
ZFW	Zero Fuel Weight

Station numbering

1	Intake inlet
2	Fan inlet
13	Fan tip outlet / Bypass duct inlet
131	Bypass duct inlet
132	Intercooler cold stream inlet
133	Intercooler cold stream outlet
14	Bypass duct outlet
23	Fan root outlet
24	Intermediate pressure compressor inlet
25	Intermediate pressure compressor outlet / Intercooler hot stream inlet
26	High pressure compressor inlet / Intercooler hot stream outlet
3	High pressure compressor outlet
307	Recuperator cold (air) stream inlet
308	Recuperator cold (air) stream outlet
31	Combustor inlet
4	Combustor outlet
41	High pressure turbine rotor inlet
43	High pressure turbine outlet
44	Intermediate pressure turbine rotor inlet
45	Intermediate pressure turbine outlet
46	Low pressure turbine rotor inlet
5	Low pressure turbine outlet / Jet pipe inlet

6	Recuperator hot (gas) stream inlet
601	Recuperator hot (gas) stream outlet
7	Jet pipe outlet
8	Core nozzle throat
18	Bypass nozzle throat
138	Intercooler nozzle throat

Symbols

A_8	Hot nozzle area in [m^2]
A_{18}	Bypass nozzle area in [m^2]
A_{138}	Intercooler nozzle area in [m^2]
A_{eff}	Effective flow area in [m^2]
AFR	Air to Fuel Ratio in [-]
Alt	Altitude in [m] or [ft]
Arel5	Low pressure turbine relative capacity in [-]
Arel8	Hot nozzle relative throat area in [-]
Arel18	Bypass nozzle relative throat area in [-]
Arel138	Intercooler nozzle relative throat area in [-]
Alpha8	Hot nozzle petal angle in [deg]
Alpha18	Bypass nozzle petal angle in [deg]
Alpha138	Intercooler nozzle petal angle in [deg]
BPR	ByPass Ratio in [-]
c	Turbine blade chord in [mm]
C_f	Fan streamline deviation correction factor in [-]
C_p	Isobaric heat capacity (specific heat at constant pressure) in [J/(kg·K)]
C_p^o	Isobaric heat capacity of a real gas in [J/(kg·K)]
C_v	Isochoric heat capacity (specific heat at constant volume) in [J/(kg·K)]
D_pNO_x/F_{oo}	NO_x certification parameter in [g/kN]
dP2Q1	Intake fractional pressure loss in [-]
dP133Q132	Intercooler cold stream fractional pressure loss in [-]
dP14Q131	Bypass duct fractional pressure loss in [-]
dP24Q23	IPC inlet duct fractional pressure loss in [-]
dP26Q25	Intercooler hot stream fractional pressure loss in [-]
dP4Q31	Combustor fractional pressure loss in [-]

dP308Q307	Recuperator cold (air) stream fractional pressure loss in [-]
dP31Q3	High pressure compressor diffuser fractional pressure loss in [-]
dP601Q6	Recuperator hot (gas) stream fractional pressure loss in [-]
dP7Q5	Jet pipe fractional pressure loss in [-]
Eff26	Intercooler effectiveness in [-]
Eff601	Recuperator effectiveness in [-]
$EINO_x$	NO_x emissions index in [g/kg fuel]
EPNL	Effective Perceived Noise Level in [dB]
$EPNL_i$	Effective Perceived Noise Level of source i in [dB]
$EPNL_{Tot}$	Total Effective Perceived Noise Level from all sources in [dB]
ETA4	Combustor efficiency in [-]
ETAm4	High pressure spool mechanical efficiency in [-]
ETAm44	Intermediate pressure spool mechanical efficiency in [-]
ETAm46	Low pressure spool mechanical efficiency in [-]
ETA13	Fan tip isentropic efficiency in [-]
ETA23	Fan root isentropic efficiency in [-]
ETA25	Intermediate pressure compressor isentropic efficiency in [-]
ETApol13	Fan tip polytropic efficiency in [-]
ETApol23	Fan root polytropic efficiency in [-]
ETApol25	Intermediate pressure compressor polytropic efficiency in [-]
ETApol3	High pressure compressor polytropic efficiency in [-]
ETApol43	High pressure turbine polytropic efficiency in [-]
ETApol45	Intermediate pressure turbine polytropic efficiency in [-]
ETApol5	Low pressure turbine polytropic efficiency in [-]
F_N	Net thrust in [kN]
F_N, Tot	Total propulsion system thrust in [kN]
$F_o o$	ICAO ISA SLS take-off net thrust in [kN]
FAR	Fuel to Air Ratio in [-]
FAR_{stoich}	Stoichiometric Fuel to Air Ratio in [-]
FL	Flight Level in [100ft]
FPR	Fan Pressure Ratio in [-]
h	Specific enthalpy in [J/kg]
H	Turbine blade height in [mm]
H/C	Hydrogen to Carbon ratio in [-]
Hum	Specific humidity in dry air in [kg H_2O/kg dry air]
Hum_{SL}	Specific humidity in dry air at sea-level in [kg H_2O/kg dry air]

IC Eff	Intercooler effectiveness in [-]
IC W_{cold}/W_{hot}	Intercooler cold to hot mass flow ratio in [-]
L/D	Lift to Drag ratio in [-]
LHV	Lower Heating Value of fuel in [J/kg]
m	Number of noise sources in [-]
M	Mach number in [-]
M_0	Flight Mach number in [-]
M_{cr}	Cruise flight Mach number in [-]
N	Rotational speed in [rpm]
OPR	Overall Pressure Ratio in [-]
P	Total pressure in [kPa]
P_2	Fan inlet total pressure in [kPa]
P_{13}	Bypass duct inlet total pressure in [kPa]
P_{24}	Intermediate pressure compressor inlet total pressure in [kPa]
P_{26}	High pressure compressor inlet total pressure in [kPa]
P_3	High pressure compressor delivery total pressure in [kPa]
P_{31}	Combustor inlet totalpressure in [kPa]
P_{41}	High pressure turbine rotor inlet total pressure in [kPa]
P_{44}	Intermediate pressure turbine rotor inlet total pressure in [kPa]
P_{46}	Low pressure turbine rotor inlet total pressure in [kPa]
$P_{c,in}$	Compressor inlet total pressure in [kPa]
P13Q2	Fan tip pressure ratio in [-]
P23Q2	Fan root pressure ratio in [-]
P25Q24	Intermediate pressure compressor pressure ratio in [-]
P3Q26	High pressure compressor pressure ratio in [-]
PR	Component pressure ratio in [-]]
PR_c	Compressor pressure ratio in [-]]
PW	Required work in [MW]
PWX4	High pressure shaft power off-take in [kW]
PWX44	Intermediate pressure shaft power off-take in [kW]
PWX46	Low pressure shaft power off-take in [kW]
R	Specific gas constant in [J/(kg·K)]
$R_{A/C}$	Aircraft range in [km]
S	Turbine blade pitch in [mm]
SFC	Specific Fuel Consumption in [g fuel/(kN·s)]
SR	Specific Range in [m/kg fuel]

T	Total temperature in [K]
T_{13}	Bypass duct inlet total temperature in [K]
T_{24}	Intermediate pressure compressor inlet temperature in [K]
T_{26}	High pressure compressor inlet temperature in [K]
T_{30}	High pressure compressor delivery temperature in [K]
T_{31}	Combustor inlet temperature in [K]
T_4	Combustor outlet temperature in [K]
T_{41}	High pressure turbine rotor inlet temperature in [K]
T_{44}	Intermediate pressure turbine rotor inlet temperature in [K]
T_{46}	Low pressure turbine rotor inlet temperature in [K]
T_f	Fuel injection temperature in [K]
T_{flame}	Combustor primary zone flame temperature in [K]
T_{in}	Component inlet total temperature in [K]
$T_{c,in}$	Compressor inlet total temperature in [K]
T_s	Static temperature in [K]
T133Q132	Intercooler cold stream temperature change in [K]
T26Q25	Intercooler hot stream temperature change in [K]
T308Q307	Recuperator cold (air) stream temperature change in [K]
T601Q6	Recuperator hot (gas) stream temperature change in [K]
TF	Technology Factor exponent in [-]
U	Turbine blade speed in [m/s]
V	Velocity in [m/s]
W_1	Intake inlet mass flow in [kg/s]
W_2	Fan inlet mass flow in [kg/s]
W_{24}	Intermediate pressure compressor inlet mass flow in [kg/s]
W_{26}	High pressure compressor inlet mass flow in [kg/s]
$W_{A/C}$	Aircraft weight in [kg]
W_c	Corrected mass flow in [kg/s]
W_f	Fuel mass flow in [kg/s]
W131Q132	Intercooler splitter bypass ratio in [-]
W132Q25	Intercooler cold to hot mass flow ratio in [-]
WAR	Water to Air Ratio in [-]
x	Mass fraction in [-]
y	Mole fraction in [-]
Z	Zweifel number in [-]
α_1	Turbine stage inlet flow angle in [deg]

α_2	Turbine stage outlet flow angle in [deg]
γ	Isentropic coefficient / Ratio of specific heats in [-]
Δh	Turbine stage enthalpy drop in [J/(kg·s)]
ΔPW_c	Compression work variation in [%]
ΔT_{comb}	Combustor temperature rise in [K]
ΔT_{ISA}	Ambient temperature deviation from ISA conditions in [K]
$\Delta T_{c,out}$	Compressor outlet total temperature variation in [K]
$\eta_{c,is}$	Compressor isentropic efficiency in [-]
$\eta_{c,pol}$	Compressor polytropic efficiency in [-]
λ	Lambda in [-]
μ	Dynamic viscosity in [Pa·s]
ϕ	Specific entropy in [J/(kg·K)]
ψ	Turbine stage loading coefficient in [-]

Subscripts

calc	Calculated
d	Dissociation
nd	No dissociation
ref	Reference

Chapter 1

Introduction

1.1 Problem area

Public awareness and political concern over the environmental impact of civil aviation growth (predicted at 5.9% per year in 2007 [1]) has improved substantially during the past 30 years. As the environmental awareness increases, so does the effort associated with addressing NO_x and CO_2 emissions by all the parties involved. In the Vision 2020 report [2], made by the Advisory Council for Aeronautical Research in Europe on European aeronautics, goals are set to reduce noise and emissions produced by the ever increasing global air traffic. Emissions legislation, set by the International Civil Aviation Organisation and it's Committee on Aviation Environmental Protection, is becoming ever more stringent, creating a strong driver for investigating novel aero engine designs that produce less CO_2 and NO_x emissions.

On the other hand, airline companies need to continuously reduce their operating costs in order to increase, or at least maintain, their profitability. This introduces an additional design challenge as new aero engine designs need to be conceived for reduced environmental impact as well as direct operating costs. Decision making on optimal engine cycle selection needs to consider mission fuel burn, direct operating costs, engine and airframe noise, emissions and global warming impact. A tool following a Techno-economic, Environmental and Risk Assessment (TERA) approach is required to conceive and assess engine designs with minimum environmental impact and lowest cost of ownership in a variety of

emissions legislation scenarios, emissions taxation policies, fiscal and air traffic management environments.

Within the European collaborative project VITAL (enVIronmenTALly friendly aero engines) [3], key low pressure spool technologies for three different turbofan architectures are being investigated, targeting step reductions in engine CO_2 and noise emissions. As part of the VITAL effort, a number of universities cooperate on establishing a platform for multidisciplinary system analysis, the TERA2020 environment. The tool is targeted towards identifying an appropriate design space where more complex and time-consuming tools could be utilised; it is capable of evaluating the technology progress achieved within the project on engine/aircraft system level as well as performing scenario studies of next generation turbofan engines. The activities within the VITAL project specifically target year 2020 entry into service, thus the acronym TERA2020.

Within the European collaborative project NEWAC (NEW Aero engine Core concepts) [4], enabling technologies are also researched for four new engine core concepts and three different lean-burn combustion concepts, with the objective of improving core thermal efficiency and reducing NO_x emissions. The TERA2020 tool from VITAL, is being developed further to assess the economic and environmental impact of the new technologies being researched in NEWAC and to undertake sensitivity and optimisation studies about the new engine configurations. New technologies researched under the umbrella of NEWAC include: intercooling, intercooling with recuperation, improved compressor blade aerodynamic design and blade tip rub management, aspirated compression systems, active control of compressor surge and tip clearance, and active control of a cooled cooling air system.

1.2 Fuel efficient aero engine designs

CO_2 emissions are directly proportional to fuel burn, and therefore any effort to reduce them needs to focus on improving fuel consumption. Fuel burn for a turbofan engine can typically be improved by:

1. Reducing engine weight and size.
2. Reducing engine Specific Fuel Consumption (SFC).

Reducing engine weight results in a lower aircraft maximum take-off weight, which in turn leads to reduced thrust requirements for a given aircraft lift to drag ratio. Reducing engine size – predominantly engine nacelle diameter and length – reduces nacelle drag and therefore also leads to reduced thrust requirements. For a given engine SFC, a reduction in thrust requirements essentially results in lower fuel consumption.

Lower engine SFC can be achieved by improving propulsive efficiency and thermal efficiency. Improving component efficiencies, as well as reducing other losses in the cycle, such as duct pressure losses and cooling flows, is another way of improving engine SFC. Modern CFD-assisted 3D blade designs however, are already quite aggressive and limited benefit may be envisaged by such future advancements in terms of loss reduction [5].

In the following sections, three important research questions will be set with respect to improving engine thermal and propulsive efficiency, and simultaneously reducing CO_2 and NO_x emissions.

1.2.1 Propulsive efficiency

Improvements in propulsive efficiency – and hence engine SFC at a given thermal efficiency – can be achieved by designing an engine at a lower specific thrust (i.e. net thrust divided by fan inlet mass flow). This results in a larger fan diameter, at a given thrust, and therefore in increased engine weight, which can partially, or even fully, negate any SFC benefits. Propulsive efficiency improvements at a constant weight are directly dependent on weight reduction technologies such as light weight fan designs and new shaft materials. Increasing engine bypass ratio aggravates the speed mismatch between the fan and the low pressure turbine. Introduction of a gearbox can relieve this issue by permitting the design of these two components at their optimal speeds, and can hence reduce engine weight, as well as improve component efficiency. The first research question therefore rises:

How low can we really go on specific thrust?

1.2.2 Thermal efficiency

Improvements in thermal efficiency – and hence engine SFC at a given propulsive efficiency – can be achieved for conventional cores mainly by increasing engine overall pressure ratio (OPR). At a given OPR there is an optimal level of combustor outlet temperature T_4 for thermal efficiency. However, at a fixed specific thrust and engine thrust, an increase in T_4 can result in a smaller core and therefore a higher engine bypass ratio; in some cases, a potential reduction in engine weight can more than compensate for a non-optimal thermal efficiency. Increasing OPR further than current engine designs is hindered by limitations in high pressure compressor delivery temperature at take-off. Increasing T_4 is limited by maximum permissable high pressure turbine rotor metal temperatures at take-off and top of climb. Increasing turbine cooling flows for this purpose is also fairly limited as a strategy; cooling flows essentially represent losses in the thermodynamic cycle, and increasing them eventually leads to severe thermal efficiency deficits [6, 7]. The second research question therefore rises:

How high can we really go on OPR and T_4?

1.2.3 CO_2 and NO_x emissions

Aggressive turbofan designs that reduce CO_2 emissions – such as increased OPR and T_4 designs – can increase the production of NO_x emissions due to higher flame temperatures. Designing a combustor at very low air to fuel ratio levels is also limited by the need for adequate combustor liner film-cooling air as well as maintaining an acceptable temperature traverse quality [8]. The third research question therefore rises:

What is the trade-off between low CO_2 and NO_x?

1.3 Research aim and objectives

An aero engine multidisciplinary design tool, TERA2020 (Techno-economic, Environmental and Risk Assessment for 2020), that helps to automate part of the

aero engine conceptual design process, was further developed in this project in order to be successfully utilised for exploring the three research questions presented in Section 1.1. The tool is based on a modular design and features a sophisticated explicit conceptual design algorithm. TERA2020 considers a large number of disciplines typically encountered in conceptual design, such as: engine performance, engine aerodynamic and mechanical design, aircraft design and aerodynamic performance, emissions prediction and environmental impact, engine and airframe noise, as well as production, maintenance and direct operating costs. Individually developed modules are integrated together in an optimiser environment; a large amount of information is available after every design iteration and can be used for many purposes such as technology impact assessment, sensitivity and parametric studies and multi-objective optimisation.

In a nutshell, the work described in this thesis attempts to:

1. Present important aspects of the development of a sophisticated explicit algorithm that can help automate part of the aero engine conceptual design process.

2. Discuss the derivation of new models – and the further development of existing ones – that are suitable for optimising the novel engine configurations studied under the NEWAC project.

3. Present system numerical improvements with respect to improving computational speed, reducing non-convergence cases, and eliminating numerical noise problems hindering TERA2020 optimisation capability in the VITAL project.

4. Assess the impact of fluid modelling uncertainty on performance calculations and emissions predictions at aircraft system level and identify accuracy limitations in assessing novel engine core concepts as imposed by current practice in thermo-fluid modelling.

5. Quantify potential benefits from novel technologies for three low pressure spool turbofan architectures, as developed under the VITAL project.

6. Quantify potential benefits from the introduction of heat-exchanged cores with variable geometry features in future aero engine designs, as developed under the NEWAC project.

7. Quantify potential benefits from the introduction of novel lean-burn combustion technology, as developed under the NEWAC project, coupled with future novel aero engine designs.

1.4 Thesis overview

The main contents of this thesis have been organised in the following chapters:

- In Chapter 2, the developed aero engine conceptual design framework is presented.
- In Chapter 3, developments carried out by the author on individual TERA2020 modules are discussed.
- In Chapter 4, the impact of fluid modelling uncertainty on performance calculations and emissions predictions at aircraft system level is assessed. Accuracy limitations in assessing novel engine core concepts as imposed by current practice in thermo-fluid modelling are identified.
- In Chapter 5, the potential benefits from various low pressure spool component advancements are presented, and the impact of failing to deliver specific component technologies is quantified, in terms of power plant noise and CO_2 emissions.
- In Chapter 6, an assessment of various novel engine core technologies and concepts coupled with lean-burn combustion concepts is presented.
- In Chapter 7, various aspects are presented of an intercooled core and conventional core turbofan engine optimisation procedure using TERA2020. A back-to-back comparison between the two engine configurations is performed and fuel optimal designs for year 2020 entry into service are proposed.
- In Chapter 8, overall conclusions are drawn from the work carried out and recommendations for future work are made.

Additional information to support the work carried out for this project is presented in the following appendices:

- In Appendix A, various aspects of project management, quality control and dissemination reflecting the development of a multi-disciplinary conceptual design tool within a collaborative environment are discussed.
- In Appendix B, information is given in spreadsheet format on the choice of design variables for the optimisation process described in Chapter 7.
- In Appendix C, some of the component characteristics used with the newly developed performance code are presented.

Chapter 2

Framework Development

Various aspects of the development of a multi-disciplinary aero engine conceptual design tool, TERA2020 (Techno-economic, Environmental and Risk Assessment for 2020), are described - as carried out under the umbrella of European Framework 6 and 7 collaborative projects VITAL, NEWAC and DREAM. The tool can assist in the transition from the traditional, human-based design procedure to a partially-automated process, and considers the following disciplines: engine performance, engine aerodynamic and mechanical design, aircraft design and performance, emissions prediction and environmental impact, engine and airframe noise, and production, maintenance and direct operating costs. The proposed explicit conceptual design algorithm minimises internal iterations, reduces system complexity and improves computational speed; through a good set of constraints, it will also give an optimal aero engine conceptual design that will be feasible in terms of engine certification and customer requirements. As part of the project overall long term ambition, the continuous refinement of the TERA2020 algorithms is leading to an independent research tool that can help quantify risks and assess the impact of gas turbine design on the environment, by comparing and helping to rank future technologies and design concepts for civil aviation on a formal and consistent basis.

N.B. *The work presented in this chapter has been a collaborative effort between Cranfield University, Rolls-Royce and Chalmers University and has been published in the following paper:*

K.G. Kyprianidis, S.O.T. Ogaji, P. Pilidis, R. Singh, A.M. Rolt, and T. Grönstedt. Aero Engine Conceptual Design - Part I: Multi-Disciplinary Framework Development. *AIAA Journal of Propulsion and Power*, 2010. under preparation.

2.1 Introduction

2.1.1 Conceptual design tools - a brief review

The current state of the art in multidisciplinary engine simulation tools is represented by NASA's (National Aeronautics and Space Administration) extended suite of tools: NPSS (Numerical Propulsion System Simulation), WATE (Weight Analysis of Turbine Engines), FLOPS (FLight OPtimization System), and ANOPP (Aircraft Noise Prediction Program). As described by Claus et al. [9] and Lytle [10], NPSS can tackle different levels of modelling fidelity, from simple thermodynamic cycle calculations to full 3D whole-engine CFD (Computational Fluid Dynamics) simulations. WATE [11–13] is an object-oriented computer code that can been used to predict the dimensions and weight of different gas turbine engine configurations at component level, based on cycle parameters from NPSS. FLOPS [14] is an aircraft conceptual design code that can be used for aircraft sizing and mission analysis using information from WATE and NPSS. ANNOP [15] is an engine and airframe noise prediction code that can predict certification noise levels and noise power distance curves, based on aircraft dimensions from FLOPS and engine information from NPSS and WATE. Several successful attempts have been made to integrate these codes together and produce engine design results at aircraft system level; for some of the most recent efforts the interested reader can refer to Antoine et al. [16] and Mercer et al. [17].

The EDS (Environmental Design Space) tool is being developed collaboratively by The Georgia Institute of Technology and the Massachusetts Institute of Technology within PARTNER (Partnership for AiR Transportation Noise and Emissions Reduction) [18]. The tool consists essentially of an integration of the NPSS, WATE, FLOPS and ANNOP codes and various emissions predictions methodologies. EDS provides the capability to estimate source noise, exhaust emissions, and performance for potential future aircraft designs under different policy

and technological scenarios. FAA (Federal Aviation Administration) is currently sponsoring the development of ETS (Environmental Tool Suite), a larger suite of tools of which EDS is part of. The main aim of this effort is to conduct research, and develop, verify, and validate analytical tools to better understand the relationship between noise and emissions and different types of emissions, as well as to provide the cost benefit analysis capability necessary for data-driven decision making. ETS is intended to be used for supporting the FAA domestic analyses and ICAO CAEP (International Civil Aviation Organisation, Committee on Aviation Environmental Protection) analyses, and therefore decision making with respect to long term and global legislation [19].

Genesis is a gas turbine aerodynamic and mechanical design tool developed by Rolls-Royce; it can be used to define the basic engine geometry, as well as predict engine weight and cost using correlations based on a database of Rolls-Royce engines. A preliminary design process for military engines that utilises a hybrid combination of Genesis, RRAP (Rolls-Royce Aerothermal Performance) and other tools is presented in Jones et al. [20]. The tool developed can be used to quickly define and refine gas turbines engines within a design procedure that considers engine performance attributes as well as Through Life Costs (TLC).

MTU Aero Engines' software package for the preliminary design of airborne and stationary gas turbines, MOPEDS (MOdular Performance and Engine Design System), is described by Jeschke et al. [21]. The tool can perform multidisciplinary and multi-point analysis considering all major gas turbine engine components and their interrelations. The transition from the preliminary design phase to the detailed design phase is also handled by the system, with preliminary design results being transferred to higher fidelity 1D and 2D models for detailed component design.

The GISMO software, as described by Avellán and Grönstedt [22], is a generic simulation and modelling environment for conceptual design and analysis of aircraft and engines. Engine performance and weight predictions are first carried out with the GeSTPAn (General Stationary and Transient Propulsion Analysis) code [23], and the results are then transferred to the aircraft design modules for further analysis; this is an iterative process, with the engine and aircraft being redesigned in every loop, and is repeated until all the aircraft performance requirements set are satisfied.

The next three codes discussed cannot be considered as full conceptual design tools. Nevertheless, they do consider some important aspects of engine and aircraft conceptual design:

GasTurb [24] is a user-friendly gas turbine performance simulation code that can evaluate the thermodynamic cycle of a predefined set of engine architectures, both at design and off-design. Recent additions to the program allow the preliminary geometrical design of a gas turbine engine including disc stress calculations.

PIANO (Project Interactive ANalysis and Optimisation) [25] is a user-friendly aircraft preliminary design and analysis tool. It can be used to design and predict the performance of conventional aircraft configurations including emissions and costs.

GSP (Gas turbine Simulation Program) [26] is a flexible object-oriented tool for gas turbine engine performance analysis [27]. Additions to the code presented by Shakariyants et al. [28, 29] have extended the tool's capabilities to in-flight exhaust emission studies, while work by Montella and van Buijtenen [30] has allowed the evaluation of the impact of component design on engine overall performance.

2.1.2 Conceptual design tools - lessons learned

The aero engine industry is in constant search for more efficient and environmentally friendly power plants. Along with a continued progress in air traffic management, aircraft structures and aerodynamics, lighter and more efficient engines are being projected. Current and future engine noise and emission certification requirements make the search for optimal engines truly multidisciplinary. Decision making on optimal engine cycle selection has to consider mission fuel burned, operating cost, engine and airframe noise and environmental impact.

Each of the conceptual design tools presented in this brief review has its' merits and shortfalls. Unnecessary nested loops/iterations in the conceptual design algorithms are often encountered which increases system complexity and reduces computational speed while lack of code modularity - present in some of them - affects the system's maintainability and extendability. More importantly, most

codes fail to consider one or more important disciplines for engine conceptual design, which can severely hinder the degree of realism during design space exploration.

A Techno-economic, Environmental and Risk Assessment (TERA) approach during the conceptual and preliminary design process for complex mechanical systems will soon become the only affordable, and hence, feasible way of producing optimized and sound designs, if the whole spectrum of possible impacts (economic, environmental etc.) is to be taken into account. A tool following the TERA approach is required to conceive and assess engine designs with minimum environmental impact and lowest cost of ownership in a variety of emissions legislation scenarios, emissions taxation policies, fiscal and air traffic management environments. This chapter presents the development of a multi-disciplinary aero engine conceptual design tool that considers the following disciplines: engine performance, engine aerodynamic and mechanical design, aircraft design and performance, emissions prediction and environmental impact, engine and airframe noise, and production, maintenance and direct operating costs. The developed conceptual algorithm is explicit; it minimises internal iterations, reduces system complexity and improves computational speed.

2.2 The development of TERA2020

2.2.1 General objectives

Decision making on near term emissions legislation and taxation policies is usefully informed through industry studies, with respect to the impact certain legislator decisions could have on the design and operation of future civil aircraft engines. A TERA approach tool intends, mainly, to address policy evaluations at a "macro level" looking more at how long term and global legislation can be addressed. TERA2020 can therefore be viewed as a common tool which in the future, and through continuous refinement with input from legislators, operators, OEMs (Original Equipment Manufacturer) and universities, could enhance the dialogue between these parties by increasing the visibility of the impact of different policy issues on a consistent and formal basis.

Another potential benefit from the development of TERA2020 within the Eu-

ropean Union (EU), could be its contribution to enhanced European competitiveness on a global level. In the past, product design and manufacture has mostly been located in and driven by the markets and the legislative requirements of Europe, North America and Japan. These were also the markets where the majority of the sales occurred. The large growth in developing economies is changing the sales destination of civil aerospace products. Important proportions of the sales now take place in these emerging economies where different design solutions for good environmental performance may apply. A TERA approach tool would allow the exploration of economic and environmental performance of alternative design concepts and technologies. This could be done in a wide range of taxation regimes, helping to identify the more competitive options in local scenarios internationally.

The general objectives set during the development of the TERA2020 tool across the three European Framework 6 and 7 collaborative projects, VITAL (enVIronmenTALly friendly aero engines) [31], NEWAC (NEW Aero engine Core concepts) [32] and DREAM (valiDation of Radical Engine Architecture systeMs) [33] are:

- A quick assessment tool for new engine technologies.
- Assess the benefits of technologies under differing economic and environmental conditions.
- Optimise a group of engine technologies by relatively simple algorithms to differing economic and environmental scenarios.
- Progressively incorporate new and novel technologies.
- Provide initial starting points for engine designs for low economic and environmental impact that could be examined in depth by more complex and time consuming OEM tools.
- Evaluate and optimise the study engines against the project objectives.
- Progressively develop the capacity to become an independent research tool of choice for joint OEM ventures and provide useful information to project partners and important stakeholders.

The long term overall ambition is that the continuous refinement of TERA2020 algorithms will lead to an independent research tool that can help quantify risks and assess the impact of gas turbine design on the environment, by comparing and helping to rank future technologies and design concepts for civil aviation on a formal and consistent basis. TERA2020 will rely on the developers of new technologies providing data from realistic assessments of their capabilities and attributes, so that the tool can evaluate the costs and benefits at whole engine and whole aircraft level.

2.2.2 Origins of the TERA concept

Work in Cranfield University on the development and adaptation of TERA models for mechanical systems can be traced back to the early 90's. TERA-oriented developments to consider drag and weight were initiated by Vicente [34] in an attempt to study the effect of bypass ratio on commercial aero engines designed for long-range subsonic aircraft.

Around the same period, Dilosquer [35] initiated a study on the relationship between long range engines and atmospheric pollution. The full spectrum of this work [36–40], essentially took the TERA approach a step further by introducing the influence of environmental impact and flight routes, in aero engine design and analysis.

The research interest soon spread to industrial gas turbine systems. Gayraud [41] identified issues in gas turbine selection for power generation and attempted to address them through techno-economic assessments. His later work [42], focusing on more complex systems, set the base for a decision support system for combined cycle schemes.

During the further development of TERA for aero applications, environmental impact assessment continued to remain a key element, as described by Whellens and Singh [43]. Further work on genetic algorithms [44] introduced multidisciplinary optimization in the TERA armory of available tools and methods. These developments served as the foundation for demonstrating how a TERA approach could assist in the transition from the traditional, human-based conceptual design process to a more automated methodology [45].

The potential environmental benefits from the use of H_2 as an aviation fuel were studied extensively by Svensson [46]. His work served as the basis for introducing the capability of performing environmental impact assessments in the TERA tool [47].

Further work on power generation schemes was carried out by Papadopoulos [48] who investigated various thermodynamic cycles using the TERA approach. Work by Polyzakis [49] focused on a techno-economic evaluation of trigeneration plants i.e. gas turbine power generation combined with absorption cooling and district heating.

Studies by Laskaridis et al. [50, 51] on the potential of more-electric aircraft and engine architectures introduced a semi-generic aircraft model for use with the TERA tool. Tsoudis [52] worked on introducing an integrated computational marine vessel operation environment, tailored to realistically approach the life cycle operation of a marine gas turbine power plant, in a TERA version for marine applications.

Work by Khan et al. [53, 54] showcases how the TERA approach could be used for liquefied natural gas equipment selection. For more details on the TERA origins, current status and future developments the interested reader is referred to Ogaji et al. [55, 56].

2.2.3 Core partners and contributions

The core university partners involved in the development of the TERA2020 tool are:

- Cranfield University (CU)
- University of Stuttgart (USTUTT)
- Chalmers University (CHALMERS)
- ISAE/SUPAERO
- National Technical University of Athens (NTUA)
- Aristotle University of Thessaloniki (AUTH)

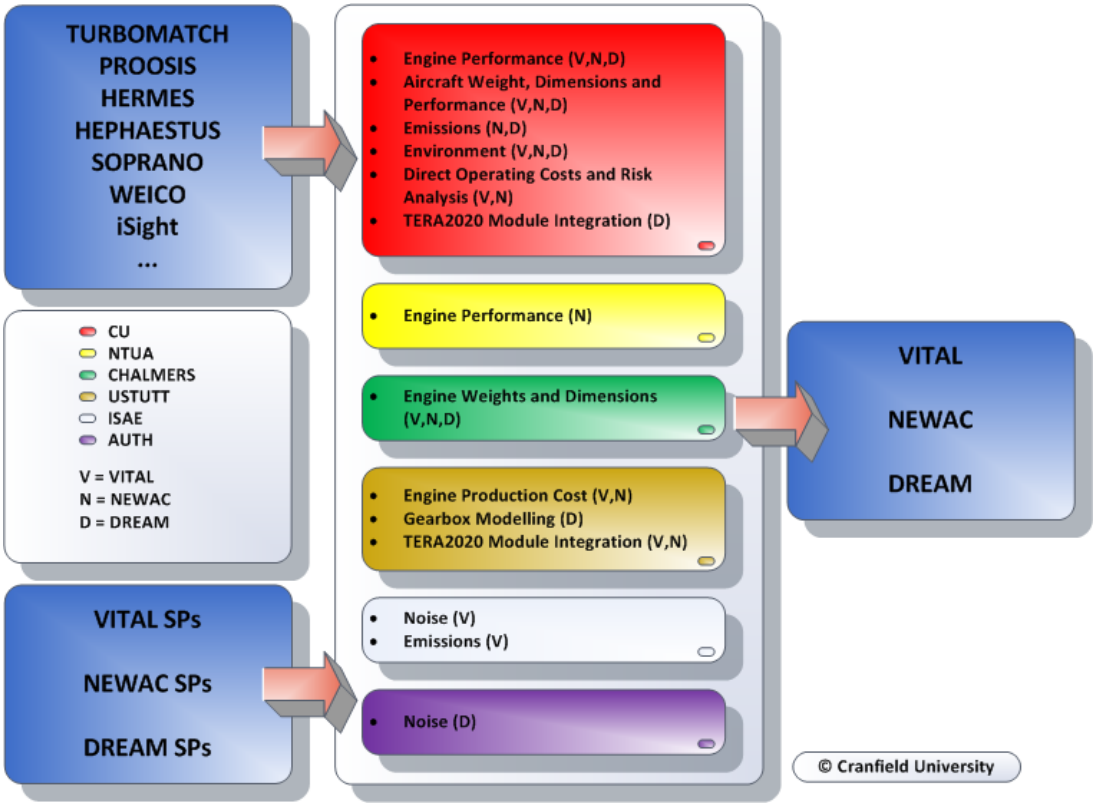

Figure 2.1: TERA2020 contributions.

- Universidad Politechnica de Madrid (UPM)

The contributions of the individual university partners to the development of the TERA2020 software are illustrated in Fig. 2.1. The development of the tool has been significantly influenced by several European OEMs, the latter providing important feedback to the university partners. The main OEMs involved in this process are:

- Rolls-Royce
- MTU Aero Engines
- Snecma
- Volvo Aero
- Rolls-Royce Deutschland
- AVIO

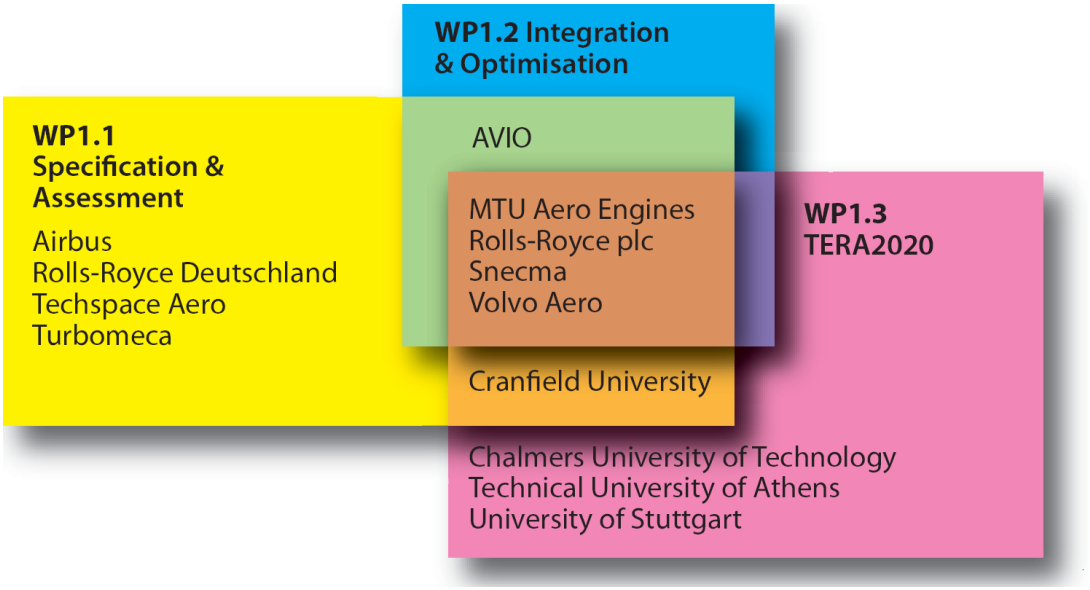

Figure 2.2: NEWAC SP1 partners [32].

- Turbomeca
- Airbus

Within NEWAC and it's Sub-Programme 1 (SP1), an assessment is carried out - at whole-engine and aircraft system level - of four novel engine designs that incorporate the new technologies researched in the other NEWAC SPs. As part of this effort, TERA2020 is used to assess the economic and environmental impact of these new technologies, and to undertake sensitivity and optimisation studies about the new engine configurations. A list of all the partners involved in NEWAC SP1, and an example of the interactions between the TERA2020 university partners and OEMs, are illustrated in Fig. 2.2.

2.3 TERA2020 conceptual design algorithm

2.3.1 Typical practice in preliminary and conceptual design

A typical industry approach is first to optimise an aircraft, or aircraft family, using generic engine data, and then to optimise the engine for a detailed set of

aircraft design requirements. The specification of this new engine starts with a set of thrust requirements, a basic design concept and initial estimates of the potential performance available from each major component and system. The next step is to construct design and off-design performance models. Major components are then sized and the gas path annulus is defined. Iterative design studies and assessments are then undertaken to refine the performance model and to complete a preliminary mechanical design for the engine. The nacelle lines can then be drawn and the overall powerplant weight and drag can be assessed [57]. More details on the preliminary design process are given by Halliwell [58], Kurzke [59] and Kyritsis and Pilidis [60].

This process relies on the experience of the preliminary design team to produce realistic physical and functional models. Each new engine design builds on ones that have gone before. When new or improved technologies are invoked they are initially modelled on the basis of target levels of performance and target space envelopes and weights. As the research activities raise the TRL (Technology Readiness Level) of each technology, so improved component efficiency estimates become available and can be used to refine the whole-engine models. In estimating effects at the whole aircraft level, exchange rates are initially used for the effects of changes in specific fuel consumption, engine weight and nacelle drag on the aircraft's takeoff weight and fuel burned [57].

2.3.2 The developed framework

TERA2020 is a software tool that helps to automate part of the aero engine design process. The tool spans typical aero engine conceptual design and preliminary design, featuring a sophisticated explicit modular design, as illustrated in Fig. 2.3, addressing major component design as well as aircraft system level performance.

Individually developed modules are integrated together in an optimiser environment; a large amount of information is available after every design iteration and can be used for many purposes such as technology impact assessment, sensitivity and parametric studies, multi-objective optimisation etc.

The selected modular design architecture leads to important system advantages such as:

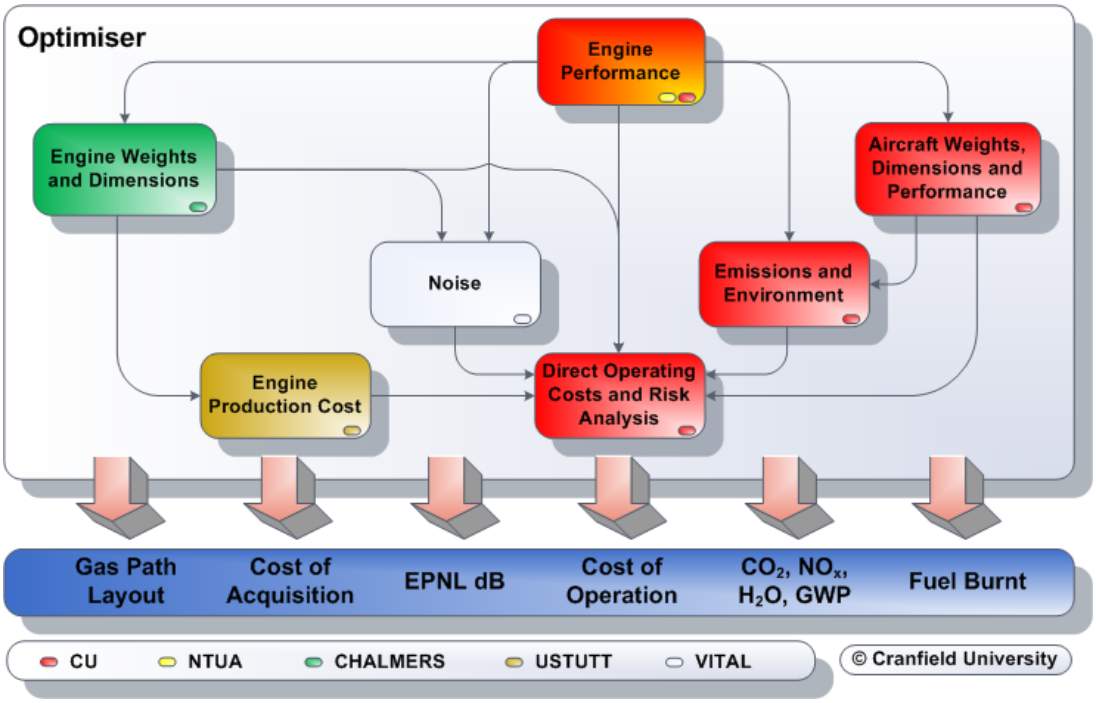

Figure 2.3: NEWAC TERA2020 modular structure.

- Accelerated tool development and lower maintenance cost - Improvements in an individual module are possible without modifications to the rest of the modules i.e. the whole system does not need to be recompiled every time.
- Legacy code utilisation - Existing codes can be used with TERA2020 with minimal to no adaptation through the use of custom wrappers.
- Module plug-in/plug-out capability - Individual modules can easily be replaced by more sophisticated OEM propriety codes.
- Run-time flexibility - Modules can be switched-off during particular simulations to improve the speed of execution, assuming their output is not of interest to the user.

Since VITAL, NEWAC and DREAM are engine technology development programmes, a different approach - than the typical practice described in the previous section - has been adopted in TERA2020 to simplify the conceptual design process. The TERA2020 algorithm first defines an engine thermodynamic cycle from a set of performance parameters, and then performs a full gas path layout

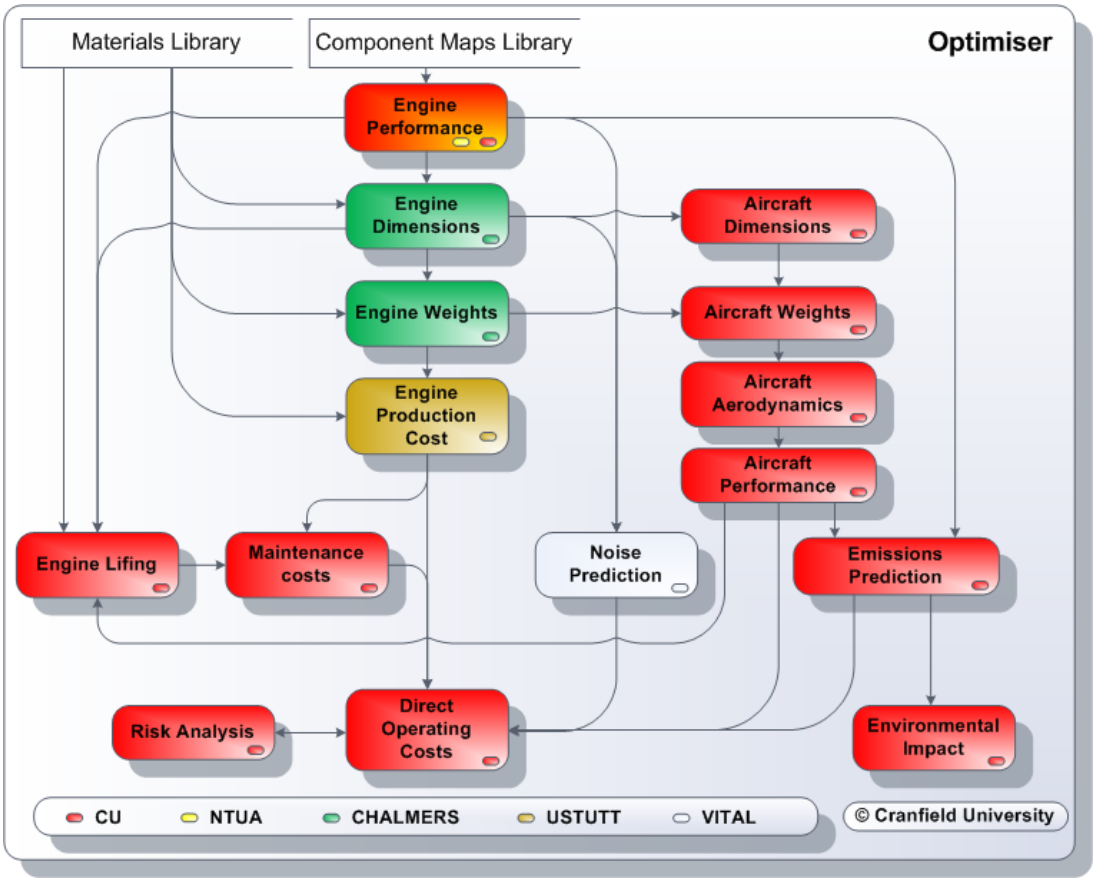

Figure 2.4: NEWAC TERA2020 conceptual design algorithm.

design. For every individual engine design, the aircraft is scaled (from a baseline design) to satisfy the defined payload-range requirement based on the new engine dimensions, weight and performance.

One of the major efforts with TERA2020 has been to remove - wherever possible - nested loops/iterations typically encountered in conventional conceptual design. **Use of the proposed explicit algorithm minimises internal iterations, reduces system complexity, improves computational speed, and through a good set of constraints it will also give an optimal aero engine conceptual design that will be feasible in terms of engine certification and customer requirements.**

TERA2020 is not an expert system; it is a tool that requires a user with some experience in engine preliminary design. The user needs to have a good understanding of engine performance and design, as well as sufficient knowledge of the capabilities of the technologies under assessment. Results can have meaningful

interpretations only when the underlying assumptions in the TERA algorithm are well understood by the user.

Architectural details of the TERA2020 tool, as originally developed for the VITAL project, are given in [61]. The TERA2020 conceptual design algorithm as developed for NEWAC is illustrated in Fig. 2.4, while details are given in the following paragraphs for each module.

2.3.3 The TERA2020 modules

2.3.3.1 Engine performance

As discussed earlier, the TERA2020 algorithm first starts by defining an engine thermodynamic cycle from a set of input performance parameters. During this procedure, the top of climb condition (Alt = 35000 [ft], M_{cr}, ISA +10 [K]) is set as the performance design point for the purpose of component map scaling and nozzle area calculations. The user may alter the engine cycle at top of climb by varying typical performance parameters such as fan pressure ratio, bypass ratio, overall pressure ratio, IPC/HPC (Intermediate Pressure Compressor / High Pressure Compressor) work split, combustor outlet temperature (T_4), cooling mass flow ratios, component efficiencies, heat exchanger effectiveness etc.

Climb, cruise and descent ratings are calculated as extended performance tables. Important engine operating conditions are also simulated as steady state off-design points, including:

- Hot day end of runway take-off (Sea-level, M = 0.25, ISA +15 [K])
- ICAO emissions certification take-off 100% F_N (ISA SLS)
- ICAO emissions certification climb-out 85% F_N (ISA SLS)
- ICAO emissions certification approach 30% F_N (ISA SLS)
- ICAO emissions certification idle 7% F_N (ISA SLS)
- ICAO noise certification sideline (Alt = 300 [m], M = 0.26, ISA +10 [K])
- ICAO noise certification cutback/flyover (Alt = 300 [m], M = 0.26, ISA +10 [K])

- ICAO noise certification approach (Alt = 118 [m], M = 0.222, ISA +10 [K])

For all these off-design operating points and ratings, the user may alter the main engine control parameter (T_4 or F_N) as well as any secondary control parameters such as low pressure turbine capacity, nozzle areas or intercooler effectiveness schedule for engines with variable geometry.

On principle, no iterations are performed for take-off and climb thrust requirements, or cooling mass flow and velocity ratio re-optimisation. Constraints for output parameters such as compressor delivery temperature, high pressure turbine rotor metal temperatures, or even time between overhaul (a value calculated in the lifing part of the economics module) are only set at the end of the TERA2020 calculation sequence.

2.3.3.2 Engine dimensions, weights and production cost

This module uses thermodynamic data from the engine performance module to perform a full gas path layout design. For the mechanical and aerodynamic design a component by component approach is used. The design procedure is carried out at the appropriate critical operating condition for each component; such conditions are typically hot day end of runway take-off and/or top of climb. The full engine geometry is subsequently used to calculate the total engine weight in a similar component by component approach.

The full engine geometry is also used for calculating the engine production cost using a bottom-up approach. The engine is broken down into components, and each component is consecutively broken down into smaller parts. The cost assessment for each part is further divided into material and manufacturing cost. The final result is an assumed typical engine and parts cost to the operator, rather than the true unit cost.

2.3.3.3 Aircraft dimensions, weights, aerodynamics and performance

The purpose of this module is to scale the aircraft to the new engine design and predict the block fuel for the given payload-range requirements. It uses the climb, cruise and descent rating extended performance tables, as well as additional

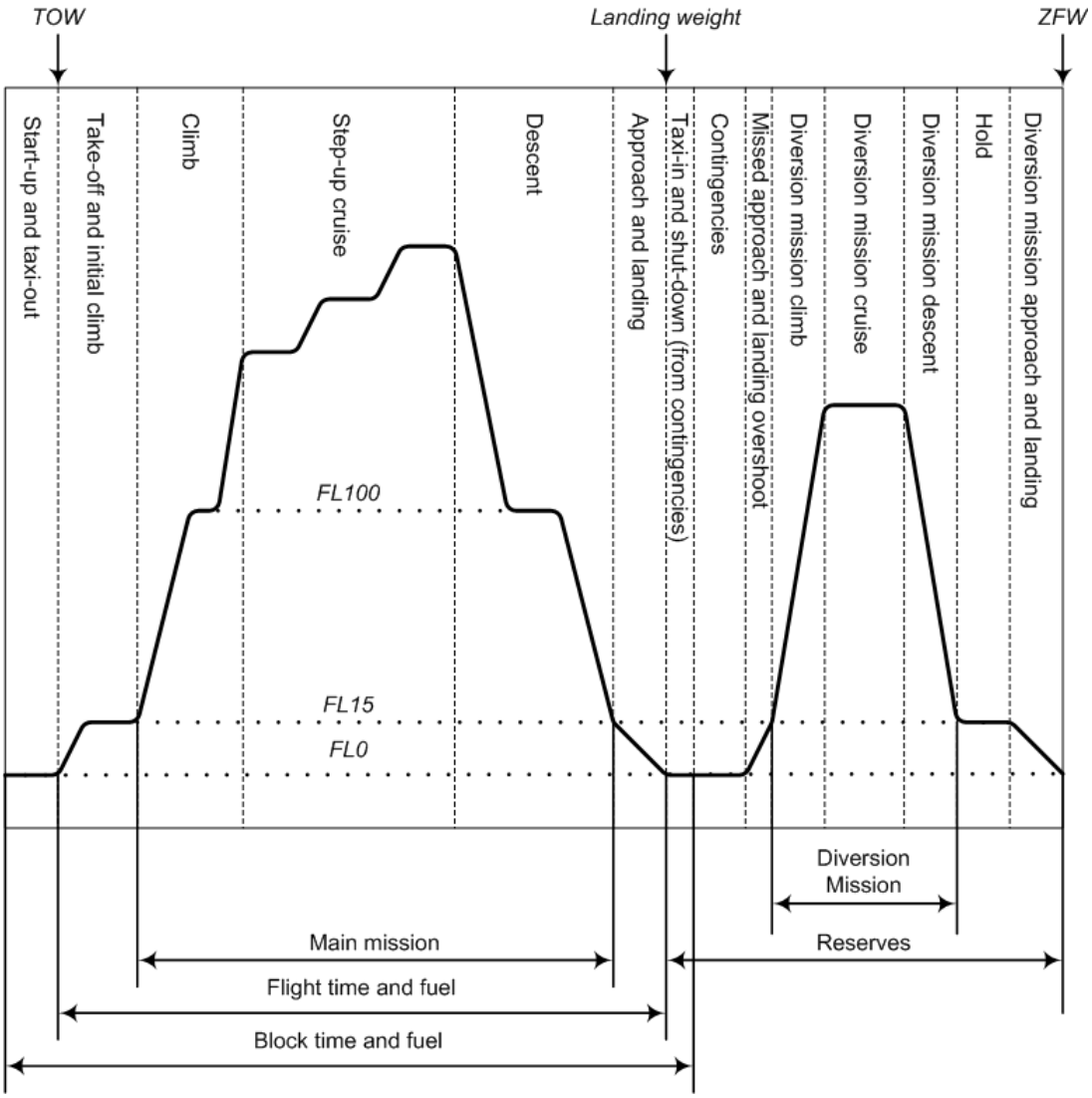

Figure 2.5: NEWAC TERA2020 typical flight cycle.

performance data for take-off, approach and landing, taxi and hold. The engine weight and dimensions, calculated upstream in the TERA2020 sequence, are also considered.

The aircraft drag polar and weight breakdown are predicted at component level from the aircraft geometry and high lift device settings for the take-off and approach phases. Fuel burned is calculated for the entire flight mission profile, including reserves, according to the requirements defined for international flights by FAA [62] and JAA (Joint Aviation Authorities) [63], as illustrated in Fig. 2.5. Cruise is performed at the optimum altitude for specific range (fixed cruise Mach

number) using a step-up cruise procedure as the aircraft gets lighter. A comprehensive take-off field length calculation is performed for all engines operating and one engine inoperative conditions up to 1500 [ft].

During design space exploration a rubberised[1] aircraft wing model is used to capture "snowball effects" with respect to maximum take-off weight variation. It offers a simplified method for aircraft scaling, that covers the major aircraft/engine conceptual design interactions i.e. first order effects. The given aircraft configuration is adapted, on a constant wing loading and aspect ratio criterion, in order to suit the new engine design (i.e. performance, weight and geometry) as well as to satisfy the defined payload-range requirements. Once the aircraft geometry has been set for the aircraft design range, a second set of fuel burned calculations is performed for the business range with the aircraft geometry fixed this time. All aircraft performance data fed to the modules downstream in the TERA sequence are for the business range.

As the aircraft gets lighter during the flight mission profile, less thrust is required for cruise; therefore the engine will gradually be operated at a lower T_4. A lighter, smaller and more efficient engine means that the aircraft will be lighter to begin with, resulting in a lower maximum take-off weight design requirement. The aircraft wing will therefore be resized to meet the new lift requirements while the tail plane is also resized to retain aircraft stability. Changing the aircraft wing and tail area essentially means that their weight will change, hence, the overall aircraft operating empty weight will change (first snowball effect). It also means that the drag polar will change (second snowball effect). The weight of other components also changes in some cases; for example the landing gear systems will be resized using the new maximum take-off weight design requirement. The fuel tank volume is recalculated for the new wing size and a check is made to confirm that the fuel tank volume is sufficient for the given mission. The overall aircraft scaling procedure eventually results in lower cruise thrust and T_4 requirements. In conclusion, the required cruise thrust, T_4 and specific fuel consumption will not only vary during the cruise phase to account for the aircraft getting lighter - due to the mass of fuel consumed - but will also vary for every new individual engine design during the design space exploration.

It is therefore hard to set a fixed mid-cruise point for which consistent analysis

[1]Rubberised refers to an aircraft geometry and weight that is optimised to meet the performance specification of the integrated engine.

could be performed for the entire design space - this being a typical approach used in conceptual design with fixed aircraft geometry assumption. For example, for a 12500 [km] design range mission, the cruise calculation is broken into more than 800 segments/points. The mid-cruise point could in this case be selected to be the middle point in the distance covered during cruise, but then care should be taken in analysing it's variations (in terms of thrust, specific fuel consumption, and T_4 requirements) as one would have to keep in mind that it's not only affected by engine performance effects but by aircraft design as well. Also care would need to be taken during optimisation since this selection could result in numerical noise every time the middle point coincides with a step-up cruise altitude change. To avoid potential numerical unsmoothness issues, when single point mid-cruise analysis is required, TERA2020 considers a time-averaged engine cruise operating point which is based on the scaled aircraft actual performance results.

On principle, no iterations are performed for take-off and climb thrust requirements. Constraints for output parameters such as FAR (Federal Aviation Regulations) take-off field length, time to height etc. are only set at the end of the TERA2020 calculation sequence.

2.3.3.4 Emissions and environmental impact

This module uses thermodynamic data from the engine performance module to predict the emissions levels for the ICAO LTO (Landing and Take-Off) cycle, as well as interpolated thermodynamic data from the aircraft module, for the business case mission, to predict the emissions levels for the entire flight profile.

The D_pNO_x/F_{oo} figure is calculated and compared against ICAO Annex 16 Volume II legislative limits [64], as well as the medium and long term technology goals set by CAEP [65]. A large number of public domain semi-empirical correlations are available in the module, each of which being suitable for a particular combustor concept such as rich burn single annular, rich burn dual-annular, or lean burn design.

The environmental impact of the engine/aircraft combination is predicted using the NO_x, CO_2 and H_2O(g) emissions estimates for the entire business case flight profile. The environmental impact is predicted in terms of global warming potential, based on a parametric model with a selected time horizon of 100 years [47]

- rather than employing a sophisticated 3D climate model.

2.3.3.5 Noise

This module uses thermodynamic data from the engine performance module, detailed engine component geometry from the engine dimensions and weights module, and aircraft geometry and flap settings during take-off and approach. These data are used for calculating the noise produced, by all major sources, for the main ICAO noise certification points i.e sideline, flyover/cutback, and approach. The trajectory points as well as the relevant times required to reach each point, are fixed, and therefore improvements in aircraft take-off performance are not accounted for. Heat exchanger, auxiliary nozzle effects and combustion noise for lean burning concepts are not considered, but airframe noise is accounted.

A cumulative EPNL (Effective Perceived Noise Level) figure is calculated according to the ICAO Annex 16 certification procedures and compared against the certification limits [66]. The resulting margin is fed to the optimiser and at the end of the calculation procedure the design will be judged for its feasibility.

2.3.3.6 Economics

This module calculates the DOC (Direct Operating Costs) for the engine/aircraft combination over a given time period using a large amount of data from all upstream modules in the TERA2020 sequence. Various elements can be accounted for including:

- Aircraft utilisation times
- Inflation
- Fuel price volatility
- Lifing considerations
- Noise, CO_2 and NO_x taxes

The maintenance part of the DOC depends mainly on production cost and time between overhaul calculations. Time between overhaul calculations involve a

high pressure turbine stress, creep and fatigue analysis using material information from the TERA2020 common material properties library and the component geometry as designed upstream in the TERA sequence; cooling effectiveness, thermal barrier coating effects, and average T_{41} values for take-off, cruise, climb, descent, and reverse-thrust operation are considered. Weibull distributions are utilised to account for the uncertainty of other engine components failing, including the high pressure compressor, combustor, and life-limited parts.

The module can also perform risk analysis, to account for uncertainty in various input parameters, but this is an extremely time consuming process. This potential capability of TERA2020 is currently reserved for single engine designs, since it cannot yet be fully exploited for design space exploration because the code executes too slowly. This capability is expected to be further explored in future TERA2020 projects and eventually lead to the removal of the current TERA2020 deterministic analysis limitation and allow for robust design.

2.3.4 Engine design feasibility and optimisation

In order to speed up the execution of individual engine designs, TERA2020 attempts to minimise internal iterations in the calculation sequence through the use of the explicit algorithm described in the previous sections. Aero-engine designs however are subject to a large number of constraints and these need to be considered during conceptual design.

Constraints in TERA2020 are applied through the optimiser environment procedures at the end of the calculation sequence i.e. after the the economics module has been executed. During a numerical optimisation TERA2020 will select a new set of input design parameters for every iteration and the resulting combination of aircraft and engine will be assessed. Using user specified objective functions the optimiser will home in on the best engines, determining the acceptability/feasibility of each engine design through the constraints set by the user. Infeasible designs will be ruled out, while non-optimum design values will result in engine designs with non-optimum values for the objective function selected. The optimiser will therefore avoid regions in the design pool that result in infeasible or non-optimum engine designs.

Design constraints set by the user can include among others:

- Take-off T_{30} and other important performance parameters.
- FAR take-off field length for all engines operating and balanced field length for one engine inoperative conditions.
- Time to height.
- LTO D_pNO_x/F_{oo} vs. ICAO certification limits and CAEP medium and long term goals.
- Cumulative EPNL vs. ICAO certification limits.
- Engine time between overhaul.

For example, during a block fuel optimisation all engine aircraft combinations which do not fulfil the take-off and time to height criteria set will be ignored as infeasible. Due to the underlying physics of the TERA2020 system, this will lead to an optimum engine and aircraft combination for the defined objective function. All large engines will produce heavier aircraft with more drag and thus higher block fuel weight. Engines which are too small will not deliver enough thrust to satisfy the take-off and time to height criteria.

2.4 Conclusion

The research effort presented in this chapter focused on various aspects of the development of a multi-disciplinary aero engine conceptual design tool for assessing the impact of technology advancements on future turbofan engine emissions and direct operating costs. Firstly, a brief review of some conceptual design tools was carried out and the merits and shortfalls of such tools were discussed. The development of a new conceptual design tool, TERA2020, was presented; this work was based on lessons learned from previous efforts and considered the following disciplines: engine performance, engine aerodynamic and mechanical design, aircraft design and performance, emissions prediction and environmental impact, engine and airframe noise, and production, maintenance and direct operating costs.

The main findings can be summarised as follows:

- From the conceptual design tools reviewed, most codes failed to consider one or more important disciplines for engine conceptual design, which can severely hinder the degree of realism during design space exploration.. Unnecessary nested loops/iterations in the conceptual design algorithms were often encountered which increased system complexity and reduced computational speed, while lack of code modularity - present in some of them - affected the system's maintainability and extendability.
- To conceive and assess engines with minimum environmental impact and lowest cost of ownership in a variety of emission legislation scenarios, emissions taxation policies, fiscal and air traffic management environments, a Techno-economic, Environmental and Risk Assessment (TERA) approach tool is required.
- The new tool developed, TERA2020, can assist in the transition from the traditional, human-based aero engine conceptual design procedure to a partially-automated process.
- The proposed explicit conceptual design algorithm minimises internal iterations, reduces system complexity and improves computational speed; through a good set of constraints, such an algorithm will give an optimal aero engine conceptual design that will be feasible in terms of engine certification and customer requirements.

As part of the project overall long term ambition, the continuous refinement of the TERA2020 algorithms is leading to an independent research tool that can help quantify risks and assess the impact of gas turbine design on the environment, by comparing and helping to rank future technologies and design concepts for civil aviation on a formal and consistent basis.

2.5 Outlook

Various aspects of the development of a multi-disciplinary aero engine conceptual design tool, TERA2020, have been discussed in this chapter. In the next chapter, details will be given on developments carried out on individual TERA2020 modules by the author. A brief description of TERA2020 modules developed by other project partners will also provided.

Chapter 3

Module Development

In this chapter, details are given on developments carried out on individual TERA2020 (Techno-economic, Environmental and Risk Assessment for 2020) modules by the author; this includes the derivation of a semi-empirical NO_x correlation for modern rich-burn single-annular combustors. A brief description of TERA2020 modules developed by other project partners is also provided.

N.B. *Parts of the work presented in this chapter have been a collaborative effort between Cranfield University and Aristotle University of Thessaloniki and have been published in the following papers:*

> K.G. Kyprianidis and A.I. Kalfas. Dynamic Performance Investigations of a Turbojet Engine using a Cross-Application Visual Oriented Platform. *RAeS The Aeronautical Journal*, 112(1129):161-169, March 2008.
>
> K.G. Kyprianidis, R.F. Colmenares Quintero, D.S. Pascovici, S.O.T. Ogaji, P. Pilidis, and A.I. Kalfas. EVA - A Tool for EnVironmental Assessment of Novel Propulsion Cycles. In *ASME TURBO EXPO 2008 Proceedings, GT-2008-50602*, Berlin, Germany, June 2008.

3.1 Engine performance

This section provides a brief review of existing gas turbine performance codes, and discusses various aspects of the development of a performance code tailored to meet the needs of the TERA2020 tool.

3.1.1 Gas turbine performance codes - a brief review

In the past four decades many gas turbine performance simulation programs have been developed. During this period, these programs have evolved from simple engine specific performance codes to complex object-oriented generalized performance tools capable of simulating arbitrary engine configurations.

The first static generalised code known to the author, GENENG/GENENG II, was developed at the NASA (National Aeronautics and Space Administration) Lewis Research Center in the United States by Koening and Fishbach [67,68] and was tested on several engine cycles. The code could simulate the design point and off-design performance of turbofan engines with two or three streams and up to three spools, and turbojet engines with one or two spools. Novel features in the program for obtaining sub-derivatives of these configurations essentially provided the user with the capability of simulating variable cycle engines.

At Cranfield University in Britain, another static generalized simulation program, TURBOMATCH, was developed by MacMillan [69]. Based on the TURBOMATCH scheme, Palmer and Cheng-Zong [70] developed the generalized simulation code TURBOTRANS. Owing to its modular structure the code was capable of simulating the dynamic behavior of arbitrary gas turbine engines with arbitrary control systems. The term arbitrary refers to radically new, non-standard, engine configurations, and can be used for example in the case of a gas turbine engine with four different control systems; including the main fuel flow, the afterburner fuel flow, the bypass ratio and the nozzle control systems.

In The Netherlands, NLR's (Nationaal Lucht- en Ruimtevaartlaboratorium) need for a generalized simulation program with a graphical user interface resulted in the development of GSP (Gas turbine Simulation Program) [26,27,71]. The software uses a friendly object-oriented environment that makes it quite flexible in terms of adapting to the specific needs that arise with new projects. It was orig-

inally developed at the Delft Technical University based on NASA's DYNGEN code [72].

At Chalmers University of Technology in Sweden, Grönstedt [23, 73] used a pseudo object-oriented approach in developing GeSTPAn (General Stationary and Transient Propulsion Analysis), a generalized simulation program capable of predicting the steady state and transient performance of virtually any practical aero engine configuration.

A study by Drummond et al. [74] of NASA revealed the need for abandoning older methods and moving on to the development of object-oriented simulation programs. The argumentation behind this transition is based on the fact that the development of a new engine design is strongly linked to the development of each engine component. Therefore, the need for linking various computational tools together grows stronger as new engine designs become increasingly more complicated. To ease integration efforts, new tools should be developed using object-oriented languages based on a common framework.

NASA's generalized simulation program NPSS (Numerical Propulsion System Simulation) [9, 10] is based on the NCP (National Cycle Program) architectural framework and forms the current state of the art in gas turbine performance simulation. The NCP program provides the object-oriented platform necessary for linking different computational tools together [75].

PROOSIS (PRopulsion Object Oriented SImulation Software) [76–78] is a flexible and extensible object-oriented gas turbine performance simulation environment developed by a consortium of European universities, research institutes and corporate companies. The tool features an advanced graphical user interface allowing for modular model building using either the standard or any custom library of engine components.

3.1.2 Code development

While the cost of a personal computer and its accommodating hardware has decreased significantly since its first appearance in the 1980's, this is not the case with simulation software. Software development costs have been increasing constantly and will continue to do so in the near future. High demands by users

for graphical user interfaces and generalized features, impede the development process and tend to lead to continuous modification of complex and expensive codes. Furthermore, in the case of legacy codes, the people capable of carrying out significant modifications are often limited to the original authors.

Developments in programming tools and software engineering methods have eased the process of creating new applications. Main examples of this trend are the new object oriented programming systems and visual development environments. Latest practice among new releases is the inclusion of an internal programming language within the main application and the possibility of linking to other applications and their programming environments through a common platform or architecture (also referred to as cross-application environments).

Several issues were encountered with the use of the TURBOMATCH code within the VITAL (enVIronmenTALly friendly aero engines) [31] and NEWAC (NEW Aero engine Core concepts) [32] projects, including:

- Insufficient modelling fidelity for several components with respect to the needs of the NEWAC project (fan, variable geometry turbine, intercooler, recuperator, variable geometry dual-nozzle, secondary air system and thermo-fluid model). Also the use of component characteristics is restricted mainly to a small hard-coded selection.
- Inflexible formulation of the mathematical model to be solved limiting the number of parameters that can be used to control the engine, and especially for configurations with variable geometry features.
- Convergence, numerical noise, and computational speed issues.

In order to resolve these issues and rigorously model the performance of the engine configurations studied within NEWAC, a semi-generic gas turbine performance simulation code was developed. The code has its roots in earlier work carried out by the author at Aristotle University of Thessaloniki (AUTH); the original source code was based on a cross-application visual-oriented platform and was successfully used for predicting the transient performance of a military turbojet engine [79, 80]. For the purposes of this project, the code was extensively modified in order to conform to object-orientation programming standards (inheritance, polymorphism, data binding etc.) as described in [81, 82], and partially conforms to international standards [83–87] with respect to nomenclature,

Figure 3.1: Engine performance model components.

interface, object oriented environment and standard performance methodology. The code was also extended with more rigorous models based on public domain information [6, 23, 69, 71, 88–93] for the following engine components: fan, compressor, secondary air system, variable geometry cooled turbine, variable geometry nozzle, intercooler, and recuperator.

Further improvements to the scheme focused on the development of a current state of the art numerical solver (described in Section 3.5) and a rigorous thermo-fluid model (described in Chapter 4). The former, significantly improved computational speed and reduced non-convergence cases, and essentially eliminated numerical noise problems. These three issues, formed an important bottleneck in the integration of TURBOMATCH within VITAL TERA2020. To further reduce non-convergence cases, the smoothness of all component maps was significantly improved using the commercially available tools SmoothC and SmoothT [94,95].

The developed code is capable of simulating the steady state and transient performance of arbitrary engine configurations assembled from the engine components illustrated in Fig. 3.1.

3.1.3 Engine models

3.1.3.1 Deck description

Within the NEWAC project, the developed performance code is used to generate TERA2020 compatible engine performance rubber decks for: i) the short and long range applications of the direct drive fan intercooled core configuration, ii) the long range application of the geared fan intercooled recuperated core configuration, and iii) the long range application of the baseline direct drive fan conventional core configuration. The developed engine performance models are illustrated in Fig. 3.2, Fig. 3.3, and Fig. 3.4, respectively.

For each configuration, two models are created; a design point cycle model and an off-design one. No component maps are used and no iterations are performed in the former; in the latter suitable component maps are used and a mathematical model needs to be set and solved.

The code initially carries out a design point calculation at top of climb conditions (Alt = 35000 [ft], M_{cr}, ISA +10 [K]) to determine the scaling factors for the different component maps and the cross sectional areas of the bypass and core nozzles - a dual-nozzle system is used for the heat-exchanged configurations. The various off-design points can then be simulated and all the necessary engine performance data required by other TERA modules are produced. More details about the off-design cases simulated have already been given in Section 2.3.3.1.

For defining a particular engine operating point, different parameters can be selected such as combustor outlet temperature, fuel flow rate, net thrust, and fan rotational speed. Variable geometry features in the Low Pressure Turbine (LPT) and the dual-nozzle system are addressed using secondary control parameters such as Variable Guide Vanes (VGV) angle and nozzle throat areas. Where the model's mathematical description is concerned, the necessary independent variables and residuals are selected automatically by the code. The user may intervene in this process and select the parameters manually but this is not a trivial task; wrong choices can lead to mathematical models that have multiple or even no solutions. Methods from the LISIS library are used for solving the mathematical model formed (i.e. system of non-linear equations) and these are discussed in detail in Section 3.5. An example of such a mathematical model is given in Table 3.1.

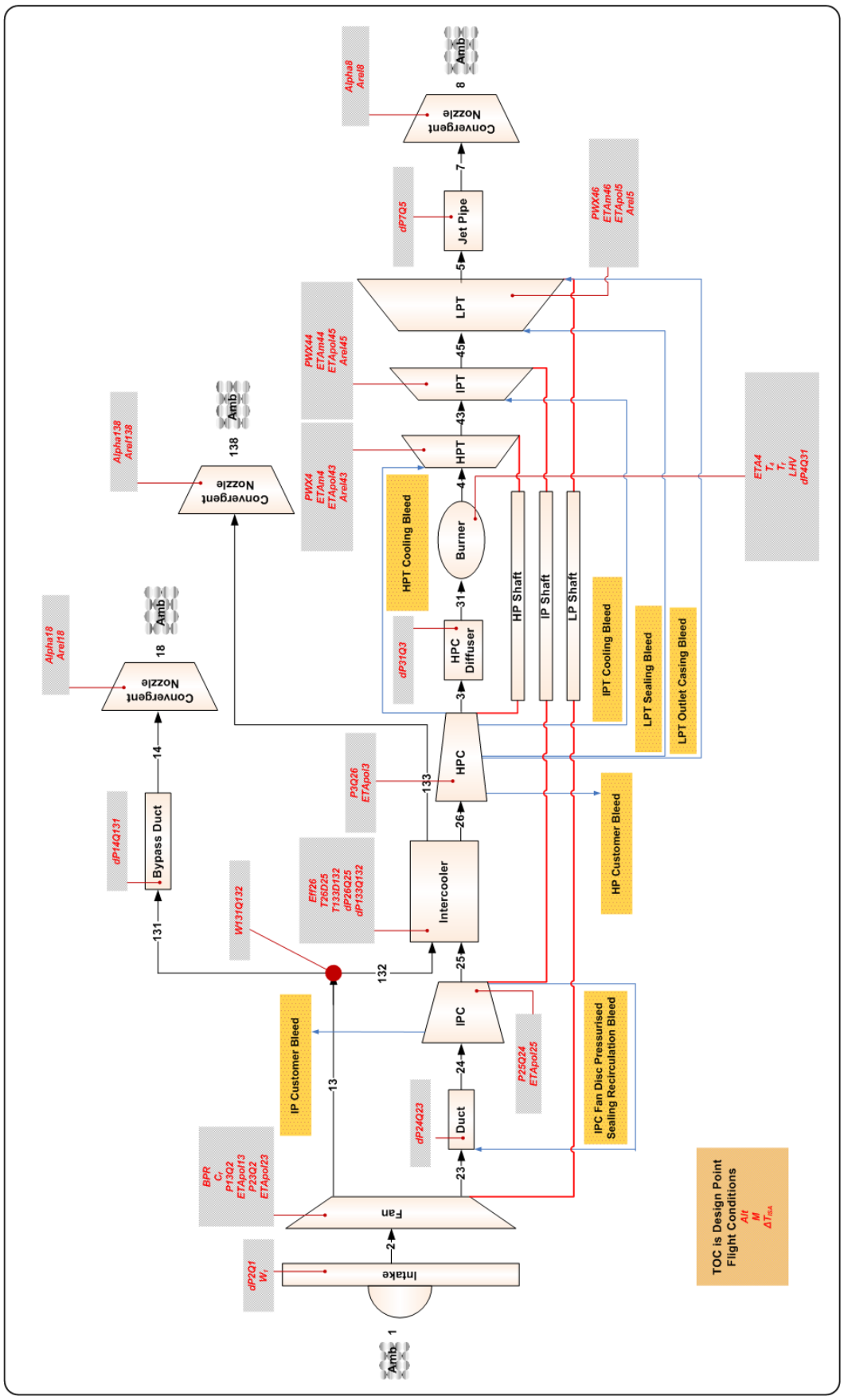

Figure 3.2: Intercooled core turbofan engine performance model.

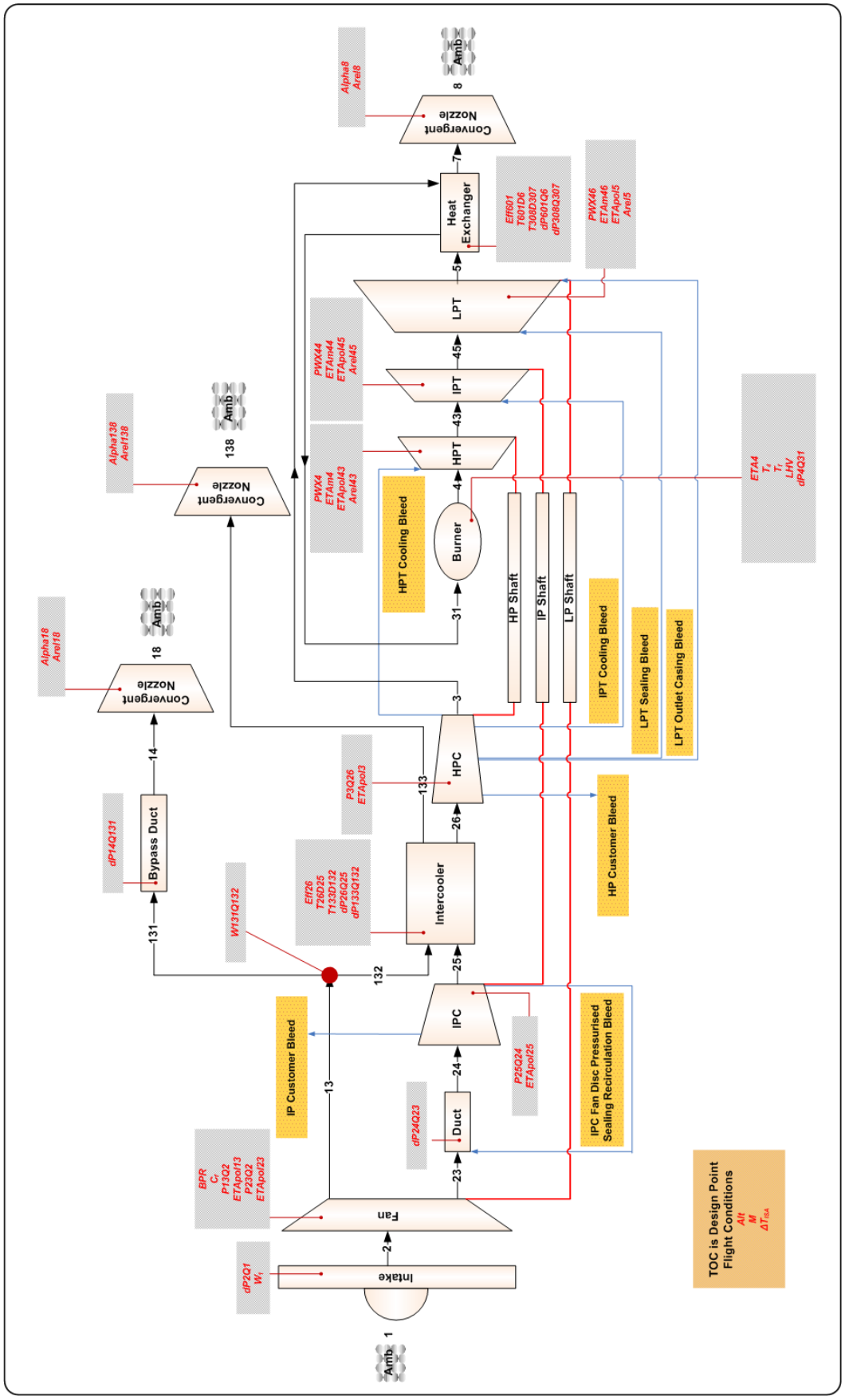

Figure 3.3: Intercooled recuperated core turbofan engine performance model.

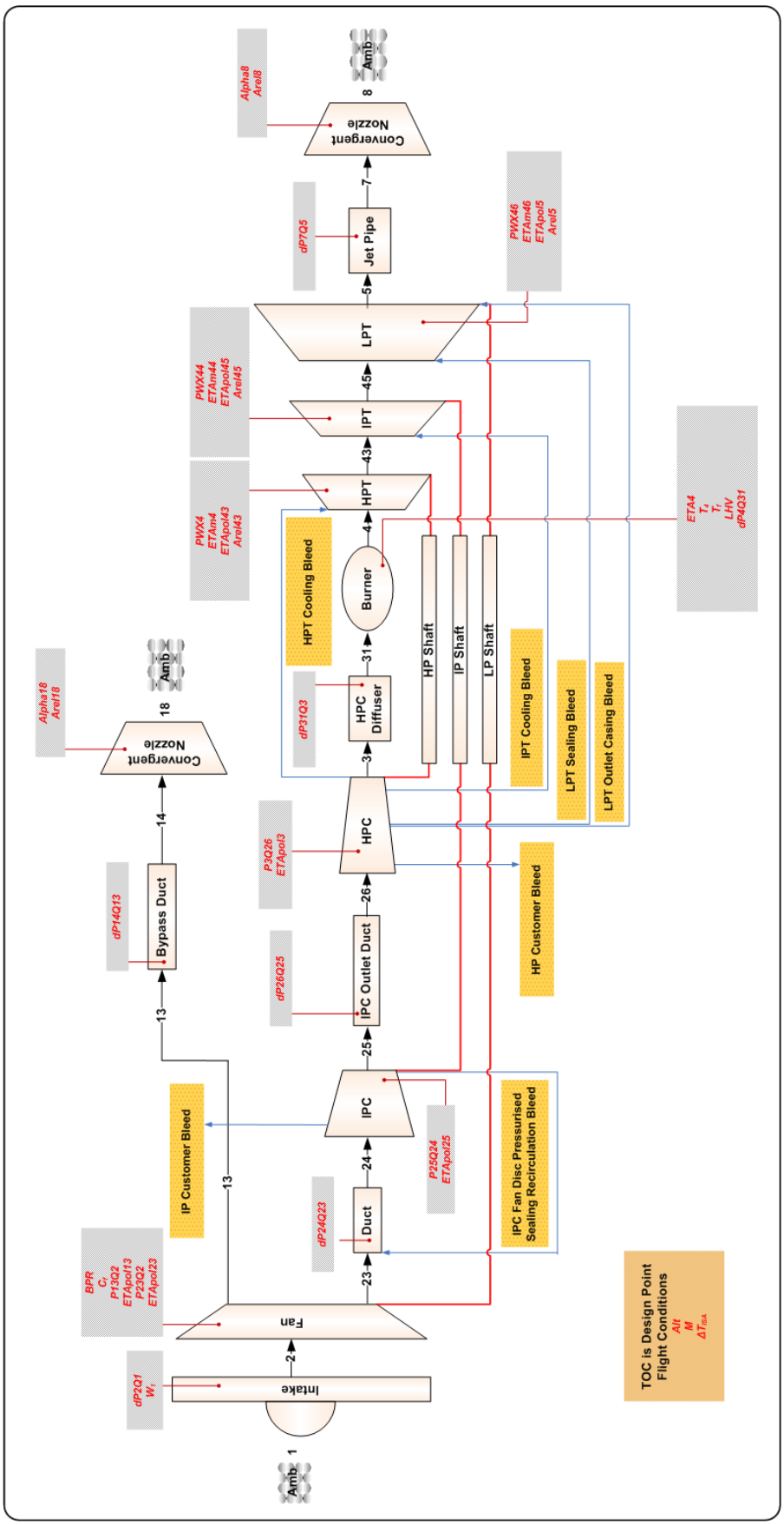

Figure 3.4: Conventional core turbofan engine performance model.

Table 3.1: Example of a mathematical model for an intercooled recuperated core turbofan engine with a variable geometry low pressure turbine and a variable geometry dual-nozzle system.

Engine component	Independent variable	Residual	Engine control parameter
Low pressure shaft	Rotational speed	Work balance	
Intermediate pressure shaft	Rotational speed	Work balance	
High pressure shaft	Rotational speed	Work balance	
Intake	Inlet corrected mass flow		
Fan	Root map beta	Root mass flow balance	
	Tip map beta	Tip mass flow balance	
	Bypass ratio		
Fan disc pressurised sealing bleed	Mass flow	Mass flow balance	
(recirculating flow)	Temperature	Temperature balance	
Intermediate pressure compressor	Map beta	Mass flow balance	
Intercooler		Effectiveness balance	Effectiveness
High pressure compressor	Map beta	Mass flow balance	
Burner	Outlet temperature		
High pressure turbine	Map beta	Mass flow balance	
Intermediate pressure turbine	Map beta	Mass flow balance	
Low pressure turbine	Map beta	Mass flow balance	Variable guide vane angle
Recuperator	Hot stream heat flux	Hot stream energy balance	
	Cold stream heat flux	Cold stream energy balance	
Core nozzle		Mass flow balance	
Intercooler splitter	Bypass ratio		
Bypass nozzle		Mass flow balance	Throat area
Intercooler nozzle	Throat area	Mass flow balance	
Performance monitor		Net thrust balance	Net thrust
Total	19	19	4

3.1.3.2 Component modelling

A brief description of the modelling carried out for each engine component is presented in this section. Only the features relevant to the engine configurations studied in this thesis are described. Some of the component characteristics used with the newly developed performance code are presented in Appendix C.

The thermo-fluid model used is discussed in detail in Chapter 4. The atmosphere component is used for calculating the ambient pressure and temperature for the given altitude and temperature difference from ISA (International Standard Atmosphere) conditions according to [96]. The intake component is used for calculating the free stream total conditions and momentum drag for a given value of flight Mach number and inlet mass flow. The outlet total pressure is then calculated assuming a certain level of pressure losses as a function of the flight Mach number [88].

In the fan component, separate characteristics are used for the fan root and fan tip. The calculations do not account for Reynolds number effects. However, the movement of the dividing streamline at deviating off-design bypass ratios is accounted for using the methodology described in [71]. Compressor characteristics are also used for the Intermediate Pressure Compressor (IPC) and High Pressure Compressor (HPC) components.

The pressure drop in the various duct components is expressed as a fraction of the component's inlet total pressure. The recirculating flow used for the fan disc pressurised sealing is simulated as a constant fraction of the IPC inlet mass flow. The IPC handling bleed flow is mixed with the main flow in the bypass duct component. This handling bleed is only required for the flight and ground idle operating points, as well as for approach. The required customer bleed flow may be extracted either from the IPC or the HPC component. The actual amount extracted varies with flight altitude.

The intercooler component is positioned between the IPC and the HPC. Intercooler effectiveness can be calculated at off-design using either the correlation presented in [88] or a scaled component characteristic; either temperature effectiveness or the standard textbook thermodynamic definition may be used. The pressure drop in the intercooler is specified as a fraction of the total pressure at the inlet of each stream, hot and cold. Both "hot" and "cold" pressure losses are

considered for each of the two streams.

The recuperator component is used for transferring heat from the LPT outlet to the combustor inlet. At off-design conditions the recuperator effectiveness is calculated using a scaled component characteristic. The pressure drop in the recuperator is specified as a fraction of the total pressure at the inlet of each stream, hot and cold. Both "hot" and "cold" pressure losses are considered for each of the two streams.

The High Pressure Turbine (HPT) cooling flow is extracted from the HPC outlet and only a part of it is consider to do work in the rotor; Nozzle Guide Vane (NGV) and blade cooling, as well as sealing requirements are considered. In the intercooled recuperated core turbofan engine configuration, the HPT cooling flow is extracted from the recuperator cold stream outlet; this practice improves the engine's Specific Fuel Consumption (SFC) since more energy can be recuperated for a given recuperator effectiveness level and despite the consequent increase in cooling air requirements [88, 97]. The Intermediate Pressure Turbine (IPT) cooling flow is extracted a bit earlier in the HPC compression process and only a part of it is consider to do work in the rotor; NGV and blade cooling, as well as sealing flow requirements are considered. The LPT sealing and outlet casing flows are extracted much earlier in the HPC compression process; a part of the former is consider to do work in the rotor.

For the burner component a correlation from [88] is used to estimate combustion efficiency based on combustor load and volume. The "can" volume is estimated at the design point from the correlation proposed in [88] assuming a typical load value for aero engine combustors. The pressure drop is expressed as a fraction of the component's inlet total pressure and both "hot" and "cold" pressure losses are considered.

For cooled turbines, the equivalent single stage efficiency definition is used in the expansion process modelling, as described in [92]. Turbine characteristics are used for the HPT, IPT, and LPT components. The fraction of the turbine cooling air that does work in the rotor is mixed with the turbine main inlet flow at the rotor inlet. The corrected mass flow values read from the turbine map correspond to this engine station. The fraction of the turbine cooling air that doesn't do work in the rotor is mixed at the outlet of the turbine rotor and is therefore not considered in the efficiency calculation. All calculations for cooling

effectiveness, rotor blade metal temperature, and cooling flow mixing pressure losses follow the approach described in [6].

Variable geometry features are considered in the LPT modelling for the intercooled recuperated core turbofan engine configuration. An efficiency penalty is applied when the VGV angle (and as a result the turbine capacity) is varied from the nominal setting. For the convergent nozzle components either constant values or component characteristics may be used for determining the discharge, thrust, and velocity coefficients. For the conventional core engine, fixed area nozzles are used for the core flow and the bypass flow. In the case of the intercooled core engine however, a variable geometry dual-nozzle system is used instead for modelling the expansion of the bypass and intercooler cold streams to ambient conditions. If required, the total nozzle throat area can be kept constant for all operating points in which case the dual-nozzle component tends to behave more like a variable area mixer in terms of performance. For the intercooled recuperated core engine, either a fixed area or a variable geometry dual-nozzle system can be used for the bypass and intercooler cold stream flows.

A fixed mechanical efficiency is assumed for the High Pressure (HP), Intermediate Pressure (IP), and Low Pressure (LP) shaft components. Power can be extracted from any off these shafts. For the year 2020 entry into service engine configurations studied in NEWAC, the assumption is made that all power is extracted from the IP shaft. For the year 2000 entry into service baseline engine set, the assumption is made that all power is extracted from the HP shaft.

3.1.3.3 Model validation

The performance models developed for the intercooled core and intercooled recuperated core turbofan engines, assuming a year 2020 entry into service technology, have been calibrated against information provided within the NEWAC project. For the intercooled recuperated core turbofan engine model for long range applications, deviations between model predictions and OEM (Original Equipment Manufacturer) specification are restricted for all performance parameters to roughly 2%. For the intercooled core turbofan engine model for long range applications, deviations between model predictions and OEM specification are also restricted for most major performance parameters to roughly 2%. For the short range applications version of this model deviations between model

predictions and OEM specification are restricted for all performance parameters to roughly 2% at top of climb and mid-cruise conditions, and to 4% at end of runway hot day take-off conditions.

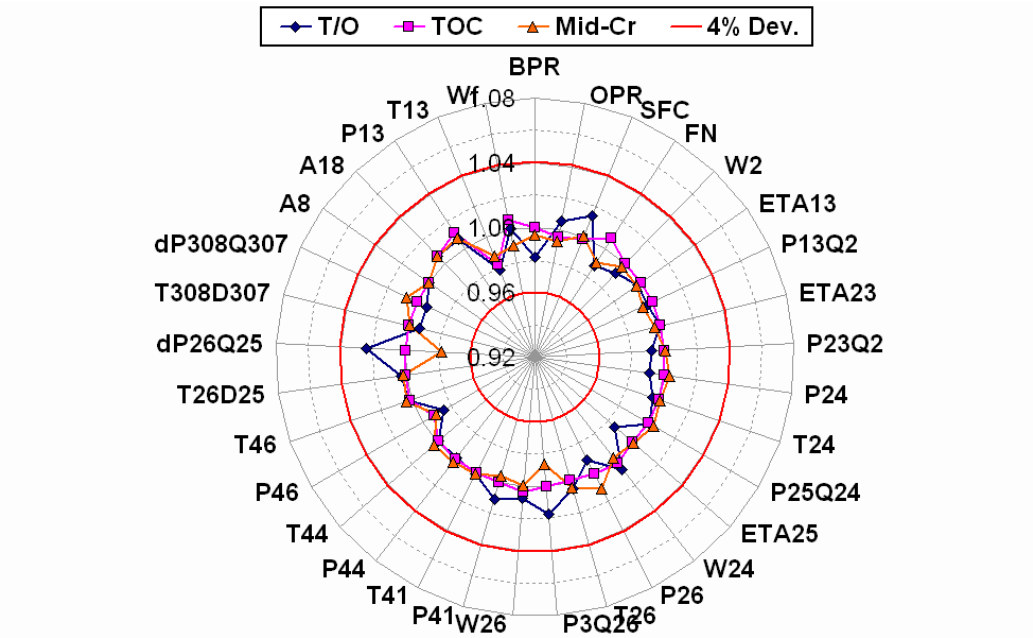

Figure 3.5: Deviations of TERA2020 performance model predictions from NEWAC specifications for the long range intercooled recuperated core turbofan engine.

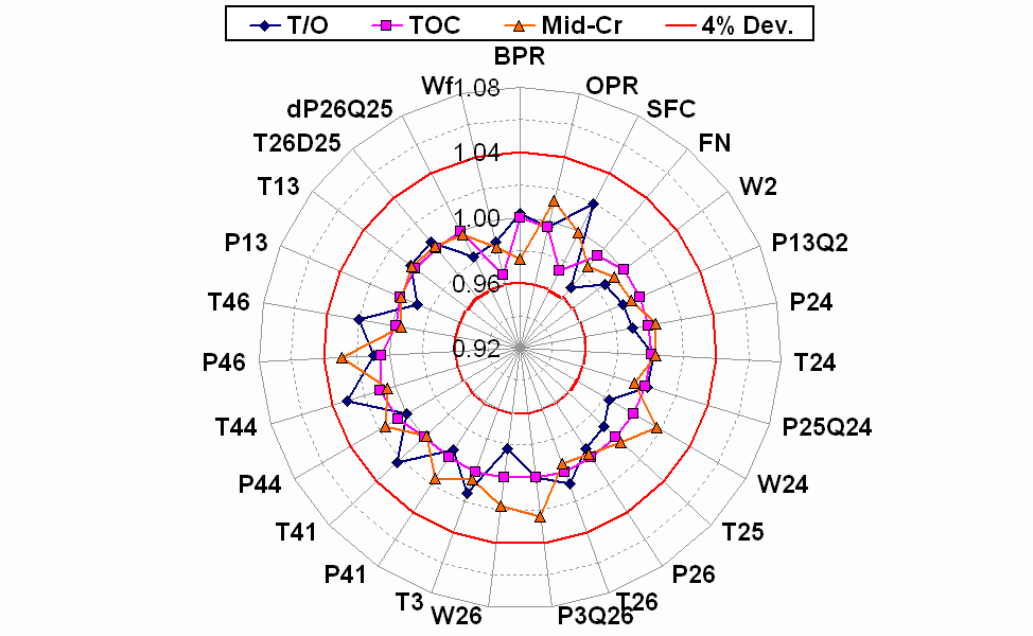

Figure 3.6: Deviations of TERA2020 performance model predictions from NEWAC specifications for the long range intercooled core turbofan engine.

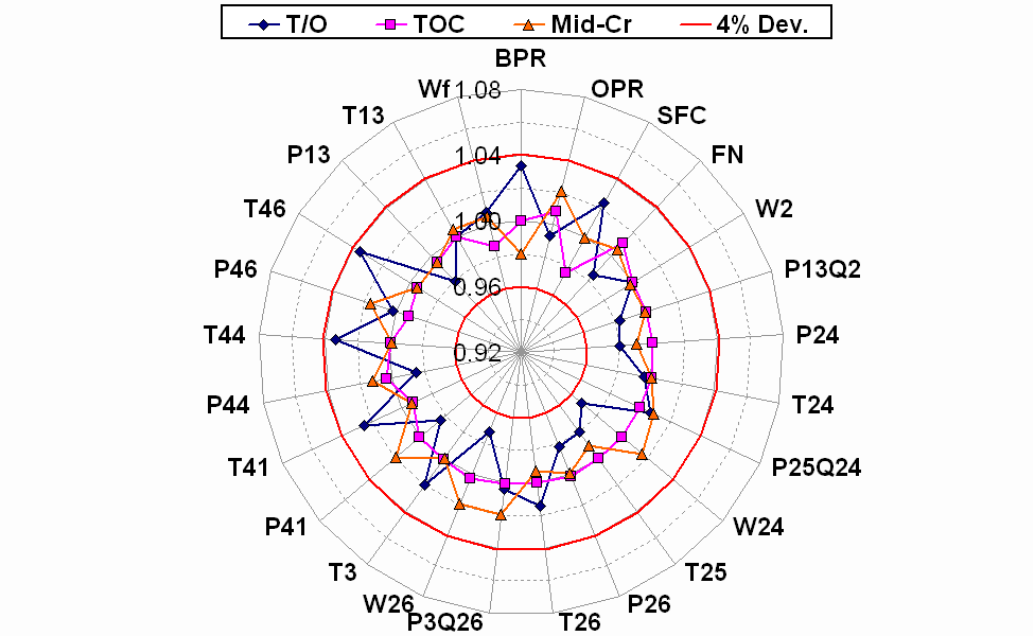

Figure 3.7: Deviations of TERA2020 performance model predictions from NEWAC specifications for the short range intercooled core turbofan engine.

3.2 HERMES

3.2.1 Introduction

HERMES is a software code developed by Cranfield University that has been integrated into TERA2020. It utilises a large amount of engine performance data as well as the engine weight and dimensions, all calculated upstream in the TERA2020 sequence, and can be used to:

- Scale a nominal aircraft configuration to fit a new engine design using a rubberised wing aircraft model that is based on first-order accuracy rules.
- Predict the block fuel for a given set of payload-range requirements for the entire flight mission including reserves.
- Predict important performance parameters used for aircraft and engine design, such as time to height and take-off field length for all engines operative and one engine inoperative conditions.

Details on the use of HERMES within NEWAC TERA2020 have been given already in Chapter 2.

3.2.2 Code modifications

The code is based on work carried out by Laskaridis et al. [50, 51] on the prediction of aircraft performance; the aircraft modelling is largely based on the work presented in [98, 99]. For the needs of NEWAC TERA2020, the author had to perform a full reconstruction of HERMES. Major code modifications include:

- Overhaul of the entire code including defragmentation, addition of object-oriented structures and scientific units control.
- Complexity reduction step with respect to I/O operations.
- Addition of aircraft component weight calculation routines to improve the rubberised wing aircraft model.

- Addition of a fuel tank volume calculation routine.
- Step-up cruise procedures can now be performed, via a switch, at the optimum altitude (fixed cruise Mach number) for minimum specific fuel consumption, maximum lift to drag ratio, or maximum specific range.
- Introduction of full diversion mission calculations.
- Modelling accuracy improvements for climb and descent calculations.
- Updated calibration of baseline long range and short range aircraft models for NEWAC.
- Isolation of physics from mathematics through a new aircraft model formulation; the new aircraft model is formed as a system of non-linear equations compared to the previous version that was based on a nested-loops scheme.
- The aircraft model is now solved using routines from the LISIS library (see Section 3.5).
- Three different calculation modes are now available: design, business case, and parametric study. Furthermore, range can now be calculated for a given fuel load.

As a result of these modifications, the code's accuracy and robustness has improved significantly, while all numerical noise issues previously encountered have essentially been eliminated. Computational speed has improved by more than two orders of magnitude and can now be considered almost negligible compared to the execution times of other TERA2020 modules.

In the previous HERMES version, the step-up cruise procedure was performed at optimum cruise altitude for maximum lift to drag ratio. The addition of new options for cruise optimal altitude selection is illustrated in Fig. 3.8. The default option used now in HERMES is maximum specific range which yields the best aircraft performance in terms of minimising block fuel.

The parametric study calculation mode can be used to perform a variety of tasks. An example of utilising this HERMES option for performing transport efficiency studies is demonstrated in Fig.3.9. As illustrated, fuel burn in [lt/(km*pax)], and therefore CO_2 emissions (in [kg/(km*pax)]), are lower at a given technology level for aircraft designed to carry a larger number of passengers for smaller distances.

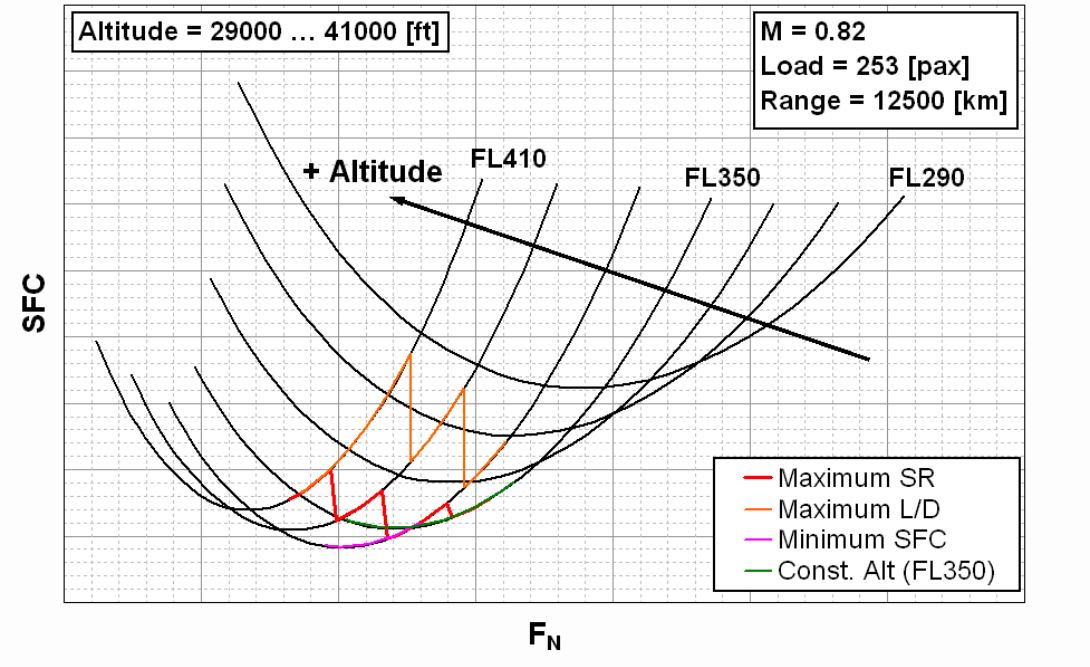

Figure 3.8: Step-up cruise procedure with HERMES and the use of different objectives for optimal altitude selection.

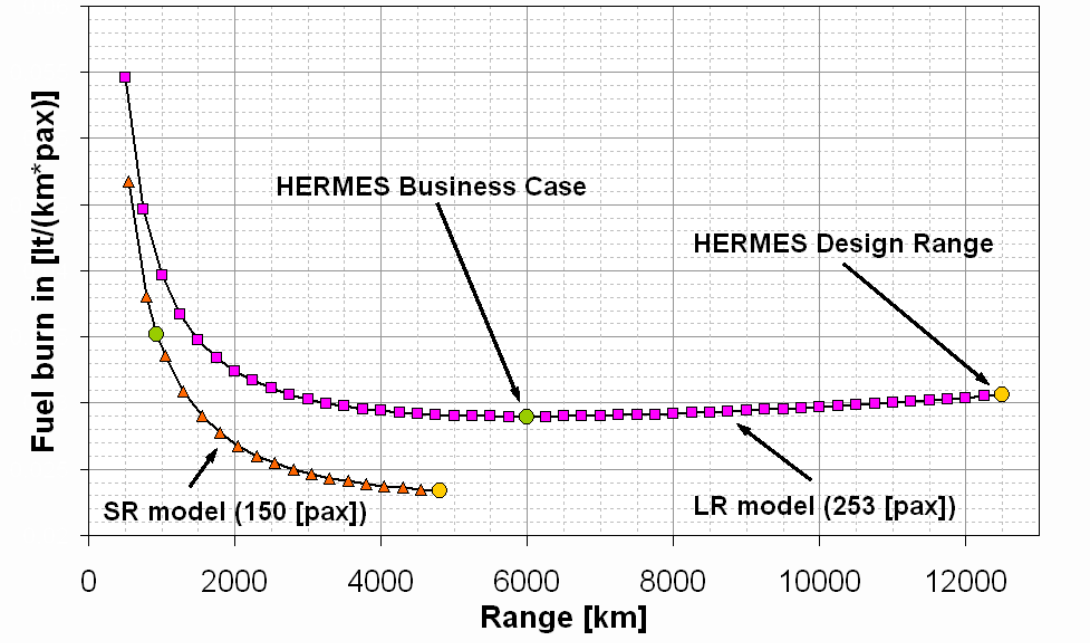

Figure 3.9: Transport efficiency studies with HERMES.

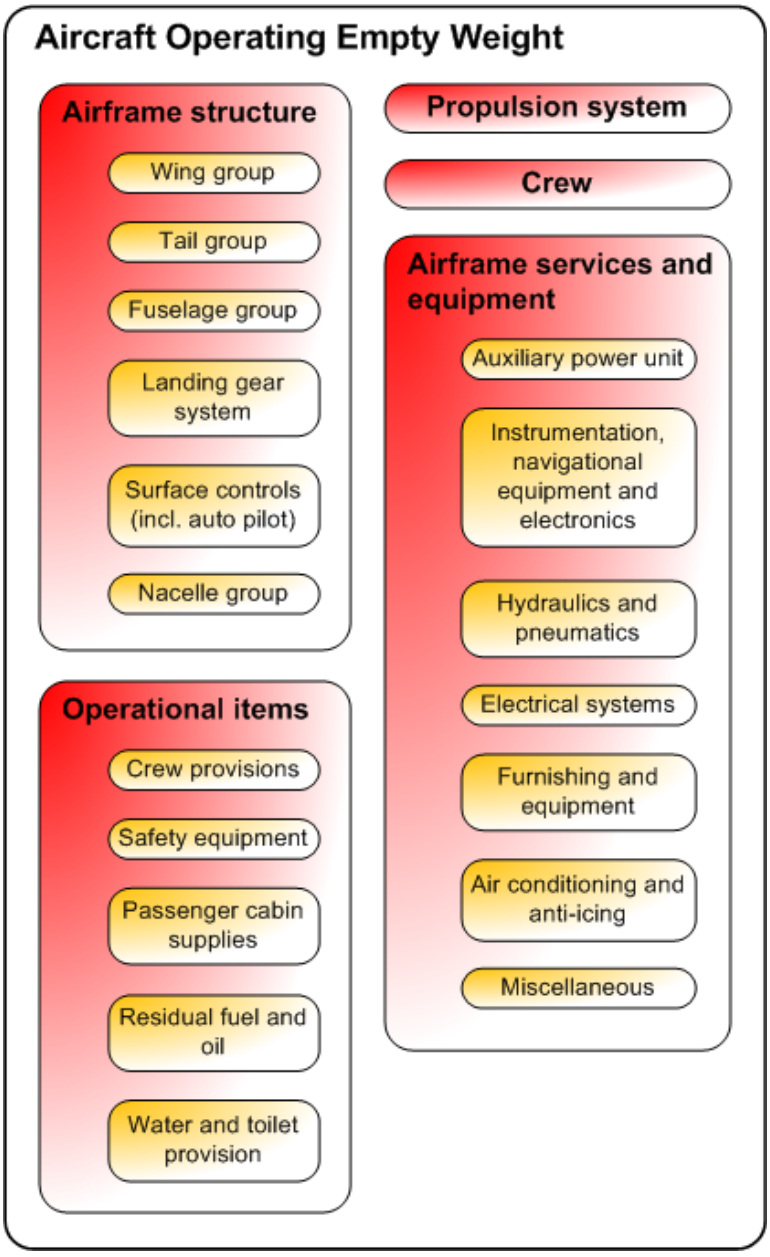

Figure 3.10: HERMES aircraft weight calculation breakdown.

Finally, the main weight groups considered in the aircraft weight calculations carried out by HERMES are illustrated in Fig. 3.10. Component weight calculations are largely based on the work presented by Torenbeek [100] and Roskam [101,102].

3.2.3 Exchange rates

Two baseline aircraft models are in use in NEWAC TERA2020; one model for long range applications and one for short range. The former model is largely based on public domain information available for the Airbus A330-200 and is designed to carry 253 [pax] for a distance of 12500 [km]. The latter model is largely based on public domain information available for the Airbus A320-200 and is designed to carry 150 [pax] for a distance of 4800 [km].

Block fuel predictions made with HERMES assume a load factor of unity and no cargo. This is by no means a typical airline practice, and validating absolute block fuel predictions with public domain airline data is not a trivial task as different airlines will follow different operational practices. For example for the long range aircraft model, the HERMES business case prediction is 10% lower than the published annually-averaged value, given in [lt/(km*pax)], by SwissAir for 2009 for the Airbus A330-200 [103]. This does not necessarily mean that the HERMES business case is not a realistic one; nor that it wouldn't fit well with operational practices followed by other airlines. Furthermore, regional Air Traffic Management (ATM) practices can skew available block fuel data, while global ATM regulations may very well change significantly by 2020. It should be noted that fuel planning in HERMES respects the requirements defined for international flights by FAA [62] and JAA (Joint Aviation Authorities) [63].

Table 3.2: Block fuel exchange rates using the HERMES baseline long range and short range rubberised wing aircraft models.

	Exchange rate	
Perturbation	LR	SR
1000 [kg] weight penalty	0.73%	1.26%
+1% SFC	1.28%	1.09%

Where conceptual design is concerned, exchange rates are perhaps a better type of parameter for evaluating the accuracy of a rubberised wing model, rather than just simply comparing absolute values. Block fuel exchange rates produced with the HEMES rubberised wing aircraft models are presented in Table 3.2 for the business case (assumed 5500 [km] for the long range model and 925 [km] for the short range model) and are considered reasonable numbers [104]. When looking at these figures, it should be kept in mind that HERMES will rescale some of the aircraft components after the 1000 [kg] weight penalty perturbation has been introduced in the model; the actual increase in aircraft operating empty weight will therefore be greater than 1000 [kg].

3.3 HEPHAESTUS

This section provides a brief review of existing emissions prediction and environmental impact models, and discusses various aspects of the development of HEPHAESTUS, an emissions and environmental impact prediction code tailored to meet the needs of the NEWAC TERA2020 tool.

3.3.1 Introduction to emissions modelling

As discussed in Chapter 1, public awareness and political concern on aviation induced pollution has improved substantially during the past 30 years; and so have the efforts to address the problem. Ref. [105] provides a good introduction to the impact of aviation induced emissions on the global atmosphere. A review on aero engine pollutant emissions, and some of the technologies currently under research for reducing them, is given by Wulff and Hourmouziadis [106]. For conceptual design of more environmental friendly aero engines with novel combustion technologies, the need rises for sufficiently accurate models for estimating pollutant emissions and their impact on the environment.

Prediction models of gaseous emissions for aero gas turbine combustors typically need to focus on the following pollutants: NO_x, CO, unburned hydrocarbons and smoke. Lefebvre [8] describes thoroughly the formation mechanisms for these pollutants, focusing on the influence of various parameters such as temperature and pressure. Combustion and emissions prediction models can be divided into the following categories [107]:

- Semi-empirical
- Phenomenological
- 3-D CRFD RANS (Computational Reactive Fluid Dynamics, Reynolds-Averaged NavierStokes equations)
- Direct Numerical Simulation (DNS)

It is evident that, although, direct numerical simulation is the most powerful of the above mentioned methods, the associated computational time and cost is

prohibitive. An additional disadvantage of all analytical methods is the requirement for a large amount of input data (i.e. boundary conditions) that are not always readily available. Semi-empirical models are well suited for conceptual design of novel engine concepts, since only a limited amount of data is usually available at the beginning of such projects. The latter constraint makes the implementation of the computationally more expensive phenomenological models (for example models based on stirred reactor networks), within TERA2020, a fairly challenging task. The author therefore argues:

> ***For a conceptual design tool like TERA2020, that combines different disciplines at a reduced level of modelling complexity, semi-empirical models pose as the best available choice.***

3.3.2 Semi-empirical correlations and P_3T_3 methods for NO_x

Over the years, a large amount of semi-empirical correlations have been proposed by several authors. These models assume that the amount of NO_x is dependent on the following three factors [8]:

- Mean residence time in the combustor
- Chemical reaction rates
- Mixing rates

A large amount of semi-empirical correlations may be found in the literature for different combustor designs. Mellor [108] provides good insight on semi-empirical correlations derived before the 1980's. Lefebvre [109] proposed a model suitable for conventional spray combustors, based on experimental data. Odgers and Kretschner [110], Malte et al. [111], Lewis [112], Rokke et al. [113], and Rizk and Mongia [114, 115] have all contributed semi-empirical models derived for industrial and aero gas turbine combustor designs. Becker and Perkavec [116], and Nicol et al. [117] provide an analytical review of various semi-empirical models

derived before the mid 1990's. Semi-empirical correlations for lean direct injection combustors calibrated with high pressure experimental data can be found in Tacina et al. [118] while earlier efforts are presented in [119]. For modern conventional aero engine combustors a large variety of semi-empirical correlations can be found in [120–122]. For more information on recent advances on the development of models as combustor design tools, reference should be made to Mongia [123].

The main disadvantage of all the above models is that they will only hold well for combustors designs of the same technology level as the original combustors that were used for deriving these correlations (via curve fitting of available experimental data). In certain occasions, though, sufficiently accurate predictions could be produced for other combustor designs if a limited amount of data is available; one would need to adapt the constants in these correlations in order to produce a good fit with the new data available [124]. On the other hand, when no experimental data are available for insight, these correlations may result in significantly inaccurate predictions.

ICAO maintains a large databank of $EINO_x$ measurements [125], taken at sea level static conditions according to ICAO Annex 16 engine emissions certification procedures [64]. For predicting emissions at altitude a variety of P_3T_3 methods may be used (also known as ratio or "reference" methods). Although also semi-empirical in nature, they are applicable to any conventional core turbofan engine for which reference NO_x data are available; these methods essentially correct ground level measurements to an altitude condition taking into account some, or all, of the following parameters:

- Combustor inlet temperature
- Combustor inlet pressure
- Combustor fuel to air ratio
- Combustor fuel mass flow
- Flight Mach number
- Specific humidity

The P_3T_3 method, discussed by Norman et al. [126], uses combustor inlet temperature and pressure, and FAR for correcting ground level measurements. Other similar methodologies include the Boeing2 fuel flow method [127, 128] and the DLR fuel flow method [129–131]. These methods take advantage of the fact that P_3 and T_3 effects can be well correlated with engine fuel flow and flight conditions, at least for turbofan engines without variable geometry; they can therefore be considered as variations of the "standard" P_3T_3 method. The main advantage of fuel flow methods, compared to the "standard" P_3T_3 method, lays with the fact that they don't require sensitive engine performance data. On the other hand, the "standard" P_3T_3 method can provide predictions that reflect better the influence of engine performance on NO_x emissions, in those cases where engine performance data are available. Existing fuel flow methods are not suitable for heat-exchanged core turbofan engines, with or without variable geometry, due to the different correlation of fuel flow and flight conditions with P_3 and T_3. Finally, all these methods ("standard" P_3T_3 and fuel flow) have one issue in common which forms their main limitation; they require $EINO_x$ measurement data at sea level static conditions to be used as reference. In those cases where reference measurement data are not available, for example during the conceptual design of a novel engine configuration, P_3T_3 methods are of limited use.

A large selection of public domain semi-empirical correlations and P_3T_3 methods, from the references discussed earlier, has been implemented in HEPHAESTUS. Each correlation is suitable for a particular combustor concept (and technology level) such as rich burn single annular, rich burn dual-annular, or lean burn design.

3.3.3 Derivation of a NO_x correlation for modern rich-burn single-annular combustors

To further enhance the NO_x predictions of HEPHAESTUS, a semi-empirical correlation was derived for modern rich-burn single annular combustor designs coupled with high OPR (Overall Pressure Ratio) cycles. The correlation is based on a large number of engine performance data produced with the Cranfield in-house library of engine performance models, and corresponding NO_x emissions measurement data from the ICAO engine emissions databank [125]. NO_x predictions produced with this correlation for a high OPR conventional core 2020 entry

Table 3.3: NO_x correlation constant and exponent default values for modern rich-burn single-annular combustor designs.

Parameter	Value
a	8.4
b	0.0209
c	0.0082
d	0.4
TF	0.0
f	19.0
$P_{31,ref}$ [kPa]	3000.0
$\Delta T_{comb,ref}$ [K]	300.0
Hum_{SL} [kg H_2O/kg dry air]	0.006344

into service turbofan engine have been verified internally within the NEWAC project [132].

The proposed NO_x correlation is described by the following equation:

$$\begin{aligned} EINO_x &= (a + b \cdot \exp(c \cdot T_{31})) \cdot \left(\frac{P_{31}}{P_{31,ref}}\right)^d \\ &\quad \cdot \exp(f \cdot (Hum_{SL} - Hum)) \\ &\quad \cdot \left(\frac{\Delta T_{comb}}{\Delta T_{comb,ref}}\right)^{TF} \end{aligned} \tag{3.1}$$

where P_{31} is in [kPa], T_{31} is in [K], Hum is in [kg H_2O/kg dry air], and ΔT_{comb} is in [K].

Default values for the constants and exponents in Eq. 3.1 are given in Table 3.3 and are suitable for modern civil aero engines currently in production coupled with rich-burn single-annular combustors, as illustrated in Fig. 3.11. These values are also suitable for a high OPR conventional core 2020 entry into service turbofan engine based on the assumption that no major leaps will occur in rich-burn technology over the next 10 years.

For very aggressive future cycles, with high combustor inlet temperature and low air to fuel ratio (AFR) values, the proposed correlation could very well be

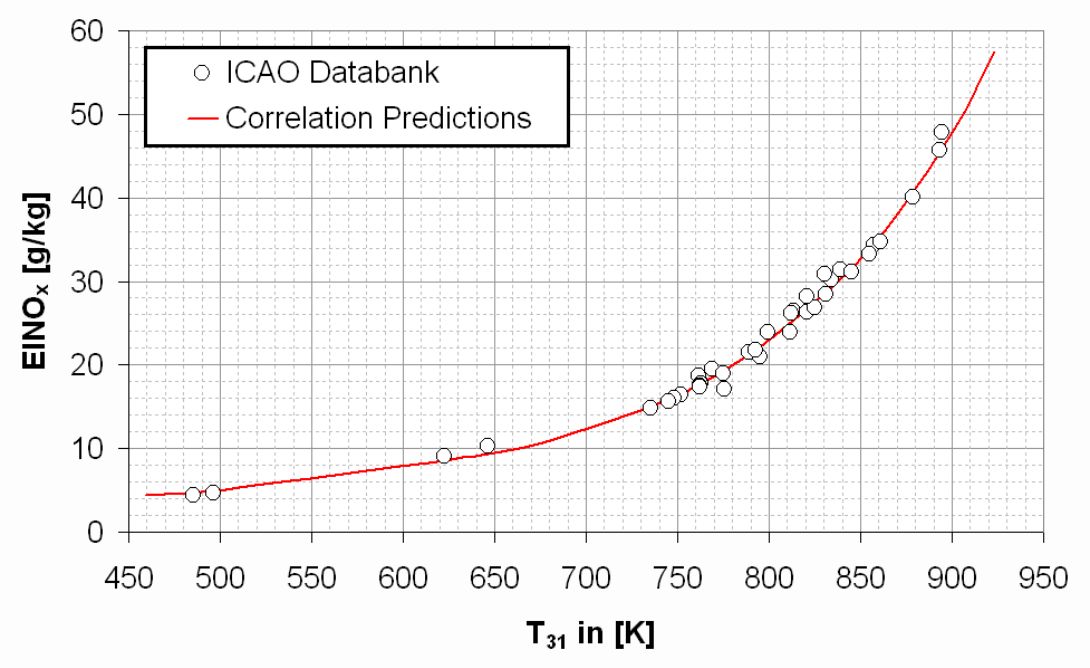

Figure 3.11: Modern rich-burn single-annular NO_x correlation fit to emissions measurement data from the ICAO databank [125].

underpredicting NO_x emission levels. Designing a conventional rich-burn single-annular combustor for such conditions could prove a challenging task, mainly due to the limitations imposed by the need for adequate combustor liner film-cooling air as well as maintaining an acceptable temperature traverse quality [8]. For such cycles, exponent *TF* may be used as a technology factor for matching either experimental data or results from higher fidelity NO_x prediction models, as illustrated in Fig. 3.12.

This procedure was successfully used to adapt the default correlation to available data for some of the more aggressive cycles studied under the NEWAC project. The deviation of the correlation predictions from available propriety data for the NEWAC engine configurations, and from public domain data for modern civil aero engines currently in production from the ICAO databank [125], is no more than 10% as demonstrated in Fig. 3.13. The accuracy of the correlation is therefore considered to be sufficient for the TERA2020 conceptual design studies.

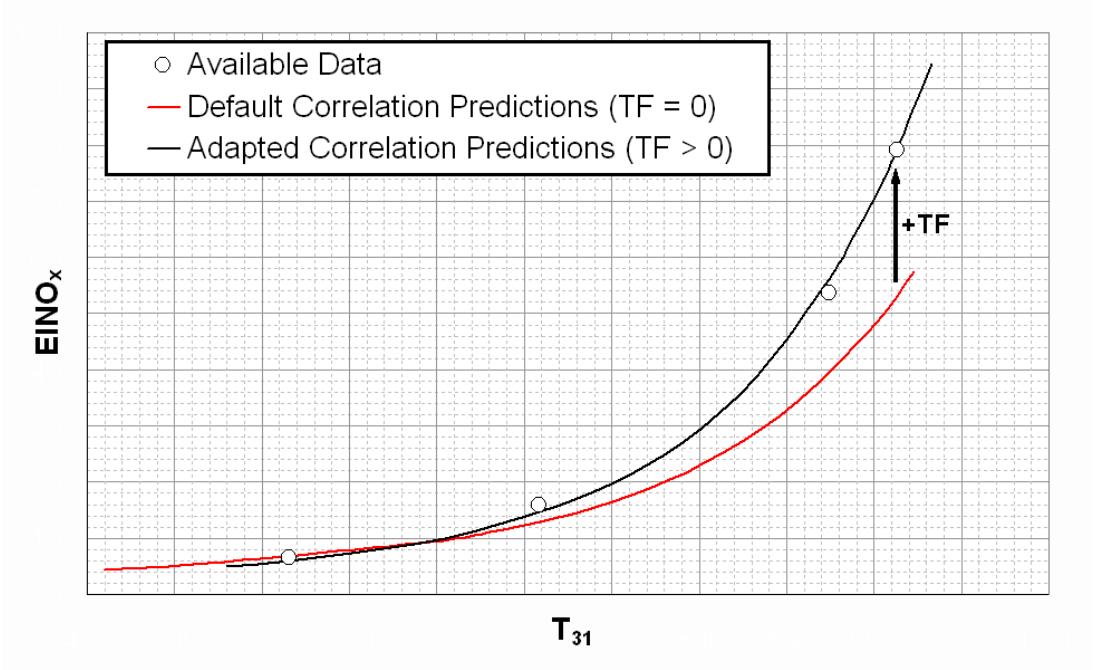

Figure 3.12: Example of using the technology factor to adapt the default correlation to available NO_x emissions data.

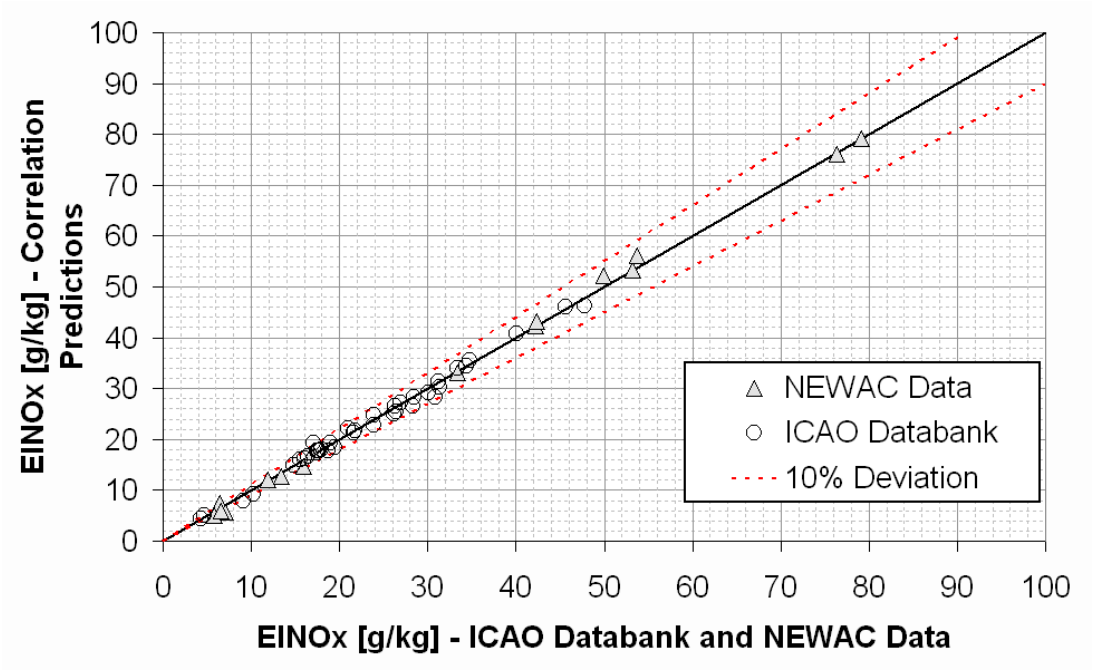

Figure 3.13: Deviation of correlation predictions from available NEWAC data and public domain data from the ICAO databank [125].

3.3.4 NO_x model for lean-burn combustion concepts

Within the NEWAC project, different lean-burn combustion concepts are being studied. Within the public domain, only a limited number of semi-empirical correlations for lean-burn combustor are available [118, 119]. These correlations were found to be unsuitable for predicting NO_x emissions from the NEWAC combustor designs mainly for two reasons:

- They have been based on data from experimental campaigns for lean-burn combustor designs that are very different from the designs studied under NEWAC; the latter designs are themselves very different from one another.
- They fail to properly consider the effects of the fuel flow split (between the pilot injectors and the main injectors) varying for different combustor operating conditions.

To further enhance the NO_x predictions of HEPHAESTUS, a new NO_x model for lean-burn combustion concepts was introduced based on information provided by Rolls-Royce Deutschland, Avio and Turbomeca within the NEWAC project. Some background information on lean-burn combustion and the NO_x modelling approach adopted for HEPHAESTUS, can be found in Segalman et al [133], Ripplinger et al. [134], Otten et al. [135], Plohr et al. [136] and Lazik et al. [137].

In the approach implemented, the combustor primary zone is first sized for cruise conditions to balance low NO_x emissions with a good combustion efficiency. This sizing exercise mainly involves calculating the primary zone AFR required to achieve a fixed flame temperature value; the latter is essentially a design parameter and the fixed value chosen is known - from experience and NEWAC experimental measurements - to provide a reasonable trade-off at first-order accuracy. With the combustor overall AFR and primary zone AFR known, the ratio of primary zone to combustor overall mass flow may be determined. The primary zone flame temperature can now be calculated for every engine operating point using the combustor inlet temperature and the combustor overall AFR.

The NO_x emissions index may be determined for every engine operating point using a simple correlation of $EINO_x$ with flame temperature, as illustrated in Fig. 3.14. Values calculated with this correlation need to be corrected for pressure; this is because the correlation is actually a simple polynomial fit based

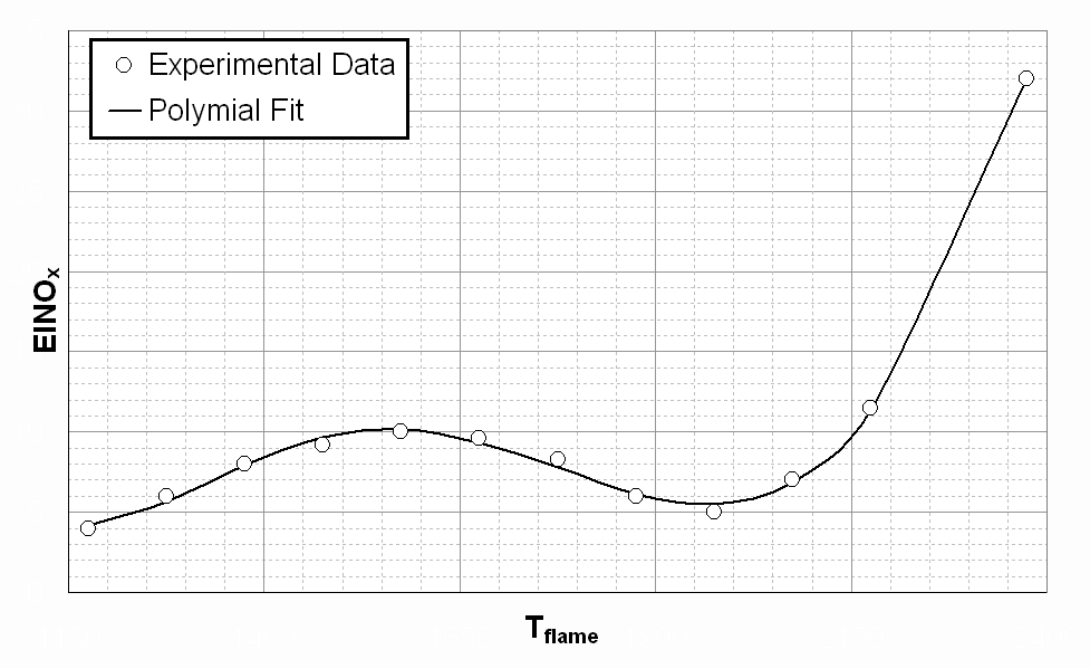

Figure 3.14: Correlation of NO_x measurements with flame temperature at a fixed combustor inlet pressure for a lean-burn combustor design.

on experimental measurements taken at a fixed combustor inlet pressure. A best-case, nominal and worst-case scenario pressure correction exponent may be applied to study the uncertainty of the predictions made.

3.3.5 Environmental impact

3.3.5.1 Global warming potential model limitations

As described already in Chapter 2, HEPHAESTUS predicts the emissions levels not only for the ICAO Landing and Take-Off cycle but also for the entire flight profile (aircraft business case mission). The D_pNO_x/F_{oo} figure is calculated and compared against ICAO Annex 16 Volume II legislative limits [64], as well as the medium and long term technology goals set by CAEP [65]. There are currently no regulatory limits set for pollutants emitted above 3000 [ft] (i.e. for the climb, cruise and descent flight phases), despite the fact that potential regulation methodologies for such purposes have been under discussion for a long time [126, 138, 139].

Table 3.4: Global warming potential figures for CO_2, H_2O(g) and NO_x versus altitude (reproduced from [47]).

Altitude [km]	CO_2 GWP	H_2O(g) GWP	NO_x GWP
0	1	0.0	-7.1
1	1	0.0	-7.1
2	1	0.0	-7.1
3	1	0.0	-4.3
4	1	0.0	-1.5
5	1	0.0	6.5
6	1	0.0	14.5
7	1	0.0	37.5
8	1	0.0	60.5
9	1	0.0	64.7
10	1	0.24	68.9
11	1	0.34	57.7
12	1	0.43	46.5
13	1	0.53	25.6
14	1	0.62	4.6
15	1	0.72	0.6

The environmental impact of a given engine/aircraft combination can be estimated by HEPHAESTUS in terms of Global Warming Potential (GWP) using NO_x, CO_2 and gaseous H_2O emissions estimates for the entire business case flight profile and a parametric GWP model from the CRYOPLANE project [47] with a selected time horizon of 100 years; this approach was chosen for its simplicity and computational speed compared to employing a sophisticated 3D climate model. GWP is an index that attempts to integrate the overall climate impacts of an emitted pollutant over a time horizon of 100 years, essentially relating the impact to that of an equivalent mass of CO_2. The GWP values for gaseous H_2O and NO_x utilised by the HEPHAESTUS environmental impact model are given in table 3.4.

It should be noted that there are large uncertainties in environmental impact results produced with GWP models. The Intergovernmental Panel on Climate Change states [140]:

To assess the possible climate impacts of short-lived species and compare those with the impacts of the long-lived greenhouse gases, a met-

ric is needed. However, there are serious limitations to the use of global mean GWPs for this purpose. While the GWPs of the long-lived greenhouse gases do not depend on location and time of emissions, the GWPs for short-lived species will be regionally and temporally dependent.

Although, GWP is now considered inadequate as a metric for short-lived species, no consensus has been reached yet by the scientific community on a validated metric for the environmental impact of aviation induced emissions [141]. To that extent, Forster et al. [142] argues that it is still premature to include the effects of short-lived species in policy schemes for aviation. Details on metrics currently under evaluation are given in [143].

3.3.5.2 Example calculations

A simple example of the kind of output that may be produced with TERA2020 when using HEPHAESTUS is presented in Fig. 3.15. The aircraft mission profile in this chart was assumed to be composed of the following flight phases: take-off, climb, cruise, descent, approach, and taxi. The dotted black line illustrates the aircraft flight path; the right hand side vertical axis has been used for plotting the flight altitude value for each point on the curve. The left vertical axis corresponds to the relativised cumulative GWP produced during the various aircraft flight phases. The cumulative GWP value at the end of the aircraft mission has been used as the denominator for the purposes of relativising the chart. This explains why the relative cumulative GWP value at the beginning of the aircraft mission is equal to zero, and why unity is approached during the final aircraft taxi, just after landing.

The pollutants considered to contribute to global warming in Fig. 3.15 are NO_x, CO_2 and H_2O with their contribution measured using GWP as a metric. Three curves have been plotted to illustrate the individual contribution of each pollutant to the cumulative GWP. According to the GWP model used, some 75% of the total GWP is produced during cruise, while nearly 20% is produced during take-off and climb. NO_x emissions during cruise contribute by nearly 20% to the total GWP produced while H_2O emissions contribute by 15%. CO_2 emissions contribute by almost 70% to the total GWP produced during the entire flight cycle.

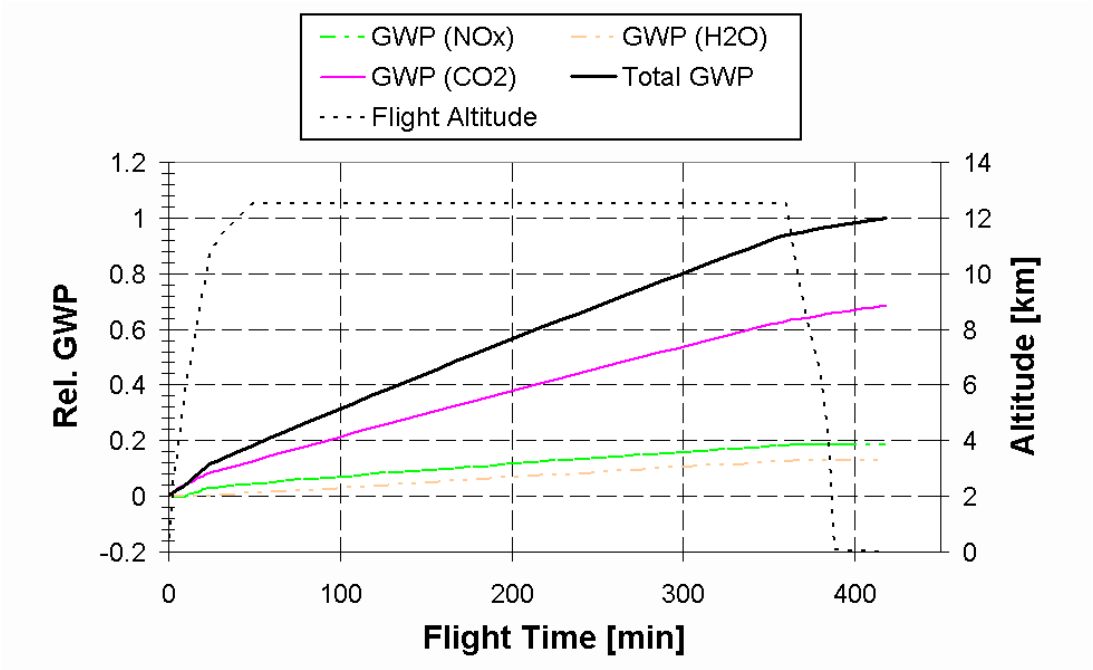

Figure 3.15: Pollutant contribution to the cumulative GWP value for a long-range flight.

As discussed earlier environmental impact results produced with GWP as a metric are subject to large uncertainties; the influence of short lived species, in particular, is highly dependent on the assumptions made in deriving the GWP model. Nevertheless, Fig. 3.15 does help illustrate how HEPHAESTUS can be used to predict the emissions levels for the entire flight profile of a given engine/aircraft combination, and also utilise these estimates to predict the environmental impact using a GWP model.

3.4 HESTIA

3.4.1 Introduction

HESTIA is a software code developed by Cranfield University that has been integrated into TERA2020 and can be used to calculate the direct operating costs for the engine/aircraft combination over a given time period. A large amount of data from all upstream modules in the TERA2020 sequence are used to account for various important elements including: aircraft utilisation times, inflation, fuel price volatility, lifing considerations, as well as noise, carbon and NO_x taxes. Some details on the interaction of HESTIA with other TERA2020 modules have been given already in Chapter 2. The main cost groups considered in the direct operating cost calculations carried out by HESTIA are illustrated in Fig. 3.16.

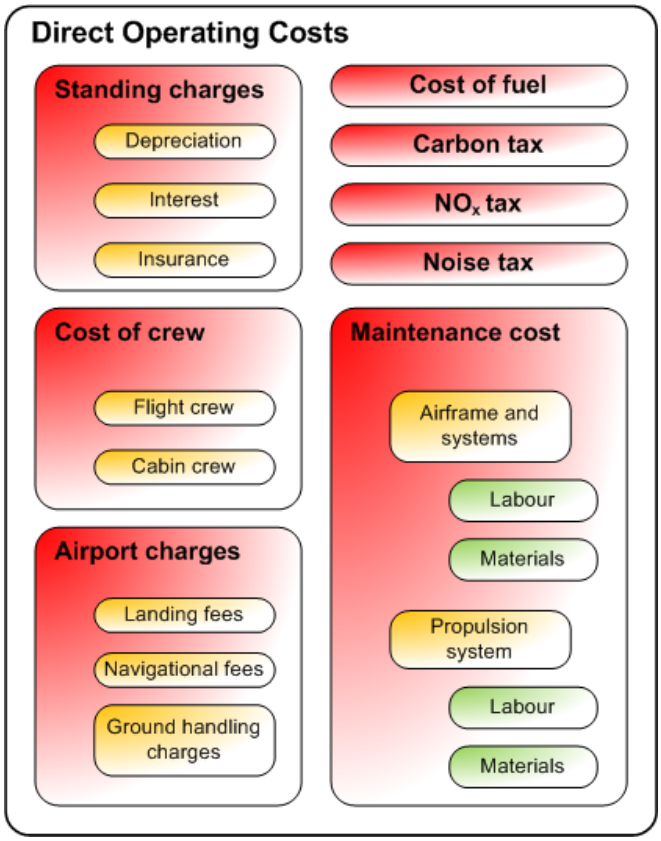

Figure 3.16: HESTIA direct operating cost calculation breakdown.

3.4.2 Code modifications

The code is based on work carried out by Pascovici et al. [144–147] on the prediction of engine/aircraft direct operating costs based on information from [98, 148]. Risk analysis capabilities were added in HESTIA by Colmenares [149], while Vigna Suria [150] worked on turbine blade and disc stress, creep and fatigue analysis. For the needs of NEWAC TERA2020, the author had to perform a partial reconstruction of HESTIA. Major code modifications include:

- Overhaul of the entire code including defragmentation.
- Complexity reduction step with respect to I/O operations.
- Replacement of simplistic iterative algorithms in the stress calculations with methods from the LISIS library.
- Calculation of direct operating cost breakdown in various formats i.e. per year, per flight, per block hour.
- Update of the materials database and blade lifing assumptions to consider year 2020 entry into service engine designs.

As a result of these modifications, the code's computational speed and robustness has improved significantly, while numerical noise issues have essentially been eliminated; the latter formed an important bottleneck in the integration of HESTIA within VITAL TERA2020 partially hindering the tool's optimisation capabilities. Furthermore, lifing assumptions, and consequently time between overhaul calculations, are now more representative of year 2020 entry into service level of technology.

3.5 LISIS

In this section, details are given on the development of LISIS, a numerical methods library for use by the developed engine performance code, as well as HERMES and HEPHAESTUS. The library was developed with the purpose of improving the computational speed and stability of these codes, as well as to eliminate the numerical noise problems hindering VITAL TERA2020 optimisation capability. As part of this research effort, an improved gradient-based algorithm for solving non-linear equation systems is proposed.

3.5.1 General objectives

The general objectives set during the development of the LISIS library are:

- Provide a generic interface to the library in order to be used by different codes without modifications.
- Improve computational speed compared to existing implementations within VITAL TERA2020.
- Reduce the frequency of non-convergence cases compared to existing implementations within VITAL TERA2020.
- Eliminate the numerical noise problems hindering VITAL TERA2020 optimisation capability.

3.5.2 Code development

For engine performance steady state simulations an algebraic equation system may be formed (see for example Fawke and Saravanumuttoo [151]) and is typically solved using a gradient-based root-finding method. Non gradient-based methods may also be employed for solving non-linear equations; their success will largely depend on the particulars of the system they are applied to. Perhaps the simplest gradient-based method available for solving multidimensional problems is the Newton-Raphson method [152]; it uses the Jacobian matrix to

iteratively solve the non-linear equation system formed. The Newton-Raphson method was selected as the starting point for developing LISIS.

In LISIS, the Jacobian may be approximated by forward or central differences, or complex-step differentiation [153, 154]. Central differences are more accurate than forward differences but at a significant computational penalty i.e. twice as many function evaluations are required to approximate the Jacobian matrix. Complex-step differentiation is the most accurate of the three options and it's accuracy is independent of the differentiation step chosen. Despite the fact that complex-step differentiation requires the same number of function evaluations as forward differences, the function evaluations themselves are computationally more expensive since complex calculus is required i.e. all real variables in the function need to be transformed into complex variables as described by Martins et al. [153].

When function evaluations are expensive, cheap approximations to the Jacobian (or better said, cheap updates to the inverted Jacobian) may be introduced in order to reduce computational time. The main idea here is that the Jacobian matrix is determined using a differentiation method only during the first iteration; for consecutive iterations cheap approximations (updates) are used for the inverted Jacobian. A whole class of algorithms have been developed that implement this idea, and are known as quasi-Newton or secant methods [155].

Through a careful study of the variations of the inverted Jacobian between engine steady state operating points that are not far away from each other (for example top of climb and max cruise), one can make a useful observation [156]: **the inverted Jacobian matrix does not vary significantly and may still be reused successfully.** The idea of reusing past information - avoiding costly Jacobian evaluations in each iteration - is not a new one. Stamatis et al. [157] describe the use of this idea for real-time transient performance simulations. Unfortunately, little detail is provided on the potential benefits for steady state simulations and the exact implementation carried out by the authors. With respect to steady state simulations, a further improvement is therefore proposed here to the class of quasi-Newton methods and has been implemented successfully in the LISIS library:

1. The Jacobian matrix is determined using one of the differentiation methods described above only during the simulation of the very first point.

2. The next simulation point(s) reuse the inverted Jacobian from the last, successfully converged, simulation point.

3. During the simulation of a given point, a Broyden update is performed on the inverted Jacobian after every iteration step as described in [158, 159].

4. The quality/accuracy of the inverted Jacobian deteriorates with every new simulation point; if the convergence rate drops below a certain threshold, the Jacobian matrix needs to be re-determined using a differentiation method in order to restore the convergence rate.

5. For consecutive simulation points whose solutions are too far from each other (i.e. for large jumps), the reused inverted Jacobian may no longer be sufficiently representative of the system. This can be detected by a slow convergence rate, numerical instabilities, and the function (model) reporting calculation errors. In such a case, the iteration for the new simulation point is restarted from the original guess of the solution vector; the Jacobian matrix is re-determined on that particular solution vector guess using a differentiation method.

A similar algorithm was investigated for steady state simulations during the development of the GeSTPAn code [23] but was never fully implemented because of convergence problems encountered when jumping between simulation points whose solutions are too far away from each other [156]. This important issue has been successfully resolved in the proposed algorithm through step 5.

Although quasi-Newton methods and the modified algorithm proposed offer improved computational speed, it should be kept in mind that cheap approximations to the inverted Jacobian may sometimes introduce deteriorated numerical stability as a trade-off. As a countermeasure, backtracking needs also be employed (i.e. line search) to improve convergence (as discussed in [23, 152]) when either:

- The function residual did not actually decrease when the full Newton step was taken.

- And/or the function (i.e. one of the engine component models) reported calculation errors.

Backtracking is of particular importance in achieving very high accuracy i.e. very small residual tolerance, and in simulating the notorious regions of a system (for example in simulating ultra-high bypass ratio engines at idle conditions - where the hot nozzle pressure ratio approaches unity and component efficiencies drop significantly).

The user can choose - via the library interface - between the original "standard" Newton-Raphson method or the quasi-Newton method described thoroughly in Broyden [158, 159]. A switch is provided for selecting one of the differentiation methods described earlier, as well as for reusing the inverted Jacobian from previous simulation points. The library integration also includes a quasi-Newton solver that utilises the Powell dogleg step procedure [160], namely MINPACK, described by Moré et al. [161, 162] and available under a freeware license through NetLib [163]. Therefore, MINPACK may also be selected for use during steady state simulations and it is worth noting that this is the solver of choice for the commercially available gas turbine performance simulation code PROOSIS.

During dynamic simulations, the original steady state set of algebraic equations representing the engine model is coupled with a set of Ordinary Differential Equations (ODE) that describe the dynamics of the system, and is hence transformed into a set of Ordinary Algebraic Differential Equations (ODAE). Grönstedt [23, 164] presents various strategies for solving ODAE systems for gas turbine dynamic simulations and after extended benchmarking concludes that the "direct approach" of treating differential and algebraic variables simultaneously seems to perform best. Stamatis et al [157] also gives benchmarking results for implicit and explicit integration schemes, while Petzold [165] provides a good reference on solving ODAE sets.

A large number of ODAE solvers, coupled with the SLATEC Common Mathematical Library, an extensive library of Fortran numerical routines, are together available under a freeware license through NetLib [163]. Three of these solvers (namely the DDASSL, the DDASPK and the DDASKR) have been integrated in the LISIS library together with some parts of the SLATEC library.

In an attempt to reduce non-convergence cases, the FITPACK higher order surface splines routines were introduced in the LISIS library; these routines are available under a freeware license through NetLib [163] and described by Dierckx [166]. Surface splines can be used to approximate component maps (i.e.

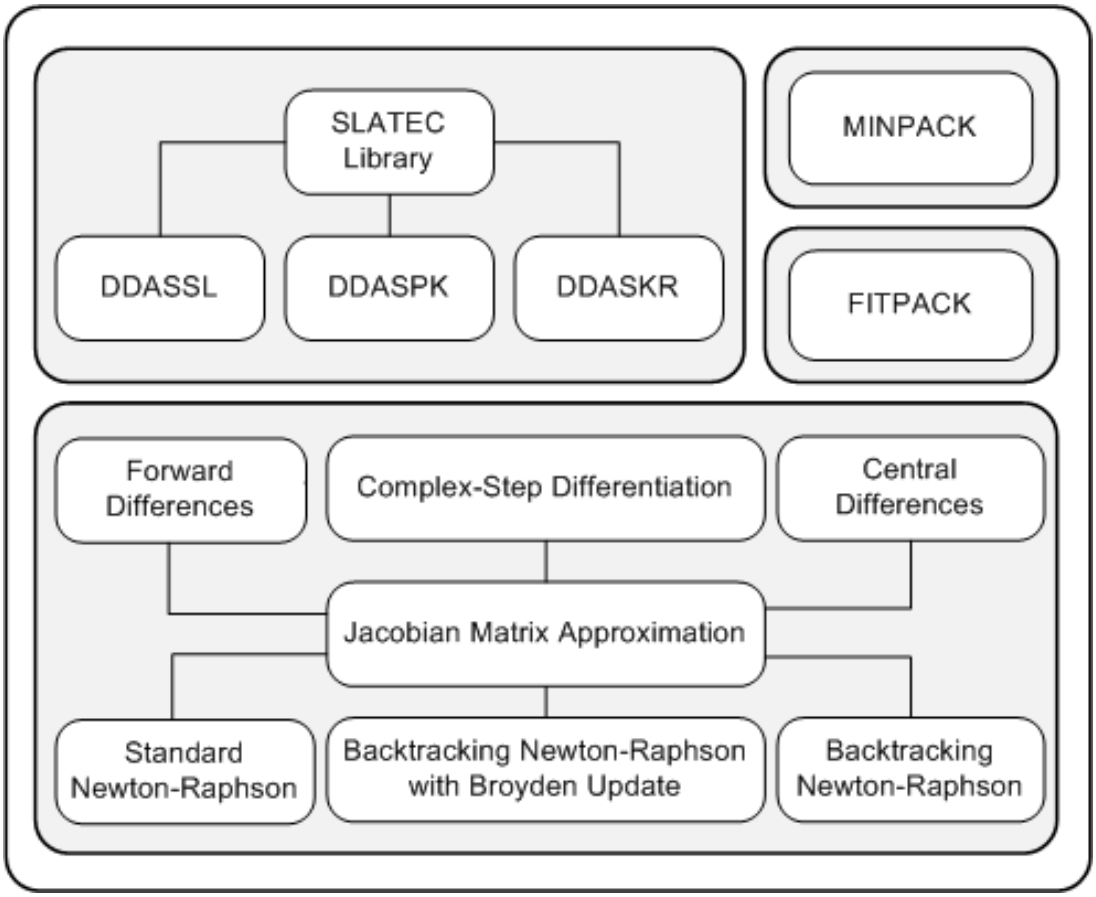

Figure 3.17: LISIS library structure.

components represented by tabulations) and hence provide first-order, second-order and third-order continuous derivatives in all map directions. Higher-order continuous derivatives are of significant importance for dynamic simulations, as discussed by Grönstedt [23, 164], while first order continuous derivatives are important for steady state simulations.

The structure of LISIS library is illustrated in Fig. 3.17. As discussed earlier the library was mainly developed for steady state and transient engine performance simulations. It is also used for solving the "inverse functions" in the thermo-fluid model as well as for solving the (non-linear) algebraic equation systems formulated by HERMES and HEPHAESTUS.

3.5.3 Benchmarks

Despite the fact that the computational power of personal computers has been rising constantly over the past decades - as predicted by Moore's Law [167] - the implementation of fast (and robust) numerical methods is of critical importance where radical design space exploration is concerned. The performance of the non-linear equation system solvers available in LISIS is presented in Table 3.5 and Table 3.6 in terms of number of functions evaluations required; the latter was chosen as a metric to make results hardware-independent (i.e. independent of computer specification), and also less dependent on the programming techniques, language, and compiler used. Convergence is assumed to have been achieved when the accuracy (tolerance) level set is reached for each (relativised) residual in the model. Various conclusions may be drawn, largely confirming expectations from the literature reviewed:

- The use of quasi-Newton methods can significantly improve computational speed but the benefit is highly dependent on the number of independent variables that formulate the function used, and the accuracy required. Results for the engine performance rubber deck (high accuracy option) indicate an up to a three-fold increase in function evaluations when quasi-Newton methods are not utilised.

- Reuse of the inverted Jacobian, between different simulation points, can significantly improve computational speed but the benefit is highly dependent on the number of independent variables that formulate the function used and its nonlinearity, the differentiation method used, and the accuracy required. Results for the engine performance rubber deck (central differences and low accuracy options) indicate an up to a twelve-fold increase in function evaluations when the inverted Jacobian is not used.

- The computational penalty associated with using central differences is dependent on the number of independent variables that formulate the function used and its nonlinearity. Reuse of the inverted Jacobian, between different simulation points, fully alleviates this penalty.

Table 3.5: Non-linear equation system solver performance (TERA2020 engine rubber deck).

	Solver		
	Broyden	MINPACK	Backtracking Newton-Raphson
Options	*No. of function evaluations*		
Nominal TERA2020 points			
Central differences, low accuracy	4756		9486
Forward differences, low accuracy	2705	2703	5015
Central differences, high accuracy	5418		14389
Forward differences, high accuracy	3367	3362	8828
Central differences, low accuracy, reuse inverted Jacobian	1171		
Forward differences, low accuracy, reuse inverted Jacobian	1086		
Central differences, high accuracy, reuse inverted Jacobian	2198		
Forward differences, high accuracy, reuse inverted Jacobian	2144		
Nominal TERA2020 points + 9000 cruise points			
Central differences, low accuracy	236307		239046
Forward differences, low accuracy	127346	127346	128663
Central differences, high accuracy	245744		466699
Forward differences, high accuracy	138103	138300	284498
Central differences, low accuracy, reuse inverted Jacobian	18800		
Forward differences, low accuracy, reuse inverted Jacobian	18723		
Central differences, high accuracy, reuse inverted Jacobian	45263		
Forward differences, high accuracy, reuse inverted Jacobian	44869		

*No. of independent variables: 12; low accuracy: 1.E-04; high accuracy: 1.E-10

Table 3.6: Non-linear equation system solver performance (HERMES and HEPHAESTUS).

Options	Solver		
	Broyden	MINPACK	Backtracking Newton-Raphson
	No. of function evaluations		
HERMES - nominal TERA2020 design point and business case			
Central differences, low accuracy	21		43
Forward differences, low accuracy	14	14	25
Central differences, high accuracy	30		66
Forward differences, high accuracy	23	23	38
HERMES - nominal TERA2020 points + 1000 business case points			
Central differences, low accuracy	8028		8085
Forward differences, low accuracy	5021	5017	5045
Central differences, high accuracy	10750		19917
Forward differences, high accuracy	7746	7736	11874
Central differences, low accuracy, reuse inverted Jacobian	2078		
Forward differences, low accuracy, reuse inverted Jacobian	2071		
Central differences, high accuracy, reuse inverted Jacobian	5746		
Forward differences, high accuracy, reuse inverted Jacobian	5875		
HEPHAESTUS - nominal TERA2020 points			
Central differences, low accuracy	3686		4480
Forward differences, low accuracy	2872	2872	3258
Central differences, high accuracy	4936		6919
Forward differences, high accuracy	4122	4122	4884
Central differences, low accuracy, reuse inverted Jacobian	2853		
Forward differences, low accuracy, reuse inverted Jacobian	2852		
Central differences, high accuracy, reuse inverted Jacobian	3722		
Forward differences, high accuracy, reuse inverted Jacobian	3721		

*No. of independent variables: 3 (HERMES) and 1 (HEPHAESTUS); low accuracy: 1.E-04; high accuracy: 1.E-14 (HERMES) and 1.E-10 (HEPHAESTUS)

3.6 Modules developed by project partners

In this section the modules i.e. software codes that have been developed for TERA2020 by other project partners are described. Details on the use of these codes within NEWAC TERA2020 have been given already in Chapter 2.

3.6.1 PROOSIS

PROOSIS is a flexible and extensible object-oriented simulation environment developed by a consortium of European universities (Cranfield University, National Technical University of Athens and Stuttgart University), research institutes and corporate companies within the integrated European Framework 6 collaborative project VIVACE [168] (Value Improvement through a Virtual Aeronautical Collaborative Enterprise). The tool performs all kinds of engine simulations as well as generic system simulation (e.g. control, thermal, hydraulic, mechanical etc.). It features an advanced graphical user interface allowing for modular model building using either the Standard or any custom library of engine components. It is capable of both steady and transient simulations as well as customer deck generation. Different calculation types (mono or multi-point design, off-design, test analysis, sensitivity, optimisation etc.) can be performed. It is also capable of performing multi-fidelity, multi-disciplinary and distributed simulations. The software is currently used in the NEWAC project for generating TERA2020 compatible rubber decks for the short and long range applications of the contra-rotating flow-control configuration and the geared turbofan with active core technologies configuration [169], as well as for the baseline short range application engine. The tool is also used in TERA2020 for DREAM (valiDation of Radical Engine Architecture systeMs) [33] to model the performance of direct drive and geared open rotor engines.

3.6.2 WeiCo

The WeiCo software module comprises two parts, the weight and dimensions part (Wei) and the plant cost part (Co), as illustrated in Fig. 3.18. The weight and dimensions code, developed by Chalmers University, utilises performance data (such as pressures, temperatures, and mass flows at different engine stations)

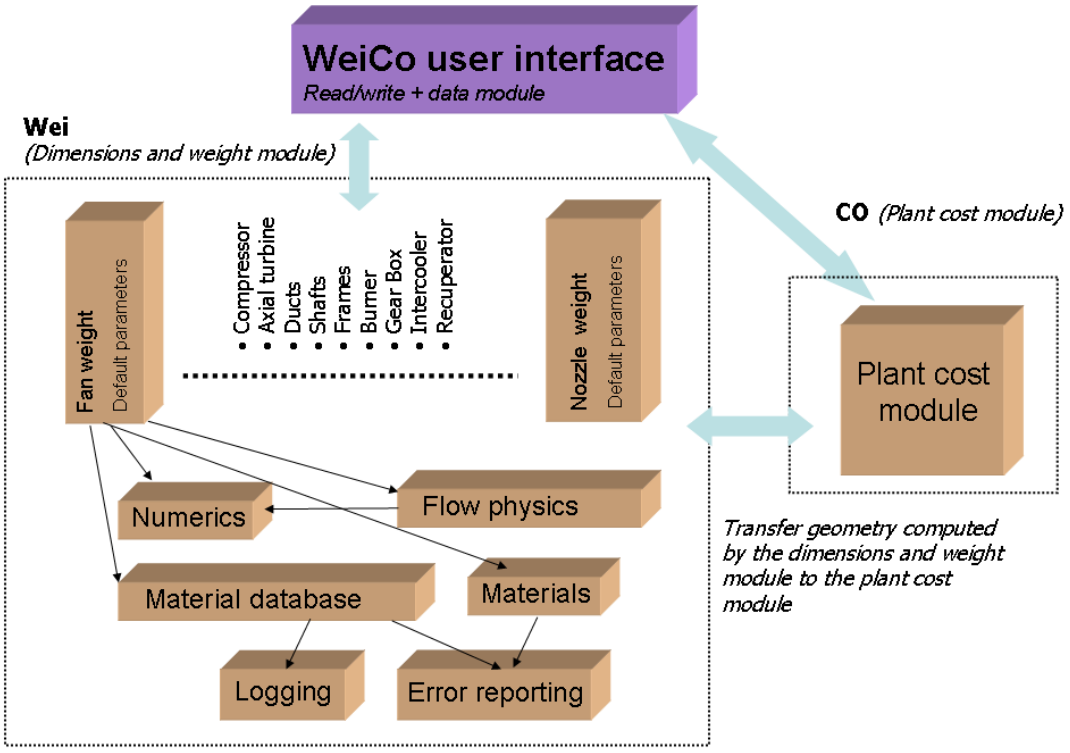

Figure 3.18: WeiCo structure (courtesy of Chalmers University).

to carry out a preliminary sizing of the engine. This will, among other things, determine the necessary number of turbomachinery stages, hub and tip radii at every stage interface, number of blades, a preliminary sizing of the combustor, a nacelle and bypass duct geometry, exhaust nozzle geometry, inlet sizing, a mechanical assessment of the shafts and compressor and turbine discs sizing. Data on turbomachinery blade speed and local Mach numbers are generated as input for the noise prediction code SOPRANO. Blade speed and geometry are used as input for life prediction through the HESTIA code. Engine weight and nacelle dimensions are used by HERMES to estimate total aircraft weight as well as nacelle drag. A complete engine weight breakdown is produced at component and subcomponent level to allow a comprehensive analysis of engine weight. Major part of the development was carried out within the VITAL project. Refined core modelling as well as development of a number of new architectures has been implemented in the NEWAC project. Current work in the DREAM project focuses on developing open rotor propeller and gearbox geometry and weight models.

The plant cost code has been developed by the University of Stuttgart and its aim is to calculate the production cost of a given engine design. This comprises scaling of a single configuration to new design constraints. The major part of the development was carried out within the VITAL project, while new models for individual components (active cooling air cooler, intercooler, recuperator, combustor injectors, air cooled oil cooler and manifolds) have been introduced within the NEWAC project. The output of the model is to be understood as production cost only which reflects realistic cost trending and scaling but does not predict absolute cost or selling prices. A meaningful comparison of cost is only achieved by looking at direct production cost while assuming equal manufacturing conditions for all investigated engines. The plant cost model uses a fully object-orientated approach in modelling production cost. This approach was chosen because an improved level of modelling flexibility is achieved; almost every possible engine configuration can be represented. To derive this kind of modelling, the breakdown of an aero engine product structure was first analysed [170]. All classes of parts with similar properties, and production cost calculation schemes, were identified. These part classes are represented as objects within the plant cost model and can be assembled to modules (according to the TERA2020 defined bookkeeping) in a flexible manner.

3.6.3 SOPRANO

The SOPRANO software was developed within the European Framework 6 collaborative project SILENCER by the Spanish consultancy company ANOTEC. The SOPRANO code will allow the assessment of noise generation at the engine/aircraft level by means of a number of semi-empirical correlations such as fan inlet and aft noise, airframe noise, combustor and turbine noise and jet noise. The current implementation of the SOPRANO code does not consider open rotor propeller or ducted counter rotating fan noise modelling. Models for the former are developed within the DREAM project by Aristotle University of Thessaloniki, while models for the latter have been developed within the the VITAL project by ISAE/SUPAERO. The noise prediction methods utilised in VITAL and NEWAC are summarized in Table 3.7. Most of the existing methods have been calibrated with data from previous and in-service engines. As new and different engine concepts are being investigated, the input conditions may be out of the validity range of the methods. Some of the models are then extrapolated

Table 3.7: Overview of implemented noise prediction methods.

Fan and compressors	Heidmann [171], and Kontos et al. [15]
Coaxial exhaust jet	Stone and Krejsa [172], SAE ARP 876D [173]
Turbine	Krejsa and Valerino [174]
Airframe	Fink [175]
Noise propagation	SAE ARP 866A [176], Chien and Soroka [177], SAE AIR 1751 [178]
Installation effects on jet noise	Blackner and Bhat [179]
Contra-rotating rotors interaction tone noise	Hanson [180], Whitfield et al. [181], Heidman [171], Kontos et al. [15]

for the optimization investigation, and assumed to be sufficient to capture the noise trends correctly.

The noise resulting from the semi-empirical models are projected down to the microphone position where the sound pressure levels are converted to effective perceived noise levels. The cumulative sum from the three ICAO certification points - sideline, flyover, and approach - is then estimated, which allows a subsequent comparison of noise generated by a particular engine/aircraft combination with the noise regulations stipulated in Vol. 1 of the ICAO Annex 16 [66]. The existence of a code like the SOPRANO code within a tool like the TERA2020 tool makes it possible to study how new engine designs will behave under different noise regulations and taxation polices. TERA2020 may for instance single out designs that can satisfy stringent noise regulations (by delivering a low noise footprint) without a major block fuel penalty.

3.7 Conclusion

The research effort presented in this chapter focused on various aspects of the development of new models and modules for NEWAC TERA2020, and the improvement of existing ones. As a result of these efforts, TERA2020 has been significantly improved. In more detail the following improvements have taken

place within NEWAC:

- Development of new TERA2020 models and modules, and improvement of existing ones, to be sufficiently accurate for multi-disciplinary conceptual design of the novel engine configurations (and technologies) studied under the NEWAC project. This includes the derivation of a semi-empirical NO_x correlation for modern rich-burn single-annular combustors.
- TERA2020 complexity reduction step - less input/output files, and more efficient data exchange.
- A nearly three-fold improvement in computational speed for the heat-exchanged cycles, compared to VITAL TERA2020. Significant reduction in the frequency of non-convergence cases and elimination of the numerical noise problems hindering VITAL TERA2020 optimisation capability.

3.8 Outlook

Details have been given on developments carried out on individual TERA2020 modules by the author, as well as a brief description of TERA2020 modules developed by other project partners. In the next chapter, a systematic assessment of the impact of thermo-fluid modelling on the accuracy of the TERA2020 tool will be carried out. Accuracy limitations in assessing novel engine core concepts as imposed by current practice in thermo-fluid modelling will be identified.

Chapter 4

System uncertainty due to thermo-fluid modelling

This chapter describes and compares fluid models, based on different levels of fidelity, which have been developed for the engine performance module in the TERA2020 (Techno-economic, Environmental and Risk Assessment for 2020) tool. The disciplines in TERA2020 utilised for these assessments are: engine performance, aircraft performance, emissions prediction, and environmental impact. The work presented aims to fill the current literature gap by: (i) investigating the common assumptions made in thermo-fluid modelling for gas turbines and their effect on caloric properties, (ii) assessing the impact of uncertainties on performance calculations and emissions predictions at aircraft system level and (iii) identifying accuracy limitations in assessing novel engine core concepts as imposed by current practice in thermo-fluid modelling.

N.B. *The work presented in this chapter has been a collaborative effort between Cranfield University and Aristotle University of Thessaloniki and has been published in the following papers:*

> K.G. Kyprianidis, V. Sethi, S.O.T. Ogaji, P. Pilidis, R. Singh, and A.I. Kalfas. Thermo-Fluid Modelling for Gas Turbines - Part I: Theoretical Foundation and Uncertainty Analysis. In *ASME TURBO EXPO 2009 Proceedings, GT-2009-60092*, Orlando, FL, USA, June 2009.

K.G. Kyprianidis, V. Sethi, S.O.T. Ogaji, P. Pilidis, R. Singh, and A.I. Kalfas. Thermo-Fluid Modelling for Gas Turbines - Part II: Impact on Performance Calculations and Emissions Predictions at Aircraft System Level. In *ASME TURBO EXPO 2009 Proceedings, GT-2009-60101*, **Cycle Innovations Committee Best Paper Award**, Orlando, FL, USA, June 2009.

K.G. Kyprianidis, V. Sethi, S.O.T. Ogaji, P. Pilidis, R. Singh, and A.I. Kalfas. Uncertainty in Gas Turbine Thermo-Fluid Modelling and its Impact on Performance Calculations and Emissions Predictions at Aircraft System Level. *Proceedings of the IMechE, Part G: Journal of Aerospace Engineering, JAERO765*, 2010. submitted for publication.

4.1 Introduction

Accurate and reliable fluid modelling is essential for any gas turbine performance simulation software as it provides a robust foundation for building advanced multi-disciplinary modelling capabilities [182]. Caloric properties for generic and semi-generic gas turbine performance simulation codes can be calculated at various levels of fidelity; selection of the fidelity level is dependent upon the objectives of the simulation and execution time constraints. Rigorous fluid modelling, however, may not necessarily improve performance simulation accuracy unless all modelling assumptions and sources of uncertainty are aligned to the same level. Certain modelling aspects such as the introduction of chemical kinetics, and dissociation effects, may reduce computational speed significantly and this could be of significant importance for radical space exploration and novel propulsion cycle assessment.

A large number of technical models are currently available in the literature for calculating caloric properties of ideal gases [84, 88, 183–192]. Bücker et al. [183] reviewed most of these models and argued that although some of them are accepted standards in various industrial sectors their mutual consistency can be rather poor. Since this could result in significant discrepancies, and even in contradictory results, a new technical model was developed in that study to be used as a standard for the prediction of caloric properties of moist air and combustion gases based on consistent sets of data.

Some of the uncertainties of thermo-fluid modelling and the potential dangers induced by certain assumptions in gas turbine performance have been discussed in the gas turbine literature [5, 94, 183, 193–195]. Nevertheless, the actual effects of error propagation still remain unclear with respect to gas turbine performance calculations and multi-disciplinary simulations at aircraft system level. Cengel [196] argues that "the assumptions made while solving an engineering problem must be reasonable and justifiable". The work presented in this chapter aims to fill the current literature gap by: i) investigating the common assumptions made in thermo-fluid modelling for gas turbines and their effect on caloric properties and ii) assessing the impact of uncertainties on performance calculations and emissions predictions at aircraft system level.

In the first part of this chapter, a comprehensive analysis of thermo-fluid modelling for gas turbines is presented and the thermo-fluid models developed for the TERA2020 (Techno-economic, Environmental and Risk Assessment for 2020) engine performance rubber decks are discussed in detail. Common technical models, used for calculating caloric properties, are compared while typical assumptions made in fluid modelling, and the uncertainties induced, are examined. Several analyses, which demonstrate the effects of composition, temperature and pressure on caloric properties of working mediums for gas turbines, are presented. The working mediums examined include dry air and combustion products for various fuels and Hydrogen to Carbon ratios (H/C). The errors induced by ignoring dissociation effects are also discussed.

In the second part of this chapter, the uncertainty induced in performance calculations by common technical models, used for calculating caloric properties, is discussed at engine level. The errors induced by ignoring dissociation are examined at three different levels: i) component level, ii) engine level, and iii) aircraft system level. Essentially, an attempt is made to shed light on the trade-off between improving the accuracy of a fluid model and the accuracy of a multi-disciplinary simulation at aircraft system level, against computational time penalties. The accuracy/uncertainty of an overall engine model will always be better than the mean accuracy/uncertainty of the individual component estimates as long as systematic errors are carefully examined and reduced to acceptable levels to ensure error propagation does not cause significant discrepancies. The results obtained demonstrate that accurate modelling of the working fluid is essential, especially for assessing novel and/or aggressive cycles at aircraft system level. Computa-

Table 4.1: Chemical composition of atmospheric dry air.

Constituent	Chemical Formula	Mole Fraction y_i	Mass Fraction x_i
Nitrogen	N_2	0.780840	0.755184
Oxygen	O_2	0.209476	0.231416
Argon	Ar	0.009365	0.012916
Carbon Dioxide	CO_2	0.000319	0.000484

tional time penalties induced by improving the accuracy of the fluid model as well as the validity of the ideal gas assumption for future turbofan engines and novel propulsion cycles are discussed.

4.2 Fluid modelling

The fluid model of a gas turbine simulation software generally consists of three types of fluids; the initial working fluid (typically air), the fuel and the products of combustion. The chemical composition of atmospheric dry air that was assumed for the purpose of this study is highlighted in Table 4.1.

Conventionally, there are two approaches for implementing technical fluid models in gas turbine performance simulation software. Caloric properties can either be obtained from linearly - and in some case logarithmically [182] - interpolated fluid tables or from polynomial functions. Generating fluid model tables, either from polynomial relationships such as those described in references [88, 187, 197, 198], and/or chemical equilibrium software such as CEA (Chemical Equilibrium with Applications) [188], Gaseq [199] and CEC (Chemical Equilibrium Composition) [200], is far more laborious and time consuming than directly implementing polynomial functions. Nevertheless, fluid tabulations offer several key advantages that have been discussed extensively by Sethi et al. [182, 201].

Often the need for analysing the effects of different working mediums and alternative fuels on gas turbine performance arises [201–203]. The engine performance module developed for TERA2020 can utilise CHEMKIN-II format libraries of polynomials to rigorously model these effects. The structure of the fluid model

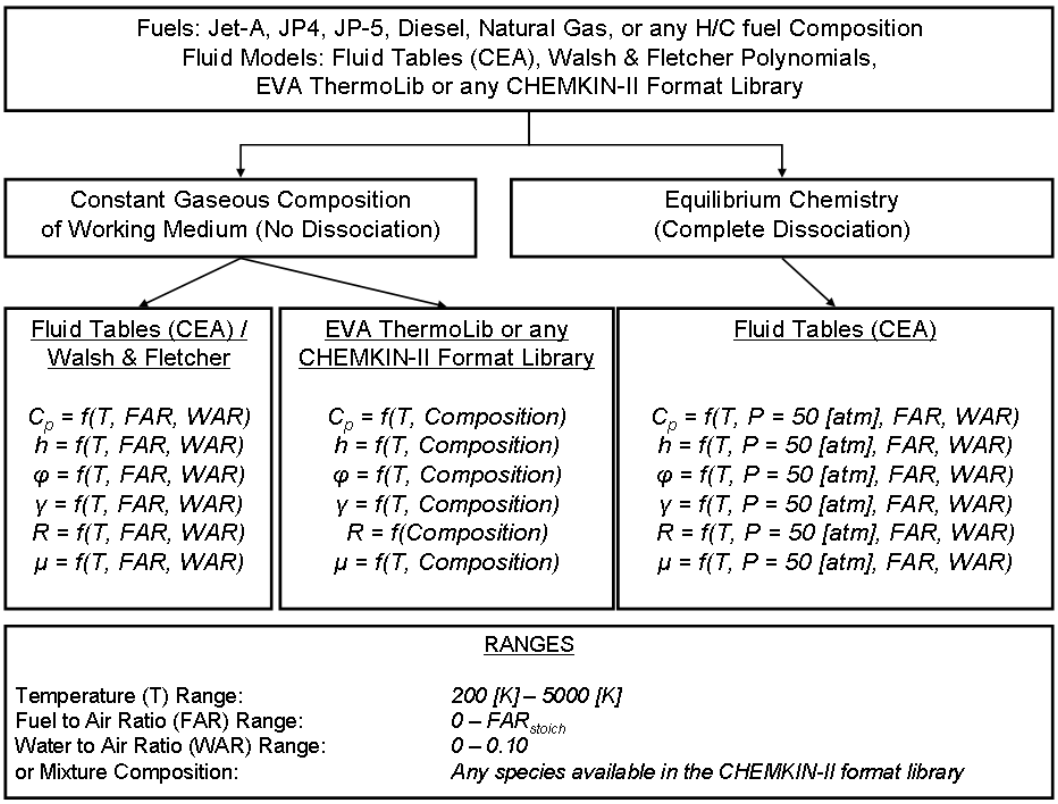

Figure 4.1: Fluid model structure.

implemented is illustrated in Fig. 4.1. The following types of technical fluid models can currently be used:

- Tables of caloric properties
- Walsh and Fletcher fluid model [88]
- Polynomial libraries based on CHEMKIN-II format [191]

The Walsh and Fletcher technical model is based on 8th order polynomial functions for combustion products of kerosene and diesel for temperatures ranging from 200 [K] to 2000[K]. Libraries in the CHEMKIN-II format, such as CEA up to 1994 [187], and GRI-Mech [192], consist of 4th order polynomial coefficients for various species and are typically valid for temperatures ranging from 200 [K] to 5000 [K]. In more recent versions of CEA [188], caloric properties are calculated with polynomial functions consisting of seven terms; these data have been

utilised via tables and their range of validity is typically the same as with the CHEMKIN-II format polynomials.

For the "no dissociation" option of the developed fluid model a constant gaseous composition of the working medium has been assumed. Composition is only allowed to change when combustion or mixing takes place; no allowances for dissociation have been made. The products of combustion for any hydrocarbon will comprise only water vapour, carbon dioxide, argon, nitrogen and oxygen (if combustion is lean). Since there is no dissociation, the composition of the products does not change even with changes in temperature as the distributions of moles and consequently mole fractions remain the same at any temperature. This implies that the mean molecular weight of the gases in the products of combustion remains constant regardless of the temperature or pressure. The no dissociation option is suitable for any hydrocarbon with the structure C_aH_b where lean and stoichiometric ideal combustion is concerned.

For the "complete dissociation" option the assumption has been made that full chemical equilibrium is reached by the working medium at every given temperature and pressure. This approach considers the complex series of reaction steps typically encounter in combustion, which can yield many major and minor constituents when the large number of potential reactions is considered. The extensive simulations carried out with the NASA CEA code [188] that support the "complete dissociation" option in the fluid model are described in detail in [201]. Detailed descriptions of the definition of equilibrium constants as well as the calculation procedures are presented in reference [204]. The composition of the main combustion products of Jet-A (i.e. the ones with mole fractions greater than $5 \cdot 10^{-6}$) for a range of temperatures assuming chemical equilibrium is presented in Table 4.2. It can be observed that dissociation becomes first noticed at 1500 [K], and increasingly important at higher temperatures.

Theoretically, as the temperature of the combustion products reduces due to cooling in the burner and due to the expansion process in the turbine, dissociation should cease, and the mixture should return to the non-dissociated species composition. In practice however, fast local chilling of the reactions - for example due to contact with the cooler walls of the combustor or due to insufficient residence times in the turbine - will result in some dissociated species still being present in the final mixture (i.e. frozen composition). Generating an accurate fluid model to account for this phenomenon is considered to be highly complex

Table 4.2: Composition of the main combustion products of Jet-A for a range of temperatures assuming chemical equilibrium (reproduced from [201]).

	Mole fraction y_i at species specified temperature in [K]				
Species	200	1500	2000	2500	3000
Ar	0.00767	0.00767	0.00767	0.00764	0.00750
CO_2	0.10239	0.10239	0.10222	0.09826	0.07677
H_2O	0.22960	0.22959	0.22911	0.22479	0.20588
N_2	0.63977	0.63959	0.63853	0.63413	0.61791
O_2	0.02057	0.02038	0.01942	0.01861	0.02360
CO	0.00000	0.00000	0.00014	0.00372	0.02325
H	0.00000	0.00000	0.00000	0.00013	0.00204
HO_2	0.00000	0.00000	0.00000	0.00001	0.00003
H_2	0.00000	0.00000	0.00007	0.00137	0.00842
NO	0.00000	0.00034	0.00210	0.00614	0.01417
NO_2	0.00000	0.00000	0.00001	0.00001	0.00002
N_2O	0.00000	0.00000	0.00000	0.00000	0.00001
O	0.00000	0.00000	0.00001	0.00028	0.00244
OH	0.00000	0.00003	0.00072	0.00490	0.01793

* P = 50 [atm], FAR = 0.06, WAR = 0.1

since the composition of the mixture will need to be determined experimentally using techniques such as chemical absorption or adsorption, infrared radiation or paramagnetism [204]. The interested reader can also refer to reference [205] for more information on advanced non-equilibrium modelling for predicting the formation of various species in gas turbine combustors.

4.3 Rationale for fully rigorous calculations

A comparison between various methodologies for thermodynamic calculations is presented in this section with respect to compressor performance.

The most crude of assumptions that can be made is that of perfect gas i.e. constant cold end gas properties with $C_p = 1004.7$ [J/(kg·K)] and $\gamma = 1.4$ [88], and can yield inaccuracies of more than a few [K] in temperature calculations.

A more accurate calculation is based again on the assumption of a constant value

Table 4.3: Comparison of various calculation methods for compression from the fully rigorous approach.

Calculation method	$\Delta T_{c,out}$ [K]*	ΔPW_c [%]*
Constant cold end C_p and γ	-15.8	-0.61
Mean C_p and γ	3.7	0.59
C_p and γ at mean component temperature	1.1	0.58
Fully rigorous approach	Ref.	Ref.
Assumptions:	Dry air (CEA [188]), $T_{c,in}$ = 351.2 [K] $P_{c,in}$ = 110.1 [kPa] $\eta_{c,is}$ = 0.863 PR_c = 10.65 and no bleeds	

*Relative to the fully rigorous approach result

of C_p and γ, but evaluated at the mean component temperature. This calculation is generally easy to perform without a computer and will yield inaccuracies of just a few [K] in temperature calculations.

The fully rigorous calculations will involve the use of the fundamental definitions of specific enthalpy and entropy and will give results whose inaccuracy is primarily dependent on the uncertainty of the ideal gas assumption and the technical model used for calculating caloric properties. The authors of reference [88] state that the uncertainty level in calculations using the fully rigorous approach is approximately 0.25%, for moderate pressures and temperatures, but give no explanation. This type of calculations is fundamental for gas turbine simulation software since errors of even a few [K] may be considered unacceptable during the conceptual design phase. As a calculation method it is certainly more cumbersome and consequently, for educational purposes, a simpler method is often sought. Nevertheless, Kurzke [193] provides a simple way of using rigorous calculation procedures i.e. enthalpy and entropy instead of C_p and γ, for teaching students gas turbine theory.

A comparison of the constant C_p and γ methods, relative to the fully rigorous approach, is presented in Table 4.3 for a compression calculation. The relatively small error in the calculation of compression power implies that the error propagation in the expansion calculations for a gas turbine system should also be small. Although, on one hand this could be true (for the expansion process only), it

tends to give the illusion that the overall system calculation will not be affected much. In reality however, the error in the prediction of the compressor delivery temperature will affect significantly the accuracy of the fuel mass flow prediction - and therefore other important performance parameters such as Specific Fuel Consumption (SFC) and block fuel estimations. Furthermore, Kurzke [5] concludes that for achieving high temperatures one needs over-proportional amounts of fuel, and that is the reason for the maximum thermal efficiency being at a temperature much lower than the stoichiometric limit. The fact that fuel mass flow, and subsequently Fuel to Air Ratio (FAR), is not proportional to the combustor temperature increase can only be taken fully into account if rigorous fluid modelling is used in the combustor component calculations. Lee et al. [195] also come to similar conclusions for gas turbine configurations with multiple combustors. It can therefore be concluded that the fully rigorous approach should be used in all performance calculations, even within the educational procedure.

4.4 Computational time considerations

Estimating the performance of a gas turbine engine at aircraft system level, for a long range mission, requires a relatively small amount of computing power. However, the required computational time for design space exploration applications - through the use of multi-disciplinary tools such as TERA2020 - is not negligible and the fluid model must therefore be chosen carefully. Tables of caloric properties where seemingly found to be a good choice with respect to reducing computational speed. Computational speed decreased by some 10% if the Walsh and Fletcher 8th order polynomials were used and some 20% if CHEMKIN-II type of libraries of 4th order polynomials were used. For the latter choice, only five species were taken into account: N_2, O_2, Ar, H_2O, and CO_2. It can be argued however, with high confidence, that these benchmarking results are highly dependent on programming practices and as a result on the quality of the code produced. A conclusion therefore cannot be drawn on whether using fluid properties or polynomials is best practice with respect to computational speed.

Nevertheless, following further analysis, it was safely concluded that when using a CHEMKIN-II type of library (or equivalent) the computational speed is inversely proportional to the number of species taken into consideration. As a rule of thumb, doubling the number of species taken into consideration will

approximately double the required computational time. Using a fluid model that calculates thermodynamic properties at species level - rather than working medium level, as would be the typical case with fluid tables - can be considered a sensible choice if the effects of utilising different working mediums and/or alternative fuels are to be taken into account rigorously. Potential computational time trade-offs should not be ignored however when considering radical design space exploration as simulations can last from a few hours to a few days.

4.5 Uncertainty for common technical models

Various technical models used for calculating caloric properties based on the ideal gas assumption are compared in Fig. 4.2. Many professional gas turbine performance simulation codes used in industry and research institutes have incorporated NASAs CEA code [188] for calculating thermodynamic properties. This model has therefore been set as the baseline for comparison with the other technical models. Four technical models have been used for the purpose of this comparison: the Walsh and Fletcher 8th order polynomials [88], a special library developed for the TERA2020 engine performance module referred to here as EVA ThermoLib, the GRI-Mech [192] library ,and an older set of 4th order polynomials used with NASAs CEA code up to 1994 [187].

An oscillating deviation from CEA calculated values can be observed for the models described in references [187, 192], as well as EVA ThermoLib. This is consistent with the fact that the later three are using 4th order polynomials based on the CHEMKIN-II format while CEA is using more recent seven-term functions. The Walsh and Fletcher polynomials are only valid up to 2000 [K], for which range they show close agreement with CEA results. Caloric properties evaluated for temperatures beyond this threshold will deviate significantly and can be completely inconsistent with values calculated with the other models and the expected trends.

There is currently no conclusive study in the gas turbine literature, known to the author, that compares and ranks the various technical models discussed in this paper in terms of accuracy. Therefore, the assumption shall be made that none of the presented models is any better than the rest, within their respected range of validity. Hence, the uncertainty in calculating the isobaric heat capac-

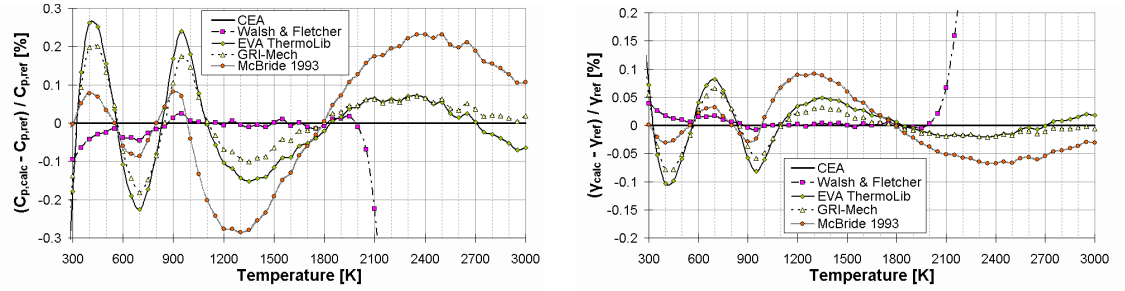

Figure 4.2: Percentage deviation of isobaric heat capacity (left) and γ (right) calculated for dry air with commonly used technical models from CEA.

ity in the range of temperatures and pressures that the ideal gas assumption holds well - is 0.3% while for γ its approximately 0.1% i.e. nearly three times lower. Essentially, the uncertainty in calculating the isobaric heat capacity from the technical models is within the same order of magnitude as the uncertainty induced by not accounting for real gas effects in modern gas turbine engines currently in service [183]. This uncertainty can propagate to gas turbine performance calculations carried out using the fully rigorous approach.

An interesting anomaly to observe is the unsmoothness of the curves in Fig. 4.2. This is mainly attributed to the implicit low precision in the output values from the CEA code. The output values from the implementation of the other technical models within the fluid model, have a much higher number of significant digits. It is therefore expected that the curves showing the percentage deviations between these models and CEA will not be very smooth. According to Cengel [196] "A result with more significant digits than that of given data falsely implies more accuracy. It is appropriate to retain all the digits during intermediate calculations and to do the rounding in the final step". For graphical comparisons the data would need to be produced with a good, and similar, number of significant digits - but that would require to access and modify the NASA proprietary CEA source code.

4.6 Ideal gas assumption and caloric properties

In this section, an attempt has been made to study the effects of temperature, FAR and lambda (λ), Water to Air Ratio (WAR), fuel and H/C ratio, and dissociation (including pressure effects) on the calculation of caloric properties using

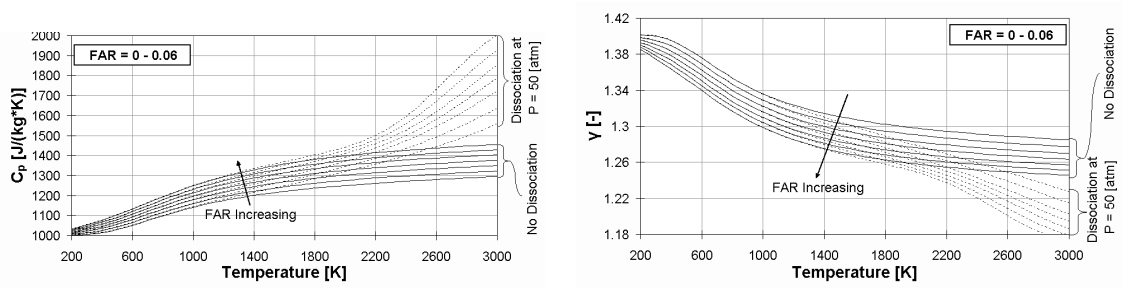

Figure 4.3: Effects of FAR and dissociation on isobaric heat capacity (left) and γ (right) for combustion products of Jet-A.

the ideal gas assumption. In some cases a comparison was made between the values calculated using rigorous ideal gas modeling and the values proposed in gas turbine textbooks to be used in "illustrative calculations for teaching purposes, or for crude ballpark estimates" [88] i.e. perfect gas assumption. Although, such simplifications are sometimes necessary within an educational framework, it is important for future engineers to understand the errors induced in their calculations. In reference [193], Kurzke clearly demonstrates how simplifications can be wrong not only quantitatively, but also qualitatively, and, hence, predict wrong trends.

Tables of caloric properties from CEA [188] have been used for producing figures illustrating the effects of dissociation and WAR. The no-dissociation and chemical equilibrium models have been discussed in earlier sections. Figures illustrating the effects of fuel chemistry have been produced using the simple no-dissociation chemistry model and a CHEMKIN-II type of library, EVA ThermoLib, discussed earlier in section 4.2.

4.6.1 Effects of dissociation on C_p and γ

The isobaric heat capacity will increase with FAR and temperature, while γ will decrease. Dissociation effects start becoming noticeable after 1500 [K], and can induce increasingly significant deviations in C_p and γ calculations for temperatures greater than 1800 [K], as can be observed in Fig. 4.3, as well as Table 4.2. To a first order, dissociation effects are highly sensitive to pressure; they are significantly less sensitive to FAR, however. The assumption of perfect gas can induce errors in the estimated values of C_p and γ of as much as 30% and 5% respectively, if dissociation effects are ignored. With dissociation effects taken

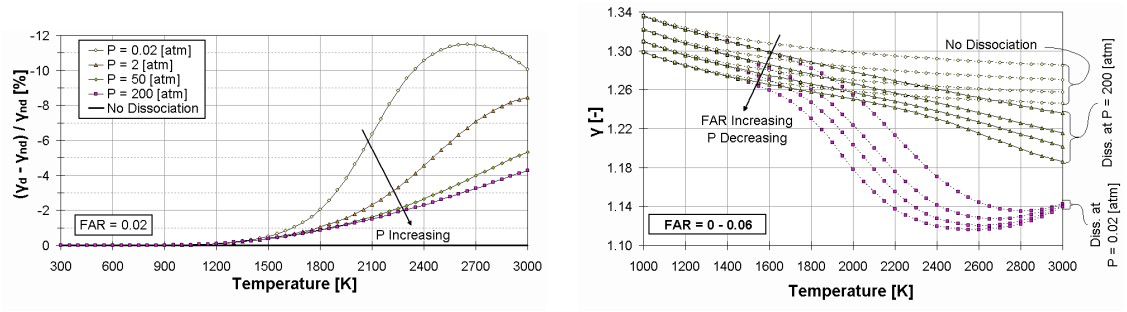

Figure 4.4: Effect of pressure on percentage deviation of γ due to dissociation of combustion products for Jet-A (left) and effects of FAR, pressure and dissociation on γ for combustion products of Jet-A (right).

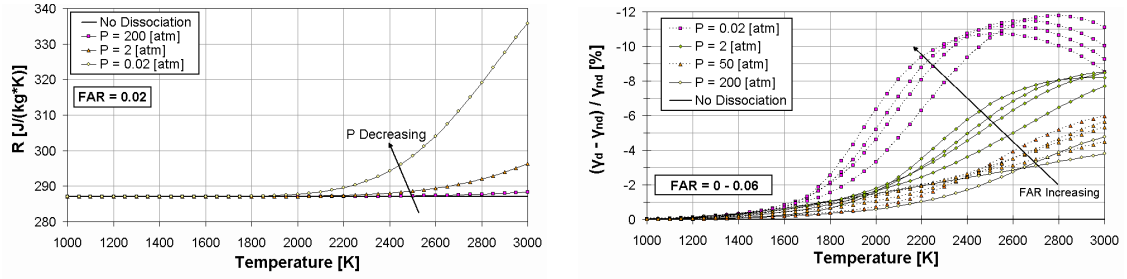

Figure 4.5: Effects of pressure and dissociation on R for combustion products of Jet-A (left) and effect of FAR and pressure on percentage deviation of γ due to dissociation of combustion products for Jet-A (right).

into account the errors will increase even further. The discrepancies induced by such assumptions for compressor calculations, as well as a qualitative analysis of the effects of dissociation, were discussed earlier.

As stated, γ is highly sensitive to pressure and this can be observed more clearly in Fig. 4.4. In general, the higher the pressure the smaller the effects of dissociation on γ and on the rest of the caloric properties will be. For very high temperatures and extremely low pressures which are unlikely to occur in modern gas turbine applications - the deviation of the value of γ compared to values obtained from the no-dissociation model can be as much as 12%. It can easily be observed in Fig. 4.4 that for high temperatures the error in calculating γ will drop by 1% to 3% for every order of magnitude increase in pressure. Modern gas turbine combustors typically function at relatively lower temperatures and significantly higher pressures and therefore the error in γ estimation is confined to 3%, which is still significantly high and should not be ignored.

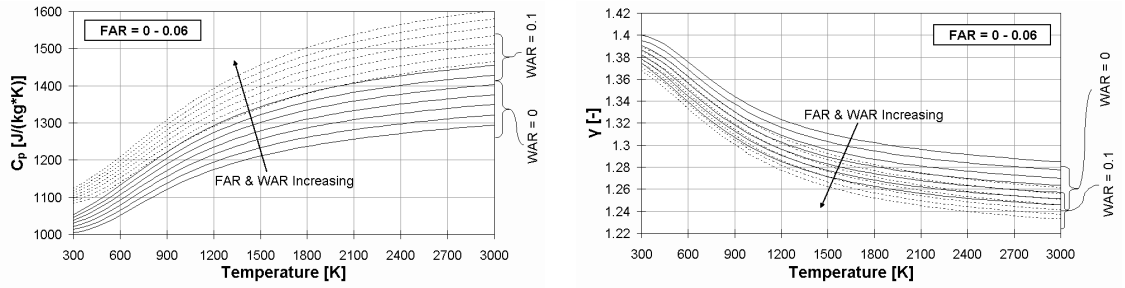

Figure 4.6: Effects of FAR and WAR on isobaric heat capacity (left) and γ (right) for combustion products of Jet-A.

Dissociation effects are relatively insensitive to FAR for high pressures. It was mentioned earlier that increasing FAR will decrease γ and this is generally true whether dissociation is taken into account or not. This rule will not apply however at high temperatures and low pressures were γ tends to become less dependent on the value of FAR. This is mainly attributed to the substantially increased value of the gas constant which offsets the increase in isobaric heat capacity, as illustrated in Fig. 4.5. This occurrence was not studied for temperatures higher than 3000 [K] since such temperatures are of limited interest for most gas turbine applications. No direct conclusion can be drawn with respect to the effect of FAR on the deviation of the chemical equilibrium value of γ compared to the value obtained from the no-dissociation model, as illustrated in Fig. 4.5.

4.6.2 Effects of water to air ratio on C_p and γ

The isobaric heat capacity will increase with water to air ratio, while γ will decrease as illustrated in Fig. 4.6. The effect of WAR is more significant on the calculation of C_p, than on γ. This is mainly attributed to the rising value of the gas constant with WAR, essentially offsetting the increase of C_p; it should be kept in mind that γ is a function of C_p and R, with the value of the latter being significantly higher for water than for dry air or combustion products of Jet-A.

4.6.3 Effects of fuel chemistry and lambda on C_p and γ

For gas turbine performance calculations, it is important to study the effects of fuel chemistry in the evaluation of caloric properties for combustion products. The isobaric heat capacity will increase with H/C ratio as illustrated in Fig.

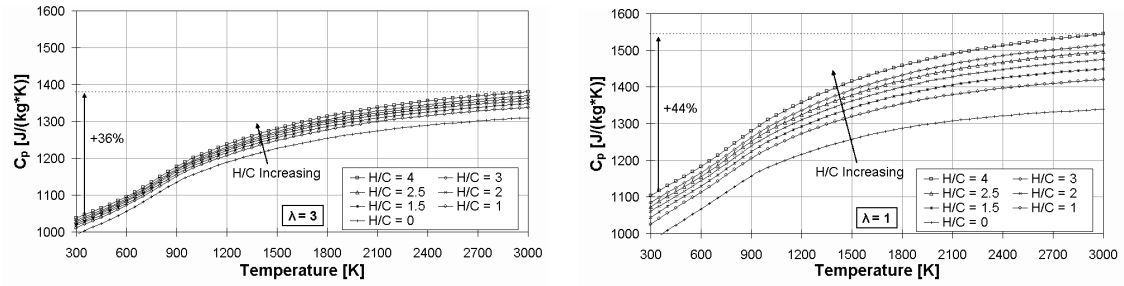

Figure 4.7: Effect of H/C ratio on isobaric heat capacity for combustion products of a weak mixture (left) and a stoichiometric mixture (right).

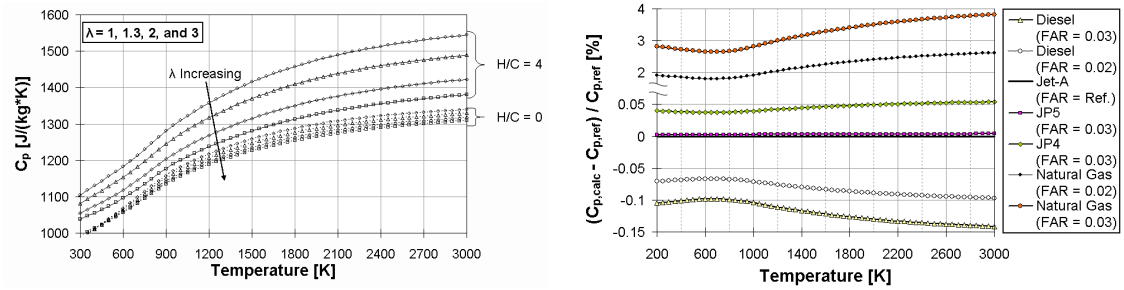

Figure 4.8: Effect of H/C ratio and λ on isobaric heat capacity for combustion products (left) and percentage deviation of isobaric heat capacity values calculated for combustion products of various fuels from Jet-A (right).

4.7. As expected, the effect of H/C ratio is more important as the mixture gets richer. Moreover, when moving from a weak mixture ($\lambda = 3$) to a stoichiometric one ($\lambda = 1$), C_p will not only become more sensitive to H/C ratio but also to temperature; it can be observed that variation of the value of isobaric heat capacity, for the same range of temperatures (300 [K] to 3000 [K]), rises from 36% for the weak mixture to as much as 44% for the stoichiometric mixture.

Some fluid models, based either on tables or polynomials, can only account for combustion products of a particular fuel. For example, the PROOSIS (PRopulsion Object Oriented SImulation Software) [76–78] standard component fluid model [182] uses caloric property tables for combustion products of Jet-A. Also, some of the polynomials in reference [88] are presented as being suitable for combustion products of kerosene and diesel. As discussed earlier, isobaric heat capacity for combustion products is dependent on the H/C ratio of the fuel used. For fuels with similar H/C ratio, minor deviations would be expected. For fuels with significantly different H/C ratios the errors should not be ignored, and therefore, for fully rigorous thermodynamic calculations, appropriate tables or

polynomials should be used. High values of FAR will also increase deviations since the mixture tends to move further away for the original dry air composition; for FAR = 0 all deviations will be zero.

Isobaric heat capacities for combustion products of various fuels are compared in Fig. 4.8. As expected, using Jet-A tables for estimating the caloric properties of JP-4, JP-5, and Diesel combustion productions will yield results with relatively small and perhaps acceptable - errors that are within the same order of magnitude as the uncertainty of the ideal-gas assumption [183]. One should note however, that these errors are systematic and will essentially stack on top of the existing uncertainty in the system. For accurate gas turbine performance calculations sources of systematic errors such as these should be removed. Especially, for combustion products of natural gas, where deviations in isobaric heat capacity compared to Jet-A can be as much as 4%, dedicated tables or polynomials should definitely be used.

4.7 Uncertainty at component level

4.7.1 Flow area calculations

At each station of the engine the working fluid can be fully defined by a unique set of twelve fluid-thermodynamic parameters. A typical fluid model for an engine performance code comprises of thermodynamic functions to calculate the unknown local flow properties, at any point (inlet, outlet or intermediate) of any gas turbine component provided one of a set of twelve compatible input options is satisfied. In this section the behavior of one of such functions has been studied with respect to dissociation. The inputs used were mass flow rate, total temperature, total pressure, FAR, and Mach number. This type of input would typically be used during design point performance calculations for calculating the effective flow area at a given engine station.

The effects of dissociation in calculating the total to static pressure ratio and velocity are highly sensitive to total temperature and Mach number, as illustrated in Fig. 4.9. For high total temperatures, the discrepancy in pressure ratio can be as much as 2% for sonic conditions, and well over 4% for supersonic conditions. Similarly, the discrepancy in velocity can be as much as 2% for low subsonic

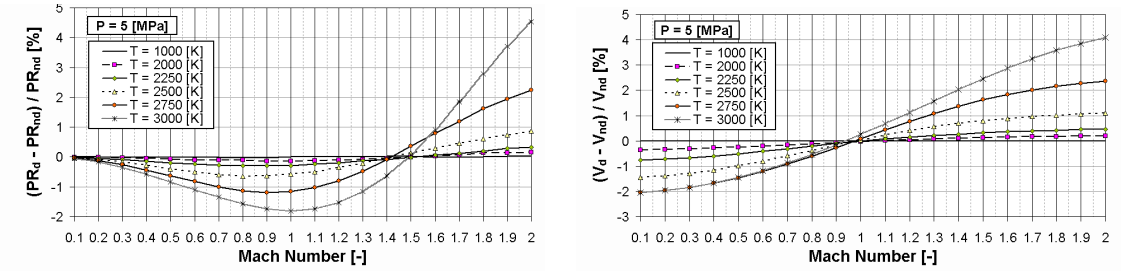

Figure 4.9: Percentage deviation of total to static pressure ratio (left) and velocity (right) for values calculated for chemical equilibrium from no dissociation values.

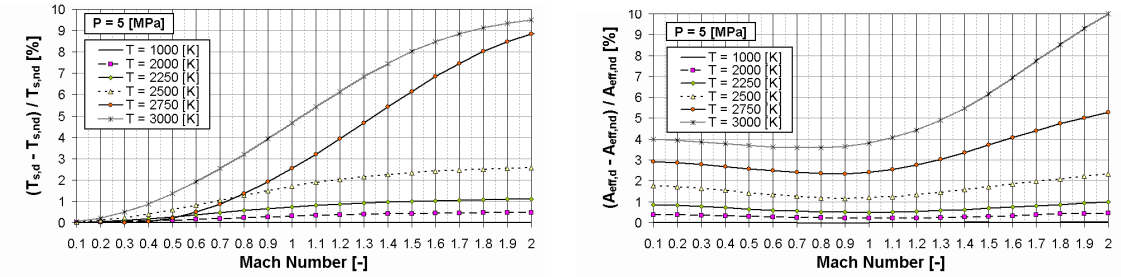

Figure 4.10: Percentage deviation of static temperature (left) and effective flow area (right) for values calculated for chemical equilibrium from no dissociation values.

conditions, and nearly 4% for supersonic conditions. As Mach number increases in the supersonic range of values, dissociation effects become more and more sensitive to total temperature.

The effects of dissociation in calculating the static temperature are also highly sensitive to total temperature and Mach number, as illustrated in Fig. 4.10. For high temperatures, the discrepancy can be as much as 5% for subsonic conditions, and well over 9% for supersonic conditions. It was concluded earlier in this work, that dissociation effects in evaluating caloric properties for relatively cold components (i.e. $T \leq 1500$ [K]) can be negligibly small. It can easily be observed in the same figure that the uncertainty in estimating the effective flow area for cold components of gas turbines, such as bypass ducts and compressors, is also negligibly small; and it is certainly smaller than the uncertainty induced by ignoring real gas effects. The same conclusion however cannot be drawn for relatively hot components. The errors induced by ignoring dissociation effects during the calculation of the effective flow area of a military afterburner running at nearly stoichiometric conditions as well as the exit area of the con-di nozzle

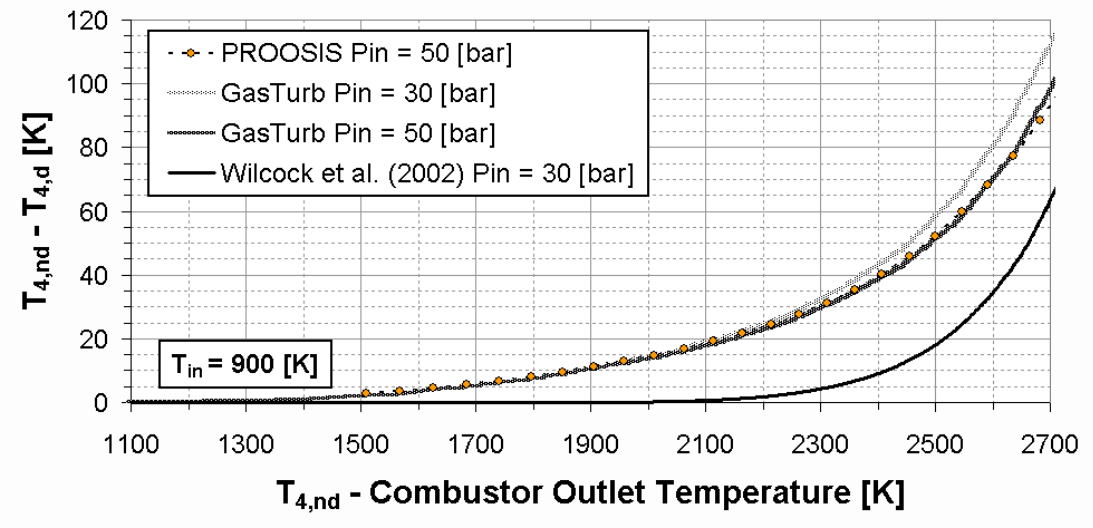

Figure 4.11: Deviation of combustor outlet temperature for values calculated for no dissociation from chemical equilibrium values for different fluid models used.

downstream, can be more than 3% and should not be ignored. Errors in velocity and effective flow area calculations for a high overall pressure ratio (OPR) gas turbine combustor can be as much as 2% and 3% respectively, and should also not be ignored.

4.7.2 Heat addition and expansion calculations

As mentioned earlier, ignoring dissociation effects for hot components can result in significant errors in performance calculations. In this section, the errors in heat addition and expansion calculations, caused by ignoring dissociation effects, are discussed.

Taking a compressor delivery temperature of 900 [K], combustion calculations were performed for a range of fuel to air ratios, both with and without accounting for the effects of dissociation. This isolated component study was performed using the fluid models from two commercially available gas turbine performance simulation codes, PROOSIS and GasTurb [24]; both codes use fluid tables produced with CEA [188] to account for dissociation effects and assume full chemical equilibrium. Results from this study are illustrated in Fig. 4.11; consistent data from reference [194] have also been plotted.

Wilcock et al. [194] concluded in their study that for combustor outlet tem-

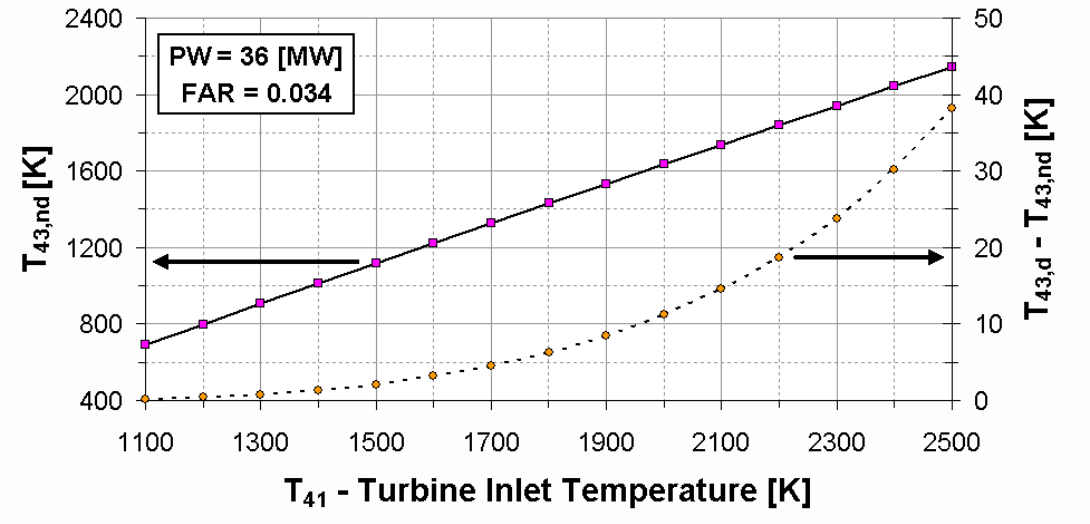

Figure 4.12: Deviation of turbine outlet temperature for values calculated for chemical equilibrium from no dissociation values.

peratures (T_4) less than 2100 [K] the inclusion of dissociation effects alters the temperature by less than 1 [K]. Their results were based on a simplified dissociation model that ignored NO_x and OH formation. It can be seen through Fig. 4.11 that when a more rigorous version of the reaction steps is considered then the results are significantly different. The actual temperature difference for combustor outlet temperatures of 2100 [K] can be as much as 20 [K], if full chemical equilibrium is considered. It can be concluded that dissociation effects in heat addition calculations become first noticed at 1500 [K], and significant at 1800 [K]. Also, increasing pressure will tend to reduce the effects of dissociation for temperatures greater than 2300 [K].

Ignoring dissociation effects in expansion calculations can also result in significant errors. Taking a work requirement (PW) of 36 [MW] and a FAR of 0.034, expansion calculations were performed for a range of turbine inlet temperatures (T_{41}), both with and without accounting for the effects of dissociation. As illustrated in Fig. 4.12, dissociation effects in expansion calculations become first noticed at 1500 [K], and significant at 1800 [K]. The actual difference in turbine outlet temperature (T_{43}) for inlet temperatures of 1800 [K] was found to be nearly 7 [K].

It must be noted, that when dissociation effects were taken into account, full chemical equilibrium was assumed as an ideal scenario, for both head addition and expansion calculations. In practice however, insufficient residence times and

fast local chilling of reactions – for example due to contact with the cooling air – will result in full chemical equilibrium not being reached in the combustor and dissociated species still being present in the final mixture in the turbine outlet (i.e. frozen composition). It can therefore be concluded that even when full chemical equilibrium is assumed, there is still significant thermo-fluid modelling induced uncertainty in the performance calculations; determining the level of this uncertainty experimentally for a particular engine design is not a trivial task, if possible at all.

4.8 Uncertainty at engine system level

In this section, an attempt was made to study how the choice of the fluid model affects engine design point performance calculations. For the purpose of this work, various technical models were used - utilising the flexibility of the developed fluid component for TERA2020. All engine technology parameters were kept constant including component efficiencies, pressure losses and maximum permissible T_4 levels. The differences encountered in the engine performance predictions are discussed.

If dissociation effects are ignored, variability in the calculated values of corrected mass flow, total pressure and total temperature throughout the gas path is confined to 1%, 1.3%, and 2 [K] band, respectively. This is illustrated in Fig. 4.13 and Fig. 4.14. If dissociation effects are taken into account then the calculated values of corrected mass flow, total pressure and total temperature can vary from the "no dissociation" values as much as 3%, 4%, and 12 [K], respectively. These large deviations originate mainly from the performance calculations in the high pressure turbine and should not be ignored. They can be attributed to the different working medium composition (and hence, different caloric properties) when dissociation effects are taken into account.

For major performance parameters the induced uncertainty from the various technical models is 0.3% and is of the same order of magnitude as with the uncertainty in the calculation of isobaric heat capacity presented earlier in this chapter. An exception to this is the hot nozzle effective area which can vary by as much as 1%, as illustrated in Fig. 4.14. If dissociation effects are taken into account then the calculated values of fuel mass flow and net thrust can vary by

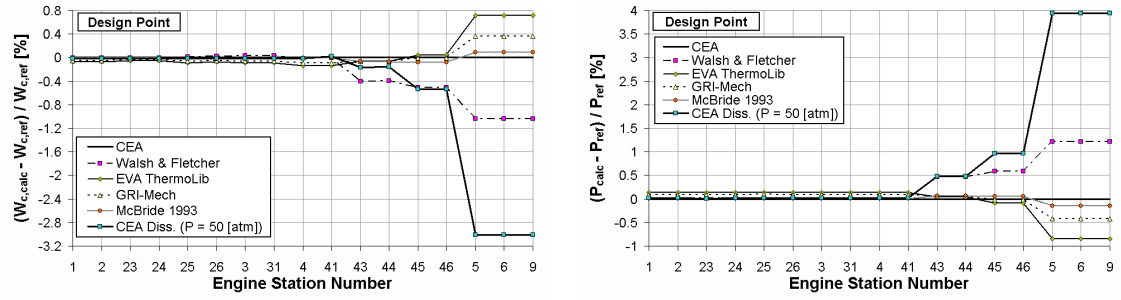

Figure 4.13: Percentage deviation of gas path corrected mass flow (left) and gas path pressure (right) predictions for an intercooled engine for different fluid models used.

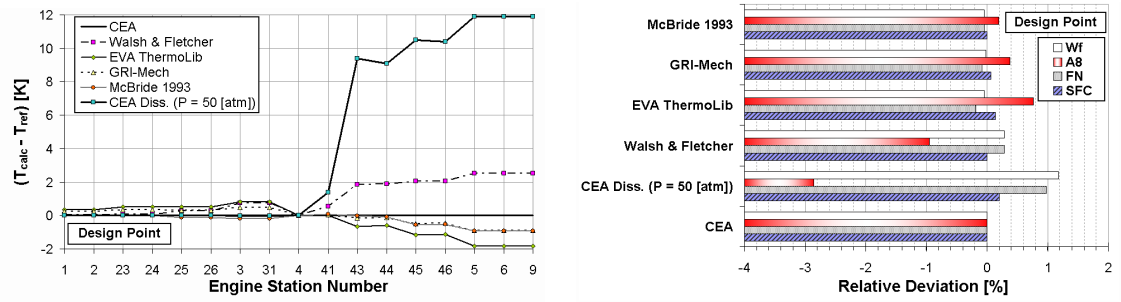

Figure 4.14: Absolute deviation of gas path temperature (left) and percentage deviation of major performance parameter (right) predictions for an intercooled engine for different fluid models used.

more than 1%, while the required hot nozzle effective area can vary by as much as 3%. The deviations in net thrust and hot nozzle effective area can mainly be attributed to propagating errors originating from the high pressure turbine expansion calculations. The deviations in fuel mass flow are attributed to the errors generated in the combustor heat addition calculations when dissociation effects are ignored. The uncertainty in heat addition and expansion calculations at high temperatures was discussed in section 4.7.2.

4.9 Uncertainty at aircraft system level

TERA2020 was utilised for analysing the variability induced at aircraft system level by implementing different fluid models in gas turbine calculations. First, the performance of an intercooled engine with year 2020 entry into service level of technology was estimated using different technical models for caloric properties. These results were fed into the aircraft performance, emissions predictions and

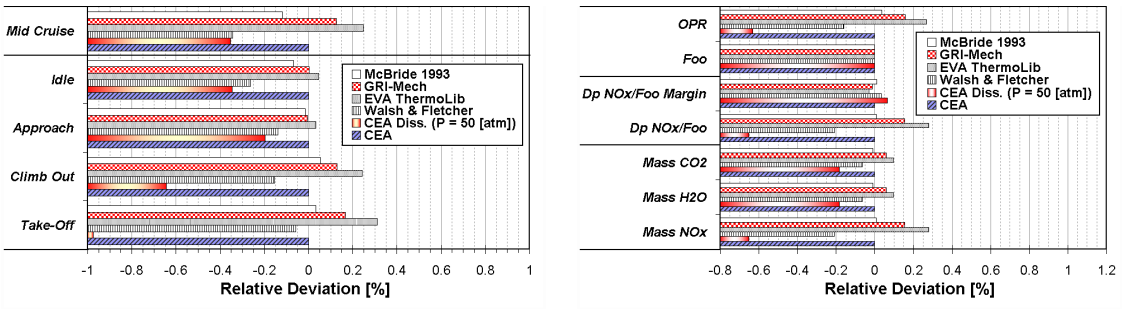

Figure 4.15: Percentage deviation of NO_x emission index (left) and typical LTO parameters (right) predictions for different fluid models used.

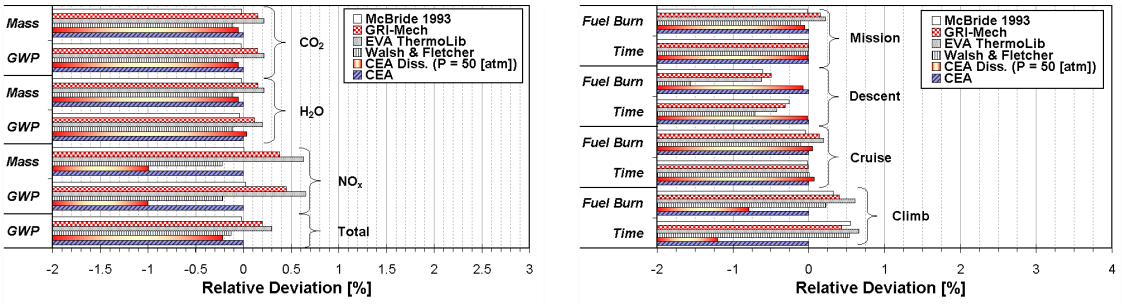

Figure 4.16: Percentage deviation of pollutant mass and GWP (left) and segment time and fuel burn (right) predictions for different fluid models used.

environmental impact modules of TERA2020. While switching from one fluid model to another, the same design point values were used such as bypass ratio, OPR, efficiency and/or pressure loss for engine components, and combustor outlet temperature. For all fluid models, the engine was run at the same thrust for the ICAO (International Civil Aviation Organization) emissions certification points [64], and at the same combustor outlet temperatures for the climb and descent ratings as well as for the mid-cruise point.

In general, the accuracy/uncertainty of an overall engine model will always be better than the mean accuracy/uncertainty of the individual component estimates as long as systematic errors are carefully examined and reduced to acceptable levels to ensure error propagation does not cause significant discrepancies. In those cases were dissociation is not important (i.e. for engine designs with relatively low combustor outlet temperatures), the uncertainty of the various technical models used for gas turbine thermo-fluid modelling can be ignored for multi-disciplinary simulations at aircraft system level. This is due to the fact that the overall level of confidence may be considerably low in highly conceptual studies; many assumptions will need to be made at this stage of the design

process and it's the overall trends that are important rather than the absolute values.

For the intercooled engine design studied herein the NO_x emission index predictions for the ICAO and mid-cruise points were found to vary by less than 1%, as can be observed in Fig. 4.15. Accounting for dissociation is essentially more important for take-off and climb-out where combustor outlet temperatures are higher. Typical parameters calculated for the ICAO LTO (Landing and Take-Off) cycle, with and without accounting for dissociation effects, can vary as much as 0.7% and 0.3%, respectively. The error in calculating the D_pNO_x/F_{oo} parameter can be considered negligible since the uncertainty of a P_3T_3 (or any other similar) semi-empirical emissions prediction model can be as much as 20% when extrapolating at the high OPR values expected for an intercooled cycle (typically much higher than 50).

The total mass of each gaseous pollutant calculated for an aircraft long range mission and its assorted Global Warming Potential (GWP) can vary as much as 1%, as illustrated in Fig. 4.16. It can be argued that taking into account dissociation effects reduces systematic errors in the calculation of pollutant mass and GWP. Nevertheless, these errors are also well within the uncertainty of the environmental impact model and can therefore be considered negligible.

The predicted climb time and corresponding fuel burn reduces by 1.2% and 0.8%, respectively, when dissociation effects are taken into account. These differences are attributed to the increased thrust being predicted for the same combustor outlet temperature; they are averaged out though by the cruise segment having to last just a little bit longer to achieve a given range. Although the variability in calculating the total time and fuel burn was found to be less than 0.25%, as illustrated in Fig. 4.16, it should be noted that ignoring dissociation effects will essentially introduce a systematic error in the predictions; for accurate block fuel predictions dissociation effects should not be ignored. It can therefore be concluded that accurate modelling of the working fluid is essential, especially for assessing novel and/or aggressive cycles at aircraft system level.

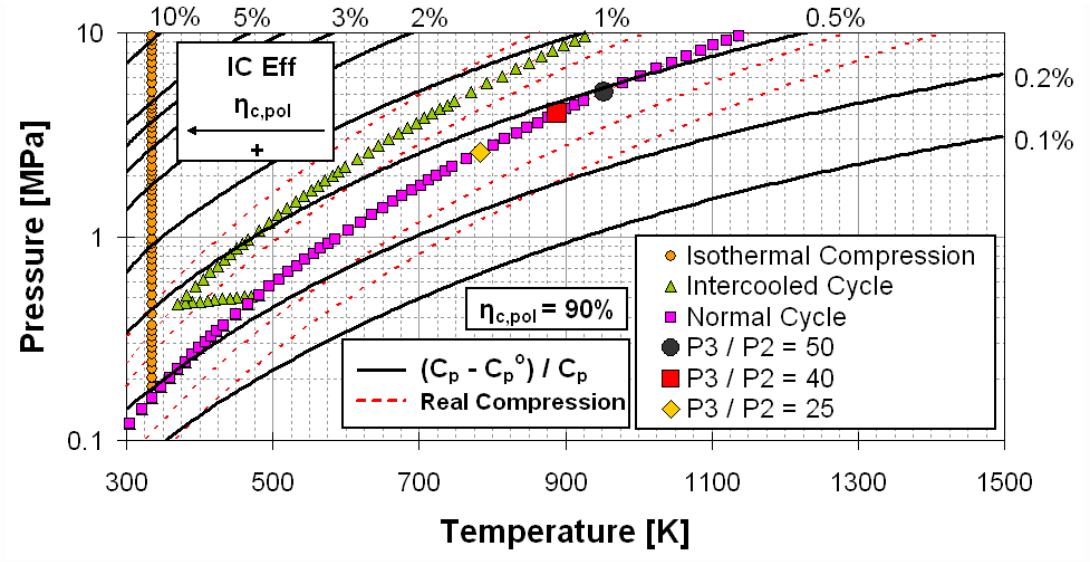

Figure 4.17: Percentage deviations of isobaric heat capacities calculated for dry air considering real gas behavior from values considering an ideal gas mixture (adapted for novel cycles from [183]).

4.10 Validity of the ideal gas assumption

The assumption of real gas is rarely used for aero engine calculations i.e. C_p being a function of temperature and pressure. In most gas turbine performance codes, the assumption of ideal gas (sometimes also referred to as half-ideal) is used i.e C_p being only a function of temperature. Temperatures and pressures in the gas path will typically be calculated using the enthalpy and entropy relations presented earlier in [88]. For teaching purposes often the assumption of perfect gas will be made i.e. C_p being constant.

A comparison of the calculated values of isobaric heat capacity assuming a real gas from values obtained considering an ideal gas - performed for a range of temperatures and pressure of dry air - is presented in Fig. 4.17 (continuous black lines). Compression lines for normal and intercooled cycles have been plotted for ISA (International Standard Atmosphere) SLS (Sea-Level Static) conditions; the ideal isothermal compression line has also been included. The plotted dashed lines in this chart are compression lines of dry air for a polytropic efficiency of 90% and various ambient temperatures.

For current and future novel propulsion cycles the following trends are illustrated

in this chart:

- It is only within a small region of low temperatures and high pressures (upper left corner) that the discrepancies are seriously high. The ideal gas law holds well for aero engines currently in service.
- For an intercooled cycle with a high OPR the discrepancies cannot be ignored for rigorous performance calculations.
- Increasing OPR - which is the current technological trend in aero engine design - diminishes the validity of the ideal gas assumption.
- Increasing the compression polytropic efficiency - which is the current technological trend in component design - diminishes the validity of the ideal gas assumption.
- An increase in intercooler hot stream temperature drop (i.e. effectiveness) will diminish the validity of the ideal gas assumption. This is especially true at lower IPC pressure ratios if an intercooled turbofan design is considered.
- If the ideal isothermal compression process is to be considered - perhaps within a novel cycle assessment - then the ideal gas assumption will not hold and significant calculation errors will be induced.

Finally, if dissociation effects are considered, the errors induced by assuming an ideal gas instead of a real gas are still negligible for turbine calculations since expansion is done at generally high temperatures. It can be concluded that real gas behavior is not negligible at high pressures and low temperatures and particularly when approaching the condensation point of water.

4.11 Conclusion

The research effort presented in this chapter mainly focused on a comprehensive analysis of typical thermo-fluid modelling for gas turbine performance codes and the potential induced uncertainty in the calculations. The fluid model developed for the engine performance module of TERA2020 was described and the assumptions made and the uncertainties induced were examined. Several analyses, which demonstrate the effects of composition, temperature and pressure

on caloric properties of working mediums for gas turbines, have been presented. The working mediums examined include dry air and combustion products for various fuels and H/C ratios. The errors induced by ignoring dissociation effects have also been discussed. The uncertainty induced in calculations by a) using common technical models for evaluating fluid caloric properties and b) ignoring dissociation effects was examined at three different levels: i) component level, ii) engine level, and iii) aircraft system level. Essentially, an attempt was made to shed light on the trade-off between improving the accuracy of a fluid model and the accuracy of a multi-disciplinary simulation at aircraft system level, against computational time penalties. The validity of the ideal gas assumption for future turbofan engines and novel propulsion cycles was discussed.

The main findings can be summarised as follows:

- In general, dissociation becomes first noticed at 1500 [K], and significant at 1800 [K].
- Using constant values of isobaric heat capacity and γ, instead of fully rigorous calculations, can result in large calculation errors, and even in the prediction of wrong trends. It should therefore be avoided even for crude estimates within the educational procedure.
- The uncertainty of various technical models for evaluating the isobaric heat capacity was found to be considerably high (0.3%). This uncertainty is within the same order of magnitude as the uncertainty induced by not modelling real gas effects in modern gas turbine engines.
- For combustion products of natural gas dedicated tables or polynomials should be used. Errors in evaluating the isobaric heat capacity can be as much as 4%, if the tables or polynomials used were originally produced for combustion products of Jet-A.
- Errors induced by not accounting for dissociation effects in velocity and effective flow area calculations, for military afterburners or high OPR combustors, are significant. For heat addition and expansion calculations, the errors are also significant at temperatures greater than 1800 [K].
- The effects of dissociation on major performance parameters during design-point and off-design performance calculations are significant.

- Dissociation effects can generally be ignored for NO_x emissions predictions with P_3T_3 methods, and perhaps for NO_x environmental impact assessments; the errors induced are more than an order of magnitude smaller compared to the uncertainty of the semi-empirical prediction methods that are typically used.

- The uncertainty of the various technical models used for gas turbine fluid modelling can be ignored in many cases for multidisciplinary simulations at aircraft system level. This is due to the fact that the overall level of confidence for such a simulation may be considerably low in highly conceptual studies since many assumptions would need to be made at this stage of the design process. For accurate block fuel predictions dissociation effects should not be ignored as this introduces a systematic error in the calculations.

- For an intercooled cycle with a high OPR the ideal gas assumption does not hold very well and if the ideal isothermal compression process is to be considered significant calculation errors should be expected.

The main conclusion coming out of this work is that the uncertainties in gas turbine thermo-fluid modelling are not negligible, and should not be ignored in neither analytical gas turbine studies or within the educational procedure. Future engineers need to be well aware of the induced uncertainty in their calculations and treat their assumptions and results accordingly. Although, some of the simplifications made were certainly justifiable for the first turbofan engine designs - if one considers the computational means available during that period - performance engineers should use them nowadays under caution for conceptual design of future propulsion systems.

The accuracy/uncertainty of an overall engine model will always be better than the mean accuracy/uncertainty of the individual component estimates as long as systematic errors are carefully examined and reduced to acceptable levels to ensure error propagation does not cause significant discrepancies. The results obtained demonstrated that accurate modelling of the working fluid is essential, especially for assessing novel and/or aggressive cycles at aircraft system level. Where radical design space exploration is concerned, improving the accuracy of the fluid model will need to be carefully balanced with the computational time penalties involved.

A strong theoretical foundation was produced in this work but additional effort still needs to be taken to address further issues including empirical estimation of fluid composition following fast chilling of products of dissociation, using simple but robust models. Future research activities could address further issues including an analysis of the trade-off between improving the accuracy of multi-disciplinary simulations at aircraft system level - by accounting for real gas effects - against computational time penalties induced by the increased modelling complexity.

4.12 Outlook

The development of a multi-disciplinary aero engine conceptual design tool, TERA2020, was discussed in Chapter 2, while details on individual TERA2020 modules were given in Chapter 3. In this chapter, a systematic assessment of the impact of thermo-fluid modelling on the accuracy of the TERA2020 tool was carried out, while accuracy limitations in assessing novel engine core concepts as imposed by current practice in thermo-fluid modelling were identified. In the next chapters, TERA2020 will be used for studying the potential of novel low pressure spool and core technologies for reducing engine emissions.

Chapter 5

Low pressure system component advancements

Improvements in engine propulsive efficiency, as a way of reducing emissions from turbofan engines, is discussed in terms of specific thrust reduction; the TERA2020 tool is used for quantifying the potential benefits from novel technologies for three low pressure spool turbofan architectures. The impact of failing to deliver specific component technologies has been quantified, in terms of power plant noise and CO_2 emissions.

N.B. *The work presented in this chapter has been a collaborative effort between Cranfield University, Chalmers University, Volvo Aero, and ISAE/SUPAERO and has been published in the following papers:*

> K.G. Kyprianidis, D. Au, S.O.T. Ogaji, and T. Grönstedt. Low Pressure System Component Advancements and its Impact on Future Turbofan Engine Emissions. In *ISABE 2009 Proceedings, ISABE-2009-1276*, Montreal, Canada, September 2009.
>
> T. Grönstedt, A. Lundbladh, S.O.T. Ogaji, P. Pilidis, R. Singh, and K.G. Kyprianidis. Aero Engine Conceptual Design - Part II: Low Pressure System Component Advancements and its Impact on Future Turbofan Engine Emissions. *AIAA Journal of Propulsion and Power*, 2010. under preparation.

5.1 Introduction

Several efforts in the past have successfully targeted the development of models capable of making multidisciplinary assessments of gas turbine engines at a preliminary design stage, and these were discussed in Chapter 2. However, the nature of the work available in the public domain has been to convincingly present the capability of the tools by means of some application examples, rather than to focus on generating results that could be generalised.

Within the European research project VITAL (enVIronmenTALly friendly aero engines) [31], a number of low pressure system component technologies are being investigated. The emerging progress will allow the design of new power plants capable of providing a step change in engine fuel burned and noise generated. An aero engine conceptual design tool like TERA2020 (Techno-economic, Environmental and Risk Assessment for 2020), can prove useful in assessing the impact of engine component technology progress at aircraft system level for the three VITAL configurations, i.e. the Direct Drive TurboFan (DDTF), the Geared TurboFan (GTF) and the Counter-Rotating TurboFan (CRTF). By using the tool to establish sensitivity factors a rapid assessment of the impact of research on the three architectures may be performed. The sensitivities may be formulated in such a way that they, whenever possible on a preliminary design stage, relate component design parameters with engine/aircraft performance. This approach distinguishes itself from the more simplistic approach of assuming an achievement on the module level. For instance, a Low Pressure Turbine (LPT) weight reduction may be computed as a consequence of an increased stage loading parameter relating the stage loading directly to the aircraft performance rather than implicitly through module weight.

For the purposes of this work, sensitivities are firstly produced relating parameters traditionally used to describe component performance, such as allowable shaft torque, low pressure turbine stage loading, fan blade weight and system level parameters. Using these sensitivities an assessment of the impact of failing to deliver specific technology advancements, as researched under the VITAL project, is performed; the impact has been quantified, in terms of power plant noise and CO_2 emissions. Inversely, these results also indicate the relative importance of researching certain component technologies for different engine architectures.

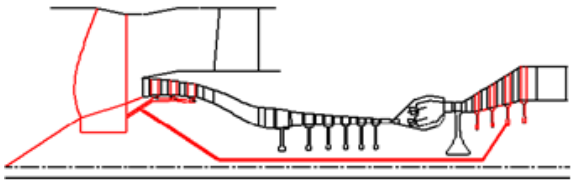

(a) Direct drive turbofan.

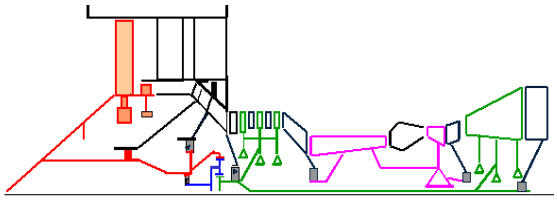

(b) Geared turbofan.

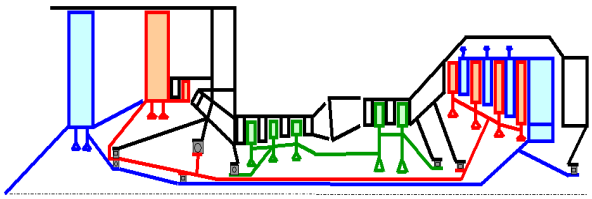

(c) Contra-rotating turbofan.

Figure 5.1: The VITAL engine configurations [206].

5.1.1 The VITAL engine configurations

The VITAL project concentrates on new technologies for the low pressure system of the engine, which enables the development of low noise and low weight fan architectures for very high bypass ratio engines. To achieve these objectives, the VITAL project investigates three different low pressure configurations, leading to low noise high efficiency power plants. The three configurations are the DDTF supported by Rolls-Royce, the GTF by MTU and the CRTF by Snecma, illustrated in Fig. 5.1(a), Fig. 5.1(b) and Fig. 5.1(c) respectively.

The DDTF architecture offers a re-optimised trade-off between fan and turbine requirements considering the low weight technologies introduced by the VITAL programme. The GTF considers combining a fan with a reduction gear train, to allow different rotating speeds for the fan on one hand, and the booster and turbine on the other. The CRTF offers a configuration with two fans turning in opposite directions, allowing for even lower rotational speeds, since the two fan rotors split the loads involved.

5.1.2 Enabling technologies

The technologies being built into the VITAL engines include [3, 206]:

- New fan concepts with the emphasis on two types: counter-rotating and lightweight fans.
- New booster technologies for different operational requirements; low and high speed, associated aerodynamic technologies, new lightweight materials and associated coating and noise reduction design.
- Polymer composites and corresponding structural design and manufacturing techniques are studied in parallel with advances in metallic materials and manufacturing processes.
- Shaft torque density capabilities through the development of metal matrix composites (MMC) and multi metallic shafts.
- Low pressure turbine weight savings through ultra high lift airfoil design, ultra high stage loading, lightweight materials and design solutions.
- Technologies for installations of high bypass ratio engines related to nozzle, nacelle and thrust reverser.

5.2 Establishing the sensitivities

5.2.1 Weight and aerodynamics considerations

Engine efficiency is quantified through the specific fuel consumption parameter SFC, which relates aircraft range $R_{A/C}$ through the specific range parameter SR:

$$R_{A/C} = \int SR \ dW_{A/C} \tag{5.1}$$

Where $W_{A/C}$ is the aircraft weight, and SR can be obtained from:

$$SR = \frac{V}{F_{N,Tot} \cdot SFC} \tag{5.2}$$

Specific range SR relates the total propulsion system thrust $F_{N,Tot}$ with flight velocity V and specific fuel consumption SFC. For a given range $R_{A/C}$ the change in aircraft weight $W_{A/C}$ is equal to the block fuel. The thrust requirement along the mission is dependent both on flight trajectory and aircraft controls as well as the aircraft takeoff weight and aerodynamic characteristics. From this, it is understood that engine efficiency improvements will require less fuel to be carried, which in turn will reduce aircraft wing size and aircraft empty weight, reducing thrust requirement further. It must therefore be appreciated that to establish sensitivities for a given technology a rubberized aircraft model is required and its thrust requirement must be integrated over a specified mission to find the requested values. Similarly engine weight reductions will translate to reduced aircraft takeoff weight which will reduce the aircraft thrust requirement and consequently decrease block fuel. The sensitivities of the technologies component models have to be formulated in such a way that they, whenever possible on a conceptual design stage, relate traditional component design parameters with engine/aircraft performance. This is done in this work either through aerodynamic improvements or weight reductions.

5.2.2 Noise considerations

Based on modelling the Sound Pressure Levels (SPL) generated by the engine components and the aircraft, time-integrated Effective Perceived Noise Levels (EPNL) can be estimated. In terms of noise performance, the engine is associated with the legislative limits set by ICAO [66] for particular engine operating conditions. These limits depend on the number of engines and on the maximum take-off weight of the aircraft. Thus, as the engine performance modelling can predict its off-design operation, it is possible to calculate the EPNL with respect to the three noise certification flight conditions: the sideline, the flyover and the approach points [66]. The different noise sources (fan noise, LPT noise, jet noise etc.) sum up logarithmically through the relation:

$$EPNL_{Tot} = 10log \sum_{i=1,m} 10^{\frac{EPNL_i}{10}} \tag{5.3}$$

The noise sensitivity of source i on EPNL_{Tot}, can be described by the following partial derivative:

$$\frac{\partial EPNL_{Tot}}{\partial EPNL_i} \tag{5.4}$$

It is clear from Eq. 5.3 that the absolute noise levels EPNL_i for all engine related noise sources as well as the airframe have to be established. Therefore, detailed noise source modelling and component modelling has to be carried out for the establishment of the noise sensitivities. The models produced for TERA2020 provide the noise sources as expected from the fundamental models and thermodynamics, for all VITAL engine configurations. Data such as rotational speeds pressures and temperatures, blade speeds and tip Mach numbers are used to establish the component noise contributions as described previously. The separate sources are then combined into an EPNL value expressing the overall noise generation of engines and the airframe. The logarithmic sum, accounting for the combined effect of the various noise sources, can be calculated using Eq. 5.3. Thus, the models developed are able to predict the relative contributions from the different components/sources of the engines. Any changes in noise for a given component/source will then be directly translated to an EPNL change for the combined airframe/engine system.

5.2.3 Step change considerations

Sensitivity factors are determined by carrying out mission analysis with the rubberised wing aircraft model. First, a 1% deficiency in the technology parameters is introduced and then a mission study is carried out; the impact of the change in the generated noise and CO_2 emissions can then be computed. It should be pointed out that some of the parameters relating weight and aerodynamic technology have to be introduced as step changes. These parameters are:

- Switch from conventional intermediate case materials to cold composites (part in bypass stream)
- Switch from conventional manufacturing of intermediate case to titanium fabrication
- Switch to new materials and new manufacturing techniques in the turbine exhaust case
- Switch of shaft material (Aermet100 material to metal matrix shaft)
- Sufficient pressure ratio in the first booster stage to remove a stage
- Sufficient stage loading in the low pressure turbine to remove a stage

To accommodate these step changes in establishing the sensitivities the following algorithm is used:

- First, the change is modelled as fully introduced.
- The weight impact of this change is then estimated.
- Finally the change in CO_2 generation due to a one percent weight change is calculated.

5.3 Impact of technology shortcomings

5.3.1 Sensitivity factors and technology analysis

The main aim of the work presented in this chapter has been to compute useful sensitivity factors and combine them with published information on the technologies developed under the umbrella of the VITAL project [3, 206], in order to assess the impact of failing to deliver expected year 2020 technology for the VITAL engine configurations, in terms of power plant noise and CO_2 emissions. The impact of failing to deliver expected VITAL component aerodynamic improvements and weight reductions, as well as noise improvements has been quantified and is presented in Tables 5.1, 5.2, 5.3, 5.4, 5.5, 5.6, 5.7, 5.8 and 5.9. These results indicate the relative importance of researching certain component technologies for different engine architectures.

Table 5.1: Direct drive turbofan for short range applications weight and aerodynamic technology analysis.

Weight and Aero Technology Objectives	**Sensitivity**	**VITAL Technology Objective**	**Technology Failure Impact**
	$\Delta CO_2(\%)$	$\Delta X(\%)$	$\Delta CO_2(\%)$
Fan blade weight reduction	0.0057		
Fan disc weight reduction	0.0017	30	0.56
Fan statics weight reduction	0.0112		
Fan efficiency improvement	0.8197	2	1.64
Booster first stage pressure ratio	0.0403	15	0.60
Engine structures weight reduction through use of cold composites	0.0090	25	0.23
Engine structures weight reduction through use of titanium fabrication	0.0040	15	0.06
Hot structures weight reduction through materials and manufacturing techniques	0.0039	18	0.07
Shaft weight reduction through material change (allowable stress)	0.0058	50	0.29
Low pressure turbine ultra high lift (Zweifel number)	0.0102	25	0.26
Low pressure turbine ultra high aspect ratio	0.0206	20	0.41
Low pressure turbine ultra high stage load	0.0250	25	0.63
Thrust reverser weight change	0.0253	30	0.76
		Total	5.50

Table 5.2: Direct drive turbofan for long range applications weight and aerodynamic technology analysis.

Weight and Aero Technology Objectives	**Sensitivity**	**VITAL Technology Objective**	**Technology Failure Impact**
	$\Delta CO_2(\%)$	$\Delta X(\%)$	$\Delta CO_2(\%)$
Fan blade weight reduction	0.0088		
Fan disc weight reduction	0.0016	30	1.03
Fan statics weight reduction	0.0239		
Fan efficiency improvement	1.7921	2	3.58
IPC first stage pressure ratio	0.0141	15	0.21
Engine structures weight reduction through use of cold composites	0.0200	25	0.50
Engine structures weight reduction through use of titanium fabrication	0.0075	15	0.11
Hot structures weight reduction through materials and manufacturing techniques	0.0045	18	0.08
Shaft weight reduction through material change (allowable stress)	0.0102	50	0.51
Low pressure turbine ultra high lift (Zweifel number)	0.0116	25	0.29
Low pressure turbine ultra high aspect ratio	0.0234	20	0.47
Low pressure turbine ultra high stage load	0.0396	25	0.99
Thrust reverser weight change	0.0421	30	1.26
		Total	9.04

Table 5.3: Geared turbofan for short range applications weight and aerodynamic technology analysis.

Weight and Aero Technology Objectives	**Sensitivity**	**VITAL Technology Objective**	**Technology Failure Impact**
	$\Delta CO_2(\%)$	$\Delta X(\%)$	$\Delta CO_2(\%)$
Fan blade weight reduction	0.0069		
Fan disc weight reduction	0.0022	30	0.66
Fan statics weight reduction	0.0128		
Fan efficiency improvement	0.8533	2	1.71
Booster first stage pressure ratio	0.0046	15	0.07
Engine structures weight reduction through use of cold composites	0.0103	25	0.26
Engine structures weight reduction through use of titanium fabrication	0.0043	15	0.06
Hot structures weight reduction through materials and manufacturing techniques	0.0030	18	0.05
Shaft weight reduction through material change (allowable stress)	0.0028	50	0.14
Low pressure turbine ultra high lift (Zweifel number)	0.0086	25	0.22
Low pressure turbine ultra high aspect ratio	0.0173	20	0.35
Low pressure turbine ultra high stage load	0.0159	25	0.40
Thrust reverser weight change	0.0260	30	0.78
		Total	4.69

Table 5.4: Geared turbofan for long range applications weight and aerodynamic technology analysis.

Weight and Aero Technology Objectives	**Sensitivity**	**VITAL Technology Objective**	**Technology Failure Impact**
	$\Delta CO_2(\%)$	$\Delta X(\%)$	$\Delta CO_2(\%)$
Fan blade weight reduction	0.0081		
Fan disc weight reduction	0.0015	30	0.90
Fan statics weight reduction	0.0205		
Fan efficiency improvement	1.1451	2	2.29
Booster first stage pressure ratio	0.0248	15	0.37
Engine structures weight reduction through use of cold composites	0.0202	25	0.51
Engine structures weight reduction through use of titanium fabrication	0.0079	15	0.12
Hot structures weight reduction through materials and manufacturing techniques	0.0030	18	0.05
Shaft weight reduction through material change (allowable stress)	0.0056	50	0.28
Low pressure turbine ultra high lift (Zweifel number)	0.0198	25	0.50
Low pressure turbine ultra high aspect ratio	0.0397	20	0.79
Low pressure turbine ultra high stage load	0.0141	25	0.35
Thrust reverser weight change	0.0389	30	1.17
		Total	7.33

Table 5.5: Counter-rotating turbofan for short range applications weight and aerodynamic technology analysis.

Weight and Aero Technology Objectives	**Sensitivity**	**VITAL Technology Objective**	**Technology Failure Impact**
	$\Delta CO_2(\%)$	$\Delta X(\%)$	$\Delta CO_2(\%)$
Fan blade weight reduction	0.0065		
Fan disc weight reduction	0.0025	30	0.69
Fan statics weight reduction	0.0140		
Fan efficiency improvement	0.9036	2	1.81
Booster first stage pressure ratio	0.0434	15	0.65
Engine structures weight reduction through use of cold composites	0.0084	25	0.21
Engine structures weight reduction through use of titanium fabrication	0.0040	15	0.06
Hot structures weight reduction through materials and manufacturing techniques	0.0040	18	0.07
Shaft weight reduction through material change (allowable stress)	0.0055	50	0.28
Low pressure turbine ultra high lift (Zweifel number)	0.0090	25	0.23
Low pressure turbine ultra high aspect ratio	0.0181	20	0.36
Low pressure turbine ultra high stage load	0.0156	25	0.39
Thrust reverser weight change	0.0246	30	0.74
		Total	5.48

Table 5.6: Counter-rotating turbofan for long range applications weight and aerodynamic technology analysis.

Weight and Aero Technology Objectives	**Sensitivity**	**VITAL Technology Objective**	**Technology Failure Impact**
	$\Delta CO_2(\%)$	$\Delta X(\%)$	$\Delta CO_2(\%)$
Fan blade weight reduction	0.0109		
Fan disc weight reduction	0.0043	30	1.32
Fan statics weight reduction	0.0288		
Fan efficiency improvement	1.5081	2	3.02
Booster first stage pressure ratio	0.0438	15	0.66
Engine structures weight reduction through use of cold composites	0.0156	25	0.39
Engine structures weight reduction through use of titanium fabrication	0.0077	15	0.12
Hot structures weight reduction through materials and manufacturing techniques	0.0054	18	0.10
Shaft weight reduction through material change (allowable stress)	0.0133	50	0.67
Low pressure turbine ultra high lift (Zweifel number)	0.0081	25	0.20
Low pressure turbine ultra high aspect ratio	0.0163	20	0.33
Low pressure turbine ultra high stage load	0.0187	25	0.47
Thrust reverser weight change	0.0441	30	1.32
		Total	8.58

Table 5.7: Direct drive turbofan noise technology analysis.

(a) Short range applications.

Noise Source	**Sensitivity** $\Delta X = -1$ $EPNdB$			**VITAL Technology Objective**	**Technology Failure Impact**		
	Take-off	Fly-over	Approach		Take-off	Fly-over	Approach
	$\Delta EPNL(EPNdB)$			$\Delta X(EPNdB)$	$\Delta EPNL(EPNdB)$		
Fan noise	0.730	0.540	0.390	6	4.38	3.24	2.34
LPT noise	0.002	0.002	0.003	4.5	0.01	0.01	0.01

(b) Long range applications.

Noise Source	**Sensitivity** $\Delta X = -1$ $EPNdB$			**VITAL Technology Objective**	**Technology Failure Impact**		
	Take-off	Fly-over	Approach		Take-off	Fly-over	Approach
	$\Delta EPNL(EPNdB)$			$\Delta X(EPNdB)$	$\Delta EPNL(EPNdB)$		
Fan noise	0.840	0.650	0.300	6	5.04	3.90	1.80
LPT noise	0.001	0.002	0.002	4.5	0.00	0.01	0.01

Table 5.8: Geared turbofan noise technology analysis.

(a) Short range applications.

Noise Source	**Sensitivity** $\Delta X = -1$ $EPNdB$			**VITAL Technology Objective**	**Technology Failure Impact**		
	Take-off	Fly-over	Approach		Take-off	Fly-over	Approach
	$\Delta EPNL(EPNdB)$			$\Delta X(EPNdB)$	$\Delta EPNL(EPNdB)$		
Fan noise	0.680	0.560	0.420	6	4.08	3.36	2.52
LPT noise	0.011	0.013	0.030	4.5	0.05	0.06	0.14

(b) Long range applications.

Noise Source	**Sensitivity** $\Delta X = -1$ $EPNdB$			**VITAL Technology Objective**	**Technology Failure Impact**		
	Take-off	Fly-over	Approach		Take-off	Fly-over	Approach
	$\Delta EPNL(EPNdB)$			$\Delta X(EPNdB)$	$\Delta EPNL(EPNdB)$		
Fan noise	0.780	0.640	0.310	6	4.68	3.84	1.86
LPT noise	0.020	0.022	0.049	4.5	0.09	0.10	0.22

Table 5.9: Geared turbofan noise technology analysis.

(a) Short range applications.

Noise Source	**Sensitivity** $\Delta X = -1$ $EPNdB$			**VITAL Technology Objective**	**Technology Failure Impact**		
	Take-off	Fly-over	Approach		Take-off	Fly-over	Approach
	$\Delta EPNL(EPNdB)$			$\Delta X(EPNdB)$	$\Delta EPNL(EPNdB)$		
Fan noise	0.660	0.340	0.280	6	3.96	2.04	1.68
LPT noise	0.003	0.004	0.003	4.5	0.0135	0.018	0.0135

(b) Long range applications.

Noise Source	**Sensitivity** $\Delta X = -1$ $EPNdB$			**VITAL Technology Objective**	**Technology Failure Impact**		
	Take-off	Fly-over	Approach		Take-off	Fly-over	Approach
	$\Delta EPNL(EPNdB)$			$\Delta X(EPNdB)$	$\Delta EPNL(EPNdB)$		
Fan noise	0.700	0.470	0.340	6	4.20	2.82	2.04
LPT noise	0.004	0.008	0.004	4.5	0.02	0.04	0.02

5.3.2 Weight and aerodynamics analysis summary

It can be observed that engine configurations for short range applications with year 2020 projected technology will be less affected by failure to deliver low pressure component advancements than their long range application counterparts, as illustrated graphically in Fig. 5.2. Inversely, reducing CO_2 emissions, through the technologies researched within VITAL, seems to be more challenging for engines designed for short range applications. The overall benefits in terms of CO_2 emissions, as a result of achieving the VITAL technologies, range from 4.7% to 5.5% for short range applications, and from 7.3% to 9% for long range applications. The study increases confidence in the TERA2020 tool since the scenario of total failure (i.e. no progress achieved in any of the VITAL technology areas for the time period from 2000 to 2020) results in a total CO_2 penalty very close to the overall goals of the VITAL project predicted by industry.

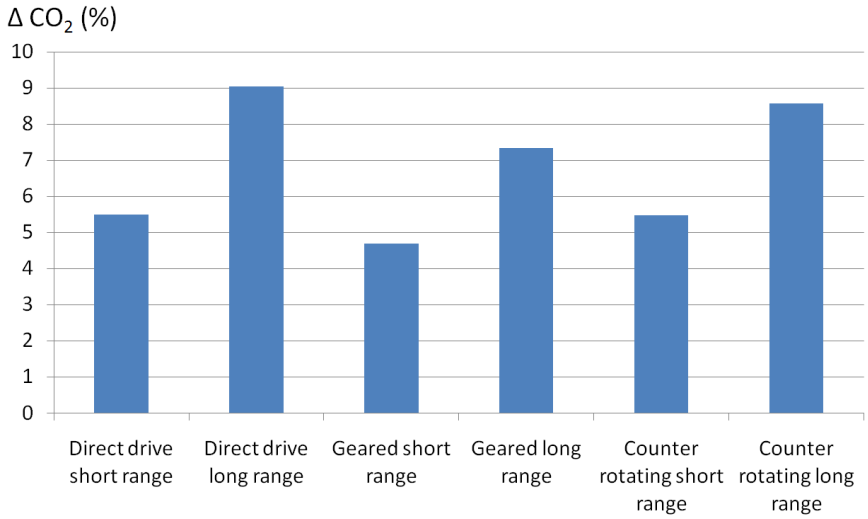

Figure 5.2: Impact of total technology failure.

The larger "snowball" factor, i.e. the impact of a technology change after the engine/aircraft matching has been reoptimised, typically expected for long range applications, is confirmed by the tables. It should also be emphasized that although the sensitivity factors, when multiplied with an achieved technology progress, give a good estimate of its impact, the ultimate measure of technology progress requires a complete reoptimisation of the engine/aircraft system for the given mission.

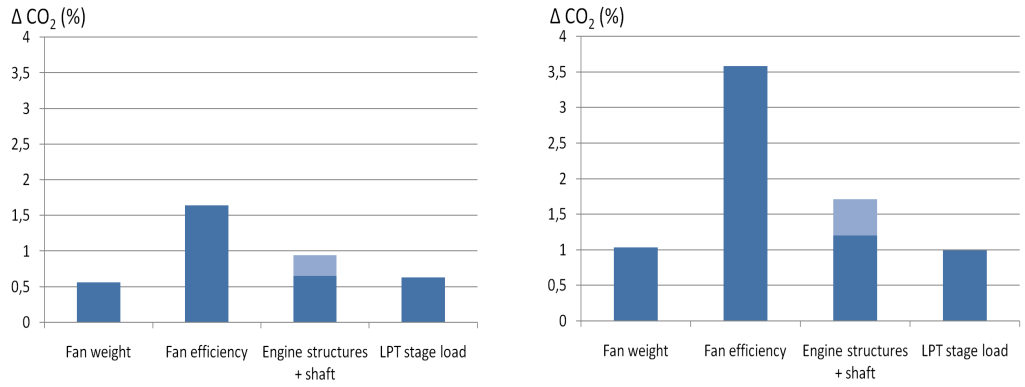

(a) Direct drive short range

(b) Direct drive long range

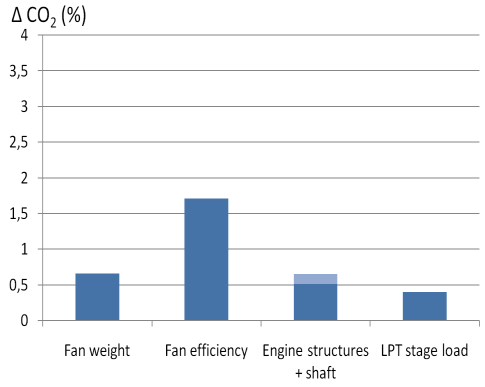

(c) Geared short range

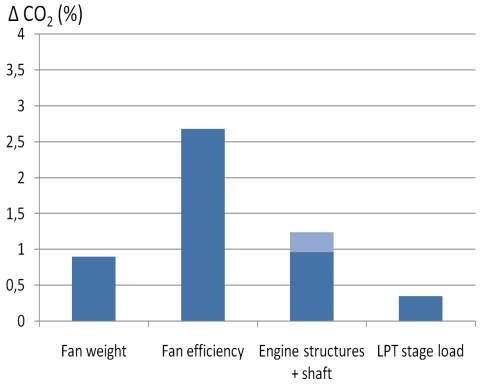

(d) Geared long range

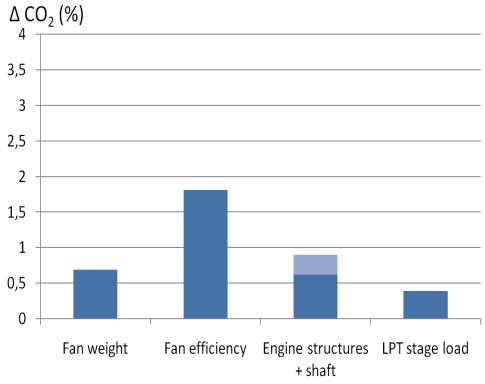

(e) Counter-rotating short range.

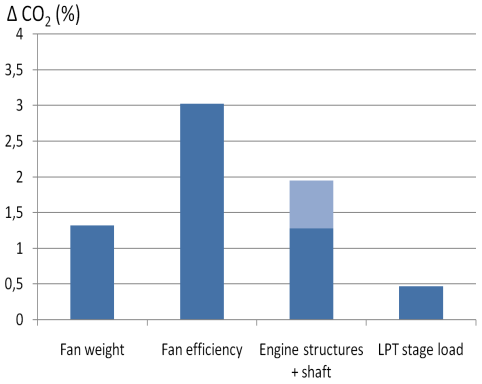

(f) Counter-rotating long range.

Figure 5.3: Impact of individual technology failure.

Looking closer at these results, it can be observed for the VITAL ultra high bypass ratio engines that fan efficiency improvements as well as fan and thrust reverser weight reductions will dominate the projected CO_2 benefits, with an emphasis on long range missions. Failure to achieve these technological goals

will effectively more than halve any CO_2 benefits expected from reducing engine specific thrust and increasing bypass ratio. It can also be observed that although all engine configurations will benefit from the VITAL technologies, some will benefit more than others from certain improvements. For example, low pressure turbine weight reductions and aerodynamic improvements are much more critical for direct drive configurations than geared solutions, as illustrated in Fig. 5.3. Similarly, the impact of improvements in shaft torque density is captured in TERA2020 through a reduced shaft diameter resulting in reduced shaft and surrounding components weight; for geared configurations the benefits predicted are smaller mainly due to the lower shaft torque values encountered.

5.3.3 Noise analysis summary

As can be observed from the presented noise assessments, expected VITAL low pressure turbine noise improvements will not be a key contributor to overall engine noise, with the exception of the geared turbofan engine. The projected future reduction in specific thrust of ultra high bypass ratio engines leads to reduced blade speeds both in the turbine and fan components. In combination with an increased bypass ratio the relative impact of low pressure turbine noise is therefore suppressed.

On the other hand, fan noise remains the most critical noise source for high bypass ratio engines during take-off and fly-over. For approach conditions fan noise continues to remain an important source of overall engine noise while airframe noise becomes the critical contributor.

The relative importance of jet noise as a function of the mission is also quite marked in the sensitivities produced. Since engines optimized for shorter missions generally have higher specific thrust and corresponding jet velocities, jet noise is relatively more important for engines designed for short range missions. In the present work, no jet noise or airframe noise reduction technology assessments are presented due to lack of published information on the VITAL achievements for these noise sources in terms of EPNL.

5.3.4 Example of capturing technology progress

In this work, the LPT stage loading coefficient, ψ, is defined as:

$$\psi = \frac{\Delta h}{\frac{1}{2} \cdot U^2} \tag{5.5}$$

where Δh is the enthalpy drop and U the blade speed. The Zweifel number, Z, quantifies high lift blading and is used to determine the number of blades for a given blade row through the expression:

$$Z = 2 \cdot H \cdot \frac{S}{c} \cdot \cos^2 \alpha_2 \cdot (\tan \alpha_1 - \tan \alpha_2) \tag{5.6}$$

H is the blade height, S is the blade pitch and c is the blade chord. The α_1 and α_2 represent inlet and outlet flow angles respectively. Through the Zweifel number blade lift will relate to blade numbers which will relate to LPT weight which gives engine weight and finally through TERA2020 a block fuel estimate is obtained.

An example of how TERA2020 can be used to capture technology progress is given in Fig. 5.4. The cross sectional images of a three spool ultra-high bypass ratio turbofan configuration with a direct drive fan are given for two levels of technology; year 2000 entry into service and year 2020 entry into service with VITAL low pressure system technology incorporated. Performance data is in both instances set to represent technology levels expected to be available for year 2020 entry into service engines. Note that some parts of the shafts as well as bearings are omitted in the two figures although they are included in the total weight estimate. Note also that the tool estimates technology improvement both in the core and the low pressure system.

The two cross sectional drawings illustrate the level of detail of the output produced by TERA2020 while performing cycle optimization; the need for advanced low pressure turbine aerodynamics becomes critical for engines of low specific thrust, and hence low fan pressure ratio and corresponding rotational speeds. The conventional LPT operates with a stage loading coefficient of 4.5 resulting

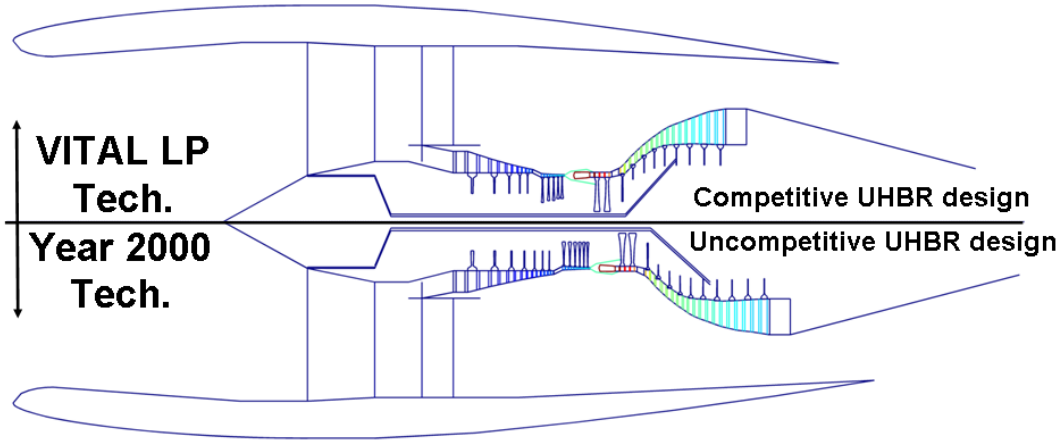

Figure 5.4: Future ultra high bypass ratio engine designed using year 2020 VITAL low pressure spool objective technology (upper half) and year 2000 entry into service technology (lower half).

in a nine stage turbine, whereas the year 2020 LPT uses a value of 5.2. It is also demonstrated how improved aerodynamics of the intermediate and high pressure compressor components will contribute to a lighter and more compact engine. Finally, the use of an MMC shaft can make a future engine more compact and more space made available for the high pressure turbine discs. The Ultra-High Bypass Ratio (UHBR) engine design illustrated in the upper half of Fig. 5.4 may be considered as an optimal one assuming all 2020 technology targets are met. On the other hand, the UHBR engine design illustrated in the bottom half of the figure may be considered as uncompetitive one since important size, weight and SFC penalties (for year 2000 entry into service technology) would shift the optimal specific thrust and bypass ratio levels to higher and lower values respectively.

5.4 Conclusion

In this chapter the TERA2020 tool was used to establish a number of sensitivity factors relating traditionally used component design parameters to engine/aircraft performance parameters. The resulting sensitivity factors allow a straightforward evaluation of the system level impact of component technology research progress. In particular, results were provided for the three VITAL engine configurations, with respect to aerodynamics, weights and noise, for two different

mission definitions. The sensitivity factors were combined with published information on the technologies developed under the umbrella of the VITAL project in order to assess the impact of failing to deliver expected year 2020 technology for the engine configurations in question. More specifically, the impact of failing to deliver specific component improvements has been successfully quantified, in terms of power plant noise and CO_2 emissions and was discussed extensively.

The study also increases confidence in the TERA2020 tool since the scenario of total failure (i.e. no progress achieved in any of the VITAL technology areas for the time period 2000 to 2020) results in a total CO_2 penalty very close to the overall goals of the VITAL project predicted by industry. In the author's opinion, all three engine configurations are optimal designs for the year 2020 and each has its own merits with respects to low technology risk and improved reliability, as well as reduced noise, CO_2 and NO_x emissions. Their commercial competitiveness will therefore largely depend on how the aviation market evolves in the years to come until 2020. Perhaps the most important aspect of this work is that the presented results essentially provide the means for making estimates of the relative merits of future technology investment; the relative importance of certain future aero engine research activities were highlighted for particular engine configurations.

5.5 Outlook

Improvements in engine propulsive efficiency, as a way of reducing emissions from turbofan engines, have been discussed in this chapter in terms of specific thrust reduction. In the next chapter, TERA2020 will be used for addressing the need for higher engine thermal efficiency mainly by exploring benefits from the potential introduction of heat-exchanged cores in future aero engine designs. A thorough discussion on the main drivers that could support such initiatives will be presented.

Chapter 6

Assessment of core technologies and concepts

Improvements in engine propulsive efficiency, as a way of reducing emissions from turbofan engines, were discussed in Chapter 5 in terms of specific thrust reduction. To address the need for higher engine thermal efficiency, TERA2020 is again utilised, this time for exploring benefits from the potential introduction of heat-exchanged cores in future aero engine designs. A thorough discussion on the main drivers that could support such initiatives is presented.

N.B. *The work presented in this chapter has been a collaborative effort between Cranfield University and Chalmers University and has been published in the following paper:*

> K.G. Kyprianidis, T. Grönstedt, S.O.T. Ogaji, P. Pilidis, and R. Singh. Assessment of Future Aero Engine Designs with Intercooled and Intercooled Recuperated Cores. In *ASME TURBO EXPO 2010 Proceedings, GT-2010-23621*, Glasgow, United Kingdom, June 2010.
>
> K.G. Kyprianidis, T. Grönstedt, S.O.T. Ogaji, P. Pilidis, and R. Singh. Assessment of Future Aero Engine Designs with Intercooled and Intercooled Recuperated Cores. *ASME Journal of Engineering for Gas Turbines and Power, GTP-10-1056*, 2010. accepted for publication.

6.1 Enabling core technologies

For conventional cores, increasing OPR and T_{41} depends on future advancements in material and cooling technology. Assuming that only mild further improvements can be achieved in these research fields in the near future, the design focus for more aggressive thermal efficiency improvements could well be redirected to the introduction of heat-exchanged cores in future turbofan designs.

A common textbook misconception about intercooling is that the thermal efficiency of an intercooled core will always be lower than a conventional core's for a fixed OPR and specific thrust. The argument behind this is that the heat removed by the intercooler will largely need to be reintroduced in the combustor by burning more fuel, while the reduction in compression work will only partially compensate for the loss in cycle efficiency, at a fixed specific thrust and T_{41}. Adding the expected intercooler pressure losses in the cycle calculations would further worsen the SFC deficit and make the increase in specific thrust less marked.

However, cycle calculations based on half-ideal gas properties and no dissociation (i.e. isobaric heat capacity dependent on temperature), presented by Walsh and Fletcher [88], give a slightly different picture on intercooling. For a given T_{41}, the optimal OPR for an intercooled core will be much higher than that for a conventional core. Comparing the two concepts at their optimal OPR levels, for a given technology level, can make the intercooled core more attractive with respect to thermal efficiency and not just specific thrust. Canière et al. [207] and da Cunha Alves et al. [208] also reached the same conclusion about the thermal efficiency of the intercooled cycle while studying this concept for gas turbines used in power generation.

Papadopoulos and Pilidis [209] worked on the introduction of intercooling, by means of heat pipes, in an aero engine design for long haul applications. Xu et al. [210] performed a mission optimization to assess the potential of a tubular intercooler. Recent work by Xu and Grönstedt [211] presents a refined tubular configuration estimating a potential block fuel benefit of 3.4%. The work addresses the limitation that short high pressure compressor blade lengths and related low compression efficiencies may impose on engines designed for short range missions, and suggest a novel gas path layout as a remedy to this con-

straint. A design study of a high OPR intercooled aero engine is described in Rolt and Baker [57], while details on the aerodynamic challenges in designing a duct system to transfer the core air into and out of the intercooler are presented by Walker et al. [212].

The introduction of recuperation in an aero engine, for high thermal efficiency at low OPR, has also been the focus of different researchers. Lundbladh and Sjunnesson [213] performed a feasibility study for intercooled and intercooled recuperated engines that consider cycle benefits, weights and direct operating costs. Boggia and Rud [97] provide an extended discussion on the thermodynamic cycle and the technological innovations necessary for realizing the intercooled recuperated core concept. Various aspects of the thermomechanical design of a compact heat exchanger have been presented in [214, 215]. For a comprehensive review on the development activities for recuperated aero engines since the late 60's the interested reader can refer to McDonald et al. [216–218].

In this study it will be shown that an intercooled core may well be designed for a significantly higher OPR, than could otherwise be achieved with a conventional core design, and can hence lead to thermal efficiency benefits, as described in [219]. It will also be demonstrated that high thermal efficiency can also be achieved at low OPR values by means of an intercooled recuperated core coupled with a variable geometry LPT.

6.2 Intercooled core

Some theoretical observations coupled with an assessment at aircraft system level are presented in this section for a future aero engine concept, featuring an intercooled core with a direct drive front fan, as illustrated in Fig. 6.1. The concept is an Ultra High Bypass Ratio (UHBR) design based on 3-shaft layout, with the intercooler mounted inboard of the bypass duct; the installation standard includes a flow splitter and an auxiliary variable geometry nozzle.

All performance calculations assume a year 2020 EIS turbofan engine for long haul applications, and all quoted numbers are at TOC conditions (FL350, ISA +10 [K], M = 0.82). F_N and propulsive efficiency were kept constant in this study by varying BPR and FPR at constant W_2. T_{41} was kept constant, while

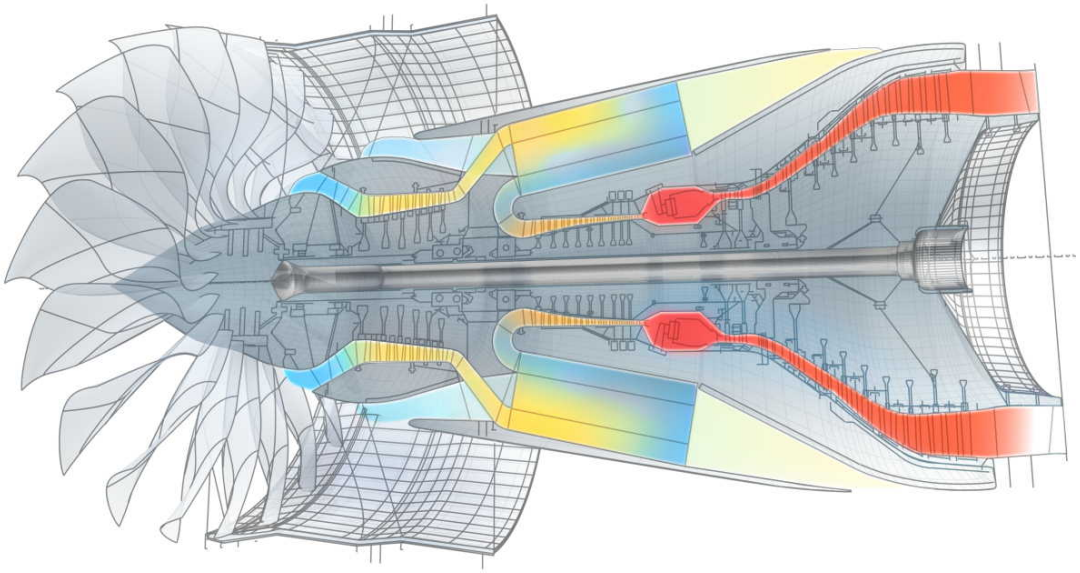

Figure 6.1: Artistic impression of the intercooled core turbofan engine [32].

the HPT and IPT cooling flows were recalculated to maintain a fixed rotor blade metal temperature. The HPC pressure ratio was varied to maintain a fixed OPR.

6.2.1 Intercooling at OPR = 50

Some minor benefits in terms of SFC by introducing intercooling in a turbofan engine with an OPR of 50 are illustrated in Fig. 6.2 for constant (but not equal) turbomachinery polytropic efficiency levels and ideal intercooling i.e. no intercooler pressure losses in the cold and hot stream. As expected, maximising thermal efficiency benefits from intercooling requires a low IPC pressure ratio. For no intercooling, shifting pressure ratio from the IPC to the more efficient HPC can also improve SFC, but a more in-depth analysis could show that this benefit may be limited by HPT design constraints. Core size reduces and hence BPR increases considerably with increasing intercooler effectiveness, as illustrated in Fig. 6.3, in order to maintain the engine specific thrust and W_2 constant; for a given OPR this can partially help compensate the intercooler weight penalty as will be discussed in the aircraft system level assessment section.

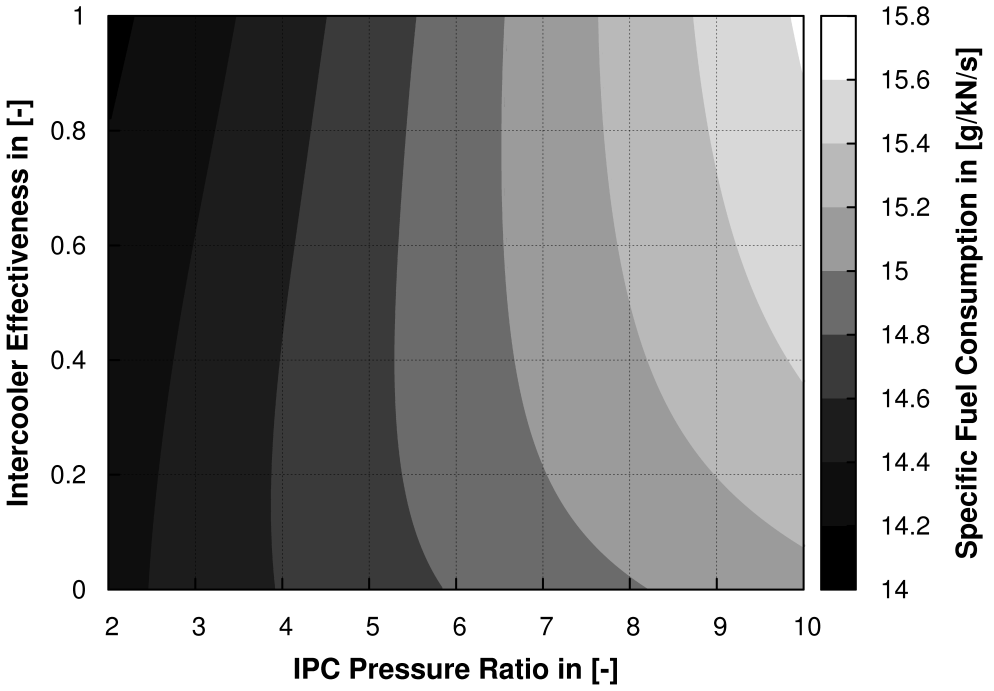

Figure 6.2: SFC benefits from introducing ideal intercooling at OPR = 50.

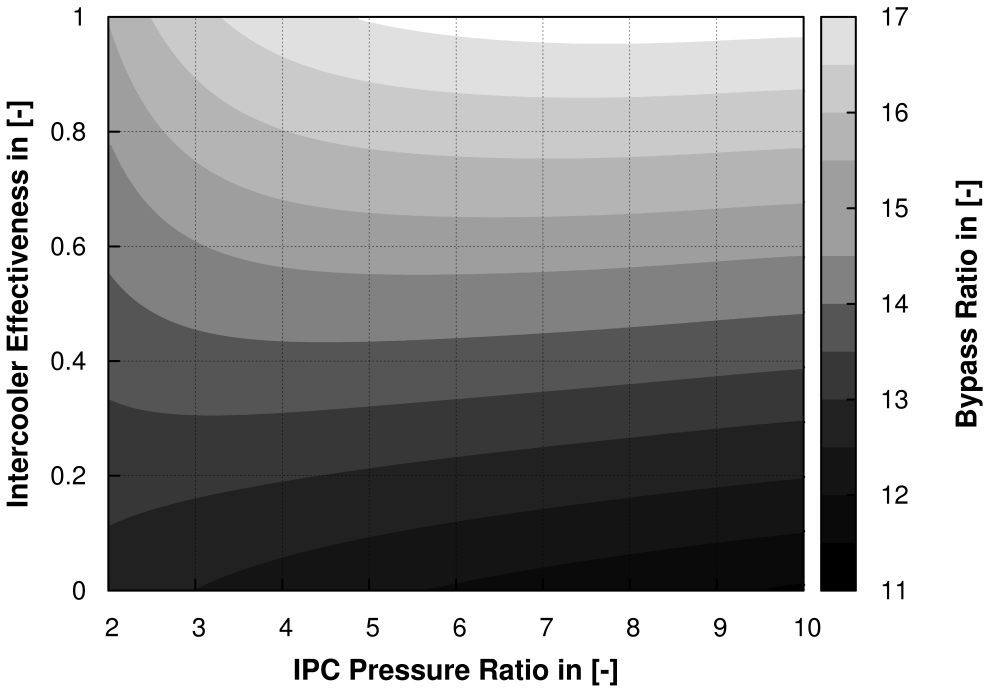

Figure 6.3: BPR variation from introducing ideal intercooling at OPR = 50.

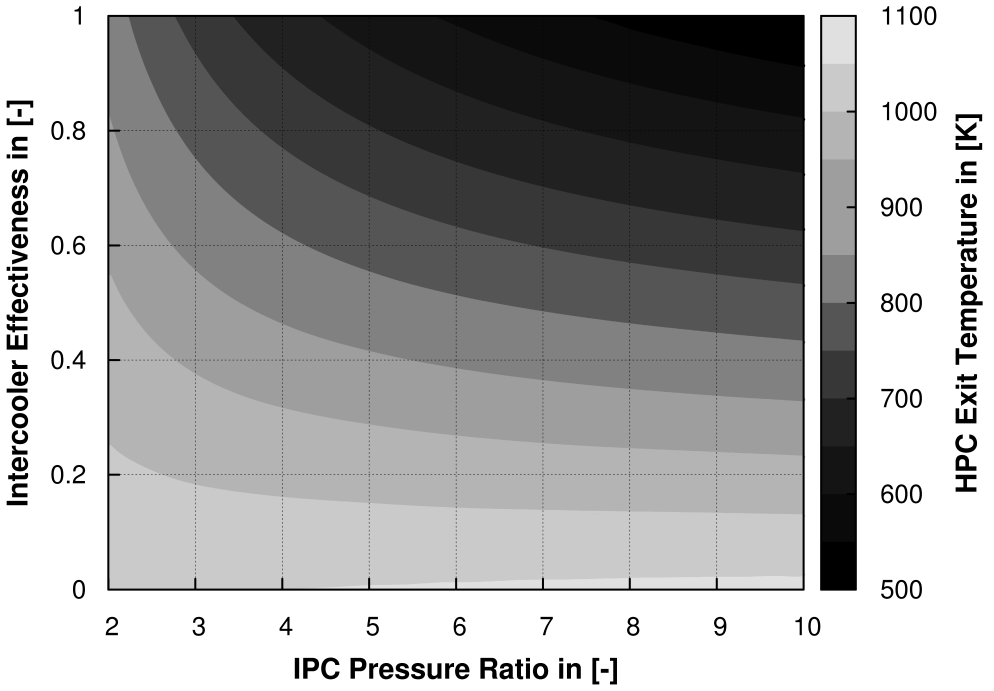

Figure 6.4: Ideal intercooling and HPC delivery temperature at OPR = 80.

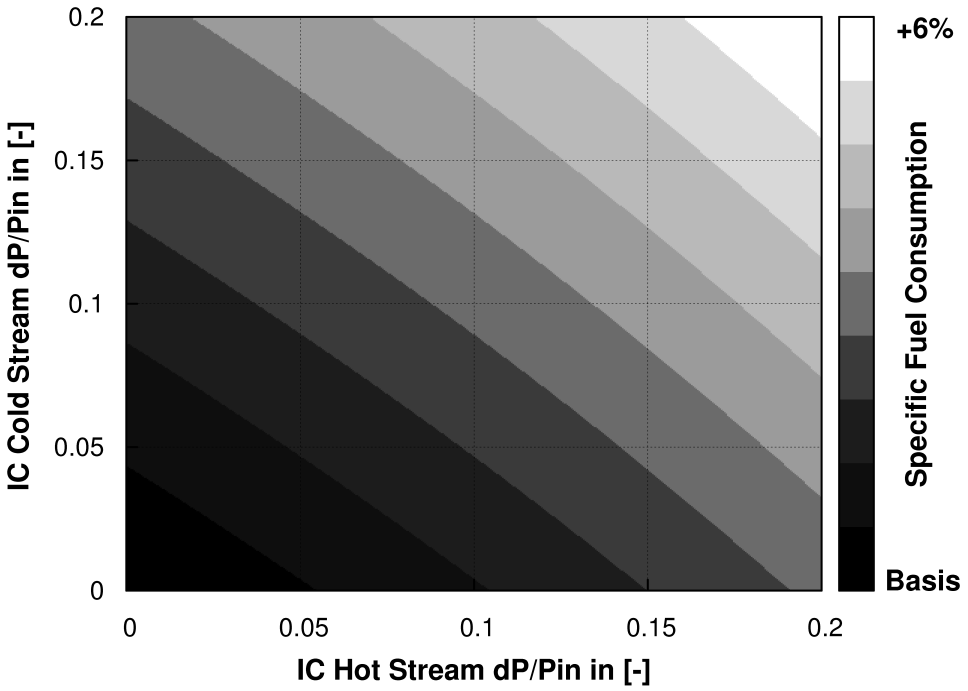

Figure 6.5: The effect of intercooler pressure losses at OPR = 80.

6.2.2 Intercooling at OPR = 80

With an intercooled core, a significantly higher OPR can be realized, for a given HPC delivery temperature limitation imposed by material technology; this is illustrated in Fig. 6.4 for an intercooled engine with an OPR of 80. The trends illustrated in Fig. 6.2 and Fig. 6.3 are still valid at this higher OPR, but the SFC levels are significantly reduced due to the improvement in thermal efficiency; BPR levels are also significantly reduced due to the higher OPR reducing core specific work output at a fixed F_N, W_2 and T_{41}. The importance of keeping intercooler pressure losses low is illustrated in Fig. 6.5; pressure loss levels that are too high could well negate any SFC benefits from an intercooled core.

6.2.3 Variable geometry

The results and analysis presented in the previous sections focused mainly on design point performance. Significant performance benefits may be achieved however at off-design conditions by utilising a variable geometry auxiliary nozzle, or a variable area mixer, to control the amount of cooling flow going through the intercooler, and hence the effectiveness and pressure loss levels at different operating points, as described in [219]. The off-design performance calculations presented in this section were carried out again with TERA2020 using a "frozen" intercooled core engine design for short range applications.

An example of how the auxiliary nozzle variable geometry setting can be utilised to increase net thrust at take-off conditions is illustrated in Fig. 6.6. During this off-design operation, the auxiliary nozzle area is increased to allow more cooling mass flow to go through the intercooler and hence raise heat transfer. An optimal nozzle setting can be identified for this operation; this is due to the fact that intercooler pressure losses also increase, and eventually negate the net thrust benefits associated with higher intercooler effectiveness. The projected benefit from this operation is up to 2% in F_N.

An example of how the auxiliary nozzle variable geometry setting can be utilised to reduce engine SFC during cruise conditions is illustrated in Fig. 6.7. During this off-design operation, the auxiliary nozzle area is reduced to allow less cooling mass flow to go through the intercooler and hence reduce heat transfer. As a result the intercooler pressure losses reduce and hence SFC is also reduced.

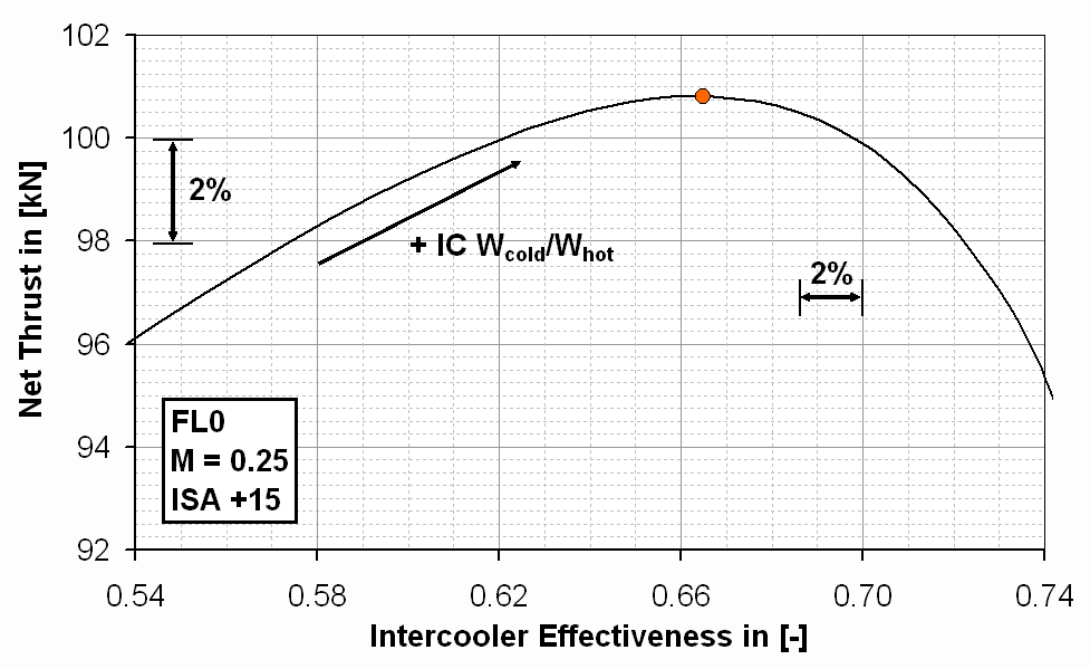

Figure 6.6: Optimising the operation of a variable intercooler nozzle at take-off for an intercooled aero engine for short haul applications.

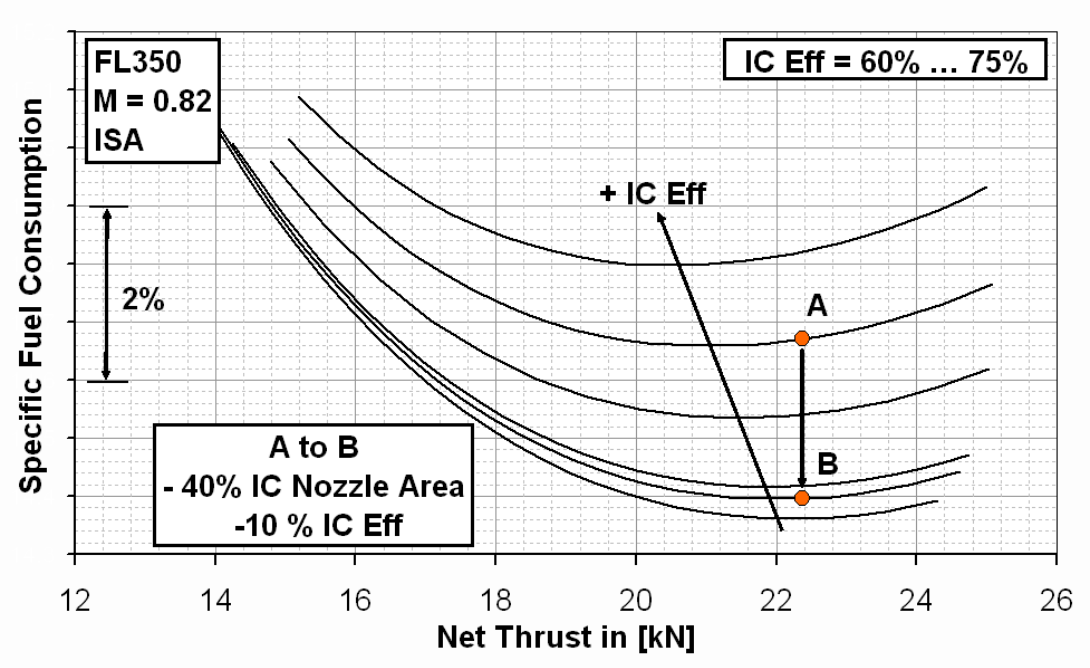

Figure 6.7: Optimising the operation of a variable intercooler nozzle at cruise for an intercooled aero engine for short haul applications.

A major limitation of this type of operation is of course the amount of area variation than can be achieved by a variable geometry nozzle while retaining an acceptable thrust coefficient. As illustrated in Fig. 6.7, a 2% reduction in SFC requires as much as 40% reduction in the auxiliary nozzle area; designing such a variable geometry nozzle would certainly be a challenging task.

6.2.4 Performance assessment at aircraft system level

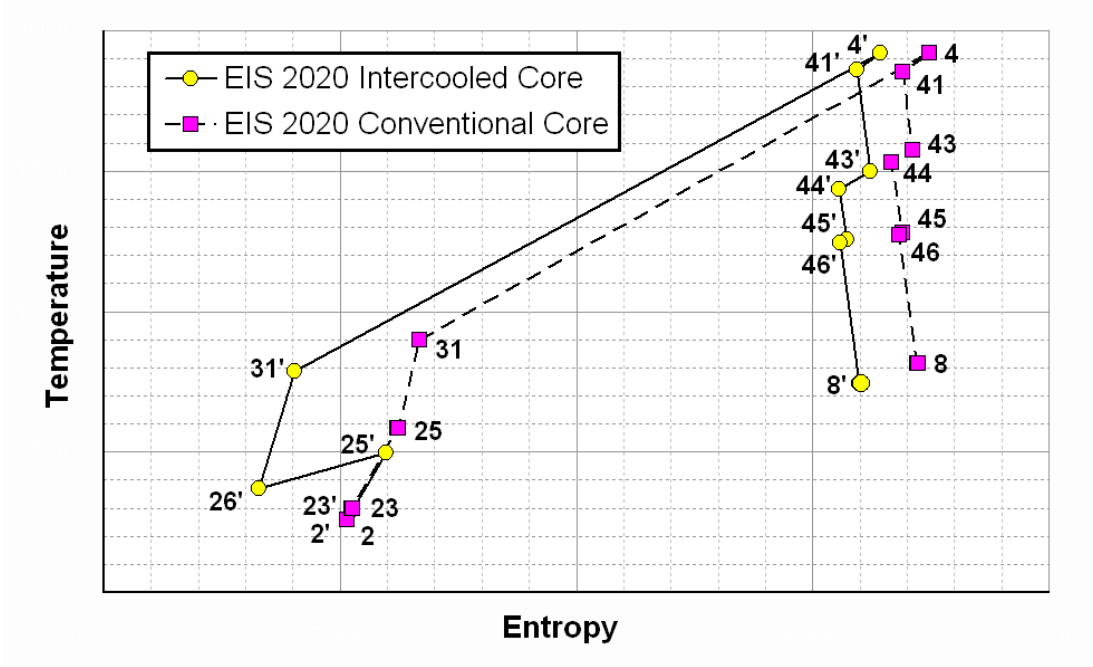

Figure 6.8: T-S diagram for the selected intercooled core and conventional core cycles at top of climb conditions.

For the results presented in Table 6.1, a year 2020 EIS turbofan engine with a conventional core was set up as the baseline. The intercooled core engine is an ultra high OPR design with also year 2020 EIS level of technology, and features a tubular heat-exchanger, while the fan for both engines has the same diameter and flow per unit of area. The OPR value for an intercooled core is no longer constrained by a maximum allowable HPC delivery temperature, but mainly from a minimum HPC blade height instead. An aggressive single stage HPT design was chosen for the mechanical layout, which set a maximum limit on the HPC pressure ratio, and hence a minimum limit on the IPC pressure ratio.

Table 6.1: Comparison of an intercooled engine with a conventional core turbofan engine at aircraft system level.

	Conventional core EIS 2020	Intercooled core EIS 2020
MTOW [1000 kg]	206.5	202.6
OEW [1000 kg]	113.0	111.2
Engine dry weight	Ref.	-5.9%
LPT weight	Ref.	-27.1%
Core weight	Ref.	-32.5%
Added components weight (as % of engine dry weight)	-	7.7%
Block fuel weight	Ref.	-3.2%
Mid-cruise SFC	Ref.	-1.5%
Mid-cruise thermal efficiency (Core + transmission efficiency)	Ref.	+0.007
Mid-cruise propulsive efficiency	Ref.	+0.000

The thermodynamic cycle at top of climb conditions for the selected intercooled core and conventional core cycles is illustrated qualitatively in the T-S plane in Fig. 6.8.

For this assessment, the TERA2020 tool was not only used for predicting engine performance but also for establishing the gas path layout for each engine configuration; this involved carrying out component thermo-mechanical and aerodynamic design, at the appropriate operating conditions, as well as predicting engine weight at component level. The TERA2020 rubberised wing aircraft model was utilised to account for snowball effects. The aircraft was initially scaled on a constant wing loading basis to achieve the design range mission of 12500 [km] with 253 [pax]. Consecutively, the scaled aircraft was used in conjunction with a typical business case mission of 5500 [km] for predicting block fuel.

Business case block fuel benefits of approximately 3.2% are predicted for the intercooled engine, mainly due to the reduced engine weight and the core's higher thermal efficiency which results in a better SFC. **These intercooling benefits are highly dependent on achieving technology targets such as low intercooler weight and pressure losses**; the predicted lower dry weight, compared to the conventional core engine, can be attributed to various reasons. The

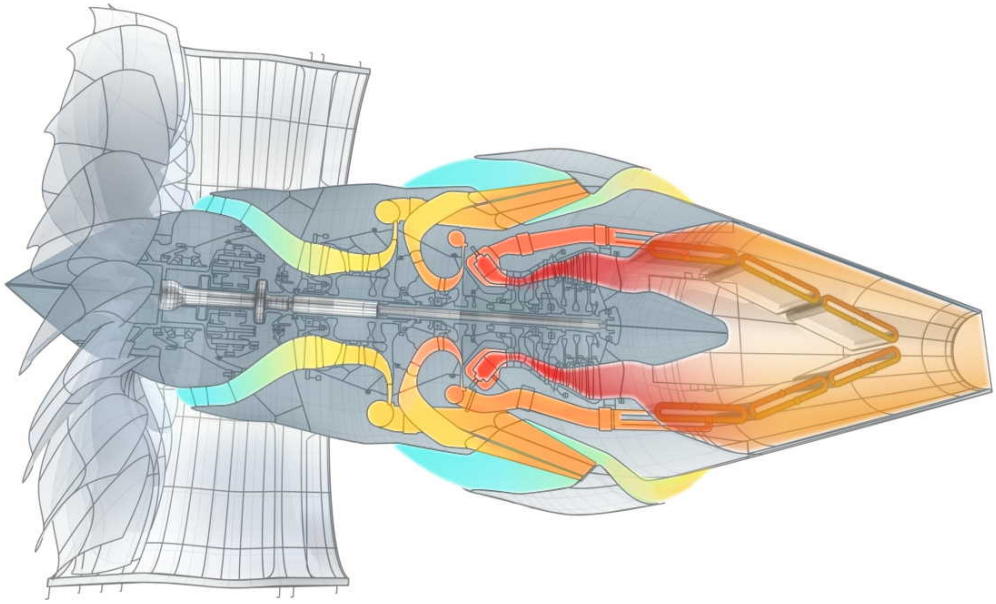

Figure 6.9: Artistic impression of the intercooled recuperated core turbofan engine [32].

intercooler weight penalty is largely compensated by the higher core specific output allowing a smaller core size and hence a higher BPR at a fixed thrust and fan diameter. The high OPR provides an additional sizing benefit, for components downstream of the HPC, by reducing further the corrected mass flow and hence flow areas. The intercooled core LPT was designed in this study with one less stage which reduced both engine weight and length, despite the high cycle OPR requiring a greater number of HPC stages. These observations are summarised in Table 6.1 with the added components weight group considering the intercooler and its installation standard; this group is not considered in the core weight group which also does not consider the core nozzle or the LPT and its casing.

6.3 Intercooled recuperated core

Some theoretical observations coupled with an assessment at aircraft system level are presented in this section for a future aero engine concept for long haul applications, featuring an intercooled recuperated core with a geared front fan, as illustrated in Fig. 6.9. The concept is again a year 2020 EIS UHBR design,

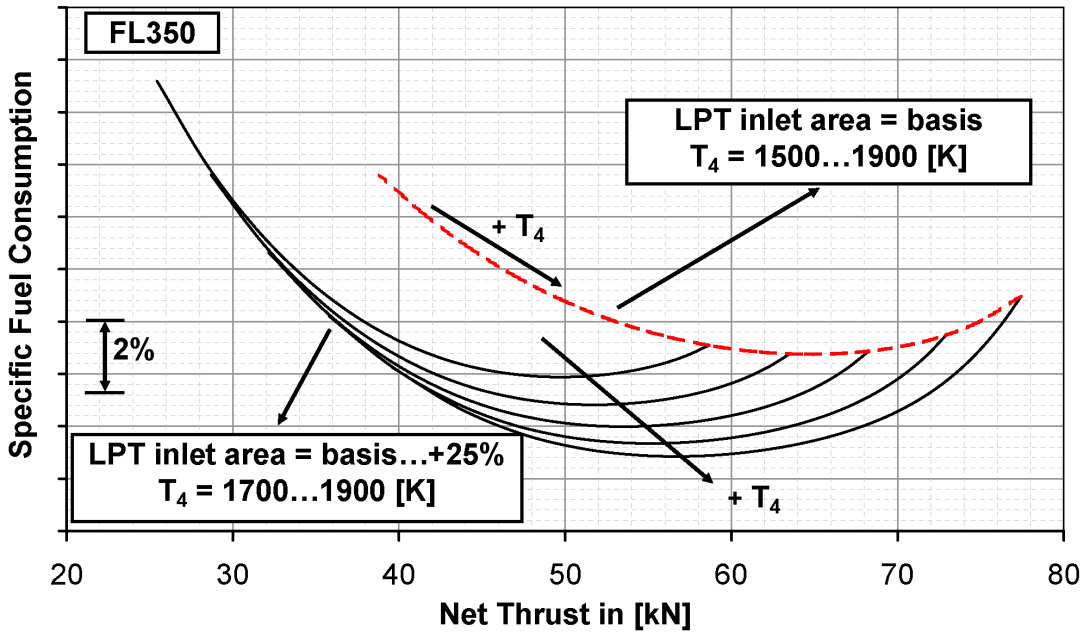

Figure 6.10: LPT variable geometry benefits for an intercooled recuperated aero engine.

in terms of expected component efficiencies and weights, and is also based on 3-shaft layout.

6.3.1 Variable geometry

High thermal efficiency for an intercooled recuperated aero engine depends on high levels of heat transfer in the recuperator; this in turn requires high temperature levels at the recuperator inlet, which at cruise conditions implies the use of high T_4 levels. An aero engine however also needs to maintain high levels of thrust at certain operating conditions, such as TOC and T-O. Off-design effects would typically dictate an engine design with reduced T_4 levels at cruise conditions, in order to maintain acceptable levels of HPT metal temperature at high power conditions. Therefore, the use of variable geometry in the LPT of an intercooled recuperated aero engine presents significant SFC benefits.

The idea of varying the inlet guide vane nozzle area in the LPT has been discussed in detail by Boggia and Rud [97] and Walsh and Fletcher [88], but has not been quantified. An attempt to quantify these benefits for an engine design optimised for long haul applications is presented in Fig. 6.10. As can be observed,

raising T_4 at cruise by as much as 200 [K], while using the variable geometry to control the engine thrust can result in an SFC benefit of more than 2% (black continuous lines). This SFC reduction, at constant specific thrust (and hence approximately constant propulsive efficiency), comes from the improvement of the engine's thermal efficiency. A short discussion on the effect of elevated cruise temperatures on HPT life is given in the NO_x emissions assessment section.

It can also be observed in Fig. 6.10 that running the exact same engine design without utilising the variable geometry results in a significantly less efficient operation of the engine (red dotted line). A re-optimised cycle at constant specific thrust - considering cruise SFC as well as engine weight - could help reduce the SFC deficit, but the benefits from higher cruise T_4 levels are still evident; the optimum thrust for aircraft-engine matching tends to lie very close to the right hand side of the SFC loop. This makes variable geometry a key factor to a performance optimised intercooled recuperated aero engine; essentially the cycle can be optimised for cruise SFC by reducing the LPT inlet area (i.e. LPT capacity) at these conditions, while a sufficient level of thrust can be maintained at top of climb by opening up the turbine nozzles.

For the same TOC design point, reducing the LPT inlet area by 20% at mid-cruise, while maintaining a constant thrust, has the following major off-design performance effects:

1. T_4 increases by as much as 200 [K] in order to maintain constant thrust.
2. HPT blade metal temperature increases by more than 130 [K], but is still cooler than the TOC metal temperature.
3. BPR increases significantly at a nearly constant fan mass flow and pressure ratio.
4. IPC corrected mass flow and pressure ratio drops.
5. IC mass flow ratio (W_{cold}/W_{hot}) and hence effectiveness increase, but temperature change drops.
6. HPC corrected mass flow and pressure ratio increases.
7. OPR reduces.

8. Recuperator effectiveness hardly varies, but the heat flux increases significantly; temperature change in both streams nearly doubles.

9. Combustor inlet temperature increases significantly.

10. Thermal efficiency improves by as much as 0.015, while propulsive efficiency remains approximately constant, and as a result SFC also improves accordingly.

6.3.2 Component aerodynamic design

The off-design behavior of the IPC, with and without LPT inlet area variation, is illustrated in Fig. 6.11 and Fig. 6.12, respectively; constant efficiency contours at 1% intervals have been drawn to show variations from the peak value in the compressor map. At take-off the LPT nozzles need to open up significantly in order to achieve the necessary thrust. This means that the IPC aerodynamic design will need to be carried out at T-O, to ensure that the compressor does not choke under these conditions.

The off-design behavior of the HPC is illustrated in a similar manner through Fig. 6.13 and Fig. 6.14. During cruise, the LPT inlet nozzle area will need to be reduced in order for the recuperator inlet temperature to rise at constant thrust. This operation results in a significantly elevated HPC corrected mass flow and pressure ratio at cruise; aerodynamic design for the HPC needs to be carried out at cruise conditions to ensure again that the compressor does not choke.

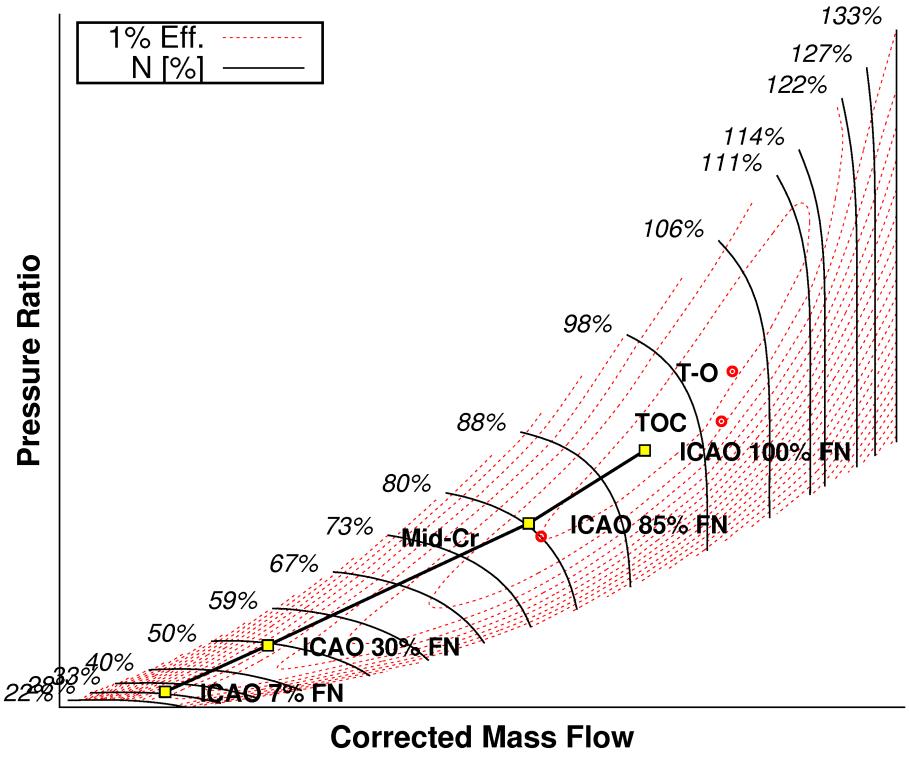

Figure 6.11: IPC operating points with LPT inlet area variation.

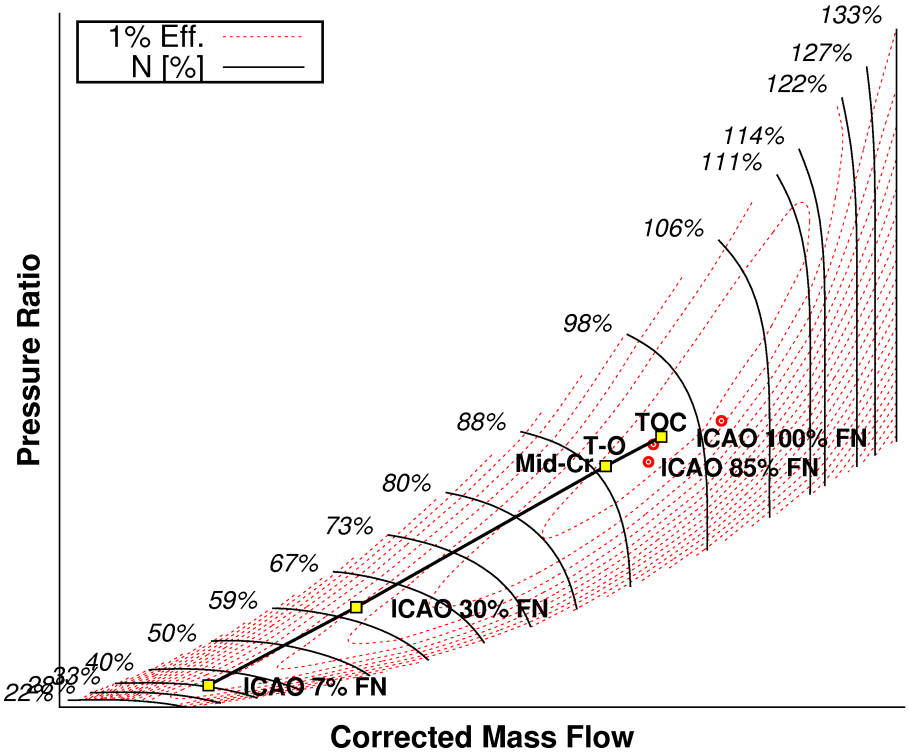

Figure 6.12: IPC operating points without LPT inlet area variation.

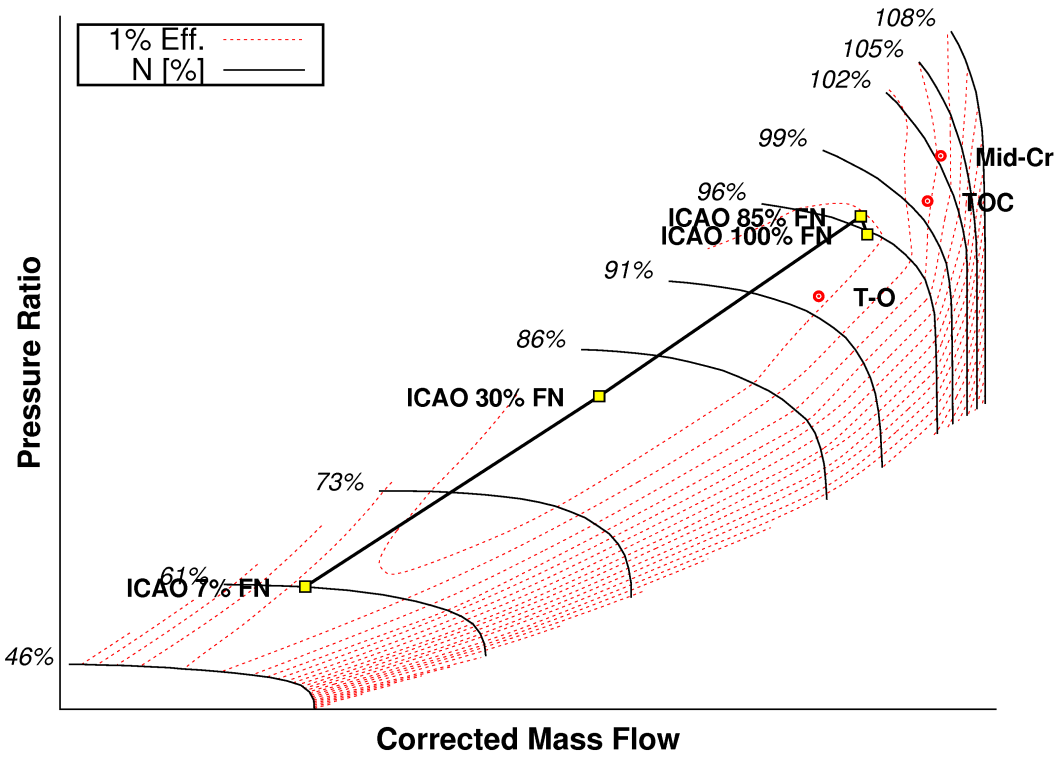

Figure 6.13: HPC operating points with LPT inlet area variation.

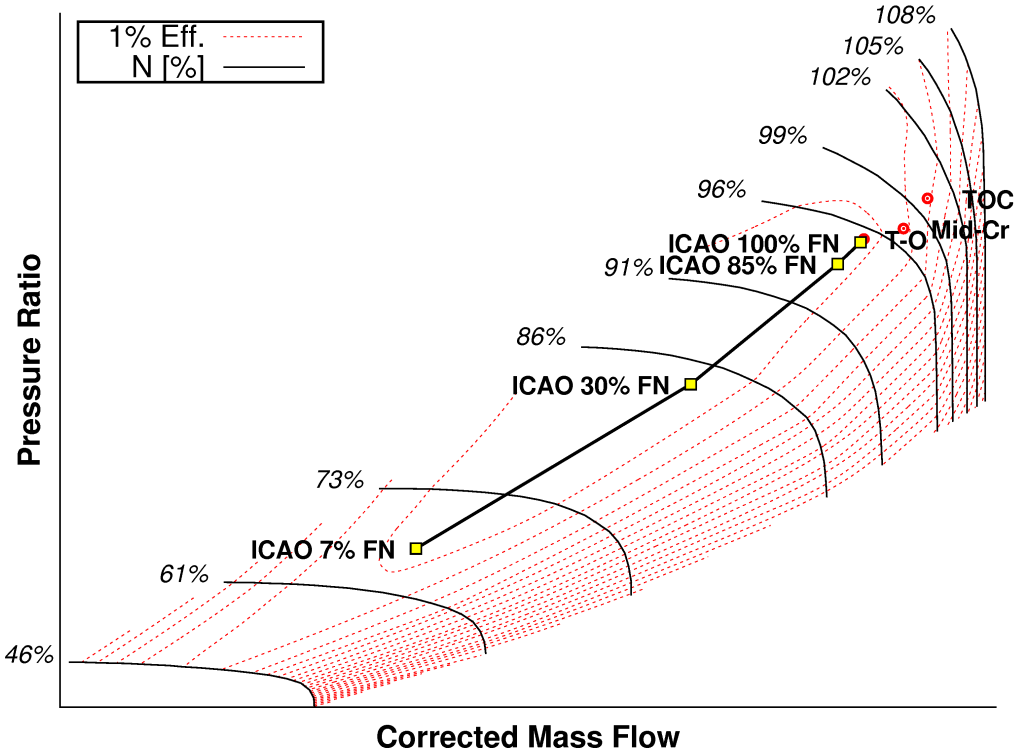

Figure 6.14: HPC operating points without LPT inlet area variation.

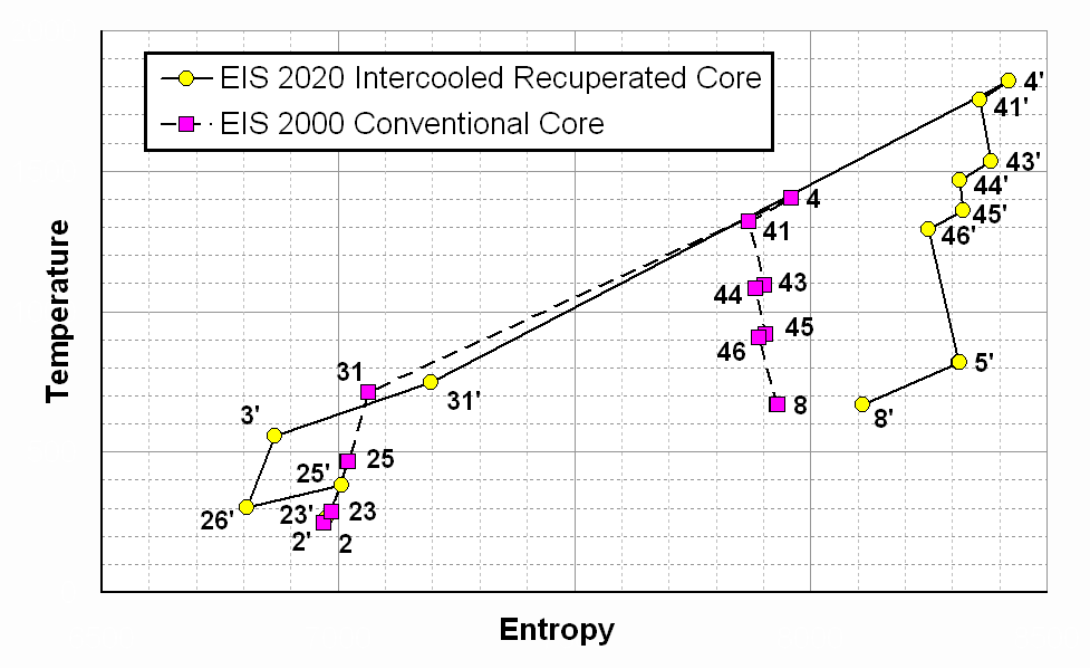

Figure 6.15: T-S diagram for the selected intercooled recuperated core and conventional core cycles at mid-cruise conditions.

6.3.3 Performance assessment at aircraft system level

For the results presented in Table 6.2, a year 2000 EIS turbofan engine with a conventional core was set up as the baseline. The intercooled recuperated engine on the other hand is an UHBR design with a year 2020 level of technology. The TERA2020 tool was used for performing the aircraft system level analysis, in a similar manner to the intercooled core assessment. The thermodynamic cycle at mid-cruise conditions for the selected intercooled recuperated core and conventional core cycles is illustrated qualitatively in the T-S plane in Fig. 6.15.

Significant business case block fuel benefits of nearly 22% are predicted for the geared intercooled recuperated core engine due to its higher thermal and propulsive efficiency. The use of HPT cooling air bled from the recuperator exit [88,97] results in a 1.3% SFC improvement due to more energy being recuperated from the exhausts, at a fixed effectiveness level - and despite the considerable increase in cooling air requirements (+3.5% of core mass flow). The predicted dry weight for the intercooled recuperated configuration is higher compared to the conventional core engine. There is a weight benefit from the use of EIS 2020 light-weight materials in most major engine components, as well as from the high speed LPT

Table 6.2: Comparison of an intercooled recuperated engine with a conventional core turbofan engine at aircraft system level.

	Conventional core EIS 2000	IRA EIS 2020
MTOW [1000 kg]	230.0	207.4
OEW [1000 kg]	119.6	116.3
Thrust/weight	Ref.	-12%
Engine dry weight	Ref.	+16.5%
Nacelle weight	Ref.	+29.7%
Fan weight	Ref.	+36.6%
LPT weight	Ref.	-17.1%
Added components weight (as % of engine dry weight)	-	25.4%
Block fuel weight	Ref.	-21.6%
Mid-cruise SFC	Ref.	-18.3%
Mid-cruise thermal efficiency (Core + transmission efficiency)	Ref.	+0.024
Mid-cruise propulsive efficiency	Ref.	+0.120

- due to the reduced stage count. Also, the relatively low engine OPR and the use of an intercooler increases core specific output, resulting in a smaller core. The introduction however of the gearbox, intercooler and recuperator components inevitably results in a significant weight penalty. It should be noted that a lower level of specific thrust, and hence a larger fan diameter, has been assumed for the intercooled recuperated core engine; this results in both a heavier fan and a heavier nacelle. These observations are summarised in Table 6.2 with the added components weight group considering the intercooler and recuperator and their installation standard, as well as the gearbox.

6.4 NO_x emissions assessment

A NO_x emissions assessment of the presented heat-exchanged cores and corresponding baseline engines has been performed. Two different combustion concepts have been considered: conventional Rich-burn/Quick-quench/Lean-burn (RQL) and lean-burn combustion technology. The results were produced using a combination of basic combustor design rules, feedback from the OEMs in-

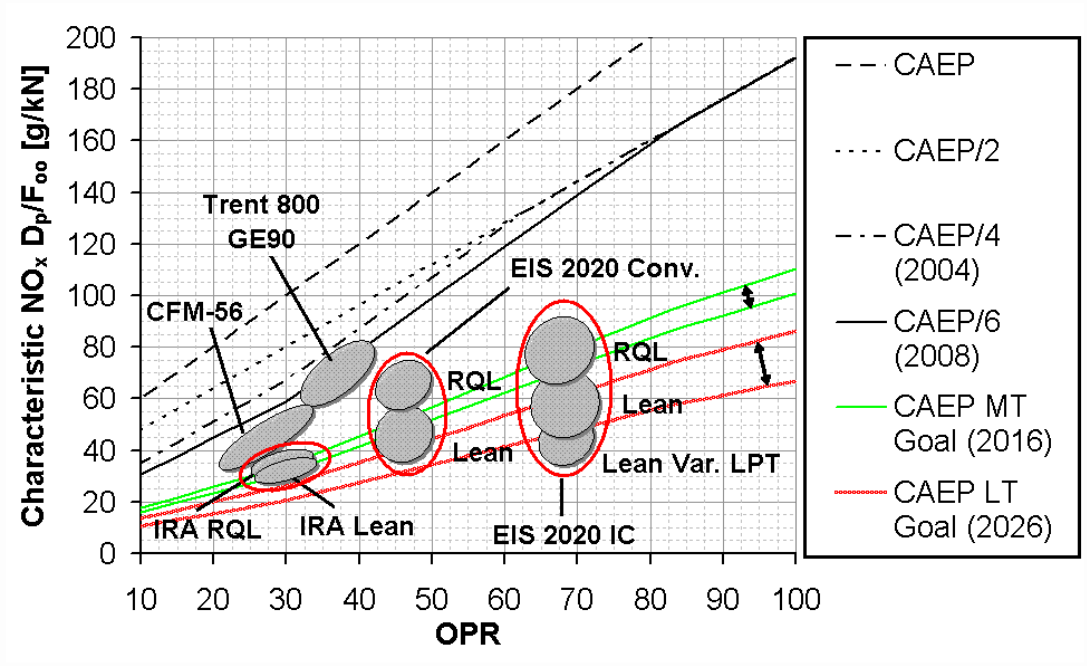

Figure 6.16: NO_x emissions assessment for future conventional and heat-exchanged core aero engine designs.

volved in the NEWAC project, and public domain semi-empirical correlations. A comparison of the results obtained against ICAO Annex 16 Volume II legislative limits [64], as well as the medium and long term technology goals set by CAEP [65], is illustrated in Fig. 6.13. Balloons have been used to indicate the uncertainty in the NO_x predictions due to the lower technology readiness level associated with the introduction of such combustor designs in the proposed future cycles.

A sufficient margin against the ICAO CAEP/6 LTO NO_x certification limit may be achieved for the year 2020 EIS conventional and intercooled cores; the cruise NO_x emission index would rise considerably however due to the high OPR. The introduction of lean-burn combustion technology has the capacity to reduce cruise NO_x and improve the certification margin significantly, negating the cycle effects of high OPR and low Air to Fuel Ratio (AFR).

For the intercooled recuperated core, although the margin against the ICAO CAEP/6 LTO NO_x certification limit, for both lean-burn and RQL combustion technology, is similar to the margin for the year 2020 EIS conventional core turbofan engine, the absolute NO_x emissions for the LTO cycle are actually

significantly lower. This is a consequence of the ICAO LTO NO_x legislative limits being quite strict for low OPR engines, while providing a better LTO NO_x allowance for high OPR engines.

Despite the generally low OPR, cruise NO_x may still remain an important concern for an intercooled recuperated configuration, if lean-burn combustion technology is not introduced. During cruise, the need for high heat exchange levels in the recuperator results in high combustor inlet temperatures and low AFR values; designing a conventional RQL technology combustor for such conditions could still prove a challenging task. To this extent, the intercooled recuperated concept essentially lends itself to lean-burn combustion technology. Due to the variable geometry LPT, the primary zone temperature during cruise will not be so far away from the take-off value when compared to conventional engine designs. It can therefore prove easier to balance the combustor primary zone design to achieve both low NO_x and CO emissions at cruise conditions, as well as retain low NO_x levels at high power conditions such as take-off. Substituting the RQL combustor with a lean-burn design, can reduce NO_x emissions but the effect would be less profound compared to lean-burn combustion technology coupled with high OPR cycles.

Similarly, introducing a variable geometry LPT in an intercooled core with lean-burn combustion technology can improve LTO NO_x and the margin from the ICAO CAEP/6 certification limit by nearly 10%, at a given level of cruise NO_x. This involves running the intercooled core approximately 60 [K] hotter during cruise in order to achieve the same thrust levels. The reduction in LTO NO_x levels is mainly the result of bringing the primary zone temperature during cruise closer to the take-off value; the latter results in the lean-burn combustor design - balanced for NO_x and CO at cruise - retaining acceptable NO_x levels at high power conditions such as ICAO 100% F_N. Running the engine hotter at cruise also improves SFC by nearly 1%.

It is worth noting that the effect of elevated cruise temperatures on HPT life, and consecutively on engine time between overhaul and maintenance costs is not profound, for the temperature increase proposed. The main reason behind this is that HPT life is dominated by the time spent at take-off and climb, with cruise effects being of secondary order due to the significantly lower operating temperatures encountered. Moreover, modulating T_{41} to remain constant at the higher cruise thrust range (i.e. flat temperature profile), could actually prove

beneficial in terms of thermal fatigue [97]. Sulphidation on the other hand could become an issue, and therefore care should be taken during design.

6.5 Conclusion

This chapter explored and quantified potential block fuel and NO_x benefits from introducing heat-exchanged cores in future aero engine designs, as studied within the European collaborative project NEWAC. SFC improvements from introducing an intercooled core of an OPR of 80 were discussed and the potential of utilising a variable geometry auxiliary nozzle to tweak the performance was assessed. Potential benefits from introducing a variable geometry LPT in an intercooled recuperated core were also quantified. Important observations were made with respect to the need to carry out the HPC aerodynamic design at cruise conditions, and the IPC aerodynamic design at T-O conditions, if a variable geometry LPT is introduced.

The performance of heat exchanged cores, with year 2020 EIS level of technology, was compared to conventional core turbofan engines at aircraft system level, and the results showed considerable benefits in terms of block fuel. An emissions assessment was also carried out, and the necessity of introducing lean-burn combustion technology in order to keep cruise NO_x at acceptable levels was demonstrated. Significant benefits in terms of LTO NO_x reduction were predicted from the introduction of a variable geometry LPT in an intercooled core with lean-burn combustion technology. Additional research effort could be undertaken to address heat-exchanger failure modes, noise and direct operating costs.

6.6 Outlook

Improvements in engine propulsive efficiency, as a way of reducing emissions from turbofan engines, have been discussed in Chapter 5 in terms of specific thrust reduction. In this chapter, the need for higher engine thermal efficiency was addressed by exploring benefits from the potential introduction of heat-exchanged cores in future aero engine designs. In the next chapter, TERA2020

will be used for assessing the combined potential of novel low pressure spool and core technologies for reducing engine emissions. A back-to-back comparison of an intercooled core engine with a conventional core engine will be performed and optimal designs for year 2020 entry into service will be proposed.

Chapter 7

Towards the optimal 2020 ducted turbofan

In this chapter, TERA2020 is used for assessing the combined potential of novel low pressure system and core technologies for reducing engine emissions. Various aspects are presented of an intercooled core and conventional core turbofan engine optimisation procedure using TERA2020. A back-to-back comparison between the two engine configurations is performed and fuel optimal designs for year 2020 entry into service are proposed.

7.1 Introduction

7.1.1 Future aero engine designs - An evolving vision

Numerous feasibility studies have been published over the years focusing on future engine and aircraft designs that can reduce fuel consumption; a brief review of some of these publications will be carried out here.

Gray and Witherspoon [220] provide one of the earliest discussions on the subject of improving engine fuel efficiency by looking at conventional and heat exchanged cores, as well as non-steady flow combustion processes and open rotor configurations. A similar study focusing on geared and open rotor arrangements as well as heat exchanged cycles is presented by Hirschkron and Neitzel [221].

Jackson [222] provides an interesting discussion on how specific thrust levels were expected to evolve in the mid-70's based on the economic and technological projections of that time period; the author provides an update to that discussion based on current economical and technological projections in [223]. Wilde [224], Young [225], and Pope [226] provide a good reference on how the future for civil turbofan engines for medium and long range applications was envisaged in the late 70's. Some early discussions on future trends in commercial aviation from the aircraft manufacturer's and airliner's perspective can be found in [227, 228] and [229], respectively.

A review on the several technical and economic obstacles that were identified in the late 80's with respect to the realization of the Ultra-High Bypass Ratio (UHBR) turbofan concept is provided by Borradaile [230] and Zimbrick and Colehour [231]. Peacock and Sadler [232] give an update on the subject, focusing further on engine design constraints and the technology advancements required for producing a competitive UHBR configuration. Potential year 2020 scenarios are explored by Birch [233] while Ruffles [234] provides an overview of current aero engine technology and some insight on the future of aircraft propulsion. Finally, for a review on the development of civil propulsion from the early 50's to recent years the interested reader is referred to Saravanamuttoo [235].

7.1.2 Optimal specific thrust levels for 2020

The potential uninstalled Specific Fuel Consumption (SFC) benefits from reducing specific thrust for a year 2020 entry into service conventional core turbofan engine are illustrated in Fig. 7.1. These design-point calculations were produced assuming constant engine Overall Pressure Ratio (OPR) and Turbine Entry Temperature (TET), and reflect mid-cruise conditions and optimal By-Pass Ratio (BPR) for SFC; off-design performance effects as well as nacelle drag and engine weight were not considered. As can be observed, reducing specific thrust can improve the propulsive efficiency but inevitably worsens the transmission efficiency. At a Fan Pressure Ratio (FPR) of roughly 1.2 there seems to be no thermodynamic benefit from further reducing specific thrust. A similar behaviour is observed in the ideal case of the fan and low pressure turbine polytropic efficiencies being equal to unity, as illustrated in Fig. 7.2.

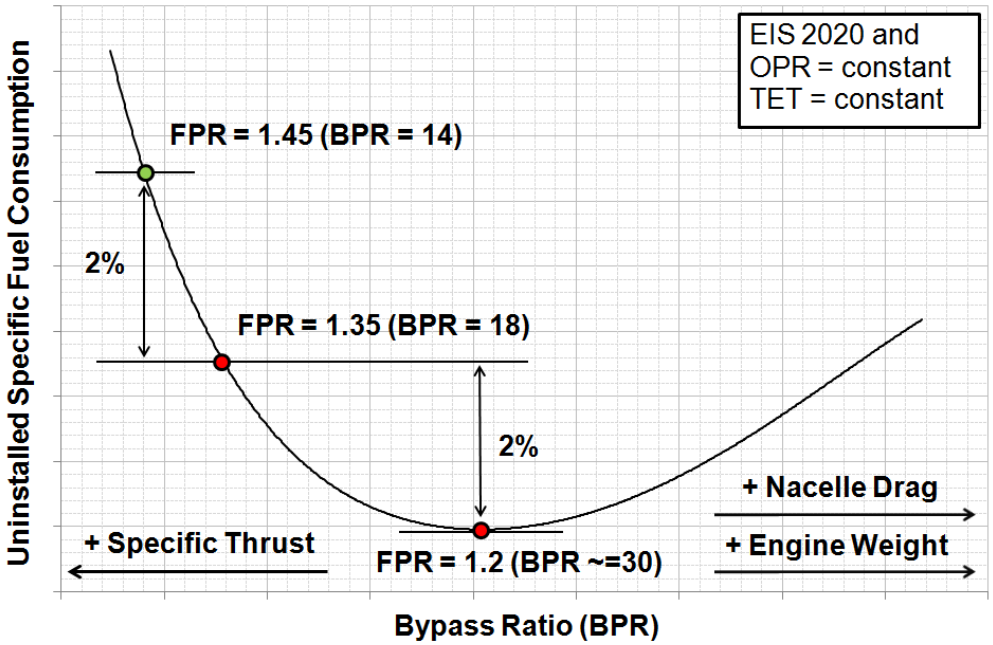

Figure 7.1: Uninstalled specific fuel consumption benefits from reducing specific thrust for a year 2020 entry into service conventional turbofan engine.

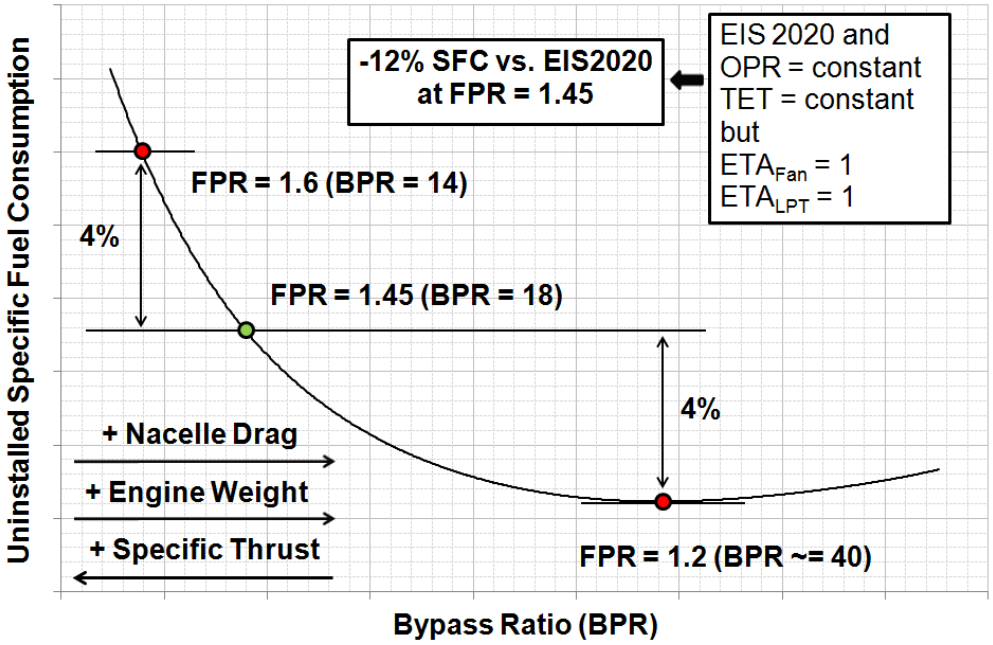

Figure 7.2: Uninstalled specific fuel consumption benefits from reducing specific thrust for a year 2020 entry into service conventional turbofan engine with fan and low pressure turbine polytropic efficiencies equal to unity.

Some important observations can be made:

- Improving fan and low pressure turbine polytropic efficiency directly improves SFC; the potential SFC benefits from reducing specific thrust however remain largely unaffected. As fan tip pressure ratio reduces, pressure losses in the bypass duct tend to have an increasingly dominant effect on transmission efficiency and, therefore, on the impact of propulsive efficiency improvements on SFC.

- Improving fan and low pressure turbine polytropic efficiency increases the optimal BPR value, at a constant specific thrust. Although not illustrated in Fig. 7.1 and Fig. 7.2, improving core specific output and component efficiency will have a similar effect. Bypass ratio can therefore be considered as a good indicator of engine technology level.

- Limited SFC improvement may be envisaged by reducing specific thrust beyond a fan pressure ratio of 1.45. The increased fan diameter will result in significant engine weight and nacelle drag penalties which can very well negate the projected uninstalled SFC benefits. A larger fan, low pressure turbine and nacelle will also increase the production cost significantly.

For determining the fuel optimal specific thrust and BPR levels, the effects of engine weight and nacelle drag on aircraft performance need to be considered, hence the need for the TERA2020 (Techno-economic, Environmental and Risk Assessment for 2020) tool. Block fuel benefits from reducing specific thrust for a year 2020 entry into service direct drive fan conventional core engine for long range applications have been calculated and are illustrated in Fig. 7.3. The engine take-off (T/O) thrust at ISA SLS conditions is 66000 [lbf] and all FPR and BPR values quoted are at mid-cruise conditions. A 10 [in] increase in fan diameter and a 4% reduction in FPR (which roughly translates to a 14% reduction in specific thrust) results in a 2% improvement in mid-cruise uninstalled SFC; using the exchange rates reported in Chapter 3 this would imply an improvement in block fuel of some 2.6%. Nevertheless, the engine weight has increased significantly by roughly 17% and in conjunction with the higher nacelle drag the block fuel benefit reduces to merely 0.85%. More details on the fuel optimal design proposed and the constraints set to derive it are given in Section 7.2. It is worth noting that a recent study by Hemmer et al. [236], albeit based on significantly more

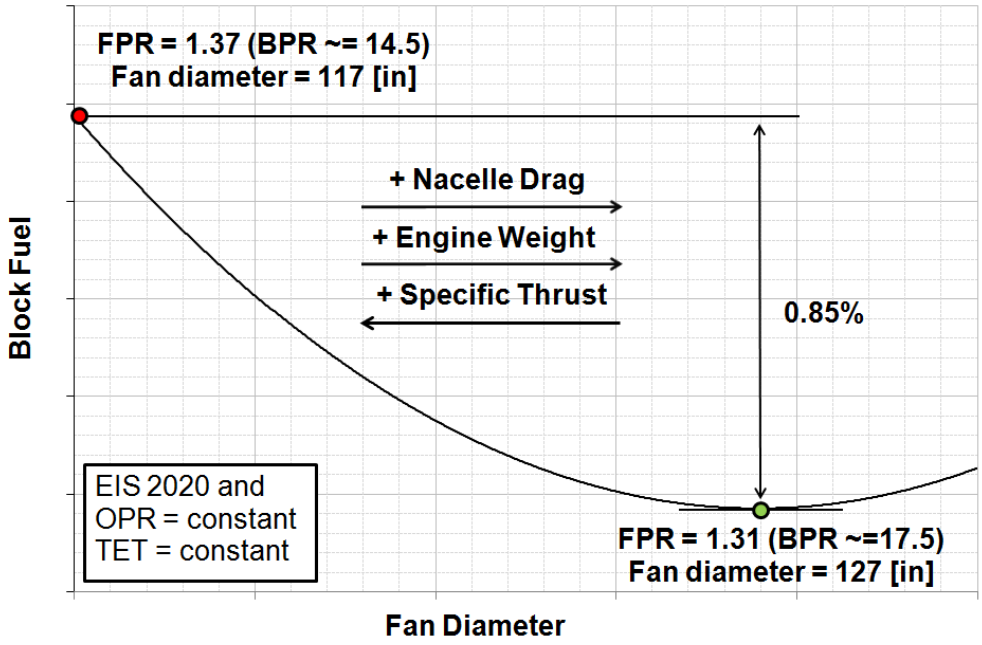

Figure 7.3: Block fuel benefits from reducing specific thrust for a year 2020 entry into service conventional turbofan engine for long range applications.

pessimistic OPR and TET levels than what was assumed here, concluded on similar fuel optimal FPR levels for the geared and contra-rotating architectures for long range applications.

From the flat curve presented in Fig. 7.3, it is clear that only limited benefits in block fuel may be envisaged by reducing specific thrust as these are highly dependent on the engine thrust to weight ratio. Technology risk considerations (i.e. shortcomings in meeting projected engine weight and turbomachinery efficiency targets) will probably move the fuel optimal level of specific thrust to higher values. Noise considerations (i.e. stringent noise legislation) may very well dictate fan size and specific thrust levels that are not fuel optimal, as has been the case in the past [232]. The optimal specific thrust level for minimum direct operating costs is highly dependent on the assumptions made for the volatility of economic parameters such as fuel price and interest rates. Furthermore, production and maintenance costs tend to be proportional to engine weight which is inversely proportional to specific thrust at a given technology level and fan diameter at a given thrust. It can therefore be concluded that the commercial competitiveness of reduced specific thrust turbofan designs will largely depend on how the aviation market evolves in the years to come until 2020.

With potential block fuel benefits from improving propulsive efficiency being rather mild, it is worth investigating if the introduction of heat-exchanged cores could change this picture. In the next section, a back to back comparison will be carried out between a conventional core and an intercooled core turbofan engine with year 2020 entry into service level of technology for long range applications. The effects of introducing intercooling will be assessed with respect to improving engine fuel efficiency. Differences in the optimal specific thrust levels between the two configurations will be discussed.

7.2 Optimising a turbofan engine

In Chapter 6, a comparison was carried out between a conventional core and an intercooled core turbofan engine with year 2020 entry into service level of technology for long range applications. Both configurations had the same fan diameter and were designed to meet the same thrust requirements. An attempt will be made here to re-optimise those powerplants using TERA2020 by allowing the specific thrust (and hence the propulsive efficiency) to vary. Rather than setting fixed thrust requirements, the rubberised wing aircraft model will be fully utilised instead. The engine/aircraft combination will be optimised to meet a particular set of customer requirements i.e. payload-range, take-off distance, time to height and time between overhaul. It is expected that different conclusions will be drawn when comparing the two powerplants at their optimal specific thrust levels.

7.2.1 Design space constraints

For every engine design there are numerous practical limitations that need to be considered. The design space constraints set for this study are given in Table 7.1 and are considered applicable for a year 2020 entry into service turbofan engine. A large amount of information, in spreadsheet format, is provided in Appendix B on the choice of design variables for the optimisation process.

For a conventional core the High Pressure Compressor (HPC) delivery temperature, and hence the engine Overall Pressure Ratio (OPR), is typically constrained by the mechanical properties of the HPC disc or HPC rear drive cone or High

Table 7.1: Design space constraints.

	Lower bound	Upper bound
FAR take-off distance	-	2.5 [km]
Climb to 35000 [ft]	-	22.5 [min]
IPC design pressure ratio (intercooled core)	2.7	-
HPC design pressure ratio (intercooled core)	-	25.0
HPC design pressure ratio (conventional core)	-	5.5
HPC delivery temperature	-	970 [K]
HPC last stage blade height	10 [mm]	-
Combustor outlet temperature	-	2050 [K]
Turbine blade mean metal temperature (external surface)	-	1350 [K]
Auxiliary nozzle area variation	Ref.	+50%
Time between overhaul	23000 [hr]	-

Pressure Turbine (HPT) disc material [57]. For an intercooled core, the OPR value is no longer constrained by a maximum allowable HPC delivery temperature. Nevertheless, the intercooling process increases the air density in the gas path and as a result the compressor blades tend to become smaller. Losses from tip clearances become increasingly important and a minimum compressor blade height limitation needs to be applied to maintain state of the art compressor efficiency. Core architecture selections for the conventional core set an upper limit to the HPC design pressure ratio that can achieved when driven by a single-stage HPT. With respect to the intercooled core, a two-stage HPT has been assumed to relieve the restriction set on the HPC pressure ratio; the minimum design pressure ratio for the Intermediate Pressure Compressor (IPC) is limited by icing considerations during the descent flight phase. The maximum area variation that may be achieved by the variable area auxiliary nozzle is also constrained by mechanical (and aerodynamic) considerations.

Designing a combustor at very low air to fuel ratio levels is also limited by the need for adequate combustor liner film-cooling air as well as maintaining an acceptable temperature traverse quality [8]; this sets an upper bound on combustor outlet temperature. Furthermore, a maximum permissible mean metal

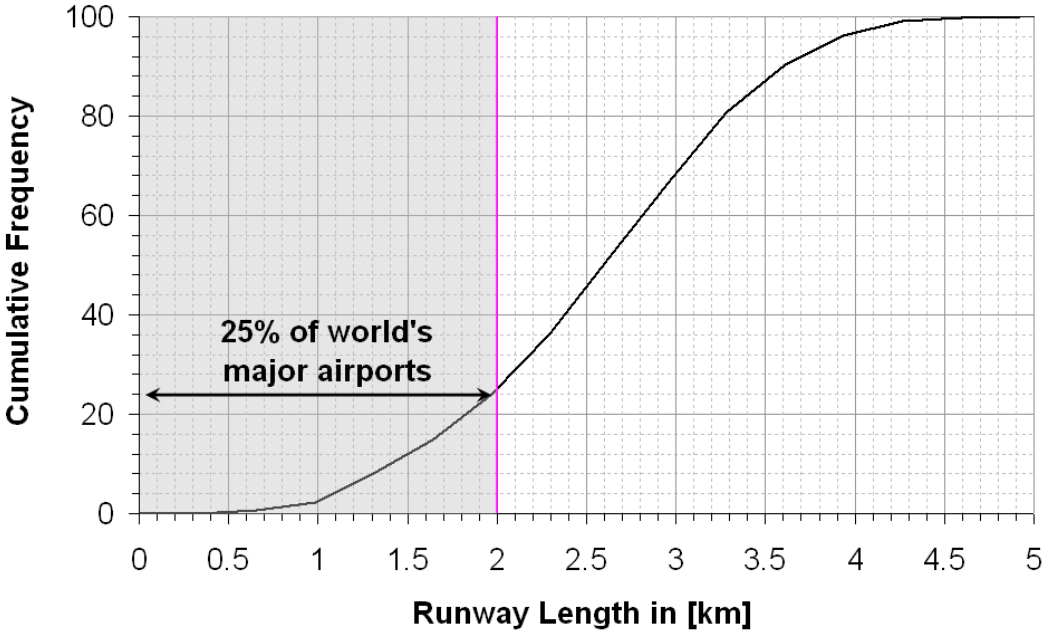

Figure 7.4: Cumulative distribution of world's major runway lengths (based on data from [98]).

temperature needs to be set to consider turbine blade material limitations. A lower bound on engine time between overhaul also needs to be set to limit the frequency of workshop visits.

As discussed in Chapter 2, a rubberised aircraft wing model is used in the TERA2020 explicit design algorithm. Rather than using fixed engine thrust requirements, a maximum FAR (Federal Aviation Regulations) take-off field length and a maximum time to height for a load factor of 1 and ISA conditions can be set instead. The choice of both is typically based on customer operational requirements. The aircraft needs to be able to: (i) take-off from a large number of airports around the world and (ii) climb to the initial cruise altitude sufficiently fast to ease operations with local air traffic control (and hence reduce waiting time on the ground). A cumulative distribution of the world's major runway lengths, based on data from [98], is illustrated in Fig. 7.4. The aircraft used in this study is designed to carry 253 [pax] for a distance of 12500 [km]; the figure of merit used in the optimisation is block fuel and is based on a business case of 5500 [km] with an assumed load factor of 1.

Table 7.2: Comparison of the fuel optimal intercooled and conventional core turbofan engine designs.

	Conventional core EIS 2020	Intercooled core EIS 2020
Fan diameter [in]	127	118
ISA SLS take-off thrust [lbf]	66000	65000
Overall pressure ratio	62.3	82.0
IPC pressure ratio	8.0	4.1
HPC pressure ratio	5.5	14.9
Fan mass flow [kg/s]	588	507
Core mass flow [kg/s]	36.3	34.3
Mid-cruise fan tip pressure ratio	1.31	1.36
Mid-cruise bypass ratio	17.7	17.3
Mid-cruise SFC	Ref.	-0.6%
Mid-cruise thermal efficiency (core + transmission efficiency)	Ref.	+0.015
Mid-cruise propulsive efficiency	Ref.	-0.02
Engine dry weight	Ref.	-12.6%
Fan weight	Ref.	-23.5%
LPT weight	Ref.	-33.2%
Core weight	Ref.	-19.9%
Added components weight (as % of engine dry weight)	-	12.2%
Nacelle weight	Ref.	-18.0%
MTOW [1000 kg]	208.5	203.3
OEW [1000 kg]	116.2	112.6
Block fuel weight	Ref.	-2.6%

*Performance parameters at top of climb conditions unless stated otherwise

7.2.2 Fuel optimal designs

Optimising a turbofan engine design for minimum block fuel essentially has to consider the trade-off between better thermal and propulsive efficiency and lower engine weight nacelle drag. The cycle optimisation results for the two power-plants are given in Table 7.2. Significant block fuel benefits are projected for the intercooled core engine but they are smaller than what was predicted earlier in Chapter 6. This is mainly attributed to the minimum blade height requirement

setting a lower limit on the intercooled core size for a given OPR. Increasing the fan diameter at a fixed tip speed inevitably reduces rotational speed, increases torque and hence increases Low Pressure (LP) shaft diameter; this further aggravates the problem since the HPC hub to tip ratio needs to increase. As a result, the optimal specific thrust for the intercooled core is higher compared to the conventional core turbofan engine. Although the high OPR intercooled core benefits from a higher core and transmission efficiency, and hence a better thermal efficiency, the conventional core benefits from a higher propulsive efficiency. In the next sections, the design space around the proposed fuel optimal designs will be explored and important observations will be made.

7.2.3 Approximating the design space

In order to graphically illustrate the design space, a large number of TERA2020 simulations had to be carried out; these simulations focused around the fuel optimal designs presented in Section 7.2.2. Polynomial response surface models were derived that interpolate between a given number of known designs. Typical design space discontinuities encountered as a result of turbomachinery stage count changes are inevitably distorted in polynomial approximations. For this reason, an error analysis was carried out to determine the discrepancy levels between the surrogate models and the actual design space; the approximation errors for engine weight and aircraft block fuel were found to be less than 1% and 0.2%, respectively.

7.2.4 Fan and core sizing

As discussed earlier, propulsive efficiency benefits from reducing specific thrust (and hence increasing fan diameter) can very well be negated by the resulting combination of: i) increased engine weight, ii) increased nacelle (and interference) drag, and iii) reduced transmission efficiency. This section will discuss various aspects of fan and core sizing for the conventional core and intercooled core configurations.

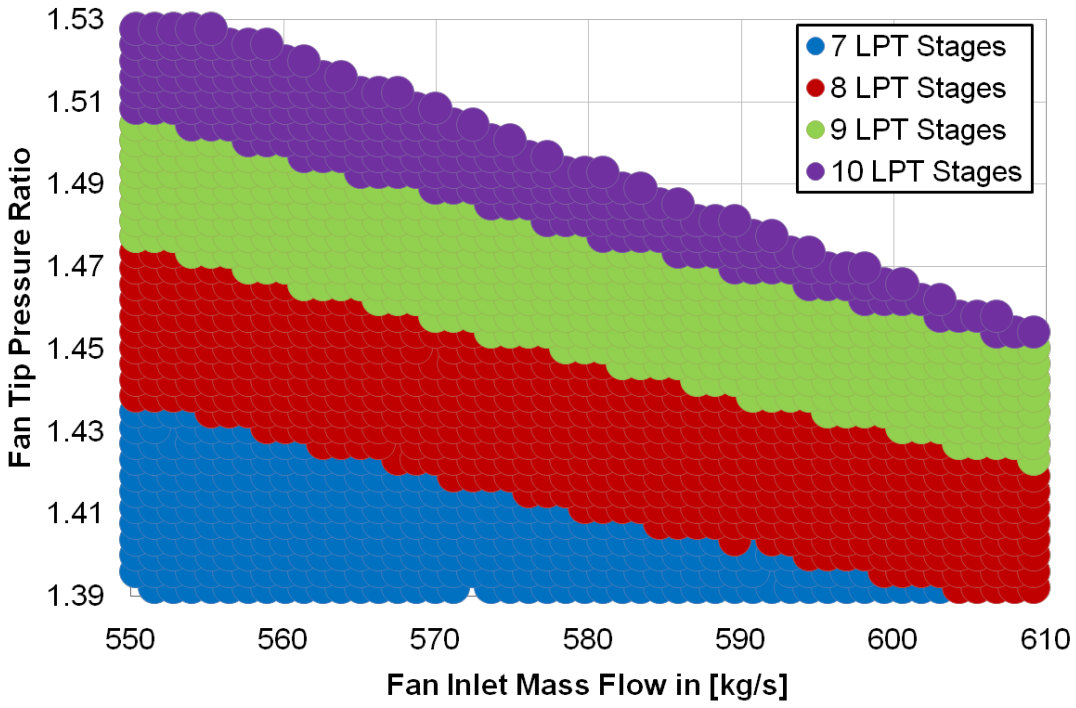

Figure 7.5: Variation of low pressure turbine stage count with fan inlet mass flow and fan tip pressure ratio for a fixed size conventional core.

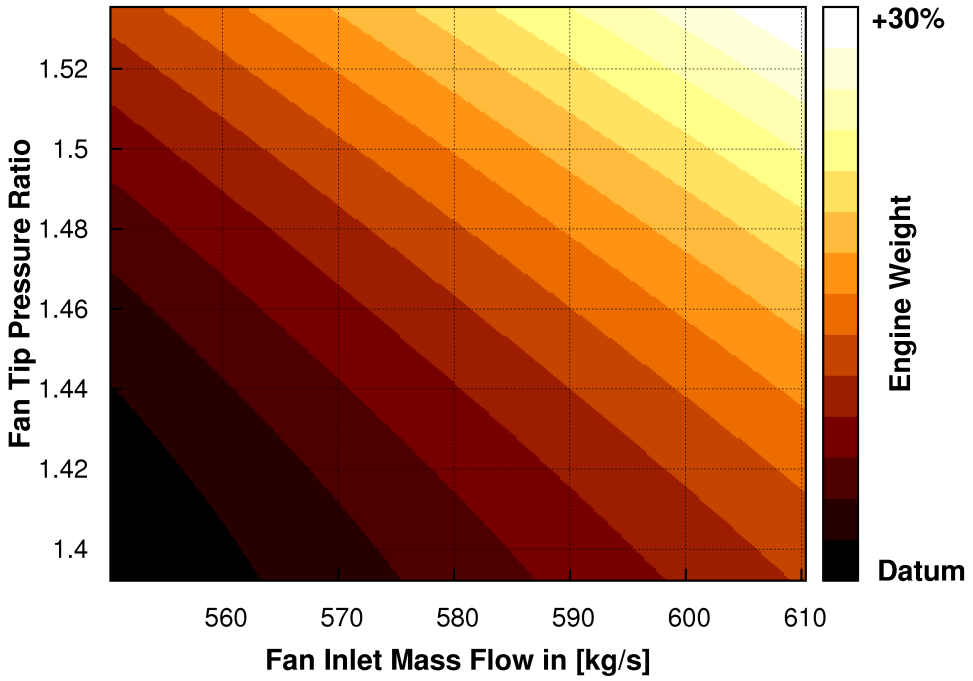

Figure 7.6: Variation of engine weight with fan inlet mass flow and fan tip pressure ratio for a fixed size conventional core.

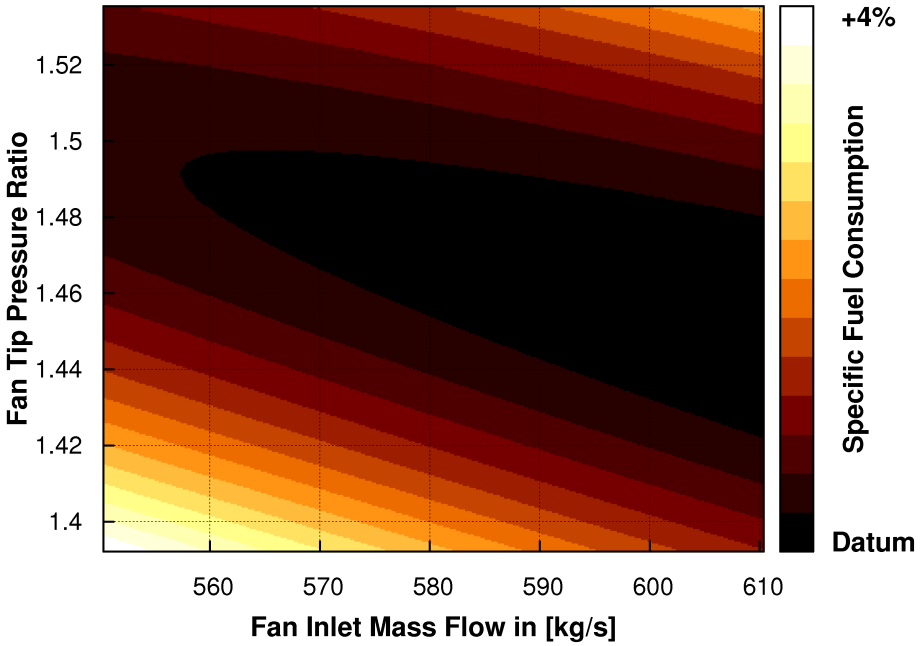

Figure 7.7: Variation of engine specific fuel consumption with fan inlet mass flow and fan tip pressure ratio for a fixed size conventional core.

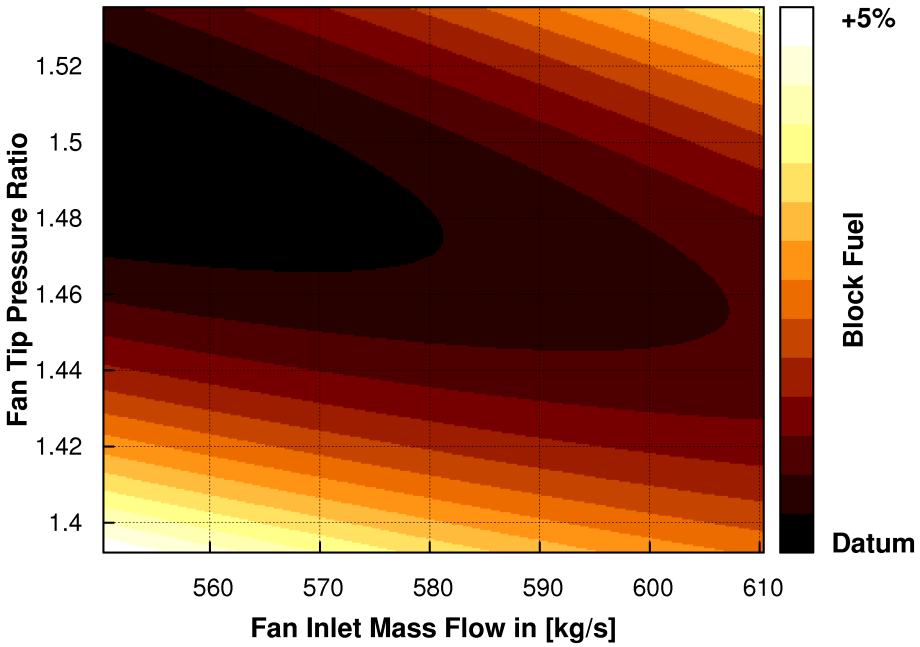

Figure 7.8: Variation of aircraft block fuel with fan inlet mass flow and fan tip pressure ratio for a fixed size conventional core.

When sizing the engine fan, assuming a fixed size core, large design space discontinuities are encountered due to Low Pressure Turbine (LPT) stage count changes, as illustrated in Fig.7.5. As discussed earlier, the use of smooth surrogate models for approximating discontinuous spaces inevitably results in approximation errors, and it is worth noting that the addition of an extra LPT stage results in approximately 150 [kg] of additional weight. Nevertheless, with the fan and nacelle weight (including the thrust reverser) each being roughly double the LPT weight and directly proportional to the fan diameter, the weight trends illustrated in Fig. 7.6 can be considered reasonable.

The improvement in mid-cruise uninstalled SFC from reducing specific thrust is illustrated in Fig. 7.7. If installation effects are ignored, then selecting a higher fan diameter (and hence a higher bypass ratio at a fixed size core) will result in better SFC; this observation is in agreement with Fig. 7.1 presented earlier. Nevertheless, the increased nacelle drag and engine weight move the optimal level of specific thrust for minimum block fuel to smaller fan diameters, as illustrated in Fig. 7.8.

Looking at the trends illustrated in Fig. 7.8 in isolation, and then comparing with the optimal design proposed in Section 7.2.2, one would be incline to draw the conclusion that the fuel optimal fan diameter should be even smaller. However, as one moves towards the upper left corner of Fig. 7.8 the engine take-off and top of climb thrust reduces. In order to satisfy the time to height and FAR take-off distance constraints set in Section 7.2.1 - at constant specific thrust - it is therefore necessary to increase the engine size i.e. increase fan and core size simultaneously which leads to: i) higher engine weight, ii) higher nacelle drag, and iii) non-optimum engine/aircraft matching i.e. mid-cruise conditions away from the bottom of the SFC loop (see Fig. 3.8).

Most of the conclusions drawn in this section are applicable to both the conventional core and the intercooled core configurations. Nevertheless, the intercooled core is constrained by a minimum blade high requirement for the last HPC stage. At a fixed core OPR and intercooler effectiveness, this constraint sets a minimum limit for the core mass flow; as a consequence a minimum limit is also set on specific thrust at a fixed engine thrust. This makes the intercooled core more favourable for very high thrust engines.

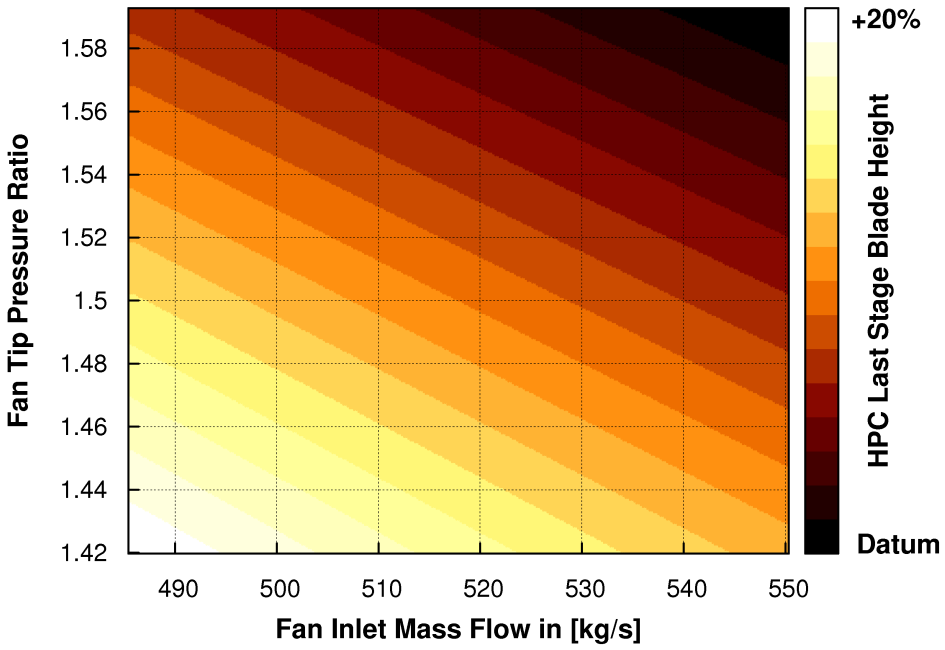

Figure 7.9: Variation of HPC last stage blade height with fan inlet mass flow and fan tip pressure ratio for a fixed size intercooled core.

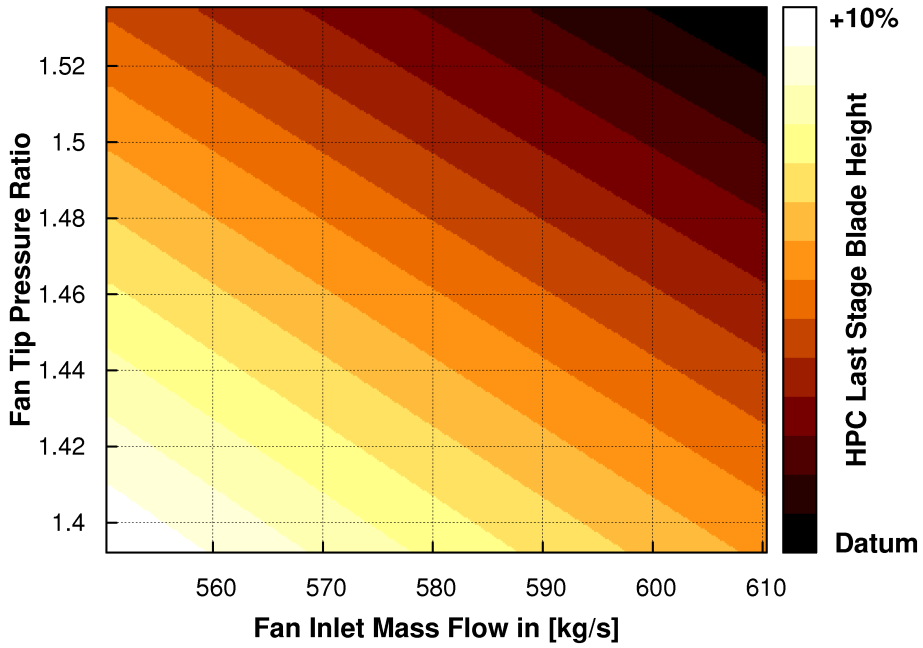

Figure 7.10: Variation of HPC last stage blade height with fan inlet mass flow and fan tip pressure ratio for a fixed size conventional core.

Bigger direct drive fans rotating at low speeds result in high torque requirements which increase the LP shaft outer diameter. The HPC inner diameter has to be pushed out and therefore, for a given flow area, the resulting blade height tends to reduce, as illustrated in Fig. 7.9 - the problem is less marked for a conventional core as illustrated in Fig. 7.10. For a given blade height requirement the core mass flow needs to be increased and it can therefore be concluded that an intercooled core would favour a geared fan arrangement, over a direct drive one, since it could alleviate some of the restrictions set on the cycle. An aft fan arrangement as the one presented in [230] could further relieve this issue; the disruptive elements associated with such an arrangement however, would make 2020 an ambitious target for entry into service. Furthermore, cooling requirements for struts in the mid-frame could potentially negate some of the thermal efficiency benefits predicted for the intercooled core.

7.2.5 IPC/HPC work split

Increasing engine OPR improves thermal efficiency and hence SFC, as illustrated in Fig. 7.11. The optimal OPR level for the conventional core is constrained by the maximum allowable HPC delivery temperature set, as illustrated in Fig. 7.12. For an intercooled cycle, this limitation is alleviated but only to give its place to a minimum blade height requirement which consequently sets a minimum allowable core size constraint. The optimal OPR level for the intercooled core at a fixed specific thrust is therefore a trade-off between a better core efficiency and a smaller core size.

If one assumes constant component polytropic efficiencies then SFC benefits will arise for the conventional core from shifting pressure ratio to the more efficient High Pressure (HP) shaft. As the HPC pressure ratio rises beyond the upper limit set, the core configuration would inevitably need to be changed to a two-stage HPT. This would introduce higher cooling flow requirements (and hence losses) and would also make the core heavier and longer, negating the originally projected benefits. Efficient intercooling requires that the IPC has significantly less pressure ratio than the HPC [88]. For that reason, a two-stage HPT has been assumed for the intercooled core while a minimum IPC design pressure ratio was set two avoid potential icing problems during decent.

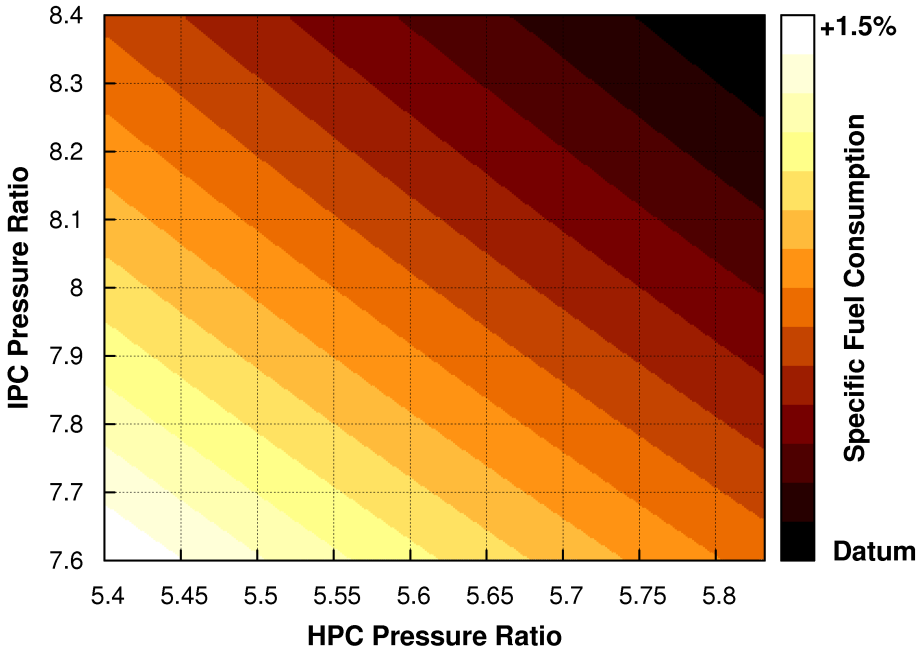

Figure 7.11: Variation of mid-cruise specific fuel consumption with IPC and HPC pressure ratio for a fixed size conventional core.

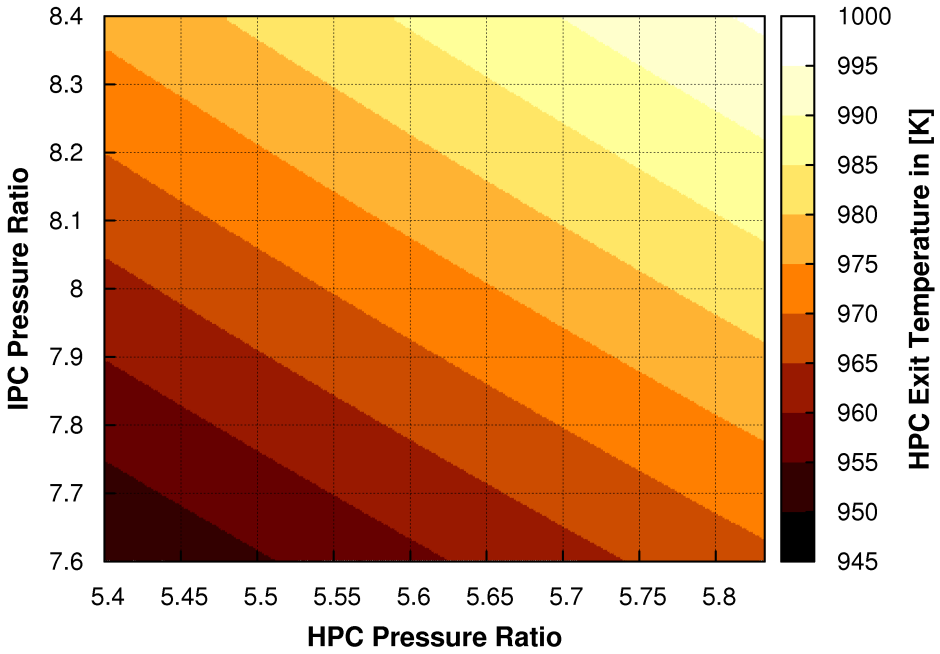

Figure 7.12: Variation of take-off HPC exit temperature with IPC and HPC pressure ratio for a fixed size conventional core.

7.2.6 Engine ratings

Rating an engine is a highly complex process that has to consider aircraft performance requirements, fuel consumption, and engine lifing. Turbine blade lifing requirements and cooling technology set a maximum allowable blade metal temperature constraint; cooling flows therefore need to increase with increasing combustor outlet temperature (T_4) levels. The maximum T_4 level may also be constrained by combustor design considerations. For example liner cooling requirements essentially reduce the amount of air available for mixing and hence NO_x tend to increase [132]; detail design studies are required for establishing the optimal trade-off between cycle efficiency and acceptable NO_x levels. For these reasons an upper limit was set to T_4 that was considered to be a reasonable trade-off for year 2020 entry into service turbofan engines. The same limit was used for both the conventional core and the intercooled core. Although, the intercooled core benefits from lower combustor inlet temperatures the air to fuel ratio is lower for a given T_4. Furthermore, high pressure levels in the intercooled cycle will affect the influence of luminosity on gas emissivity, and hence the temperature difference across the liner [8].

For a given OPR there is an optimal mid-cruise T_4 for SFC. Nevertheless, running the cycle hotter at top of climb (than the optimal for mid-cruise SFC) tends to reduce engine weight, as illustrated in Fig. 7.13. These benefits come mainly from the reduction in LPT weight although a further reduction in weight is possible by reducing core size (mainly in the case of the conventional core) since core output is increasing with T_4. On the other hand, running the cycle hotter at hot day take-off tends to increase engine weight. An increase in T_4 at top of climb generally requires an increase in T_4 at take-off in order to maintain a constant FAR take-off field length; T_4 at top of climb is therefore constrained by a hot-day take-off T_4 limitation. Furthermore, with modern large engines on long range aircraft typically being heavily derated at take-off conditions milder than hot-day, top of climb T_4 will need to be lower than hot-day take-off T_4 as to not compromise engine life [57]. An optimal block fuel trade-off therefore arises as illustrated in Fig. 7.14.

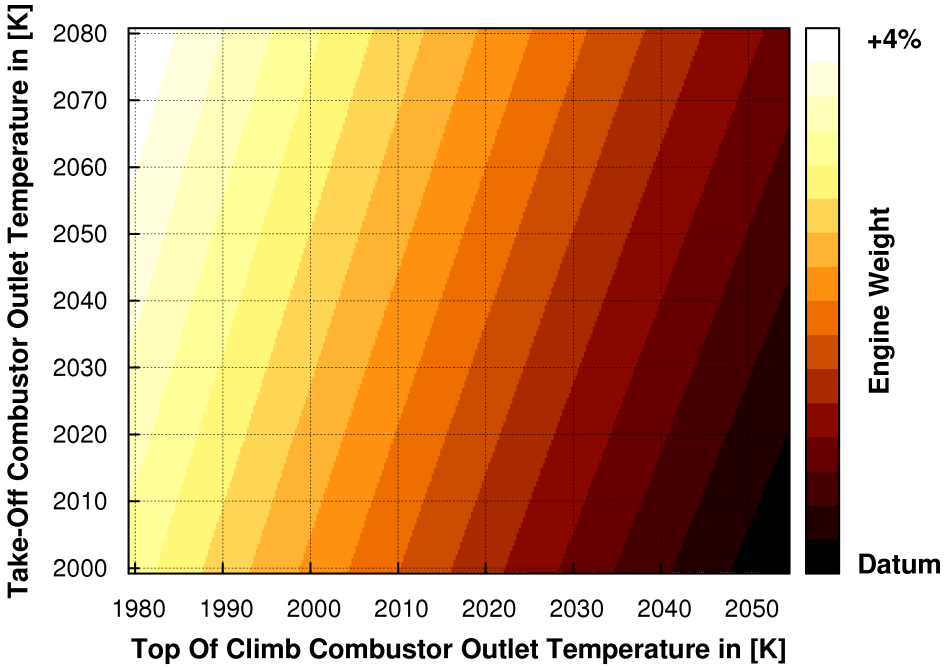

Figure 7.13: Variation of engine weight with combustor outlet temperature at take-off and top of climb conditions for a fixed size conventional core.

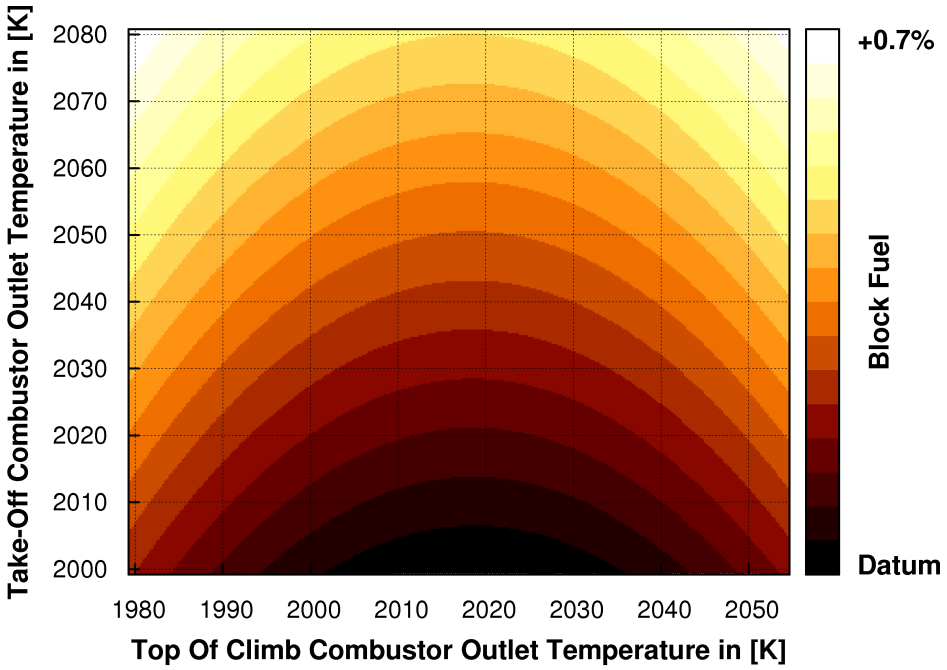

Figure 7.14: Variation of aircraft block fuel with combustor outlet temperature at take-off and top of climb conditions for a fixed size conventional core.

7.2.7 Intercooler effectiveness

In TERA2020, the aerodynamic design for most engine components is carried out at top of climb conditions. However, the intercooler component is sized at end of runway hot day take-off conditions (kink point) were the highest heat transfer levels are encountered; at cruise conditions the variable geometry dual-nozzle system is utilised to reduce the intercooler mass flow ratio (W132Q25) and hence reduce intercooler pressure losses. This practice results in better SFC and hence lower block fuel, as illustrated in Fig. 7.15.Nevertheless, there is a limit to this benefit set by a maximum allowable nozzle area variation, as illustrated in Fig. 7.16.

As discussed in detail in Chapter 6, high intercooler effectiveness can increase thrust at take-off, for a given combustor outlet temperature, but the benefits are soon negated by the increasing intercooler weight and pressure losses. The effect of intercooler effectiveness on weight is illustrated in Fig. 7.17; as can be observed intercooler effectiveness at top of climb conditions has only a secondary order effect. As intercooler weight increases so does block fuel; an optimal trade-off therefore exists between intercooler effectiveness, core size, and OPR.

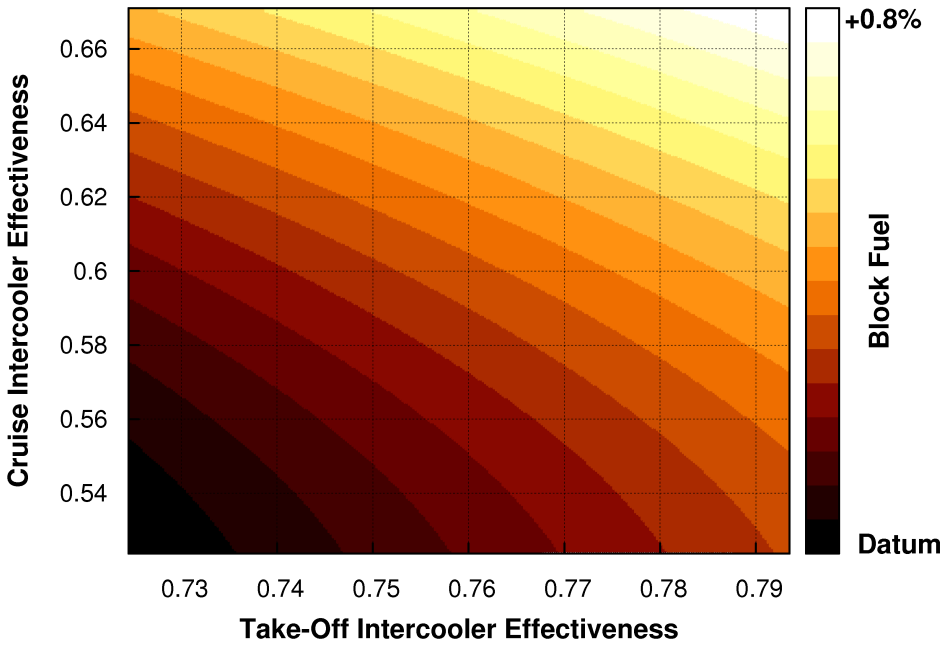

Figure 7.15: Variation of block fuel with intercooler effectiveness at take-off and cruise conditions.

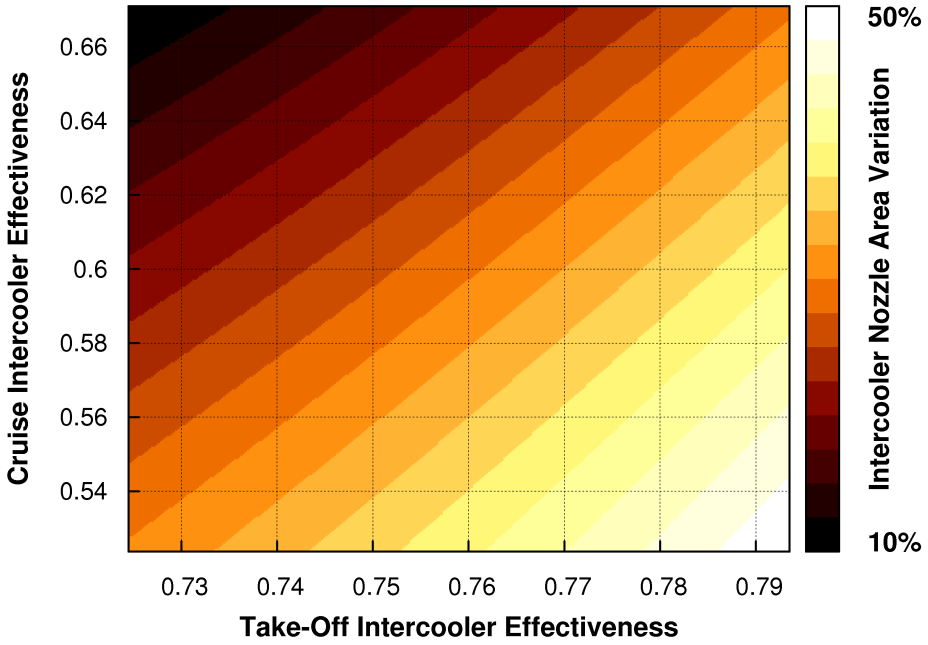

Figure 7.16: Variation of intercooler nozzle area with intercooler effectiveness at take-off and cruise conditions.

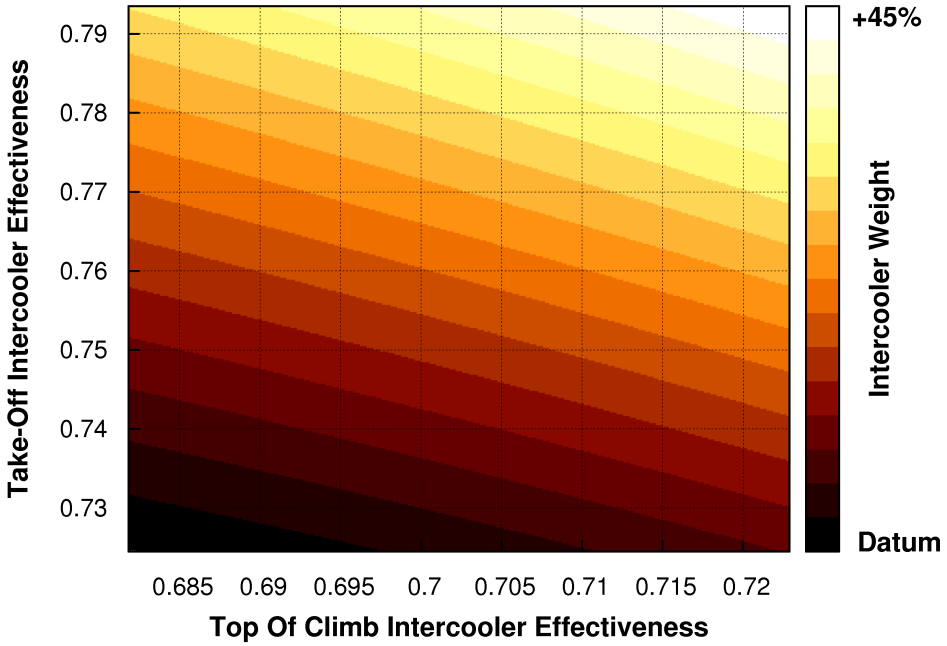

Figure 7.17: Variation of intercooler weight with intercooler effectiveness at top of climb and take-off conditions.

7.3 Sensitivity analysis of optimal designs

The study presented in this section aims to deliver averaged exchange rates which can be used to investigate the effect of technology parameter deviations on block fuel. Information on how these perturbations were introduced in the TERA2020 calculations is given in Appendix B.

The sensitivity parameters compiled allow for system level quantification of the importance of research on specific component technologies i.e. they can be used to assess the importance of progress in specific component technologies for each engine configuration in a similar manner to the assessment presented in Chapter 5. Inversely, these exchange factors also help quantify the impact of technology shortcomings. The exchange rates presented should be perceived as fractional percentage variations from the technology target value that was assumed when deriving the fuel optimal designs presented in Section 7.2.2.

7.3.1 Conventional core

The sensitivity analysis for the conventional core configuration is illustrated in Fig. 7.18. As expected for a low specific thrust engine, the low pressure system component technology has the greatest influence on performance; significant fuel benefits are expected by improving fan and LPT efficiency. Inversely, shortcomings in meeting projected technology targets for the low pressure system will have a major impact on overall engine/aircraft performance.

As fan tip pressure ratio reduces, pressure losses in the bypass duct tend to have an increasingly dominant effect on transmission efficiency and, therefore, on the impact of propulsive efficiency improvements on SFC. By combining Fig. 7.3 and Fig. 7.18 it can be observed that a 10% increase in bypass duct pressure losses will halve the projected block fuel benefits from a 10 [in] increase in fan diameter and the consequent reduction in specific thrust.

Failure to deliver the expected efficiency levels for the compressor components will increase combustor inlet temperatures resulting in higher NO_x levels and reduced component life; combustor designs are highly sensitive to inlet conditions and it is highly likely that a significant shortcoming in compressor efficiency would result in a re-design of the combustor.

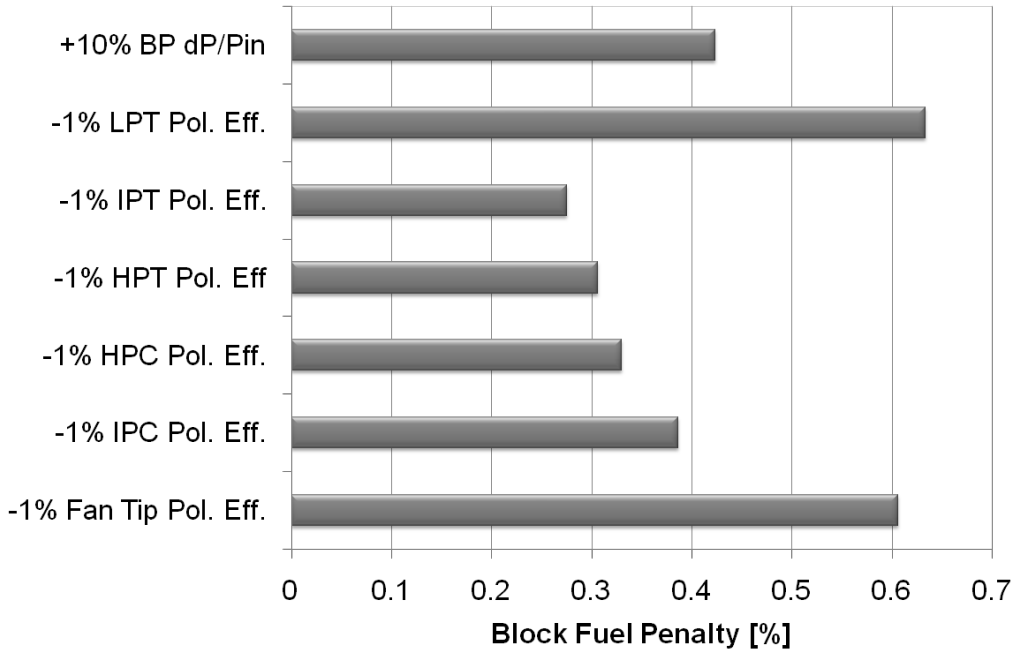

Figure 7.18: Sensitivity analysis around the fuel optimal design for the conventional core configuration.

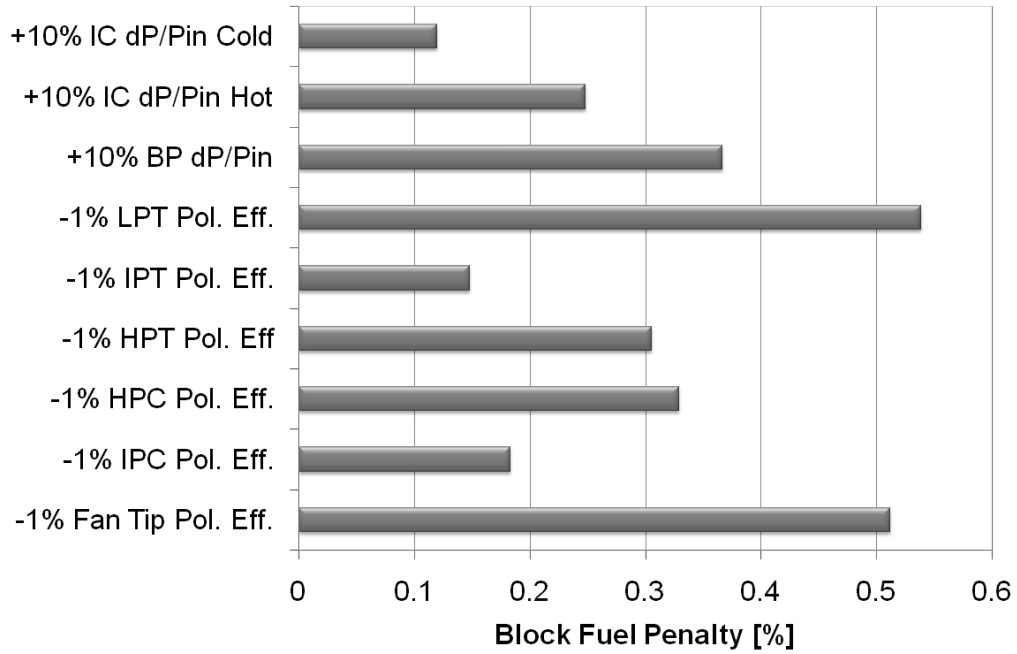

Figure 7.19: Sensitivity analysis around the fuel optimal design for the intercooled core configuration.

7.3.2 Intercooled core

The sensitivity analysis for the intercooled core configuration is illustrated in Fig. 7.19. The influence of the low pressure system component technology on performance is less marked for the intercooled core configuration compared to the conventional core; the difference in the exchange rates is directly proportional to the difference in specific thrust between the two optimal designs.

The efficiency of the IPC and IPT has a significantly smaller influence on block fuel, compared to the conventional core configuration, which reflects the significantly smaller pressure ratio placed on the Intermediate Pressure (IP) shaft. On the other hand, the efficiency of the HPC and HPT has a similar influence on block fuel, compared to the conventional core configuration, despite the significantly larger pressure ratio placed on the HP shaft. This can be explained by the fact that intercooling significantly reduces HP compression work.

As can be observed, intercooler pressure losses have a significant effect on block fuel. Losses in the intercooler hot stream are more important compared to losses in the cold stream, while losses in the cold stream become increasingly important as the intercooled mass flow ratio (W132Q25) increases. Failure to achieve the intercooler pressure loss targets set can significantly reduce the projected block fuel benefits for the intercooled core configuration.

7.4 Conclusion

The results from the optimisation process show that the optimal specific thrust for the intercooled core is higher compared to the conventional core turbofan engine; this is mainly attributed to the HPC last stage blade height requirement limiting core size and fan diameter. Although the high OPR intercooled core benefits from a higher core and transmission efficiency, and hence a better thermal efficiency, the conventional core benefits from a higher propulsive efficiency. As a remedy to this, the introduction of a geared fan arrangement is proposed. An aft fan arrangement could probably reduce the optimal specific thrust level significantly; the disruptive elements associated with such an arrangement however, would make 2020 an ambitious target for entry into service. Furthermore, cooling requirements for struts in the mid-frame could potentially negate some

of the thermal efficiency benefits predicted for the intercooled core.

It can be concluded that considerable benefits in terms of block fuel are expected from an intercooled core, with year 2020 entry into service level of technology, compared to a conventional core turbofan engine for long range applications. **These benefits are highly dependent on achieving technology targets such as low weight and pressure losses for the intercooler**. The commercial competitiveness of an intercooled core turbofan design will largely depend on how the aviation market evolves in the years to come until 2020.

7.5 Outlook

In this chapter, TERA2020 was used for assessing the combined potential of novel low pressure spool and core technologies for reducing engine emissions. A back-to-back comparison of an intercooled core engine with a conventional core engine was performed and fuel optimal designs for year 2020 entry into service were proposed. In the next chapter, overall conclusions will be drawn reflecting the research effort presented in this thesis.

Chapter 8

Conclusion

The research effort presented in this thesis focused on the development of various elements of a multi-disciplinary aero engine conceptual design tool, within a collaborative environment. The developed partially-automated tool was successfully used for quantifying the potential benefits from novel technologies for different turbofan engine architectures, and optimal designs for year 2020 entry into service were proposed.

8.1 Major findings

The developed multi-disciplinary aero engine conceptual design tool is - at this level of integration and to such evidence that were encountered during this research - of higher fidelity than previous efforts reported in the literature. It is based on an explicit algorithm and considers the following disciplines: engine performance, engine aerodynamic and mechanical design, aircraft design and aerodynamic performance, emissions prediction and environmental impact, engine and airframe noise, and production, maintenance and direct operating costs.

The developed tool is targeted towards identifying an appropriate design space where more complex and time-consuming tools could be utilised. In many cases the modelling carried out is based on correlations that are available in the public domain or have been supplied by original equipment manufacturers within the

European collaborative projects VITAL and NEWAC. It is recognized that such correlations have a limited range of validity and are dependent on supporting engineering science base. As an appropriate design space is defined, a more rigorous iterative design procedure would typically be set involving a large number of company specialists.

The major findings of the presented research effort are:

- The tool developed can assist in the transition from the traditional, human-based aero engine conceptual design procedure to a partially-automated process. The explicit algorithm proposed minimises internal iterations, reduces system complexity and improves computational speed; through a good set of constraints, such an algorithm will give an optimal aero engine conceptual design that will be feasible in terms of engine certification and customer requirements.

- The semi-empirical correlation derived can predict with sufficient accuracy - for conceptual design - the NO_x emissions for modern rich-burn single-annular combustors. The correlation may be extrapolated with sufficient confidence for year 2020 entry into service conventional core turbofan engines.

- The improved gradient-based algorithm - used for solving non-linear equation systems - significantly improved the computational speed of the different codes it was utilised with, confirming expectations from the literature reviewed. Furthermore, the algorithm fully alleviates the computational penalty associated with the use of central differences.

- In general, dissociation becomes first noticed at 1500 [K], and significant at 1800 [K]. The effects of dissociation on major performance parameters during design-point and off-design performance calculations are significant. For accurate block fuel predictions dissociation effects should not be ignored as this introduces a systematic error in the calculations.

- Where radical design space exploration is concerned, improving the accuracy of the fluid model needs to be carefully balanced with the computational time penalties involved. For an intercooled cycle with a high overall pressure ratio the ideal gas assumption does not hold very well; if the ideal

isothermal compression process is to be considered significant calculation errors should be expected.

- The developed tool, can be successfully used for quantifying the impact of failing to deliver specific component improvements in terms of power plant noise and CO_2 emissions. The exchange rates presented essentially provide the means for making estimates of the relative merits of future technology investment for particular engine architectures.

- There is significant potential in improving the performance of heat-exchanged cycles through variable geometry. Care should be taken though with respect to the need to carry out the high pressure compressor aerodynamic design at different engine operating conditions, compared to normal practice.

- Aggressive turbofan designs that reduce CO_2 emissions can increase the production of NO_x emissions due to the higher flame temperatures and pressures encountered. The introduction of lean-burn combustion in conventional and heat-exchanged cycles can help keep cruise and LTO NO_x emissions at acceptable levels. Furthermore, combining lean-burn combustion technology with variable geometry for an intercooled cycle demonstrates significant benefits in terms of LTO NO_x reduction.

- The optimal specific thrust for an intercooled core with a direct drive fan is higher compared to a conventional core configuration. Although a high OPR intercooled core benefits from a higher core and transmission efficiency, and hence a better thermal efficiency, the conventional core benefits from a higher propulsive efficiency. As a remedy to this, the introduction of a geared fan arrangement is proposed. An aft fan arrangement could probably reduce the optimal specific thrust level significantly; the disruptive elements associated with such an arrangement however, would make 2020 an ambitious target for entry into service. Furthermore, cooling requirements for struts in the mid-frame could potentially negate some of the thermal efficiency benefits predicted for the intercooled core.

Overall, it can be concluded that considerable benefits in terms of block fuel are expected from heat exchanged cores, with year 2020 entry into service level of technology, compared to conventional core turbofan engines for long range applications. **These benefits are highly dependent on achieving technology**

targets such as low weight and pressure losses for the intercooler and recuperator components. The commercial competitiveness of these designs will largely depend on how the aviation market evolves in the years to come until 2020.

8.2 Recommendations for future work

Future work on the developed tool could focus on:

- **Consideration of engine deteriorated performance.** Specific component technologies that aim to reduce engine performance deterioration could then be assessed more rigorously in terms of block fuel and direct operating costs.
- **More detailed consideration of an engine's secondary air system.** Large cooling and sealing flows could very well reduce, or even negate, the specific fuel consumption benefits predicted for some novel technologies and concepts.
- **An enhanced link between engine performance and WeiCo.** This could assist in the transition from designing a turbine at a fixed point in the Smith chart to being able to trade turbine efficiency for stage count and weight during the optimisation process.
- **Introduction of transient performance aspects.** For example a ground idle to take-off thrust acceleration could be considered, including thermal inertia effects for heat-exchanged cycles.
- **Further development of the HERMES code.** The newly-added routines for aircraft weight breakdown calculations formed the first step in the transformation of HERMES into a capable aircraft conceptual design tool. Consideration of center of gravity, fuselage design, wing buffet, and aircraft production costing aspects are the next steps to take.
- **Introduction of Air Traffic Management (ATM) and airline fleet operational aspects.** Interesting and more realistic assessments could come out of such a development, including looking into ways of reducing an airline's environmental footprint.

- **Consideration of more disruptive technologies.** Concepts such as pulse detonation and constant volume combustion, as well as the double bypass and selective bleed cycles could be considered. The tool could also be further developed to perform a more rigorous assessment - compared to previous efforts - of distributed propulsion and supersonic flight for commercial transport.

- **Platform improvements with respect to computational speed.** More efficient data exchange and parallel-processing, could result in a nearly 10-fold reduction in computational time for a modern desktop computer, and negligible computational times for a cluster environment. This means that the computational time required for the current optimisation studies could be reduced from overnight to roughly one or two hours (without changing hardware specifications). Inversely, optimisation studies with more variables or at a higher fidelity level could be run overnight.

References

[1] Intergovernmental Panel on Climate Change. Climate Change 2007: Mitigation of Climate Change. Working Group III. IPCC Fourth Assessment Report (AR4), 2007.

[2] Advisory Council for Aeronautical Research in Europe. European Aeronautics: A Vision for 2020 – Meeting Society's Needs and Winning Global Leadership. See also URL `http://www.acare4europe.org`, January 2001.

[3] J.-J. Korsia and S. Guy. VITAL – European R&D Programme for Greener Aero-Engines. In *ISABE 2007 Proceedings, ISABE-2007-1118*, Beijing, China, September 2007.

[4] G. Wilfert, J. Sieber, A. Rolt, N. Baker, A. Touyeras, and S. Colantuoni. New Environmental Friendly Aero Engine Core Concepts. In *ISABE 2007 Proceedings, ISABE-2007-1120*, Beijing, China, September 2007.

[5] J. Kurzke. Achieving maximum thermal efficiency with the simple gas turbine cycle. In *Proceedings of 9th CEAS European Propulsion Forum: "Virtual Engine – A Challenge for Integrated Computer Modelling"*, Rome, Italy, October 2003.

[6] J.H. Horlock, D.T. Watson, and T.V. Jones. Limitations on Gas Turbine Performance Imposed by Large Turbine Cooling Flows. *ASME Journal of Engineering for Gas Turbines and Power*, 123(3):487–494, July 2001.

[7] R.C. Wilcock, J.B. Young, and J.H. Horlock. The Effect of Turbine Blade Cooling on the Cycle Efficiency of Gas Turbine Power Cycles. *ASME Journal of Engineering for Gas Turbines and Power*, 127(1):109–120, January 2005.

[8] A.H. Lefebvre. *Gas Turbine Combustion*. Taylor & Francis, PA, USA, 2nd edition, 1999.

[9] R.W. Claus, A.L. Evans, J.K. Lylte, and L.D. Nichols. Numerical Propulsion System Simulation. *Computing Systems in Engineering (ISSN 0956-0521)*, 2(4):357–364, 1991.

[10] J.K. Lytle. The Numerical Propulsion System Simulation: An Overview. NASA/TM2000-209915, NASA Glenn Research Center, June 2000.

[11] E. Onat and G. W. Klees. A method to estimate weight and dimensions of large and small gas turbine engines. NASA-CR-159481, NASA, January 1979.

[12] M.T. Tong, I. Halliwell, and L.J. Ghosn. A computer code for gas turbine engine weight and disk life estimation. *ASME Journal of Engineering for Gas Turbines and Power*, 126(2):265–270, April 2004.

[13] M.T. Tong and B.A. Naylor. An Object-Oriented Computer Code for Aircraft Engine Weight Estimation. In *ASME TURBO EXPO 2008 Proceedings, GT2008-50062*, Berlin, Germany, June 2008.

[14] L.A. McCullers. Aircraft configuration optimization including optimized flight profiles. In *NASA Symposium on Recent Experiences in Multidisciplinary Analysis and Optimization, NASA-CP-2327, Part 1, pp. 395-412*, Hampton, Virginia, USA, April 1984.

[15] K. Kontos, B. Janardan, and P. Gliebe. Improved NASA-ANOPP Noise Prediction Computer Code for Advanced Subsonic Propulsion Systems. NASA-CR-195480, NASA Lewis Research Center, Cleveland, OH, USA, August 1996.

[16] N. Antoine, I. Kroo, K. Willcox, and G. Barter. A Framework for Aircraft Conceptual Design and Environmental Performance Studies. In *10th AIAA/ISSMO Multidisciplinary Analysis and Optimization Conference Proceedings, AIAA 2004-4314*, Albany, New York, September 2004.

[17] C.R. Mercer, W.J. Haller, and M.T. Tong. Adaptive Engine Technologies for Aviation CO2 Emissions Reduction. In *42nd AIAA/ASME/SAE/ASEE Joint Propulsion Conference and Exhibit, AIAA20065105*, Sacramento, California, USA, July 2006.

[18] PARTNER. `http://web.mit.edu/aeroastro/partner/`, 2009.

[19] Canadian and US Representatives. Environmental Design Space (EDS) Progress. presented to the Seventh Meeting of CAEP, CAEP/7-IP/23, February 2007.

[20] M.J. Jones, S.J. Bradbrook, and K. Nurney. A Preliminary Engine Design Process for an Affordable Capability. In *RTO AVT Symposium on "Reduction of Military Vehicle Acquisition Time and Cost through Advanced Modelling and Virtual Simulation" Proceedings, RTO-MP-089-52*, Paris, France, April 2002.

[21] P. Jeschke, J. Kurzke, R. Schaber, and C. Riegler. Preliminary Gas Turbine Design Using the Multidisciplinary Design System MOPEDS. *ASME Journal of Engineering for Gas Turbines and Power*, 126(2):258–264, April 2004.

[22] R. Avellán and T. Grönstedt. Preliminary Design of Subsonic Transport Aircraft and Engines. In *ISABE 2007 Proceedings, ISABE-2007-1195*, Beijing, China, September 2007.

[23] U.T.J. Grönstedt. *Development of Methods for Analysis and Optimization of Complex Jet Engine Systems*. PhD thesis, Chalmers University of Technology, Gothenburg, Sweden, 2000.

[24] Kurzke, J. `http://www.gasturb.de`, 2009.

[25] Lissys Ltd. `http://www.lissys.demon.co.uk`, 2009.

[26] Nationaal Lucht- en Ruimtevaartlaboratorium. `http://www.gspteam.com`, 2009.

[27] W.P.J. Visser and M.J. Broomhead. GSP, A Generic Object-Oriented Gas Turbine Simulation Environment. In *ASME TURBO EXPO 2000 Proceedings, ASME-2000-GT-0002*, Munich, Germany, May 2000.

[28] S.A. Shakariyants, J.P. van Buijtenen, W.P.J. Visser, and A. Tarasov. A Multidisciplinary Aero-Engine Exhaust Emissions Study. In *ASME TURBO EXPO 2006 Proceedings, GT2006-90749*, Barcelona, Spain, June 2006.

[29] S.A. Shakariyants, J.P. van Buijtenen, W.P.J. Visser, and A. Tarasov. Generic Airplane and Aero-Engine Simulation Procedures for Exhaust Emission Studies. In *ASME TURBO EXPO 2007 Proceedings, GT-2007-27943*, Montreal, Canada, May 2007.

[30] F. Montella and J.P. van Buijtenen. A Simplified Method to Evaluate the Impact of Component Design on Engine Performance. In *ASME TURBO EXPO 2007 Proceedings, GT-2007-28051*, Montreal, Canada, May 2007.

[31] VITAL. `http://www.project-vital.org`, 2009.

[32] NEWAC. `http://www.newac.eu`, 2009.

[33] DREAM. `http://www.dream-project.eu`, 2010.

[34] E. Vicente. Effect of Bypass Ratio on Long Range Subsonic Engines. Master's thesis, Cranfield University, Cranfield, Bedfordshire, United Kingdom, 1994.

[35] M. Le Dilosquer. Implications of Long Range Civil Aircraft Flight Routes on Atmospheric Pollution. Master's thesis, Cranfield University, Cranfield, Bedfordshire, United Kingdom, 1993.

[36] M. Le Dilosquer, S.H. Lee, and R. Singh. An Integrated Approach to the Impact of High Altitude NOx Emissions from Subsonic Aircraft on the Atmosphere. In *2nd International Symposium on Aeronautical Science and Technology (ISASTI'96) Proceedings, pp 1317-1327*, Jakarta, Indonesia, June 1996.

[37] M. Le Dilosquer and R. Singh. Influence of Low Emissions Requirements on Aero Engine Cycle. In *IMechE Seminar Publication 1996-12 - Aeroengines and Propulsion, Selected papers from Aerotech 95, C505/23/014/95*, London, United Kingdom, 1996.

[38] M. Le Dilosquer. *Influence of Subsonic Aero Engine Design and Flight Routes on Atmospheric Pollution*. PhD thesis, Cranfield University, Cranfield, Bedfordshire, United Kingdom, 1998.

[39] S.H. Lee, M. Le Dilosquer, R. Singh, and M.J. Rycroft. Further Considerations of Engine Emissions from Subsonic Aircraft at Cruise Altitude. *Atmospheric Environment*, 30(22):3689–3695, 1996.

[40] S.H. Lee, M. Le Dilosquer, R. Singh, S.E. Hobbs, C. Giannakopoulos, P.H. Plantevin, K.S. Law, J.A. Pyle, and M.J. Rycroft. Implications of NOy emissions from subsonic aircraft at cruise altitude. *Proceedings of the Institution of Mechanical Engineers, Part G: Journal of Aerospace Engineering*, 211(3):157–168, 1997.

[41] S. Gayraud. Technical and Economical Assessment for Industrial Gas Turbine Selection. Master's thesis, Cranfield University, Cranfield, Bedfordshire, United Kingdom, 1996.

[42] S. Gayraud. Design of a Decision Support System for Combined Cycle Schemes. MPhil thesis, Cranfield University, Cranfield, Bedfordshire, United Kingdom, 1998.

[43] M.W. Whellens and R. Singh. Propulsion System Optimisation for Minimum Global Warming Potential. In *23rd ICAS Congress Proceedings*, Toronto, Canada, September 2002.

[44] M.W. Whellens, H. Taguchi, R. Singh, and P. Pilidis. Genetic Algorithm Based Optimisation of Intercooled Recuperated Turbofan Desgin. In *41st AIAA Aerospace Sciences Meeting and Exhibit Proceedings*, Reno, Nevada, USA, January 2003.

[45] M.W. Whellens. *Multidisciplinary Optimisation of Aero-Engines Using Genetic Algorithms and Preliminary Design Tools*. PhD thesis, Cranfield University, Cranfield, Bedfordshire, United Kingdom, 2003.

[46] F. Svensson. *Potential of Reducing the Environmental Impact of Civil Subsonic Aviation by Using Liquid Hydrogen*. PhD thesis, Cranfield University, Cranfield, Bedfordshire, United Kingdom, 2005.

[47] F. Svensson, A. Hasselrot, and J. Moldanova. Reduced environmental impact by lowered cruise altitude for liquid hydrogen-fuelled aircraft. *Aerospace Science and Technology*, 8(4):307–320, June 2004.

[48] T. Papadopoulos. *Gas Turbine Cycles for Intermediate Load Power Generation*. PhD thesis, Cranfield University, Cranfield, Bedfordshire, United Kingdom, 2005.

[49] A. Polyzakis. *Technoeconomical Evaluation of Trigeneration Plant: Gas Turbine Performance, Absorption Cooling and District Heating.* PhD thesis, Cranfield University, Cranfield, Bedfordshire, United Kingdom, 2006.

[50] P. Laskaridis. *Performance Investigations and Systems Architectures for the More Electric Aircraft.* PhD thesis, Cranfield University, Cranfield, Bedfordshire, United Kingdom, 2004.

[51] P. Laskaridis, P. Pilidis, and P. Kotsiopoulos. An Integrated Engine - Aircraft Performance Platform for Assessing New Technologies in Aeronautics. In *ISABE 2005 Proceedings, ISABE-2005-1165*, Munich, Germany, September 2005.

[52] E. Tsoudis. *Technoeconomic Environmental and Risk Analysis of Marine Gas Turbine Power Plants.* PhD thesis, Cranfield University, Cranfield, Bedfordshire, United Kingdom, 2008.

[53] R.S.R. Khan, J. Barreiro, Lagana M.C., K.G. Kyprianidis, S.O.T. Ogaji, P. Pilidis, and I. Bennett. An Assessment of the Emissions and Global Warming Potential of Gas Turbines for LNG Applications. In *ASME TURBO EXPO 2009 Proceedings, GT-2009-59184*, Orlando, FL, USA, June 2009.

[54] R.S.R. Khan, M.C. Lagana, S.O.T. Ogaji, P. Pilidis, and I. Bennett. Risk Analysis of Gas Turbines for Natural Gas Liquefaction. In *ASME TURBO EXPO 2010 Proceedings, GT-2010-23261*, Glasgow, United Kingdom, June 2010.

[55] S.O.T. Ogaji, P. Pilidis, and R. Hales. TERA - A Tool for Aero-engine Modelling and Management. In *Second World Congress on Engineering Asset Management and the Fourth International Conference on Condition Monitoring*, Harrogate, United Kingdom, June 2007.

[56] S.O.T. Ogaji, P. Pilidis, and V. Sethi. Advanced Power Plant Selection: The TERA (Techno-economic Environmental Risk Analysis) Framework. In *ISABE 2009 Proceedings, ISABE-2009-1115*, Montreal, Canada, September 2009.

[57] A.M. Rolt. Rolls-Royce, private communications, 2009.

[58] I. Halliwell. Preliminary Engine Design – A Practical Overview. In *34th AIAA/ASME/SAE/ASEE Joint Propulsion Conference and Exhibit, AIAA 98-3891*, Cleveland, OH, USA, July 1998.

[59] J. Kurzke. Preliminary Design. In *von Karman Institute for Fluid Dynamics Lecture Series 2002-2003, Aero Engine Design: A State of the Art*, Belgium, April 2003.

[60] V.E. Kyritsis and P. Pilidis. Principles of Thermodynamic Preliminary Design of Civil Turbofan Engines. In *ASME TURBO EXPO 2009 Proceedings, GT-2009-59815*, Orlando, FL, USA, June 2009.

[61] S. Bretschneider, O. Arago, and S. Staudacher. Architecture of a Techno and Environmental Risk Assessment Tool Using a Multi–Modular Build Approach. In *ISABE 2007 Proceedings, ISABE-2007-1103*, Beijing, China, September 2007.

[62] Federal Aviation Administration. Federal Aviation Regulation Part 121 - Operating Requirement: domestic, flag and supplemental operations. FAR 121, Washington, DC, USA.

[63] Joint Aviation Authorities. Joint Airworthiness Requirements OPS Part 1 – Commercial Air Transportation (Aeroplanes). Ammendment 14, Hoofddorp, The Netherlands, 2008.

[64] ICAO. International Standards and Recommended Practices – Environmental Protection, Annex 16 to the Convention on International Civil Aviation, Volume II - Aircraft Engine Emissions. 2nd edition plus ammendments, Montreal, Canada, 1993.

[65] P. Newton, C. Holsclaw, M. Ko, and M. Ralph. Long Term Technology Goals for CAEP/7. presented to the Seventh Meeting of CAEP, February 2007.

[66] ICAO. International Standards and Recommended Practices – Environmental Protection, Annex 16 to the Convention on International Civil Aviation, Volume I - Aircraft Noise. Chapter 3 and 4, Montreal, Canada, 2001.

[67] R.W. Koenig and L.H. Fishbach. GENENG: A Program for Calculating Design and Off-Design Performance for Turbojet and Turbofan Engines.

NASA-TN-D-6552, NASA Lewis Research Center, Cleveland, OH, USA, February 1972.

[68] L.H. Fishbach and R.W. Koenig. GENENG II: A Program for Calculating Design and Off-Design Performance of Two- and Three-Spool Turbofans with as Many as Three Nozzles. NASA-TN-D-6553, NASA Lewis Research Center, Cleveland, OH, USA, February 1972.

[69] W.L. MacMillan. *Development of a Modular Type Computer Program for the Calculation of Gas Turbine Off-Design Performance*. PhD thesis, Cranfield University, Cranfield, Bedfordshire, United Kingdom, 1974.

[70] J.R. Palmer and Y. Cheng-Zhong. TURBOTRANS: A Programming Language for the Performance Simulation of Arbitrary Gas Turbine Engines with Arbitrary Control Systems. In *ASME TURBO EXPO 1982 Proceedings, 82-GT-200*, London, United Kingdom, March 1982.

[71] W.P.J. Visser. Gas Turbine Engine Simulation at NLR. In *"Making it REAL", CEAS Symposium on Simulation Technology Proceedings, CEAS-MOD-05*, Delft, The Netherlands, October-November 1995.

[72] J.F. Sellers and C.J. Daniele. Dyngen - a program for calculating steady state and transient performance of turbojet and turbofan engines. NASA-TN-D-7901, NASA Glenn Research Center, Cleveland, OH, USA, April 1975.

[73] U.T.J. Grönstedt and P. Pilidis. Optimization of the Transient Performance of the Selective Bleed Variable Cycle Engine During Mode Transition. In *ASME TURBO EXPO 2000 Proceedings, 2000-GT-0148*, Munich, Germany, May 2000.

[74] C.K. Drummond, G.J. Follen, and C.W. Putt. Gas Turbine System Simulation: An Object-Oriented Approach. NASA-TM-106044, NASA Lewis Research Center, Cleveland, OH, USA, April 1993.

[75] A.L. Evans, G. Follen, C. Naiman, and I. Lopez. Numerical Propulsion System Simulation's National Cycle Program. In *34th AIAA/ASME/SAE/ASEE Joint Propulsion Conference and Exhibit Proceedings, AIAA-1998-3113* , Cleveland, OH, USA, July 1998.

[76] EA Internacional. PROOSIS Official Website. `http://www.proosis.com/`, 2010.

[77] A. Bala, V. Sethi, E. Lo Gatto, V. Pachidis, and P. Pilidis. PROOSIS – A Collaborative Venture for Gas Turbine Performance Simulation Using an Object Oriented Programming Schema. In *ISABE 2007 Proceedings, ISABE-2007-1357*, Beijing, China, September 2007.

[78] A. Alexiou, E. Baalbergen, K. Mathioudakis, O. Kogenhop, and P. Arendsen. Advanced Capabilities for Gas Turbine Engine Performance Simulations. In *ASME TURBO EXPO 2007 Proceedings, GT2007-27086*, Montreal, Canada, May 2007.

[79] K.G. Kyprianidis. Dynamic Simulation of Aircraft Propulsion Systems. Dipl. Eng. Thesis, Aristotle University of Thessaloniki, Thessaloniki, Greece, 2006.

[80] K.G. Kyprianidis and A.I. Kalfas. Dynamic Performance Investigations of a Turbojet Engine using a Cross-Application Visual Oriented Platform. *RAeS The Aeronautical Journal*, 112(1129):161–169, March 2008.

[81] B. Meyer. *Object-Oriented Software Construction*. Prentice-Hall PTR, Englewood Cliffs, NJ, USA, 2nd edition, March 2000.

[82] E. Akin. *Object–Oriented Software Programming via Fortran 90/95*. Cambridge University Press, Cambridge, United Kingdom, 1st edition, 2003.

[83] Society of Automotive Engineers. Real-Time Modelling Methods for Gas Turbine Engine Performance. SAE AIR 4548 Rev. A, Warrendale, PA, USA, 2001.

[84] Society of Automotive Engineers. Gas Turbine Engine Steady-State and Transient Performance Presentation for Digital Computer Programs. SAE AS681 Rev. J, Warrendale, PA, USA, 2008.

[85] Society of Automotive Engineers. Aircraft Propulsion System Performance Station Designation and Nomenclature. SAE AS755 Rev. D, Warrendale, PA, USA, 2004.

[86] Society of Automotive Engineers. Application Programming Interface Requirements for the Presentation of Gas Turbine Engine Performance on Digital Computers. SAE ARP4868, Warrendale, PA, USA, 2001.

[87] Society of Automotive Engineers. Gas Turbine Engine Performance Presentation and Nomenclature for Digital Computers Using Object-Oriented Programming. SAE ARP 5571 Draft 6.0, Warrendale, PA, USA, August 2004.

[88] P.P. Walsh and P. Fletcher. *Gas Turbine Performance*. Blackwell Science, United Kingdom, 1st edition, 1998.

[89] RTO Applied Vehicle Technology Panel Task Group AVT-036. Performance Prediction and Simulation of Gas Turbine Engine Operation for Aircraft, Marine, Vehicular, and Power Generation. RTO-TR-AVT-036, NATO, France, February 2007.

[90] P. Pilidis. *Digital Simulation of Gas Turbine Performance*. PhD thesis, University of Glasgow, Glasgow, United Kingdom, 1983.

[91] A.A. Sirinoglou. Implementation of Variable Geometry for Gas Turbine Performance Simulation Turbomatch Improvement. Master's thesis, Cranfield University, Cranfield, Bedfordshire, United Kingdom, 1992.

[92] J. Kurzke. Performance modeling methodology: Efficiency definitions for cooled single and multistage turbines. In *ASME TURBO EXPO 2002 Proceedings, 2002-GT-30497*, Amsterdam, The Netherlands, June 2002.

[93] R.E. Grey and H.D. Wilsted. Performance of Conical Jet Nozzles in Terms of Flow. NACA-TN-1757, NACA Lewis Flight Propulsion Laboratory, Cleveland, OH, USA, November 1948.

[94] J. Kurzke. How to Get Component Maps for Aircraft Gas Turbine Performance Calculations. In *ASME TURBO EXPO 1996 Proceedings, 96-GT-164*, Birmingham, U.K, June 1996.

[95] J. Kurzke. Gas Turbine Performance Simulation with GasTurb 10. `http://www.gasturb.de`, 2007.

[96] National Oceanic and Atmospheric Administration. U.S. Standard Atmosphere, 1976. USGPO-1976-O-588-286, National Aeronautics and Space Administration, U.S. Government Printing Office, Washington, D.C., USA, October 1976.

[97] S. Boggia and K. Rud. Intercooled Recuperated Gas Turbine Engine Concept. In *Proceedings of 41st AIAA/ASME/SAE/ASEE Joint Propulsion Conference and Exhibit, AIAA 2005-4192*, Arizona, USA, July 2005.

[98] L.R. Jenkinson, P. Simpkin, and D. Rhodes. *Civil Jet Aircraft Design*. Arnold, London, United Kingdom, 1st edition, 1999.

[99] ESDU. Estimation of Airframe Drag by Summation of Components – Principles and Examples. ESDU-97016, London, United Kingdom, September 1997.

[100] E. Torenbeek. *Synthesis of Subsonic Airplane Design: An Introduction to the Preliminary Design of Subsonic General Aviation and Transport Aircraft, with Emphasis on Layout, Aerodynamic Design, Propulsion and Performance*. Delft University Press and Kluwer Academic Publishers, The Netherlands, student edition, 1982.

[101] J. Roskam. *Airplane Design - Part I: Preliminary Sizing of Airplanes*. Design, Analysis and Research Corporation, Lawrence, Kansas, USA, 1st edition, 2005.

[102] J. Roskam. *Airplane Design - Part V: Component Weight Estimation*. Design, Analysis and Research Corporation, Lawrence, Kansas, USA, 1st edition, 2003.

[103] Swiss International Air Lines. Flying Smart. *Swiss Magazine, Issue 12.2009 / 1.2010*, pages 100–105, December 2009.

[104] J.A. Borradaile. private communications, 2010.

[105] J.E. Penner, D.H. Lister, D.J. Griggs, D.J. Dokken, and M. McFarland. *Aviation and the Global Atmosphere: A Special Report of IPCC Working Groups I and III in Collaboration with the Scientific Assessment Panel to the Montreal Protocol on Substances that Deplete the Ozone Layer*. Cambridge University Press, 1999.

[106] A. Wulff and J. Hourmouziadis. Technology Review of Aeroengine Pollutant Emissions. *Aerospace Science and Technology*, 1(8):557–572, December 1997.

[107] A. Tomboulides. presentation during Summer School on the LES of Reacting Flows, ERCOFTAC SIG28, September 2004.

[108] A.M. Mellor. Semi-Empirical Correlations for Gas Turbine Emissions, Ignition, and Flame Stabilization. *Progress in Energy and Combustion Science*, 6(4):347–358, 1981.

[109] A.H. Lefebvre. Fuel Effects on Gas Turbine Combustion-Liner Temperature, Pattern Factor, and Pollutant Emissions. *AIAA Journal of Aircraft*, 21(11):887–898, November 1984.

[110] J. Odgers and D. Kretschmer. The Prediction of Thermal NOx in Gas Turbines. In *1985 International Gas Turbine Symposium and Exposition Proceedings, ASME-85-IGT-126*, Beijing, China, September 1985.

[111] P.C. Malte, S. Bernstein, F. Bahlmann, and J. Doelman. NOx Exhaust Emissions for Gas-Fired Turbine Engines. In *ASME TURBO EXPO 1990 Proceedings, 90-GT-392*, Brussels, Belgium, June 1990.

[112] G.D. Lewis. A New Understanding of NOx Formation. In *ISABE 1991 Proceedings, ISABE-91-7064*, Nottingham, United Kingdom, 1991.

[113] N.A. Rokke, J.E. Hustad, and S. Berg. Pollutant Emissions from Gas Fired Turbine Engines in Offshore Practice - Measurements and Scaling. In *International Gas Turbine and Aeroengine Congress and Exposition Proceedings, ASME 93-GT-170*, Cincinnati, Ohio, USA, May 1993.

[114] N.K. Rizk and H.C. Mongia. Semianalytical Correlations for NOx, CO and UHC Emissions. *ASME Journal of Engineering for Gas Turbines and Power*, 115(3):612–619, July 1993.

[115] N.K. Rizk and H.C. Mongia. Emissions Predictions of Different Gas Turbine Combustors. In *32nd Aerospace Sciences Meeting and Exhibit Proceedings, AIAA-1994-0118*, Reno, NV, USA, January 1994.

[116] T. Becker and M.A. Perkavec. The Capability of Different Semianalytical Equations for Estimation of NOx Emissions of Gas Turbines. In *ASME TURBO EXPO 94 Proceedings, 94-GT-282*, The Hague, The Netherlands, June 1994.

[117] D.G. Nicol, P.C. Malte, and R.C. Steele. Simplified Models for NOx Production Rates in Lean-Premixed Combustion. In *ASME TURBO EXPO 94 Proceedings, 94-GT-432*, The Hague, The Netherlands, June 1994.

[118] K.M. Tacina, C.-M. Lee, and C. Wey. NASA Glenn High Pressure Low NOx Emissions Research. Technical report, NASA Glenn Research Center, Cleveland, Ohio, USA, February 2008. NASA/TM-2008-214974.

[119] R. Tacina, C.-H. Mao, and C. Wey. Experimental Investigation of a Multiplex Fuel Injector Module With Discrete Jet Swirlers for Low Emission Combustors. Technical report, NASA Glenn Research Center, Cleveland, Ohio, USA, August 2004. NASA/TM-2004-212918.

[120] Committee of Aeronautical Technologies, Aeronautics and Space Engineering Board, Commission on Engineering and Technical Systems, National Research Council. *Aeronautical Technology for the Twenty-First Century.* National Academy Press, Washington, D.C., USA, 1992.

[121] M. Lecht. Simplified NOx Emissions Prediction: Fuel Flow Methods. The NEPAir Workshop, WP2 presenation slides, November 2002.

[122] J. Tilston, J. Larkman, M. Plohr, A. Doepelheuer, T. Lischer, and N. Zarzalis. Future Engine Cycle Prediction and Emissions Study. Technical report, CYPRESS Final Publishable Report, Issue 2.0 (Version 3), August 2003.

[123] H.C. Mongia. Recent Advances in the Development of Combustor Design Tools. In *39th AIAA/ASME/SAE/ASEE Joint Propulsion Conference and Exhibit Proceedings, AIAA-2003-4495*, Huntsville, Alabama, USA, July 2003.

[124] A. Tsalavoutas, M. Kelaidis, N. Thoma, and K. Mathioudakis. Correlations Adaptation for Optimal Emissions Prediction. In *ASME TURBO EXPO 2007 Proceedings, GT2007-27060*, Montreal, Canada, May 2007.

[125] ICAO. Engine Emissions Databank. `http://www.caa.co.uk`, February 2009.

[126] P.D. Norman, D.H. Lister, M. Lecht, P. Madden, K. Park, O. Penanhoat, C. Plaisance, and K. Renger. Development of the Technical Basis for a New Emissions Parameter Covering the Whole Aircraft Operation: NEPAIR, Final Technical Report. NEPAIR/WP4/WPR/01, September 2003.

[127] R.L. Martin, C.A. Oncina, and J.P. Zeeben. A Simplified Method for Estimating Aircraft Engine Emissions. Technical report, Boeing Company, 1994.

[128] S.L. Baughcum, T.G. Tritz, S.C. Henderson, and D.C. Pickett. Boeing Method 2 Fuel Flow Methodology Description. In *Scheduled Civil Aircraft Emission Inventories for 1992: Database Development and Analysis, NASA Langley Research Center, NASA-CR-4700*, Hampton, VA, USA, April 1996.

[129] F. Deidewig, A. Dopelheuer, and M. Lecht. Methods to Assess Engine Emissions in Flight. In *20th ICAS Congress Proceedings, Vol. I*, Sorrento, Italy, September 1996.

[130] A. Dopelheuer and M. Lecht. Influence of Engine Performance on Emission Characteristics. In *RTO AVT Symposium on "Gas Turbine Engine Combustion, Emissions and Alternative Fuels" Proceedings, RTO-MP-14*, Lisbon, Portugal, October 1998.

[131] A. Dopelheuer. Aircraft Emission Parameter Modelling. *Air & Space Europe*, 2(3):34–37, 2000.

[132] S. Bake. Rolls-Royce Deutschland, private communications, 2009.

[133] I. Segalman, R.G. McKinney, Sturgess G.J., and L.-M. Huang. Reduction of NOx by Fuel-Staging in Gas Turbine Engines - A Commitment to the Future. In *AGARD Conference on "Fuel and Combustion Technology for Advanced Aircraft Engines" Proceedings, AGARD CP 536, Paper 29*, May 1993.

[134] T. Ripplinger, N. Zarzalis, G. Meikis, C. Hassa, and Brandt M. NOx Reduction by Lean Premixed Prevaporised Combustion. In *RTO AVT Symposium on "Gas Turbine Engine Combustion, Emissions and Alternative Fuels" Proceedings, RTO-MP-14, Paper 7*, Lisbon, Portugal, October 1998.

[135] T. Otten, M. Plohr, and R. von der Bank. Gegenüberstellung des Emissions - Verbesserungspotentials von Brennkammertechnologien und Anderen Weiterentwicklungen am Lufttransportsystem.

[136] M. Plohr, R. von der Bank, and T. Schilling. Vergleich des Emissionsverhaltens Effizienter Hochbypasstriebwerke Mittlerer Schubgrösse für den ICAO LTO-Zyklus und Flugmissionen - Ergebnisse Einer Studie auf Basis von Korrelationsmethoden.

[137] W. Lazik, T. Doerr, and S. Bake. Low NOx Combustor Development for the Engine3E Core Engine Demonstrator. In *ISABE 2007 Proceedings, ISABE-2007-1190*, Beijing, China, September 2007.

[138] M.T. Metcalfe, R.A. Eaton, and D.M. Snape. The Impact of Air Transport on the Environment. In *ISABE 1991 Proceedings, ISABE-91-7021*, Nottingham, United Kingdom, 1991.

[139] P. Madden. Development of Emissions Methodology to Account for the Global Atmospheric Impact of Aviation. In *IMechE Conference Proceedings, Volume 9, pp. 251-272, C545/063*, United Kingdom, 1998.

[140] Intergovernmental Panel on Climate Change. Climate Change 2007: The Physical Science Basis. Working Group I. IPCC Fourth Assessment Report (AR4), 2007.

[141] J.-M. Rogero. Airbus, private communications, 2009.

[142] P.M. de F. Forster, K.P. Shine, and N. Stuber. It is premature to include non-CO_2 effects of aviation in emission trading schemes. *Atmospheric Environment*, 40(6):1117–1121, February 2006.

[143] A. Kollmuss and A. Myers Crimmins. Carbon Offsetting & Air Travel Part 2: Non-CO_2 Emissions Calculations. SEI discussion paper, Stockholm Environment Institute, Stockholm, Sweden, June 2009.

[144] D.S. Pascovici, F. Colmenares, S.O.T. Ogaji, and P. Pilidis. An Economic and Risk Analysis Model for Aircrafts and Engines. In *ASME TURBO EXPO 2007 Proceedings, GT2007-27236*, Montreal, Canada, May 2007.

[145] D.S. Pascovici, F. Colmenares, and S.O.T. Ogaji. Operating Cost and Risk Analysis for Aircraft and Engines. In *ISABE 2007 Proceedings, ISABE-2007-1106*, Beijing, China, September 2007.

[146] D.S. Pascovici. *Thermo Economic and Risk Analysis for Advanced Long Range Engines*. PhD thesis, Cranfield University, Cranfield, Bedfordshire, United Kingdom, 2008.

[147] D. Pascovici, S. Ogaji, R. Singh, and E. Zanenga. Optimisation of Direct Operating Costs of Future Ultra High Bypass Ratio Aero Engines. In *ISABE 2009 Proceedings, ISABE-2009-1342*, Montreal, Canada, September 2009.

[148] J. Roskam. *Airplane Design - Part VIII: Airplane Cost Estimation: Design, Development, Manufacturing and Operating*. Design, Analysis and Research Corporation, Lawrence, Kansas, USA, 1st edition, 2002.

[149] R.F. Colmenares Quintero. *Techno-economic and Environmental Risk Assessment of Innovative Propulsion Systems for Short-Range Civil Aircraft*. PhD thesis, Cranfield University, Cranfield, Bedfordshire, United Kingdom, 2009.

[150] O. Vigna Suria. A Flexible Lifing Model for Gas Turbines: Creep and Low Cycle Fatigue Approach. Master's thesis, Cranfield University, Cranfield, Bedfordshire, United Kingdom, September 2006.

[151] A.J. Fawke and H.I.H. Saravanamuttoo. Digital Computer Methods for Prediction of Gas Turbine Dynamic Response. SAE-710550, pp. 1805-1813, Society of Automotive Engineers, February 1971.

[152] W.H. Press, S.A. Teukolsky, W.T. Vetterling, and B.P. Flannery. *Numerical Recipes in Fortran 90: The Art of Parallel Scientific Computing - Volume 2*. Cambridge University Press, United Kingdom, 2nd edition, 1996.

[153] J.R.R.A. Martins, P. Sturdza, and J.J. Alonso. The Complex-Step Derivative Approximation. *ACM Transactions on Mathematical Software*, 29(3):245–262, September 2003.

[154] J.R.R.A. Martins, P. Sturdza, and J.J. Alonso. The Connection Between The Complex-Step Derivative Approximation and Algorithmic Differentiation. In *39th Aerospace Sciences Meeting and Exhibit Proceedings, AIAA-2001-0921*, Reno, Nevada, USA, January 2001.

[155] Jr. Dennis, J.E. and R.B. Schnabel. *Numerical Methods for Unconstrained Optimization and Nonlinear Equations*. Prentice-Hall, Englewood Cliffs, NJ, USA, 1983.

[156] U.T.J. Grönstedt. Chalmers University, private communications, 2009.

[157] A. Stamatis, K. Mathioudakis, J. Ruiz, and B. Curnock. Real Time Engine Model Implementation for Adaptive Control & Performance Monitoring of Large Civil Turbofans. In *ASME TURBO EXPO 2001 Proceedings, 2001-GT-0362*, New Orleans, Louisiana, June 2001.

[158] C.G. Broyden. A Class of Methods for Solving Nonlinear Simultaneous Equations. *Mathematics of Computation*, 19(92):577–593, October 1965.

[159] C.G. Broyden. Quasi Newton Methods and their Application to Function Minimisation. *Mathematics of Computation*, 21(99):368–381, July 1967.

[160] M.J.D. Powell. A Fortran Subroutine for Solving Systems of Nonlinear Algebraic Equations. In *Numerical Methods for Nonlinear Algebraic Equations, Rabinowitz, P., editor, Ch. 7*, January 1970.

[161] J.J. Moré, B.S. Garbow, and K.E. Hillstrom. User Guide for MINPACK-1. ANL-80-74, Argonne National Laboratory, Argonne, Ill., USA, 1980.

[162] J.J. Moré, D.C. Sorensen, K.E. Hillstrom, and B.S. Garbow. The MINPACK Project. In *Sources and Development of Mathematical Software, W.R. Cowell, editor, Prentice-Hall, ISBN-13 978-0138235017, pp. 88-111*, April 1984.

[163] The Netlib Repository. `http://www.netlib.org/`, 2009.

[164] U.T.J. Grönstedt. Advanced Solvers for General High Performance Transient Gas Turbine Simulation Tools. In *ISABE 1999 Proceedings, ISABE-99-7102*, Florence, Italy, September 1999.

[165] L.R. Petzold. Differential/Algebraic Equations are not ODEs. *SIAM Journal on Scientific and Statistical Computing*, 3(3):367–384, September 1982.

[166] P. Dierckx. *Curve and Surface Fitting with Splines*. Oxford Science Publications, Oxford, United Kingdom, 1st edition, 1993.

[167] G.E. Moore. Cramming more Components onto Integrated Circuits. *Electronics Magazine*, 38(8), April 1965.

[168] VIVACE. `http://www.vivaceproject.com`, 2007.

[169] A. Alexiou, N. Aretakis, I. Roumeliotis, and K. Mathioudakis. Analysis for a Geared Turbofan with Active Core Technologies. In *ASME TURBO*

EXPO 2010 Proceedings, GT2010-22701, Glasgow, United Kingdom, June 2010.

[170] A. Arago, S. Bretschneider, and S. Staudacher. A Unit Cost Comparison Methodology for Turbofan Engines. In *ASME TURBO EXPO 2007 Proceedings, GT2007-27485*, Montreal, Canada, May 2007.

[171] M.F. Heidmann. Interim Prediction Method for Fan and Compressor Source Noise. NASA-TM-71763, NASA Glenn Research Center, Cleveland, OH, USA, June 1975.

[172] J.R. Stone, E.A. Krejsa, and B.J. Clark. Jet Noise Modelling for Coannular Nozzles Including the Effects of Chevrons. NASA/CR-2003-212522, NASA Glenn Research Center, Cleveland, OH, USA, September 2003.

[173] Society of Automotive Engineers. Gas Turbine Jet Exhaust Noise Prediction. SAE ARP 876 Rev. D, Warrendale, PA, USA, 1994.

[174] E.A. Krejsa and M.F. Valerino. Interim Prediction Method for Turbine Noise. NASA-TM-X-73566, NASA Lewis Research Center, Cleveland, OH, USA, November 1976.

[175] M.R. Fink. Airframe Noise Prediction Method. FAA-RD-77-29, Federal Aviation Administration, 1977.

[176] Society of Automotive Engineers. Standard Values of Atmospheric Absorption as a Function of Temperature and Humidity. SAE ARP 866 Rev. A, Warrendale, PA, USA, 1975.

[177] C.F. Chien and W.W. Soroka. Sound Propagation Along an Impedance Plane. *Journal of Sound and Vibration*, 43(1):9–20, 1975.

[178] Society of Automotive Engineers. Prediction Method for Lateral Attenuation of Airplane Noise During Takeoff and Landing. SAE AIR 1751, Warrendale, PA, USA, 1981.

[179] A.M. Blackner and T.R.S. Bhat. Installation Effects on Coaxial Jet Noise, an Experimental Study. In *Aerospace Sciences Meeting and Exhibit 98 Proceedings, AIAA-98-0080*, Reno, NV, USA, January 1998.

[180] D.B. Hanson. Noise of Counter-Rotation Propellers. *Journal of Aircraft*, 22(7):609–617, 1985.

[181] G.E. Whitfield, R. Mani, and P.R. Gliebe. High Speed Turboprop Aeroacoustic Study (counterrotation), Volume 1: Model Development. Technical report, July 1990. NASA-CR-185241.

[182] V. Sethi, F. Diara, S. Atabak, A. Jackson, A. Bala, and P. Pilidis. Advanced Modelling of Fluid Thermodynamic Properties for Gas Turbine Performance Simulation. In *ASME TURBO EXPO 2008 Proceedings, GT2008-51126*, Berlin, Germany, June 2008.

[183] D. Bücker, R. Span, and W. Wagner. Thermodynamic Property Models for Moist Air and Combustion Gases. *ASME Journal of Engineering for Gas Turbines and Power*, 125(1):374–384, January 2003.

[184] American Society of Mechanical Engineers. Gas Turbine Heat Recovery Steam Generators, Performance Test Codes. ANSI/ASME PTC 4.4-1981, New York, USA, 1981.

[185] Jr. Chase, M.W. NIST–JANAF Thermochemical Tables, 4th Edition. *American Institude of Physics, Journal of Physical and Chemical Reference Data, Monograph No. 9*, 1998.

[186] B.J. McBride, S. Heimel, J.G. Ehlers, and S. Gordon. Thermodynamic Properties to 6000 K for 210 Substances Involving the First 18 Elements. NASA Special Publication 3001, Office of Technical Services, US Department of Commerce, Washington, DC, USA, 1963.

[187] B.J. McBride, S. Gordon, and M. A. Reno. Coefficients for calculating thermodynamic and transport properties of individual species. NASA-TM-4513, NASA Glenn Research Center, Cleveland, OH, USA, 1993.

[188] S. Gordon and B.J. McBride. Computer Program for Calculation of Complex Chemical Equilibrium Composition and Applications. NASA-RP-1311, NASA Glenn Research Center, Cleveland, OH, USA, 1994.

[189] F. Brandt. *Brennstoffe und Verbrennungs–rechnung, FDBR–Fachbuchreihe Band 1.* Vulkan, Essen, Germany, 3rd edition, 2000.

[190] H.D. Baehr and C. Diederichsen. Berechnungsgleichungen für Enthalpie und Entropie der Komponenten von Luft und Verbrennungsgasen. *Brennst.-Wärme-Kraft*, 40(1/2):30–33, 1988.

[191] R.J. Kee, F.M. Rumpley, and J.A. Miller. The Chemkin Thermodynamic Data Base. Report No. SAND-8215B, Sandia National Laboratories, 1992.

[192] G.P. Smith, D.M. Golden, M. Frenklach, N.W. Moriarty, B. Eiteneer, M. Goldenberg, C.T. Bowman, R.K. Hanson, S. Song, W.C. Gardiner, Jr., V.V. Lissianski, and Z. Qin. GRI-Mech 3.0. `http://www.me.berkeley.edu/gri\_mech/`, 2009.

[193] J. Kurzke. About Simplifications in Gas Turbine Performance Calculations. In *ASME TURBO EXPO 2007 Proceedings, GT2007-27620*, Montreal, Canada, May 2007.

[194] R.C. Wilcock, J.B. Young, and J.H. Horlock. Gas Properties as a Limit to Gas Turbine Performance. In *ASME TURBO EXPO 2002 Proceedings, GT-2002-30517*, Amsterdam, The Netherlands, June 2002.

[195] A.S. Lee, R. Singh, and S.D. Probert. Simulations of gas turbines performances: influence of gas-behaviour modelling. *Proceedings of the IMechE, Part A: Journal of Power and Energy, in press*, 2010.

[196] Y.A Çengel. *Heat Transfer: A Practical Approach.* McGraw Hill, 2nd edition, 2003.

[197] U.J.I. Alvarez. *Simulation of Multi Fluid Gas Turbines.* PhD thesis, Cranfield University, Cranfield, Bedfordshire, United Kingdom, 1998.

[198] A. Guha. An Efficient Generic Method for Calculating the Properties of Combustion Products. *Proceedings of the IMechE, Part A: Journal of Power and Energy*, 215(3):375–387, 2001.

[199] C. Morley. Gaseq A Chemical Equilibrium Program for Windows. `http://www.arcl02.dsl.pipex.com/`, 2009.

[200] S. Gordon and B.J. McBride. Computer Program for Calculation of Complex Chemical Equilibrium Compositions, Rocket Performance, Incident and Reflected Shocks and Chapman-Jouguet Detonations. NASA-SP-273, NASA Glenn Research Center, Cleveland, OH, USA, 1992.

[201] V. Sethi. *Advanced Performance Simulation of Gas Turbine Components and Fluid Thermodynamic Properties.* PhD thesis, Cranfield University, Cranfield, Bedfordshire, United Kingdom, 2008.

[202] A.J.B. Jackson, A.C. Neto, M. Whellens, and H. Audus. Gas Turbine Performance Using Carbon Dioxide as Working Fluid in Closed Cycle Operation. In *ASME TURBO EXPO 2000 Proceedings, 2000-GT-153*, Munich, Germany, May 2000.

[203] W.P.J. Visser and S.C.A. Kluiters. Modelling the Effects of Operating Conditions and Alternative Fuels on Gas Turbine Performance and Emissions. Nlr-tp-98629, National Aerospace Laboratory, Amsterdam, The Netherlands, 1998.

[204] E.M. Goodger. *Transport Fuels Technology - Mobility for the Millennium.* Norwich: Landfill Press, United Kingdom, 1st edition, 2000.

[205] T. Korakianitis, R. Dyer, and N. Subramanian. Pre-integrated Nonequilibrium Combustion-Response Mapping for Gas Turbine Emissions. *ASME Journal of Engineering for Gas Turbines and Power*, 126(2):300–305, April 2004.

[206] J.-J. Korsia. VITAL – European R&D Programme for Greener Aero-Engines. In *ISABE 2009 Proceedings, ISABE-2009-1114*, Montreal, Canada, September 2009.

[207] H. Canière, A. Willcokx, E. Dick, and M. De Paepe. Raising cycle efficiency by intercooling in air–cooled gas turbines. *Applied Thermal Engineering*, 26(16):1780–1787, November 2006.

[208] M.A. da Cunha Alves, H.F. de Franca Mendes Carneiro, J.R. Barbosa, L.E. Travieso, P. Pilidis, and K.W. Ramsden. An insight on intercooling and reheat gas turbine cycles. *Proceedings of the Institution of Mechanical Engineers, Part A: Journal of Power and Energy*, 215(2):163–171, 2001.

[209] T. Papadopoulos and P. Pilidis. Introduction of Intercooling in a High Bypass Jet Engine. In *ASME TURBO EXPO 2000 Proceedings, 2000-GT-150*, Munich, Germany, May 2000.

[210] L. Xu, B. Gustafsson, and T. Grönstedt. Mission Optimization of an Intercooled Turbofan Engine. In *ISABE 2007 Proceedings, ISABE-2007-1157*, Beijing, China, September 2007.

[211] L. Xu and T. Grönstedt. Design and Analysis of an Intercooled Turbofan Engine. *ASME Journal of Engineering for Gas Turbines and Power, GTP-09-1228, in press*, December 2009.

[212] A.D. Walker, J.F. Carrotte, and A.M. Rolt. Duct Aerodynamics for Intercooled Aero Gas Turbines: Constraints, Concepts and Design Methododology. In *ASME TURBO EXPO 2009 Proceedings, GT2009-59612*, Orlando, Florida, June 2009.

[213] A. Lundbladh and A. Sjunnesson. Heat Exchanger Weight and Efficiency Impact on Jet Engine Transport Applications. In *ISABE 2003 Proceedings, ISABE-2003-1122*, Cleveland, USA, September 2003.

[214] G. Pellischek and B. Kumpf. Compact Heat Exchanger Technology for Aero Engines. In *ISABE 1991 Proceedings, ISABE-91-7019*, Nottingham, United Kingdom, September 1991.

[215] H. Schoenenborn, E. Ebert, B. Simon, and P. Storm. Thermomechanical Design of a Heat Exchanger for a Recuperated Aeroengine. *ASME Journal of Engineering for Gas Turbines and Power*, 128(4):736–744, October 2006.

[216] C.F. McDonald, A. Massardo, C. Rodgers, and A. Stone. Recuperated gas turbine aeroengines, part I: early development activities. *Aircraft Engineering and Aerospace Technology: An International Journal*, 80(2):139–157, 2008.

[217] C.F. McDonald, A. Massardo, C. Rodgers, and A. Stone. Recuperated gas turbine aeroengines, part II: engine design studies following early development testing. *Aircraft Engineering and Aerospace Technology: An International Journal*, 80(3):280–294, 2008.

[218] C.F. McDonald, A. Massardo, C. Rodgers, and A. Stone. Recuperated gas turbine aeroengines, part III: engine concepts for reduced emissions, lower fuel consumption, and noise abatement. *Aircraft Engineering and Aerospace Technology: An International Journal*, 80(4):408–426, 2008.

[219] A.M. Rolt. UK Patent GB 2 413 366 B, September 2006.

[220] D.E. Gray and J.W. Witherspoon. Fuel conservative propulsion concepts for future air transports. Technical Report SAE-760535, Society of Automotive Engineers, 1976.

[221] R. Hirschkron and R.E. Neitzel. Alternative concepts for advanced energy conservative transport engines. Technical Report SAE-760536, Society of Automotive Engineers, 1976.

[222] A.J.B. Jackson. Some Future Trends in Aero Engine Design for Subsonic Transport Aircraft. *ASME Journal of Engineering for Power*, 98:281–289, April 1976.

[223] A.J.B. Jackson. *Optimisation of Aero and Industrial Gas Turbine Design for the Environment*. PhD thesis, Cranfield University, Cranfield, Bedfordshire, United Kingdom, 2009.

[224] G.L. Wilde. Future large civil turbofans and powerplants. *RAeS Aeronautical Journal*, 82:281–299, July 1978.

[225] P.H. Young. The future shape of medium and long-range civil engines. *RAeS Aeronautical Journal*, pages 53–61, February 1979.

[226] G.G. Pope. Prospects for reducing the fuel consumption of civil aircraft. *RAeS Aeronautical Journal*, pages 287–295, August 1979.

[227] J.M. Swihart. The Promise of the Supersonics. In *AIAA 7th Annual Meeting and Technical Display Proceedings, AIAA 70-1217*, Houston, Texas, USA, October 1970.

[228] R.E. Bates and J. Morris. A McDonnell Douglas Perspective – Commercial Aircraft for the Next Generation. In *AIAA Aircraft Design, Systems and Technology Meeting Proceedings, AIAA-83-2502*, Fort Worth, Texas, USA, October 1983.

[229] R. Watts. European air transport up to the year 2000. *RAeS Aeronautical Journal*, pages 300–312, July 1978.

[230] J.A. Borradaile. Towards the optimum ducted UHBR engine. In *Proceedings of AIAA/SAE/ASME/ASEE 24th Joint Propulsion Conference, AIAA-89-2954*, Boston, Massachusetts, USA, July 1998.

[231] R.A. Zimbrick and J.L. Colehour. An investigation of very high bypass ratio engines for subsonic transports. In *Proceedings of AIAA/SAE/ASME/ASEE 24th Joint Propulsion Conference, AIAA-88-2953*, Boston, Massachusetts, USA, July 1988.

[232] N.J. Peacock and J.H.R. Sadler. Advanced Propulsion Systems for Large Subsonic Transports. *ASME Journal of Propulsion and Power*, 8(3):703–708, May-June 1992.

[233] N.T. Birch. 2020 vision: the prospects for large civil aircraft propulsion. *RAeS Aeronautical Journal*, pages 347–352, August 2000.

[234] P.C. Ruffles. The future of aircraft propulsion. *Proceedings of the IMechE, Part C: Journal of Mechanical Engineering Science*, 214(1):289–305, 2000.

[235] H.I.H. Saravanamuttoo. The Daniel and Florence Guggenheim Memorial Lecture - Civil Propulsion; The Last 50 Years. In *ICAS 2002 Congress Proceedings*, Toronto, Canada, September 2002.

[236] H. Hemmer, T. Otten, M. Plohr, M. Lecht, and A. Döpelheuer. Influence of the Bypass Ratio on Low Altitude NO_x Emissions. In *1st CEAS European Air and Space Conference Proceedings, CEAS-2007-137, pp. 1185-1193*, Berlin, Germany, September 2007.

[237] W.G. Cornell. Experimental Quiet Engine Program – Summary Report. NASA-CR-2519, NASA, Cleveland, OH, USA, March 1975.

[238] G.L. Converse. Extended parametric representation of compressor fans and turbines. Volume 3: MODFAN user's manual (parametric modulating flow fan). NASA-CR-174647, NASA, Cleveland, OH, USA, March 1984.

[239] I. Halliwell. Preliminary Engine Design – A Practical Overview for the NASA John H. Glenn Research Center. Summer 2000.

[240] R.M. Plencner. Plotting component maps in the Navy/NASA Engine Program (NNEP): A method and its usage. NASA-TM-101433, NASA Glenn Research Center, Cleveland, OH, USA, January 1989.

[241] Numeca International. Radial compressor. Announcement in the Press by Numeca International, 1999.

[242] R.G. Stabe, W.J. Whitney, and T.P. Moffitt. Performance of a High-Work Low Aspect Ratio Turbine Tested with a Realistic Inlet Radial Temperature Profile. NASA-TM-83655, NASA Lewis Research Center, Cleveland, OH, USA, January 1984.

[243] G.L. Converse. Extended parametric representation of compressor fans and turbines. Volume 2: Part user's manual (parametric turbine). NASA-CR-174646, NASA, Cleveland, OH, USA, March 1984.

[244] N.D. Walker and M.W. Thomas. Experimetal Investigation of a 4 and 1/2 Stage Turbine with Very High Stage Loading Factor. 2: Turbine Performance. NASA-CR-2363, NASA Lewis Research Center, Cleveland, OH, USA, February 1974.

Author's Publications

K.G. Kyprianidis and A.I. Kalfas. Dynamic Performance Investigations of a Turbojet Engine using a Cross-Application Visual Oriented Platform. *RAeS The Aeronautical Journal*, 112(1129):161–169, March 2008.

K.G. Kyprianidis, G. Di Lorenzo, S.O.T. Ogaji, and P. Pilidis. The TERA Approach - A Methodology for Technoeconomical, Environmental and Risk Analysis of Multidisciplinary Systems. Cranfield, Bedfordshire, United Kingdom, May 2008. presented as poster at the Cranfield University Multi-Strand Conference.

K.G. Kyprianidis, R.F. Colmenares Quintero, D.S. Pascovici, S.O.T. Ogaji, P. Pilidis, and A.I. Kalfas. EVA - A Tool for EnVironmental Assessment of Novel Propulsion Cycles. In *ASME TURBO EXPO 2008 Proceedings, GT-2008-50602*, Berlin, Germany, June 2008.

D.S. Pascovici, K.G. Kyprianidis, R.F. Colmenares Quintero, S.O.T. Ogaji, and P. Pilidis. Weibull Distributions Applied to Cost and Risk Analysis for Aero Engines. In *ASME TURBO EXPO 2008 Proceedings, GT-2008-51060*, Berlin, Germany, June 2008.

R.F. Colmenares Quintero, K.G. Kyprianidis, J. Gomez-Parada, S.O.T. Ogaji, P. Pilidis, and S. Latorre. Future Turbofans' Multi-Objective Optimization for Minimal Enviromental Impact. In *ASME TURBO EXPO 2008 Proceedings, GT-2008-50126*, Berlin, Germany, June 2008.

C. Celis, M. Mohseni, K.G. Kyprianidis, V. Sethi, S.O.T. Ogaji, A. Haslam, and P. Pilidis. Multidisciplinary Design Optimization of Aero Engines: Environmental Performance-Based Methodology. In *SYMKOM'08 Proceedings published in Cieplne Maszyny Przeplywowe - Turbomachinery, No. 133*, Lodz, Poland, September 2008.

K.G. Kyprianidis, V. Sethi, S.O.T. Ogaji, P. Pilidis, R. Singh, and A.I. Kalfas. Thermo-Fluid Modelling for Gas Turbines - Part I: Theoretical Foundation and Uncertainty Analysis. In *ASME TURBO EXPO 2009 Proceedings, GT-2009-60092*, Orlando, FL, USA, June 2009.

K.G. Kyprianidis, V. Sethi, S.O.T. Ogaji, P. Pilidis, R. Singh, and A.I. Kalfas. Thermo-Fluid Modelling for Gas Turbines - Part II: Impact on Performance Calculations and Emissions Predictions at Aircraft System Level. In *ASME TURBO EXPO 2009 Proceedings, GT-2009-60101,* ***Cycle Innovations Committee Best Paper Award***, Orlando, FL, USA, June 2009.

R.S.R. Khan, J. Barreiro, Lagana M.C., K.G. Kyprianidis, S.O.T. Ogaji, P. Pilidis, and I. Bennett. An Assessment of the Emissions and Global Warming Potential of Gas Turbines for LNG Applications. In *ASME TURBO EXPO 2009 Proceedings, GT-2009-59184*, Orlando, FL, USA, June 2009.

T. Grönstedt, D. Au, K.G. Kyprianidis, and S.O.T. Ogaji. Low Pressure System Component Advancements and its Influence on Future Turbofan Engine Emissions. In *ASME TURBO EXPO 2009 Proceedings, GT-2009-60201*, Orlando, FL, USA, June 2009.

A. Terzis, K.G. Kyprianidis, P. Zachos, A.I. Kalfas, and P. Pilidis. Comparative Performance Evaluation of a Multistage Axial Fan Assembly. In *ISABE 2009 Proceedings, ISABE-2009-1187*, Montreal, Canada, September 2009.

K.G. Kyprianidis, D. Au, S.O.T. Ogaji, and T. Grönstedt. Low Pressure System Component Advancements and its Impact on Future Turbofan Engine Emissions. In *ISABE 2009 Proceedings, ISABE-2009-1276*, Montreal, Canada, September 2009.

E. Najafi Saatlou, R. Khan, B. Al-Abri, K.G. Kyprianidis, V. Sethi, S. Ogaji, and P. Pilidis. Gas Turbine Multi-disciplinary Assessments via Technoeconomical Environmental and Risk Analysis. In *IRAN ROTATE 2010 Proceedings*, Tehran, Iran, May 2010.

K.G. Kyprianidis, T. Grönstedt, S.O.T. Ogaji, P. Pilidis, and R. Singh. Assessment of Future Aero Engine Designs with Intercooled and Intercooled Recuperated Cores. In *ASME TURBO EXPO 2010 Proceedings, GT-2010-23621*, Glasgow, United Kingdom, June 2010.

T. Grönstedt and K.G. Kyprianidis. Optimizing the Operation of the Intercooled Turbofan Engine. In *ASME TURBO EXPO 2010 Proceedings, GT-2010-22519*, Glasgow, United Kingdom, June 2010.

A.M. Rolt, M. Andreoletti, and K.G. Kyprianidis. Assessment of New Aero Engine Core Concepts and Technologies in the EU Framework 6 NEWAC Programme. In *ICAS 2010 Congress Proceedings, Paper No. 408*, Nice, France, September 2010. extended abstract submitted for publication.

K.G. Kyprianidis, V. Sethi, S.O.T. Ogaji, P. Pilidis, R. Singh, and A.I. Kalfas. Uncertainty in Gas Turbine Thermo-Fluid Modelling and its Impact on Performance Calculations and Emissions Predictions at Aircraft System Level. *Proceedings of the IMechE, Part G: Journal of Aerospace Engineering, JAERO765*, 2010. submitted for publication.

K.G. Kyprianidis, T. Grönstedt, S.O.T. Ogaji, P. Pilidis, and R. Singh. Assessment of Future Aero Engine Designs with Intercooled and Intercooled Recuperated Cores. *ASME Journal of Engineering for Gas Turbines and Power, GTP-10-1056*, 2010. accepted for publication.

K.G. Kyprianidis, S.O.T. Ogaji, P. Pilidis, R. Singh, A.M. Rolt, and T. Grönstedt. Aero Engine Conceptual Design - Part I: Multi-Disciplinary Framework Development. *AIAA Journal of Propulsion and Power*, 2010. under preparation.

T. Grönstedt, A. Lundbladh, S.O.T. Ogaji, P. Pilidis, R. Singh, and K.G. Kyprianidis. Aero Engine Conceptual Design - Part II: Low Pressure System Component Advancements and its Impact on Future Turbofan Engine Emissions. *AIAA Journal of Propulsion and Power*, 2010. under preparation.

Appendices

Appendix A

Managing the development of TERA2020

This appendix discusses project management, quality control and dissemination aspects with respect to the development of the TERA2020 (Techno-economic, Environmental and Risk Assessment for 2020) tool within the European Framework 6 and 7 collaborative projects VITAL (enVIronmenTALly friendly aero engines), NEWAC (NEW Aero engine Core concepts) and DREAM (valiDation of Radical Engine Architecture systeMs). TERA2020 is a multi-disciplinary aero engine conceptual design tool and is based on an explicit algorithm; the tool is targeted towards identifying an appropriate design space where more complex and time-consuming tools could be utilised. The author worked as the acting work-package (WP) leader for NEWAC WP1.3, "Techno-Economic and Environmental Risk Analysis". Managing the development of TERA2020 within NEWAC required considerable effort; insight is provided into the challenges faced and lessons learned are discussed.

N.B. *Excerpts from the material presented in this appendix have also been used in Chapter 2.*

A.1 European Union collaborative projects and TERA2020

A.1.1 TERA2020 general objectives

Decision making on near term emissions legislation and taxation policies is usefully informed through industry studies, with respect to the impact certain legislator decisions could have on the design and operation of future civil aircraft engines. A Techno-economic, Environmental and Risk Assessment (TERA) approach tool intends, mainly, to address policy evaluations at a "macro level" looking more at how long term and global legislation can be addressed. TERA2020 can therefore be viewed as a common tool which in the future, and through continuous refinement with input from legislators, operators, OEMs (Original Equipment Manufacturer) and universities, could enhance the dialogue between these parties by increasing the visibility of the impact of different policy issues on a consistent and formal basis.

Another potential benefit from the development of TERA2020 within the European Union (EU), could be its contribution to enhanced European competitiveness on a global level. In the past, product design and manufacture has mostly been located in and driven by the markets and the legislative requirements of Europe, North America and Japan. These were also the markets where the majority of the sales occurred. The large growth in developing economies is changing the sales destination of civil aerospace products. Important proportions of the sales now take place in these emerging economies where different design solutions for good environmental performance may apply. A TERA approach tool would allow the exploration of economic and environmental performance of alternative design concepts and technologies. This could be done in a wide range of taxation regimes, helping to identify the more competitive options in local scenarios internationally.

The general objectives set during the development of the TERA2020 tool across the three European Framework 6 and 7 collaborative projects VITAL, NEWAC, and DREAM are:

- A quick assessment tool for new engine technologies.

- Assess the benefits of technologies under differing economic and environmental conditions.

- Optimise a group of engine technologies by relatively simple algorithms to differing economic and environmental scenarios.

- Progressively incorporate new and novel technologies.

- Provide initial starting points for engine designs for low economic and environmental impact that could be examined in depth by more complex and time consuming OEM tools.

- Evaluate and optimise the study engines against the project objectives.

- Progressively develop the capacity to become an independent research tool of choice for joint OEM ventures and provide useful information to project partners and important stakeholders.

The long term overall ambition is that the continuous refinement of TERA2020 algorithms will lead to an independent research tool that can help quantify risks and assess the impact of gas turbine design on the environment, by comparing and helping to rank future technologies and design concepts for civil aviation on a formal and consistent basis. TERA2020 will rely on the developers of new technologies providing data from realistic assessments of their capabilities and attributes, so that the tool can evaluate the costs and benefits at whole engine and whole aircraft level.

A.1.2 European Union collaborative projects

The TERA2020 tool is concurrently being developed within three different EU collaborative projects VITAL, NEWAC and DREAM. TERA2020 is expected to model the engine architectures and technologies studied under these projects, in sufficient detail to perform sensitivity, parametric and optimisation studies at conceptual design level.

A.1.2.1 The VITAL project

The VITAL project is a European Framework 6 collaborative project lead by Snecma and has a total budget of 91 million euros [206]. Within VITAL, three different engine architectures have been modelled with TERA2020, for short and long range applications: the direct drive fan engine, the geared fan engine, and the contra-rotating fan engine.

A.1.2.2 The NEWAC project

The NEWAC project is a European Framework 6 collaborative project lead by MTU Aero Engines and has a total budget of 71 million euros [4]. Within NEWAC, four different engine architectures have been modelled with TERA2020: the direct drive fan intercooled core engine, the geared fan active core engine, the contra-rotating fan flow controlled core engine, and the geared fan intercooled recuperated core engine. All architectures have been modelled for short and long range applications with the exception of the intercooled recuperated concept that has been modelled only for long range applications.

A.1.2.3 The DREAM project

The DREAM project is a European Framework 7 collaborative project lead by Rolls-Royce and has a total budget of 40 million euros [33]. Within DREAM, direct drive and geared pusher open rotor engine architectures are currently being modelled with TERA2020 for short range applications.

A.1.3 NEWAC sub-programme 1 management structure

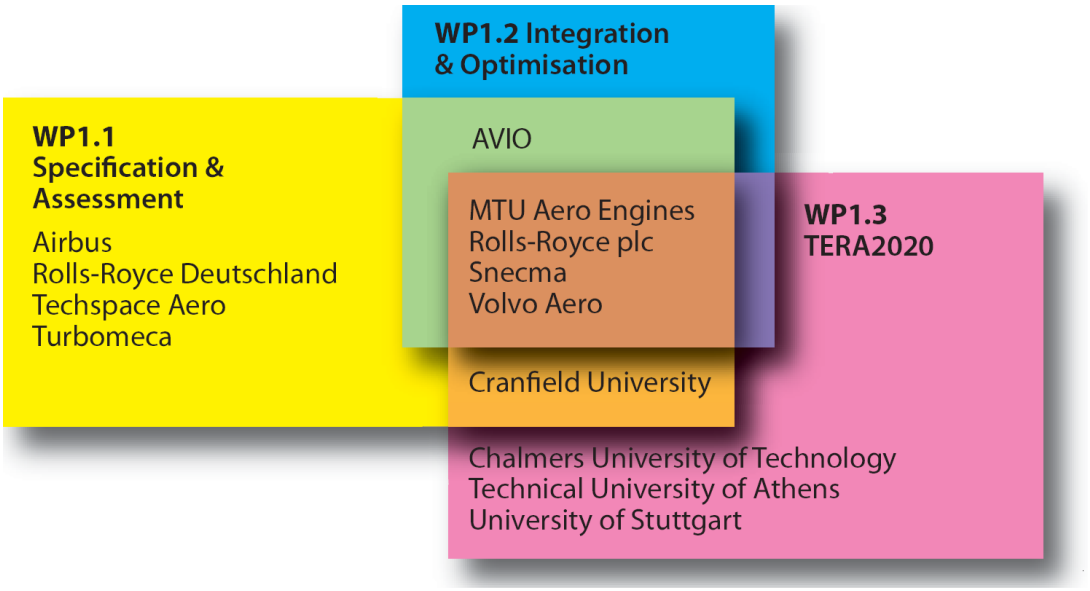

Figure A.1: NEWAC sub-programme 1 partners [32].

Within NEWAC and its sub-programme 1 (SP1), an assessement is carried out - at whole-engine and aircraft system level - of four novel engine designs that incorporate the new technologies researched in the other NEWAC SPss. As part of this effort, TERA2020 is used to assess the economic and environmental impact of these new technologies, and to undertake sensitivity and optimisation studies about the new engine configurations. The management structure of SP1 is illustrated in Fig. A.1; the schematic provides a list of all the partners involved in NEWAC SP1 and exemplifies the interactions between the TERA2020 university partners and OEMs working in different work packages.

A.1.4 TERA2020 core partners and contributions

The core university partners involved in the development of the TERA2020 tool are illustrated in Fig. A.2. while their contributions are illustrated in Fig. A.3. The development of this software has been significantly influenced by several European OEMs, the latter providing important feedback to the university partners.

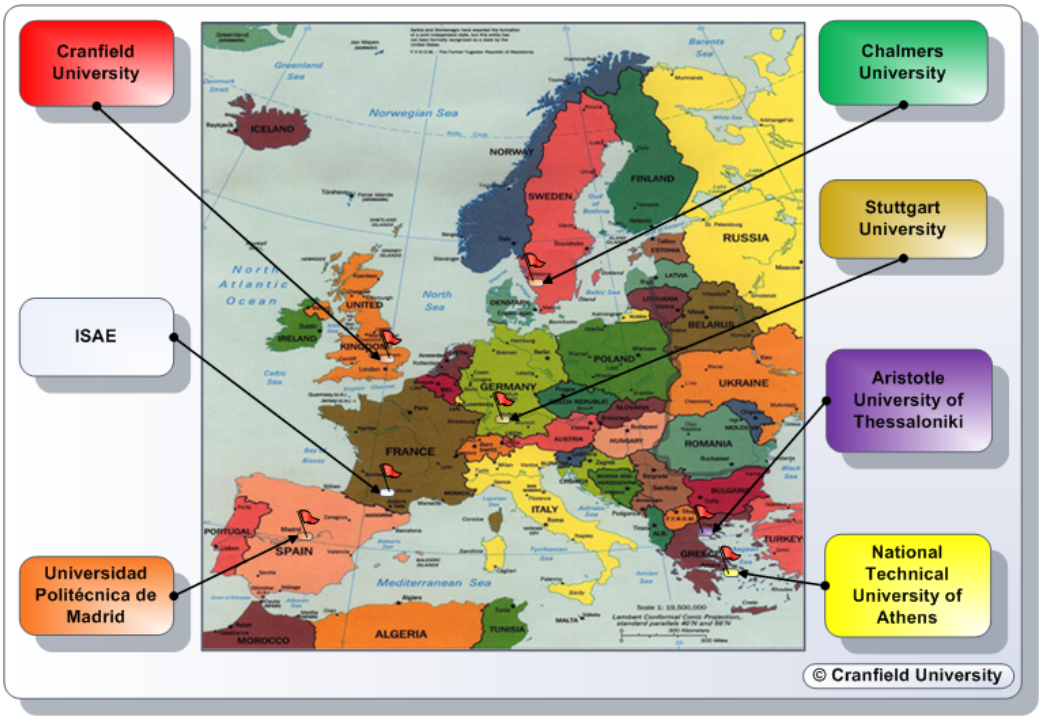

Figure A.2: TERA2020 core partners.

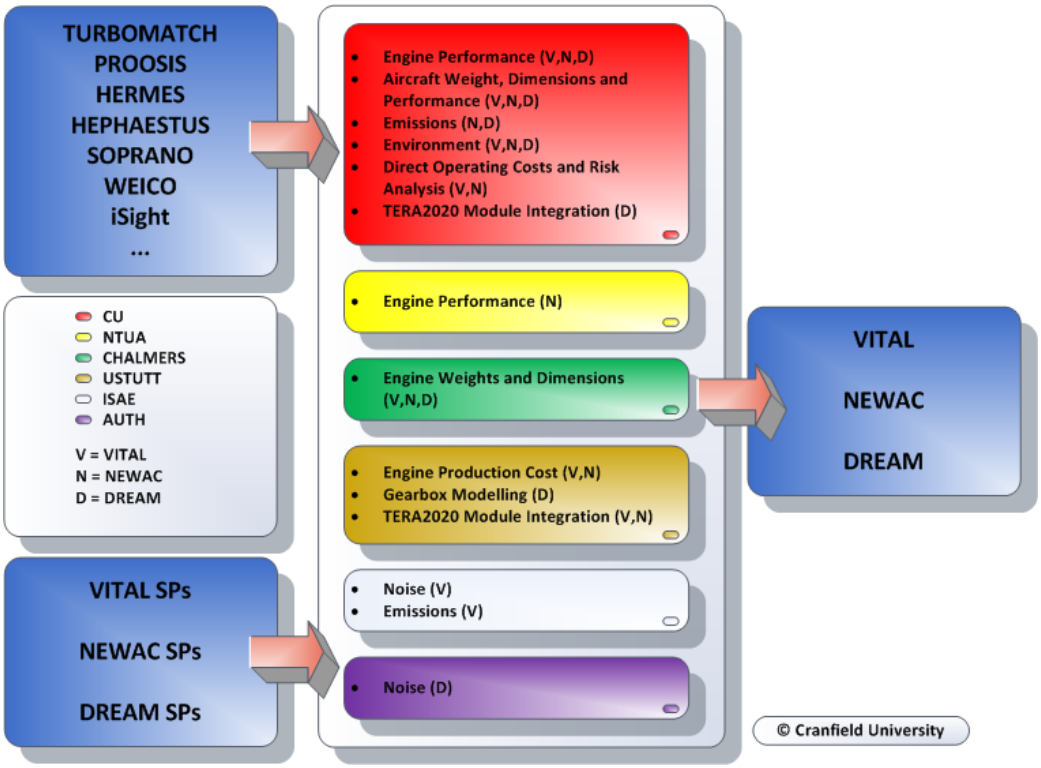

Figure A.3: TERA2020 contributions.

The OEMs involved in the NEWAC TERA2020 modelling and results peer-reviewing process are:

- Rolls-Royce
- Volvo Aero
- Rolls-Royce Deutschland
- MTU Aero Engines
- Snecma
- AVIO
- Turbomeca
- Airbus

A.2 Quality control

This section presents various aspects of quality control as applied during the development of the TERA2020 multi-disciplinary conceptual design tool within the NEWAC collaborative environment. Work planning, configuration control, communication between research teams, and documentation are discussed.

A.2.1 Work planning

The work carried out within NEWAC WP1.3 with respect to the development and use of the TERA2020 tool can be broken down into the following tasks:

- Development of new software modules and adaptation of existing ones (from VITAL TERA2020) to fit the needs of NEWAC TERA2020.
- Integration of new and existing modules in NEWAC TERA2020.
- Derivation of TERA2020 engine/aircraft models to study the novel technologies and architectures researched within the NEWAC project.
- Use of the TERA2020 tool for performing sensitivity analysis, as well as parametric and optimisation studies of the novel technologies and architectures researched within the NEWAC project.
- Dissemination of the NEWAC TERA2020 team findings to a wider audience.

A large number of milestones and deliverables were set to monitor the work carried out within NEWAC WP1.3, and to coordinate it, where possible, with the work carried out concurrently by other WPs and SPs. These management aspects are described in detail in the NEWAC DoW (Description of Work) document.

The sequence for the work carried out follows:

Stage 1 - Initial NEWAC TERA2020 (Duration: 12 months)

1. Initial software modules for TERA2020.
2. Initial TERA2020 integration and engine/aircraft models.

3. Initial TERA2020 results (assessment of baseline engine designs).
4. Peer-reviewing of initial TERA2020 results by NEWAC OEMs.
5. Dissemination of initial TERA2020 results to a wider audience.

Stage 2 - Intermediate NEWAC TERA2020 (Duration: 12 months)

1. Intermediate software modules for TERA2020 incorporating OEM feedback.
2. Intermediate TERA2020 integration and engine/aircraft models.
3. Intermediate TERA2020 results (system sensitivity analysis).
4. Peer-reviewing of intermediate results by NEWAC OEMs.
5. Dissemination of intermediate TERA2020 results to a wider audience.

Stage 3 - Final NEWAC TERA2020 (Duration: 12 months)

1. Final software modules for TERA2020 incorporating OEM feedback.
2. Final TERA2020 integration and engine/aircraft models.
3. Final TERA2020 results (engine optimisation).
4. Peer-reviewing of final results by NEWAC OEMs.
5. Dissemination of final TERA2020 results to a wider audience.

A.2.2 Configuration control

A significant lesson learned has been the importance of configuration control in the development of a multi-disciplinary conceptual design tool within a collaborative environment. Modelling assumptions need to be transparent (and of course consistent) among different disciplines; this is not a trivial task and throughout the development project a continuous effort needs to be directed to this by the team leader. It is imperative that the importance of configuration control and the consequences from not maintaining it are well understood by all the members of the development team. Frequent discussions between partners and good documentation can ease such efforts.

A.2.3 Communication between research teams

For the TERA2020 tool to achieve its goals, it was of uttermost importance that good communication channels were built at three distinct levels:

- Communication between partners in the NEWAC WP1.3 TERA2020 research team.
- Communication between the NEWAC WP1.3 TERA2020 research team and the equivalent VITAL and DREAM TERA2020 research teams.
- Communication between the NEWAC WP1.3 TERA2020 research team and the OEMs in NEWAC SP1.

Different communication channels were utilised, including:

- **Frequent link calls between partners in NEWAC WP1.3.** These helped in assessing the work progress of each partner, and adapt the short term plan accordingly.
- **NEWAC WP1.3 2-day technical review meetings once per year.** These gave the opportunity for each partner to present their work progress in detail and for the whole team to address general modelling issues with emphasis on configuration control. Long term planning (annual plan) was decided between the partners during these meetings. An important lesson learned was that the TERA2020 research team would have benefited significantly if these meetings where held quarterly; their frequency however was restricted due to budget considerations.
- **6-month visit to Chalmers university by a Cranfield TERA2020 investigator.** This gave the opportunity for a closer collaboration between the two universities, accellerating work progress and resolving modelling conflicts with respect to configuration control.
- **Frequent link calls between the work-package leaders in SP1.** These helped in assessing partner work progress and plan ahead.

- **NEWAC SP1 1-day techincal review meetings once per year (some of which were Technical Design Reviews).** These gave the opportunity for different SPs to report their latest progress to SP1, and for the SP1 team to assess the projest progress at whole engine level.
- **Meetings between NEWAC TERA2020 WP1.3 partners and OEMS in SP1 and SP6.** These gave the opportunity to the TERA2020 team to present the modelling carried out and to the OEMs to assess assumptions made and give their feedback. Information retrieved by the TERA team through this exercise significantly improve the quality of the modelling carried out and also helped improve the overall TERA2020 conceptual design algorithm.
- **Live demonstration of NEWAC TERA2020 to the EC project review team and all NEWAC partners.** This helped disseminate NEWAC TERA2020 work to the EC and the NEWAC management committee, but most importantly clarify the overall potential of the TERA2020 tool and its proximity to reaching the original objectives set.

A.2.4 Documentation

Documentation is an important aspect for any software tool development. An internal library was set up within NEWAC WP1.3 and was populated with a large number of classified documents (nearly 30). Every document in the library received a unique identification number and, where appropriate, a common document template was used. The most important documents from the VITAL TERA2020 efforts were imported into the library. A comprehensive listing of NEWAC TERA2020 internal documents including their unique identification numbers follows in the next page.

NEWAC TERA2020 Internal Documents

A. Alexiou. GTAC Performance Model Descripition and Results. Technical report, National Technical University of Athens, March 2008. NEWAC-WP1.3-NTUA-T-0308-001-R1.0.

A. Alexiou. CRFC Performance Model Descripition and Results. Technical report, National Technical University of Athens, June 2008. NEWAC-WP1.3-NTUA-T-0608-002-R1.0.

K.G. Kyprianidis. DDIC Performance Model Descripition and Results. Technical report, Cranfield University, October 2008. NEWAC-WP1.3-CU-T-1008-003-R1.0.

K.G. Kyprianidis. GTIR Performance Model Descripition and Results. Technical report, Cranfield University, February 2010. NEWAC-WP1.3-CU-T-0210-004-R1.1.

B. Lehmayr. VITAL NEWAC TERA2020 Standard Nomenclature. Technical report, University of Stuttgart, October 2009. NEWAC-WP1.3-USTUTT-T-1009-005-R1.5.

L. Xu and T. Grönstedt. DDIC TERA2020 Sensitivity Analysis. Technical report, Chalmers University, September 2009. NEWAC-WP1.3-CHALMERS-T-0909-006-R1.0.

A. Alexiou and I. Roumeliotis. CRFC TERA2020 Sensitivity Analysis. Technical report, National Technical University of Athens, July 2009. NEWAC-WP1.3-NTUA-T-0709-007-R1.0.

B. Lehmayr and S. Staudacher. GTAC TERA2020 Sensitivity Analysis. Technical report, University of Stuttgart, September 2009. NEWAC-WP1.3-USTUTT-T-0909-008-R1.0.

L. Xu and T. Grönstedt. GTIR TERA2020 Sensitivity Analysis. Technical report, Chalmers University, November 2009. NEWAC-WP1.3-CHALMERS-T-1109-009-R1.0.

K.G. Kyprianidis. DDIC Sensitivity Analysis Bounds. Technical report, Cranfield University, August 2009. NEWAC-WP1.3-CU-S-0809-010-R1.0.

K.G. Kyprianidis. GTIR Sensitivity Analysis Bounds. Technical report, Cranfield University, September 2009. NEWAC-WP1.3-CU-S-0909-011-R1.0.

K.G. Kyprianidis. NEWAC TERA2020 Engine Performance Module Specification - EVA Code. Technical report, Cranfield University, October 2009. NEWAC-WP1.3-CU-T-1009-012-R1.1.

A. Alexiou. NEWAC TERA2020 Engine Performance Module Specification - PROOSIS Code. Technical report, National Technical University of Athens, November 2008. NEWAC-WP1.3-NTUA-T-1108-013-R1.0.

K.G. Kyprianidis. NEWAC TERA2020 Engine Performance Module Specification - TURBOMATCH Code. Technical report, Cranfield University, October 2009. NEWAC-WP1.3-CU-T-1009-014-R1.1.

S. Ogaji, K.G. Kyprianidis, D.S. Pascovici, and F. Colmenares. NEWAC TERA2020 Aircraft Module Specification. Technical report, Cranfield University, October 2009. NEWAC-WP1.3-CU-T-1009-015-R1.1.

K.G. Kyprianidis. NEWAC TERA2020 Emissions Module Specification. Technical report, Cranfield University, October 2009. NEWAC-WP1.3-CU-T-1009-016-R1.1.

K.G. Kyprianidis and S. Ogaji. NEWAC TERA2020 Environmental Module Specification. Technical report, Cranfield University, October 2009. NEWAC-WP1.3-CU-T-1009-017-R1.1.

K.G. Kyprianidis, D. Au, and A. Carrere. NEWAC TERA2020 Noise Module Specification. Technical report, Cranfield University and ISAE/SUPAERO, October 2009. NEWAC-WP1.3-CU-T-1009-018-R1.1.

D.S. Pascovici, S. Ogaji, K.G. Kyprianidis, and F. Colmenares. NEWAC TERA2020 Economic Module Specification. Technical report, Cranfield University, October 2009. NEWAC-WP1.3-CU-T-1009-019-R1.1.

T. Grönstedt and L. Xu. NEWAC TERA2020 Dimensions and Weight Module Specification. Technical report, Chalmers University, December 2008. NEWAC-WP1.3-CHALMERS-T-1208-020-R1.0.

S. Staudacher, O. Arago, S. Bretschneider, and B. Lehmayr. VITAL NEWAC TERA2020 Plant Cost Module Specification. Technical report, University of Stuttgart, October 2009. NEWAC-WP1.3-USTUTT-T-1009-021-R1.0.

K.G. Kyprianidis and B. Lehmayr. NEWAC TERA2020 Demonstration to the EC Reviewers. Technical report, Cranfield University and University of Stuttgart, October 2009. NEWAC-WP1.3-USTUTT-P-1009-022-R2.0.

K.G. Kyprianidis. NEWAC WP1.3 Internal Documents List. Technical report, Cranfield University, February 2010. NEWAC-WP1.3-CU-S-0210-023-R1.3.

S. Staudacher and G. Gerrit Schütte. VITAL Optimization Techniques Review. Technical report, University of Stuttgart, October 2009. NEWAC-WP1.3-USTUTT-PDF-1009-024-R1.0.

S. Bretschneider. TERA Model iSIGHT Parameter Definitions. Technical report, University of Stuttgart, October 2009. NEWAC-WP1.3-USTUTT-PDF-1009-025-R1.4.

S. Bretschneider. Initial TERA Modules Integration into Optimiser. Technical report, University of Stuttgart, October 2009. NEWAC-WP1.3-USTUTT-PDF-1009-026-R1.0.

K.G. Kyprianidis. DDIC Optimisation Bounds. Technical report, Cranfield University, February 2010. NEWAC-WP1.3-CU-S-0210-027-R1.3.

A.3 Dissemination

Different dissemination channels were utilised, including:

- Conferences (ISABE 2009, ASME TURBO EXPO 2010, ICAS 2010)
- Journals (AIAA Journal of Propulsion and Power, ASME Journal of Engineering for Gas Turbines and Power).
- NEWAC project public workshop.

A comprehensive listing of NEWAC TERA2020 dissemination efforts follows in the next page.

NEWAC TERA2020 Publications

K.G. Kyprianidis, D. Au, S.O.T. Ogaji, and T. Grönstedt. Low Pressure System Component Advancements and its Impact on Future Turbofan Engine Emissions. In *ISABE 2009 Proceedings, ISABE-2009-1276*, Montreal, Canada, September 2009.

L. Xu and T. Grönstedt. Design and Analysis of an Intercooled Turbofan Engine. *ASME Journal of Engineering for Gas Turbines and Power, GTP-09-1228, under publication*, December 2009.

K.G. Kyprianidis, T. Grönstedt, S.O.T. Ogaji, P. Pilidis, and R. Singh. Assessment of Future Aero Engine Designs with Intercooled and Intercooled Recuperated Cores. In *ASME TURBO EXPO 2010 Proceedings, GT-2010-23621*, Glasgow, United Kingdom, June 2010.

A. Alexiou, N. Aretakis, I. Roumeliotis, and K. Mathioudakis. Analysis for a Geared Turbofan with Active Core Technologies. In *ASME TURBO EXPO 2010 Proceedings, GT2010-22701*, Glasgow, United Kingdom, June 2010.

A.M. Rolt, M. Andreoletti, and K.G. Kyprianidis. Assessment of New Aero Engine Core Concepts and Technologies in the EU Framework 6 NEWAC Programme. In *ICAS 2010 Congress Proceedings, Paper No. 408*, Nice, France, September 2010. extended abstract submitted for publication.

K.G. Kyprianidis, S.O.T. Ogaji, P. Pilidis, R. Singh, A.M. Rolt, and T. Grönstedt. Aero Engine Conceptual Design - Part I: Multi-Disciplinary Framework Development. *AIAA Journal of Propulsion and Power*, 2010. under preparation.

T. Grönstedt, A. Lundbladh, S.O.T. Ogaji, P. Pilidis, R. Singh, and K.G. Kyprianidis. Aero Engine Conceptual Design - Part II: Low Pressure System Component Advancements and its Impact on Future Turbofan Engine Emissions. *AIAA Journal of Propulsion and Power*, 2010. under preparation.

K.G. Kyprianidis, B. Lehmayr, L. Xu, and A. Alexiou. TERA2020 - Rationale, Objectives and Design Algorithm. In *NEWAC Workshop Proceedings*, Munich, Germany, June 2010. abstract submitted for publication.

B. Lehmayr, K.G. Kyprianidis, L. Xu, and A. Alexiou. TERA2020 Optimisation of NEWAC Configurations. In *NEWAC Workshop Proceedings*, Munich, Germany, June 2010. abstract submitted for publication.

Appendix B

Optimisation design variables

This appendix provides additional information in spreadsheet format on the choice of design variables for the optimisation process described in Chapter 7. Unless explicitly stated otherwise, design variables refer to top of climb engine operating conditions (ISA +10 [K], FL350, M = 0.82).

B.1 Tables

The effect of introducing a single design variable perturbation on the values of other parameters at design point and off-design conditions is described by Fig. B.1 and Fig. B.2, respectively. Similarly, Fig. B.3 describes the effect of such perturbations on the values of mechanical design parameters and objective functions.

Optimisation design variables
(TOC unless stated otherwise)

Engine parameters at design point conditions (TOC: ISA+10, FL350, M0.82 for LR and M0.78 for SR)	Units	Fan inlet mass flow	Core inlet mass flow	IC LP inlet mass flow	Fan tip pressure ratio	Fan tip polytropic efficiency	IPC pressure ratio	IPC polytropic efficiency	HPC pressure ratio	HPC polytropic efficiency	HPT polytropic efficiency	IPT polytropic efficiency	LPT polytropic efficiency	IC effectiveness TOC	IC effectiveness T/O	IC effectiveness cruise	IC LP pressure loss dP/P	IC HP pressure loss dP/P	T4 TOC	T4 T/O	T4 cruise	T4 descent/approach/idle	HPT cooling flow % core	IPT cooling flow % core	Bypass duct pressure loss	Remarks
																										This is the design point for engine performance (i.e. for determining the map scaling factors and nozzle areas). It is used by WeiCo as the aerodynamic design point for some components.
Fan inlet mass flow	kg/s	V	F	F	F	F	F	F	F	F	F	F	F	F	F	F	F	F	F	F	F	F	F	F	F	
Core inlet mass flow	kg/s	F	V	F	F	F	F	F	F	F	F	F	F	F	F	F	F	F	F	F	F	F	F	F	F	
IC LP inlet mass flow	kg/s	F	F	V	F	F	F	F	F	F	F	F	F	F	F	F	F	F	F	F	F	F	F	F	F	
Fan tip pressure ratio	-	F	F	F	V	F	F	F	F	F	F	F	F	F	F	F	F	F	F	F	F	F	F	F	F	
Fan tip polytropic efficiency	%	F	F	F	F	V	F	F	F	F	F	F	F	F	F	F	F	F	F	F	F	F	F	F	F	
IPC pressure ratio	-	F	F	F	F	F	V	F	F	F	F	F	F	F	F	F	F	F	F	F	F	F	F	F	F	
IPC polytropic efficiency	%	F	F	F	F	F	F	V	F	F	F	F	F	F	F	F	F	F	F	F	F	F	F	F	F	
HPC pressure ratio	-	F	F	F	F	F	F	F	V	F	F	F	F	F	F	F	F	F	F	F	F	F	F	F	F	
HPC polytropic efficiency	%	F	F	F	F	F	F	F	F	V	F	F	F	F	F	F	F	F	F	F	F	F	F	F	F	
HPT polytropic efficiency	%	F	F	F	F	F	F	F	F	F	V	F	F	F	F	F	F	F	F	F	F	F	F	F	F	
IPT polytropic efficiency	%	F	F	F	F	F	F	F	F	F	F	V	F	F	F	F	F	F	F	F	F	F	F	F	F	
LPT polytropic efficiency	%	F	F	F	F	F	F	F	F	F	F	F	V	F	F	F	F	F	F	F	F	F	F	F	F	
Intercooler temperature effectiveness	%	F	F	F	F	F	F	F	F	F	F	F	F	V	F	F	F	F	F	F	F	F	F	F	F	
IC LP pressure loss dP/P	%	F	F	F	F	F	F	F	F	F	F	F	F	F	F	F	V	F	F	F	F	F	F	F	F	
IC HP pressure loss dP/P	%	F	F	F	F	F	F	F	F	F	F	F	F	F	F	F	F	V	F	F	F	F	F	F	F	
T4	K	F	F	F	F	F	F	F	F	F	F	F	F	F	F	F	F	F	V	F	F	F	F	F	F	
HPT cooling flow % core	%	F	F	F	F	F	F	F	F	F	F	F	F	F	F	F	F	F	F	F	F	F	V	F	F	
IPT cooling flow % core	%	F	F	F	F	F	F	F	F	F	F	F	F	F	F	F	F	F	F	F	F	F	F	V	F	
Bypass duct pressure loss	%	F	F	F	F	F	F	F	F	F	F	F	F	F	F	F	F	F	F	F	F	F	F	F	V	
Bypass ratio	-	V	V	V	F	F	F	F	F	F	F	F	F	F	F	F	F	F	F	F	F	F	F	F	F	
Overall pressure ratio	-	F	F	F	V	F	V	F	V	F	F	F	F	F	F	F	F	V	F	F	F	F	F	F	F	Defined as: P3 / P2
IP/HP Pressure ratio split	-	F	F	F	V	F	V	F	V	F	F	F	F	F	F	F	F	V	F	F	F	F	F	F	F	It practically only varies when IPC or HPC PR is varied. Defined as: (P25 - P23) / (P3 - P23)
Fan root pressure ratio	-	F	F	F	V	F	F	F	F	F	F	F	F	F	F	F	F	F	F	F	F	F	F	F	F	
Fan root polytropic efficiency	%	F	F	F	F	V	F	F	F	F	F	F	F	F	F	F	F	F	F	F	F	F	F	F	F	
Thrust	kN	V	V	V	V	V	V	V	V	V	V	V	V	V	F	F	V	V	V	F	F	F	V	V	V	
T41	K	V	V	V	V	V	V	V	V	V	V	V	V	V	F	F	V	V	V	F	F	F	V	V	V	T41 is an output from the energy balance between the HPT cooling flow that does work in the rotor and the combustor outlet stream. For some parameter variations it practically doesn't vary.
TERA2020 technology level parameter (not varied during optimisation)	(purple shading)	F = Fixed					V = Varies																			

Figure B.1: TERA2020 design variables for the direct drive fan conventional and intercooled core engine configuration and their effect on the values of other parameters at top of climb.

Optimisation design variables (TOC unless stated otherwise)		Fan inlet mass flow	Core inlet mass flow	IC LP inlet mass flow	Fan tip pressure ratio	Fan tip polytropic efficiency	IPC pressure ratio	IPC polytropic efficiency	HPC pressure ratio	HPC polytropic efficiency	HPT polytropic efficiency	IPT polytropic efficiency	LPT polytropic efficiency	IC effectiveness TOC	IC effectiveness T/O	IC effectiveness cruise	IC LP pressure loss dP/P	IC HP pressure loss dP/P	T4 TOC	T4 T/O	T4 cruise	T4 descent/approach/idle	HPT cooling flow % core	IPT cooling flow % core	Bypass duct pressure loss	Remarks
Engine parameters at different off-design conditions (T/O: ISA+15, FL0, M0.25; ICAO T/O: ISA SLS; Mid-Cr: ISA, FL350, M0.82 for LR and M0.78 for SR)	**Units**																									
Take-off thrust	kN	V	V	V	V	V	V	V	V	V	V	V	V	V	F	V	V	V	V	F	F	V	V	V	This is the end of runway hot day T/O (kink) point. It is used by WeiCo as the mechanical design point (ISA +15K, FL0, M0.25). The aerodynamic design for some components will also be carried out at these conditions. T4 at this point is kept constant in all but a single case. T41 will vary due to off-design performance effects. The thrust produced at this point is used to deduce the ISA SLS thrust using flat take-off rating rules.
Take-off T4	K	F	F	F	F	F	F	F	F	F	F	F	F	F	F	F	F	F	V	F	F	F	F	F		
Take-off T41	K	V	V	V	V	V	V	V	V	V	V	V	V	V	F	V	V	V	V	F	F	V	V	V		
Take-off IC effectiveness	%	F	F	F	F	F	F	F	F	F	F	F	F	V	F	F	F	F	F	F	F	F	F	F		
ICAO take-off thrust	kN	V	V	V	V	V	V	V	V	V	V	V	V	V	F	V	V	V	V	F	F	V	V	V	The ICAO T/O point (ISA SLS) together with the 85%FN, 30%FN, and 7%FN ICAO points are used for determining the LTO NOx. Firstly, the thrust is determined at end of runway hot day T/O (kink point) for a given T4, and then flat take-off rating is assumed in order to deduce the thrust at ISA SLS.
ICAO take-off T4	K	V	V	V	V	V	V	V	V	V	V	V	V	V	F	V	V	V	V	F	F	V	V	V		
ICAO take-off T41	K	V	V	V	V	V	V	V	V	V	V	V	V	V	F	V	V	V	V	F	F	V	V	V		
ICAO take-off IC effectiveness	%	F	F	F	F	F	F	F	F	F	F	F	F	V	F	F	F	F	F	F	F	F	F	F		
Mid-cruise thrust	kN	V	V	V	V	V	V	V	V	V	V	V	V	V	F	V	V	V	V	F	V	F	V	V	V	This is the mid-cruise spec. point as provided by the OEMs (ISA, FL350, M0.82 for LR and M0.78 for SR). HERMES actually interpolates from extended cruise performance tables, also produced by the performance module. These tables are produced using the same fixed IC effectiveness, as well as a fixed max. and min. cruise T4. As the SFC improves and/or the engine gets lighter the rubberised aircraft also becomes lighter. The true mid-cruise point will therefore change. A time-averaged mid cruise performance point is produced by HERMES for the emissions module. The emissions module will predict NOx for the entire flight missions profile as well as ICAO LTO and the time-averaged mid cruise performance point.
Mid-cruise T4	K	F	F	F	F	F	F	F	F	F	F	F	F	F	F	F	F	F	F	V	F	F	F	F		
Mid-cruise T41	K	V	V	V	V	V	V	V	V	V	V	V	V	V	F	V	V	V	V	F	V	F	V	V	V	
Mid-cruise IC effectiveness	%	F	F	F	F	F	F	F	F	F	F	F	F	V	F	F	F	F	F	F	F	F	F	F		
TERA2020 technology level parameter (not varied during optimisation)																										

F = Fixed V = Varies

Figure B.2: TERA2020 design variables for the direct drive fan conventional and intercooled core engine configuration and their effect on the values of other parameters at different off-design conditions.

Optimisation design variables (TOC unless stated otherwise)		Fan inlet mass flow	Core inlet mass flow	IC LP inlet mass flow	Fan tip pressure ratio	Fan tip polytropic efficiency	IPC pressure ratio	IPC polytropic efficiency	HPC pressure ratio	HPC polytropic efficiency	HPT polytropic efficiency	IPT polytropic efficiency	LPT polytropic efficiency	IC effectiveness TOC	IC effectiveness T/O	IC effectiveness cruise	IC LP pressure loss dP/P	IC HP pressure loss dP/P	T4 TOC	T4 T/O	T4 cruise	T4 descent/approach/idle	HPT cooling flow % core	IPT cooling flow % core	Bypass duct pressure loss	Remarks
Mechanical/aerodynamic design	**Units**																									
LP speed	rpm	V	V	V	V	V	V	V	V	V	V	V	V	V	V	F	V	V	V	V	F	F	V	V	V	Calculated by WeiCo assuming a fixed fan corrected blade speed, fan face Mach number, and hub to tip ratio.
IP speed	rpm	V	V	V	V	V	V	V	V	V	V	V	V	V	V	F	V	V	V	V	F	F	V	V	V	A fixed IPC corrected blade speed is used with the tip radius being determined by components upstream of the IPC.
HP speed	rpm	V	V	V	V	V	V	V	V	V	V	V	V	V	V	F	V	V	V	V	F	F	V	V	V	A fixed HPC corrected blade speed is used with the tip radius being determined by components upstream of the HPC.
LP turbine efficiency T/O	%	V	V	V	V	V	V	V	V	V	V	V	V	V	V	F	V	V	V	V	F	F	V	V	V	Varies due to off-design effects. Constant at TOC in all cases but one.
Number of IPC stages	-	V	V	V	V	V	V	V	V	V	V	V	V	V	V	F	V	V	V	V	F	F	V	V	V	Allowed to vary.
Number of HPC stages	-	V	V	V	V	V	V	V	V	V	V	V	V	V	V	F	V	V	V	V	F	F	V	V	V	Allowed to vary.
Number of HPT stages	-	F	F	F	F	F	F	F	F	F	F	F	F	F	F	F	F	F	F	F	F	F	F	F	F	Fixed.
Number of IPT stages	-	F	F	F	F	F	F	F	F	F	F	F	F	F	F	F	F	F	F	F	F	F	F	F	F	Fixed.
Number of LPT stages	-	V	V	V	V	V	V	V	V	V	V	V	V	V	V	F	V	V	V	V	F	F	V	V	V	Allowed to vary.
Objective functions	**Units**																									
Mid cruise SFC	g/(kN*s)	V	V	V	V	V	V	V	V	V	V	V	V	V	F	V	V	V	V	F	V	F	V	V	V	This is the mid-cruise spec point.
Business case block fuel	kg	V	V	V	V	V	V	V	V	V	V	V	V	V	V	V	V	V	V	V	V	V	V	V	V	
Engine weight	kg	V	V	V	V	V	V	V	V	V	V	V	V	V	V	V	V	V	V	V	V	V	V	V	V	
Production cost	kEuro	V	V	V	V	V	V	V	V	V	V	V	V	V	V	V	V	V	V	V	V	V	V	V	V	
Maintenance cost	kEuro/hr	V	V	V	V	V	V	V	V	V	V	V	V	V	V	V	V	V	V	V	V	V	V	V	V	
Direct operating cost	kEuro/yr	V	V	V	V	V	V	V	V	V	V	V	V	V	V	V	V	V	V	V	V	V	V	V	V	
Global warming potential	-	V	V	V	V	V	V	V	V	V	V	V	V	V	V	V	V	V	V	V	V	V	V	V	V	
ICAO Annex 16 EPNL	db	V	V	V	V	V	V	V	V	V	V	V	V	V	F	V	V	V	V	F	V	V	V	V	V	
ICAO Annex 16 LTO NOx	g/kN	V	V	V	V	V	V	V	V	V	V	V	V	V	V	V	V	V	V	V	V	V	V	V	V	
TERA2020 technology level parameter (not varied during optimisation)		F = Fixed V = Varies																								

Figure B.3: TERA2020 design variables for the direct drive fan conventional and intercooled core engine configuration and their effect on the values of mechanical design parameters and objective functions.

Appendix C

Component characteristics

This appendix presents some of the component characteristics used with the newly developed performance code described in Chapter 3. Characteristics for the following components are included here: fan, compressor, turbine, intercooler, combustor. All turbomachinery maps have been extrapolated towards the low speed region and their smoothness has been improved using the commercially available tools SmoothC and SmoothT [94, 95]. Some characteristics from the TURBOMATCH code have also been exported.

C.1 Intercooler

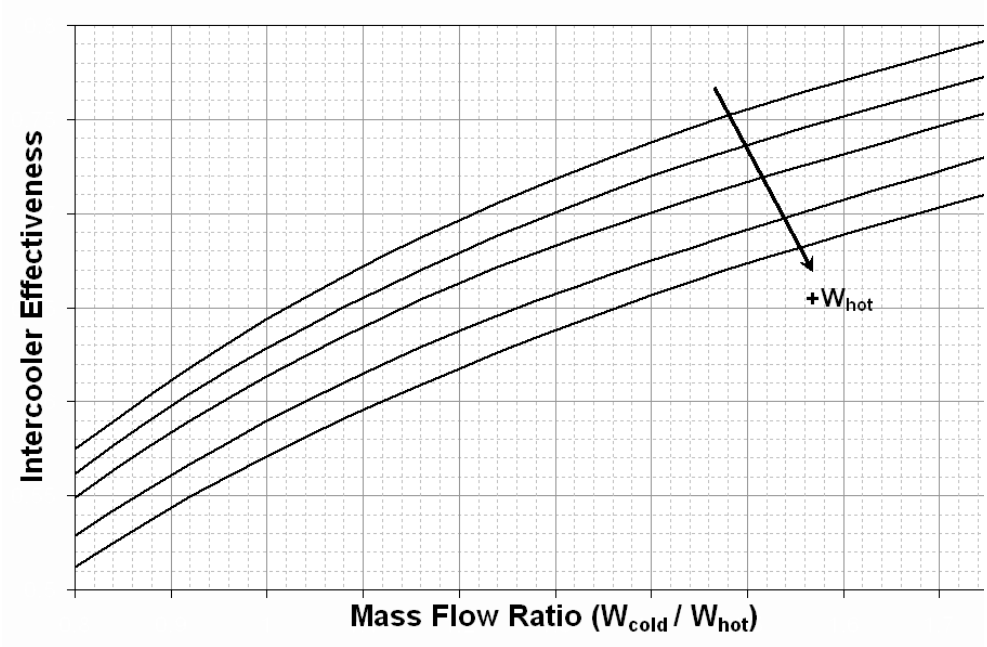

Figure C.1: Intercooler characteristic.

C.2 Combustor

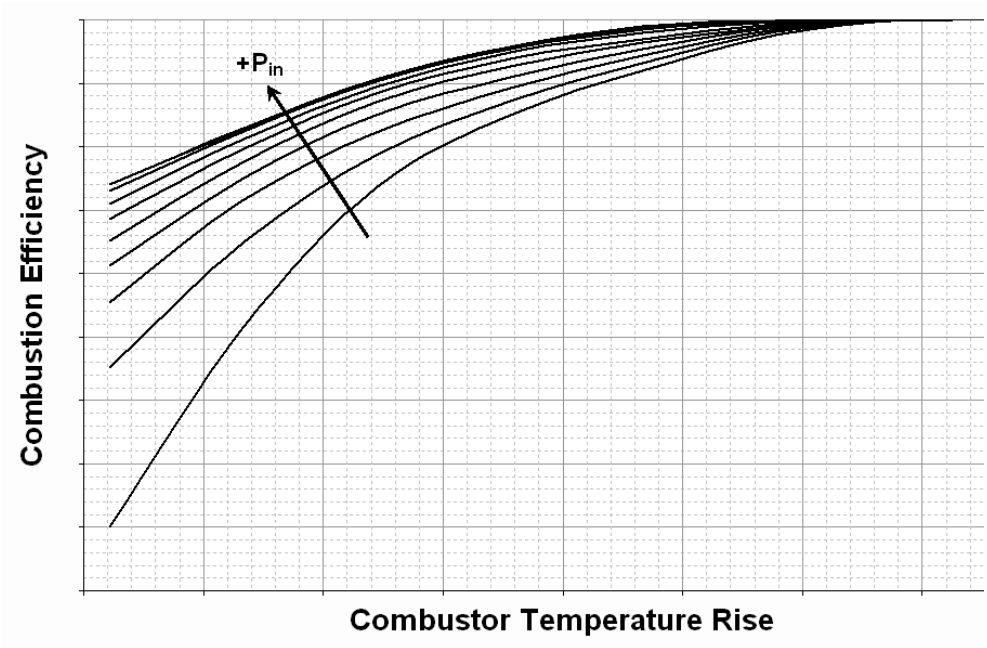

Figure C.2: Combustor characteristic.

C.3 Fan and compressor

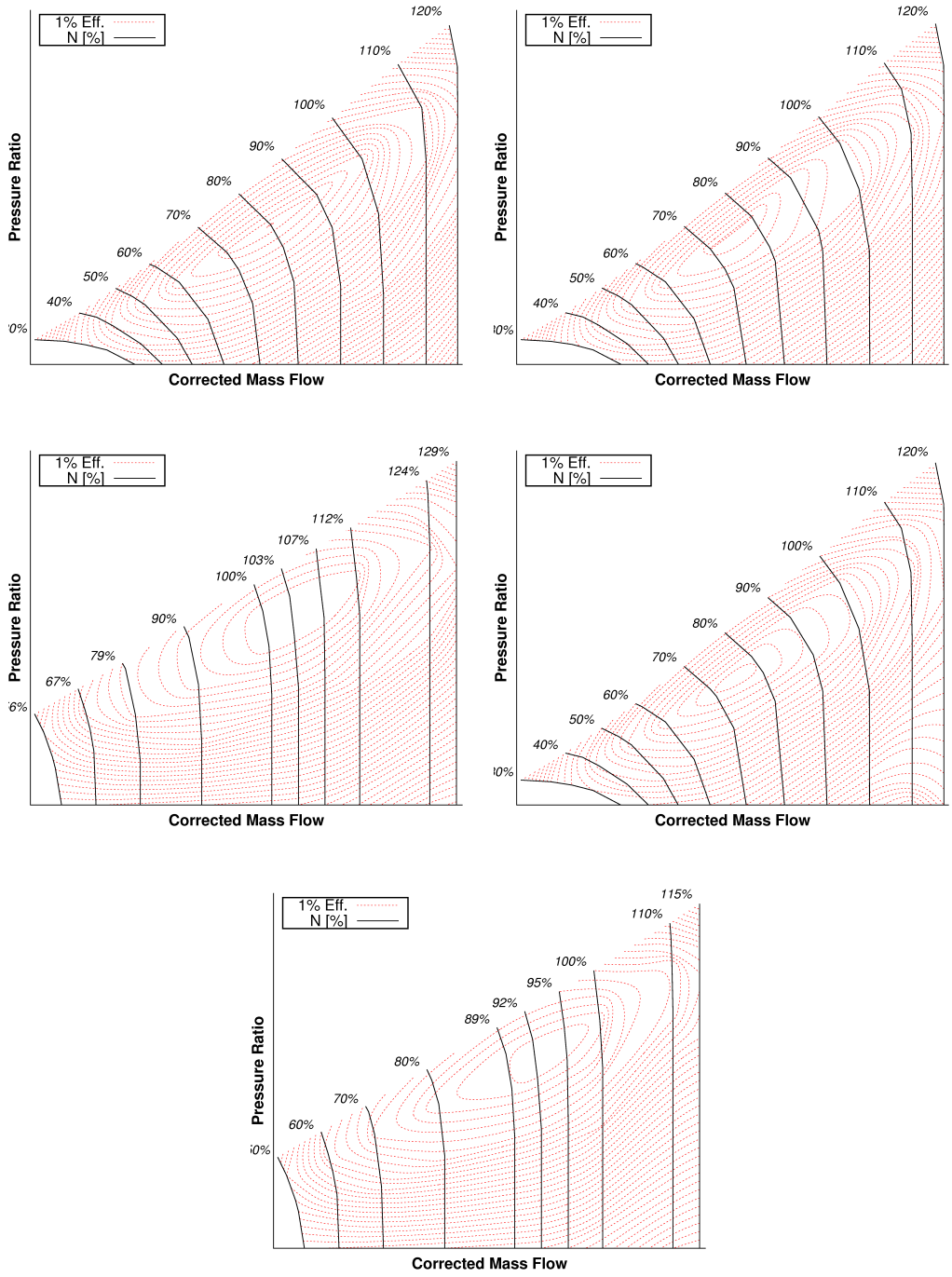

Figure C.3: TURBOMATCH fan and compressor default characteristics.

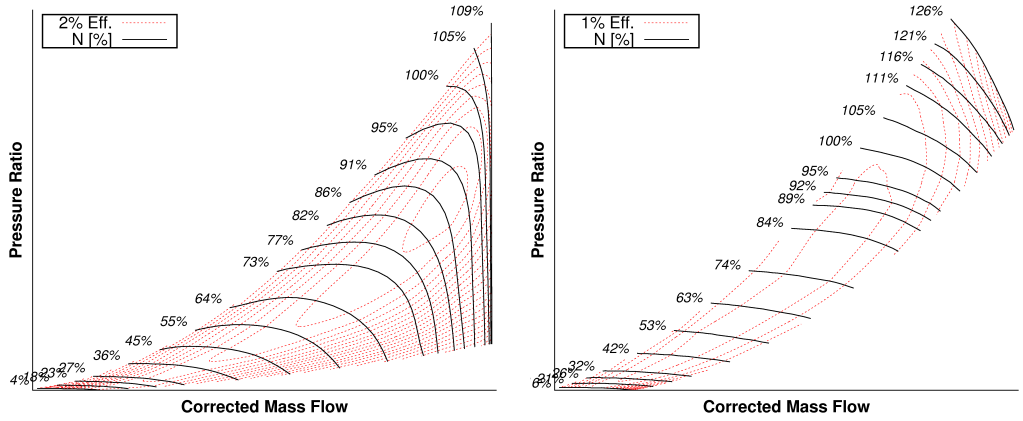

(a) Fan tip (left) and root (right) from [237].

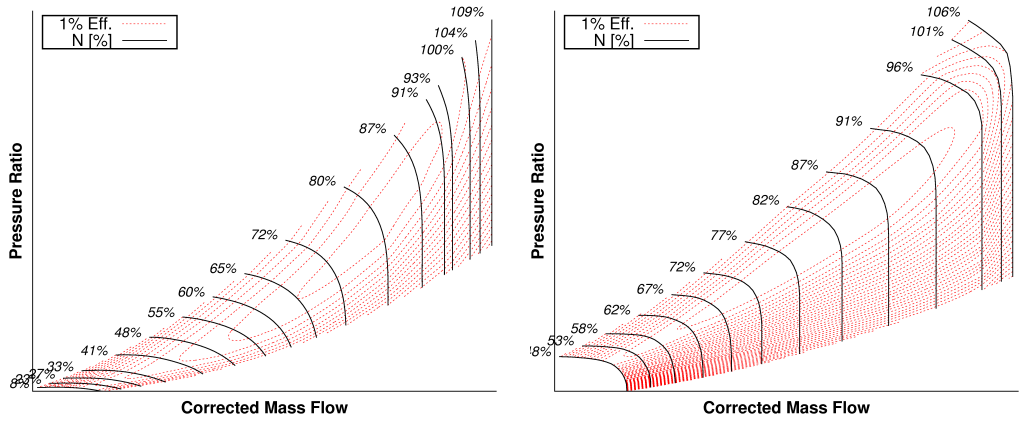

(b) Axial compressor with a design pressure ratio of 3 from [238] (left) and of 5.5 from [239] (right).

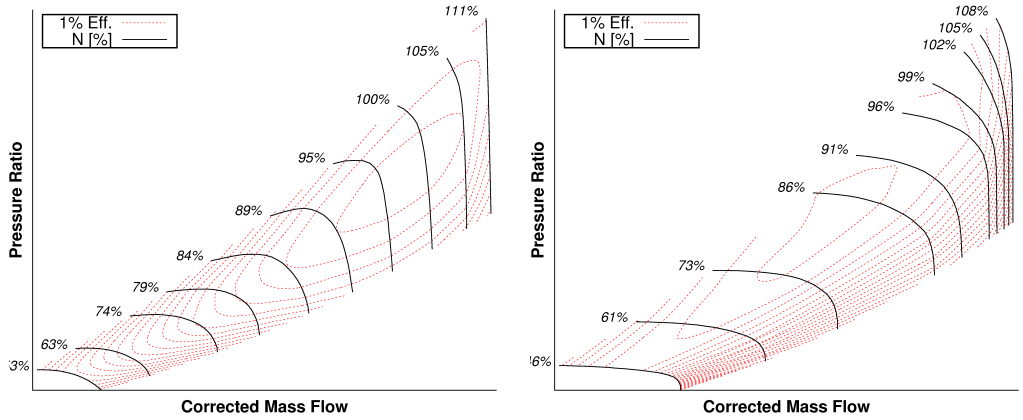

(c) Axial compressor with a design pressure ratio of 9 from [240] (left) and a radial compressor with a design pressure ratio of 4 from [241] (right).

Figure C.4: Modified fan and compressor characteristics from GasTurb [95].

C.4 Turbine

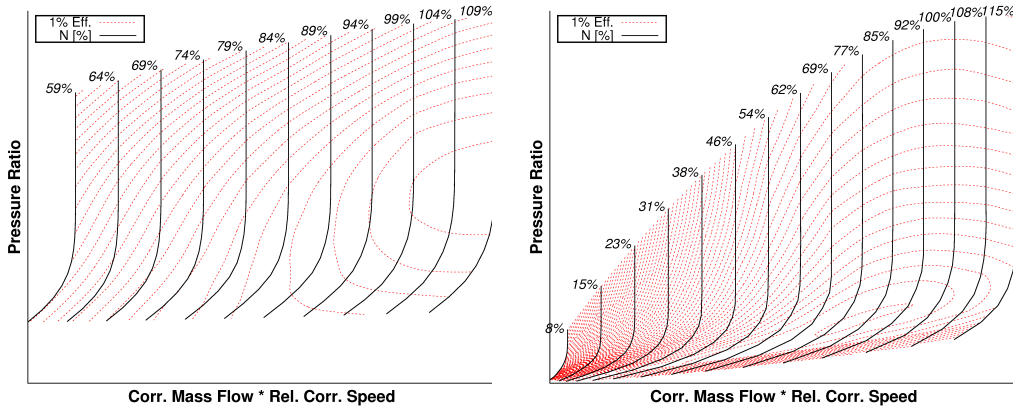

(a) High work low aspect ratio turbine from [242] (left) and variable geometry turbine ($\alpha = 68°$) from [243].

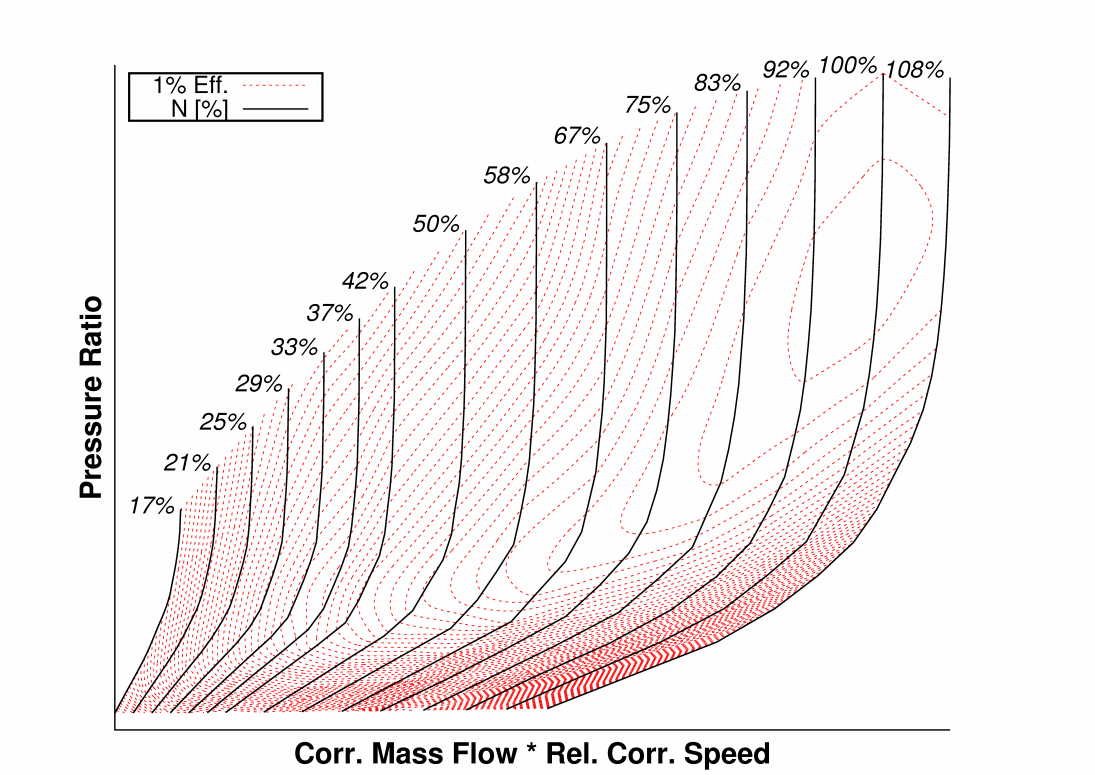

(b) Low pressure turbine from [244].

Figure C.5: Modified turbine characteristics from GasTurb [95].